GENERAL ATOMIC™

GA-A14441
UC-77

THORIUM UTILIZATION PROGRAM

QUARTERLY PROGRESS REPORT FOR THE PERIOD ENDING MAY 31, 1977

Prepared under
Contract EY-76-C-03-0167
Project Agreement No. 53
for the San Francisco Operations Office
U.S. Energy Research and Development Administration

DATE PUBLISHED: JUNE 1977

NOTICE

Printed in the United States of America
Available from
National Technical Information Service
U.S. Department of Commerce
5285 Port Royal Road
Springfield, Virginia 22161
Price: Printed Copy [redacted]; Microfiche $3.00

4/11/75

DISCLAIMER

GENERAL ATOMIC

GA-A14441
UC-77

THORIUM UTILIZATION PROGRAM

QUARTERLY PROGRESS REPORT FOR THE PERIOD ENDING MAY 31, 1977

Prepared under
Contract EY-76-C-03-0167
Project Agreement No. 53
for the San Francisco Operations Office
U.S. Energy Research and Development Administration

GENERAL ATOMIC PROJECT 3225

DATE PUBLISHED: JUNE 1977

QUARTERLY REPORT SERIES*

GA-A13178 - June 1974 through August 1974

GA-A13255 - September 1974 through November 1974

GA-A13366 - December 1974 through February 1975

GA-A13510 - March 1975 through May 1975

GA-A13593 - June 1975 through August 1975

GA-A13746 - September 1975 through November 1975

GA-A13833 - December 1975 through February 1976

GA-A13949 - March 1976 through May 1976

GA-A14085 - June 1976 through August 1976

GA-A14214 - September 1976 through November 1976

GA-A14304 - December 1976 through February 1977

*Prior to GA-A13178, the Thorium Utilization Program was reported in the Base Program Quarterly Progress Report.

ABSTRACT

This publication continues the quarterly series presenting results of work performed under the National HTGR Fuel Recycle Program (also known as the Thorium Utilization Program) at General Atomic Company. Results of work on this program prior to June 1974 were included in a quarterly series on the HTGR Base Program.

The work reported includes the development of unit processes and equipment for reprocessing of High-Temperature Gas-Cooled Reactor (HTGR) fuel, the design and development of an integrated pilot line to demonstrate the head end of HTGR reprocessing using unirradiated fuel materials, and design work in support of Hot Engineering Tests (HET). Work is also described on trade-off studies concerning the required design of facilities and equipment for the large-scale recycle of HTGR fuels in order to guide the development activities for HTGR fuel recycle.

INTRODUCTION

This report covers the work performed by General Atomic Company under U.S. Energy Research and Development Administration Contract EY-76-C-03-0167, Project Agreement No. 53. The work done under this project agreement is part of the program for development of recycle technology for High-Temperature Gas-Cooled Reactor (HTGR) fuels described in the "National Program Plan for HTGR Fuel Recycle Development" (GCR-76/19).

The objective of the program is to provide a demonstration plant for the recycle of HTGR fuels. This plant will demonstrate facility and equipment design and operating procedures which are licensable and commercially feasible for the reprocessing and refabrication of spent fuel from HTGRs. Work at General Atomic Company is concentrating on the following National Program tasks: Program Management and Analysis (Task 100); Reprocessing Technology Development (Task 200); Refabrication Technology Development (Task 300); HTGR Recycle Demonstration Facility (HRDF) design support (Task 600).

Task 100, Program Management and Analysis, includes the functions of overall planning, scheduling, budgeting, reporting, management control of the program, and coordination of activities.

Task 200, Reprocessing Technology Development, includes the definition of flowsheets, the development of components, and the definition of operating techniques, remote maintenance and or disassembly techniques, and coordination of fuel shipping and storage activities. Operations which must be developed include crushing of the fuel elements; burning the graphite in a fluidized bed-burner; separation of the fertile and fissile

particles; crushing the SiC coating on fissile particles; burning the crushed particles; dissolution of thorium and uranium in the burned, crushed particles; separation of the undissolved solids (SiC hulls, etc.) from the leachate; separation of the thorium and uranium from the fission products by solvent extraction; separation and purification of the thorium and uranium by solvent extraction; process and facility off-gas treatments to ensure releases are environmentally acceptable and in compliance with regulations; and the primary treatment of solid, liquid, and gaseous wastes from the process.

Task 300, Refabrication Technology Development, includes the definition of flowsheets, the development of components, and the definition of operating techniques, remote maintenance and/or disassembly techniques, and coordination of fuel shipping and storage activities. The refabrication begins with aqueous uranyl nitrate solution from the reprocessing facility and ends with fuel elements prepared for shipment to the reactor. The principal operations to be developed are loading the ion-exchange resin with uranium, resin carbonization, resin conversion, coating the converted resin with pyrolytic carbon and SiC, fuel rod fabrication, fuel element assembly, fuel and fuel element inspection, scrap recovery, and waste handling.

Task 600, HTGR Recycle Demonstration Facility, includes the design, construction, proof-testing, and operation of a demonstration facility for the recycle of HTGR fuel. The plant is to include all fuel cycle operations from the receiving of spent fuel elements from the reactors to shipping the refabricated fuel elements back to the reactors. The preconceptual design studies and the early conceptual design are to be used to guide the development work for reprocessing and refabrication processes and equipment. The results of the research and development tasks will in turn be used to guide the detailed design of HRDF.

CONTENTS

FIGURES

FIGURES (Continued)

FIGURES (Continued)

FIGURES (Continued)

FIGURES (Continued)

TABLES

TABLES (Continued)

TABLES (Continued)

1. SUMMARY

General Atomic Thorium Utilization Program activities progressed during the quarter essentially on schedule except for the 48-hour run on the 0.20-m burner. The head-end reprocessing equipment testing continues.

During this reporting period, testing of the UNIFRAME as an integrated system (Phase II of Activity Plan AP521001) and crushing of ∿1950 kg of scrap graphite for primary burner feed were completed. Primary burner feed preparation is continuing in conjunction with readying the system for the Phase III tests with loaded fuel elements.

The Phase II tests revealed no significant operating problems with any of the equipment including the modified secondary crusher. Material balances were within the specification of <0.5% material-unaccounted-for (MUF). Material holdup was reasonable and with minor modifications, it can be reduced still further. Process times were well within the 15-min alloted time period. However, the screener and oversize crusher were operated for the full 15 min to reduce residual material on the screen surface.

Two runs were made on the 0.40-m primary burner. These runs were the initial combustion tests on the system and included in-bed fines recycle via the gas distributor cone vertex line. The results of the runs indicated that carryover of bed fuel particles and breakage of these particles in the fines recycle loop were similar to past 0.20-m burner work (4 to 6 wt % breakage of particles fed). In the 0.40-m burner system burnout of the carbon in tailburning the recycling fines was not as efficient as previously seen in 0.20-m burner work. The lack of above-bed O_2 injection in the 0.40-m burner was considered a major factor contributing to the inefficient fines tailburning. Installation of a burner penetration for the additional O_2 was therefore planned prior to further tests. The 0.40-m

primary burner design evaluation was completed, resulting in recommendations for testing of potential design improvements on the 0.20-m primary burner.

Four attempts to complete the 48-hour run on the 0.20-m burner were made in this reporting period. The initial run attempt was shut down soon after startup when the off-gas filter ΔP and the resultant system backpressure became excessive. A startup bed containing $\sim$4 wt % moisture had inadvertently been used in a shakedown run immediately prior to this initial run attempt, and the resultant condensation on the filters induced a buildup of fines cake which could not be blown off. Filter cleaning and replacement allowed operation of increased duration in the next three tests. However, feed controller inaccuracy caused feed rates slightly in excess of burn rates and ultimately resulted in fines accumulation which exceeded the fines hopper volume. In the final run attempt, the large volume of fines was being reduced by burning in an extended fines tailburning period. A relatively short fuel particle bed reaching only the lower portion of the induction heated zone of the wall became segregated in temperature from the fines burning zone just above the bed. Ignition of a poorly mixed bed carbon layer resting on top of the short, defluidized particle bed apparently combined with the induction heater power input to cause a high localized temperature which melted the wall (burnthrough). This required that the burner be shut down.

The vessel will be repaired in conjunction with planned upgrading modification of the fines recycle system. In addition, the capability for heating small beds will be improved and the operating procedures will be modified to exclude attempting re-ignition of beds below 650°C.

Four burner runs were made on the 0.20-m secondary burner to complete a parametric study of process variables. The last three runs were made in quick succession over a 17-hour period. Each test used 60,000 g of crushed FSV TRISO fertile fuel particles as feed. Acceptance criteria were fully met in each burner run. Overall system operability was excellent.

A design evaluation is in progress to examine possible modifications to upgrade 0.20-m secondary burner equipment design. Thirteen features are being evaluated against alternative designs, with a value analysis approach being used for ranking the existing design and alternate approaches.

The 0.10-m secondary burner was used to burn 12 kg of crushed FSV TRISO fissile fuel particles. This was the first time this type of particle had been processed in the reprocessing plant. Operations were quite smooth and trouble free and all acceptance criteria were met.

The design of the engineering-scale dissolver-centrifuge system is approximately 75% complete. Procurement of the major vessels (i.e., dissolver and repulp, product, and Thorex tanks) is under way. The continuous, vertical Sharples P-850 centrifuge is ready for final testing and inspection with delivery scheduled for June. The purchase of instrumentation and the modification of the General Atomic facility for the new system will be initiated during the next quarter.

Three solvent extraction feed adjustment runs (Runs 28, 29, and 30) were completed during the quarter. The purpose of these runs was to examine the use of formic acid to aid in the semicontinuous denitration of thorium solutions in the feed adjustment step. The solutions used for feed were representative of the leacher product solution. Several difficulties developed in the operation of the feed adjustment system during these runs. In particular, the capacity of the off-gas system was inadequate when formic acid was used to enhance denitration. These runs were useful in identifying modifications which were required to permit successful operation under conditions of significant evolution of gases.

Five solvent extraction runs were completed during the quarter. Three runs (Runs 61, 64, and 65) simulated a plutonium partition column in the first cycle of the HRDF Thorex flowsheet. The Robatel centrifugal contactor and the five pulsed columns in the solvent extraction pilot plant were used.

Several operating problems were encountered in the plutonium partition runs. The low flow rates of the scrub streams created most of the problems. The low flow rates caused difficulty in controlling the column interfaces. Thorium losses from the 1PU system exceeded desirable levels in each of the runs. Some ZrNb decontamination was obtained in the 1PU system. However, effective decontamination was reduced as thorium losses from the 1PU system were reduced.

Two solvent extraction runs (Runs 66 and 67) were used to test the efficiency of the Robetel centrifugal contactor for uranium extraction under a variety of conditions. No significant operating problems occurred in Runs 66 and 67. The operating stage efficiency of the contactor was near 100% for these runs. Typical lossed from the centrifugal contactor operation were less than calculated values.

Preliminary tests have been run on ruthenium and fluoride volatility from bench-scale feed adjustment operations. Fluoride volatility averaged about 1%. However, either ruthenium tracers or a more sensitive ruthenium analytical method will be required to quantitatively measure ruthenium volatility.

Progress with testing components and subsystems of the solids handling system continues. Installation and in-place testing of rotary feeder valves has continued with satisfactory results. Evaluation of different types of samplers has progressed. Three samplers have shown particularly encouraging results.

Further experimental data have been obtained for several of the transport systems. Data analyzed to date have shown close agreement between observation and prediction. The primary burner product removal system successfully transported burner product at an elevated temperature.

The conceptual design of an engineering-scale off-gas treatment system has begun. The system includes a CO/HT oxidizer, iodine adsorber,

SO_2 adsorber, tritium/moisture removal unit, radon holdup bed, CO_2 adsorber, and NO_x converter, as well as their support and auxiliary systems such as heaters, coolers, condensers/demisters, and generators for iodine vapor and humidity. An engineering-scale semivolatile fission product removal unit and/or an electrostatic precipitator will be added to the system later after the completion of the developmental work on this unit at Idaho National Engineering Laboratory (INEL). The last step of the gaseous effluent treatment, i.e., the separation of krypton from CO_2 using the KALC process, is being developed at Oak Ridge National Laboratory (ORNL) on an engineering scale.

The processes are to be monitored and controlled via various gas analyzers. Purchase orders for the gas analyzers and sampling system have been placed and the photoionization iodine detector and the gas chromatograph unit have already been received. Molecular sieve adsorbents and catalysts have also been ordered after a preliminary sizing of the adsorption beds and catalytic reactors.

Availability requirements for major dry head-end systems were calculated as a function of reliability and maintenance downtime. Similar calculations were initiated for major wet head-end systems. The HET conceptual design work was completed. HET technical review meetings were held during the quarter to discuss facility and equipment arrangement and design, Conceptual Design Report completion, cost estimating, and future program assignments.

During the quarter, the HETP radioactive feed material shipping equipment Conceptual Design Report, which details the design effort, was published. Related activities included development of detailed costs for use in conjunction with the HETP conceptual design cost estimate and identification of all system interfaces.

Draft copies of the head-end process and off-gas treatment system sections of a topical report covering the Reprocessing Flowsheet Review

and Material Balance Study were transmitted to ORNL for use in their commercialization study activity. HTGR spent fuel element impurities were compared with specifications for impurities in the feed to the resin-loading process in the Refabrication Plant of the HRDF, and required decontamination factors were estimated. A GASP IV simulation language package was purchased for comparison with the SIMSCRIPT language package as part of the reprocessing plant simulation study. Information was provided to ORNL, RAMCO, and cognizant GA personnel as part of HTGR commercialization studies.

Alternate fuel cycles were defined for HTGRs, GCFRs, and heavy water reactors (HWRs) as part of the nonproliferation study. Specification trees and functional flow diagrams for fabrication and reprocessing of alternate fuels were prepared. A brief assessment of the state of the art of various thorium fuel cycles was made to determine future development requirements.

2. FUEL ELEMENT CRUSHING

2.1. SUMMARY

During this reporting period, testing of the UNIFRAME as an integrated system (Phase II of Activity Plan AP521001) and crushing of ∿1950 kg of scrap graphite for primary burner feed were completed. Primary burner feed preparation is continuing in conjunction with readying the system for the Phase III tests with loaded fuel elements.

The Phase II tests revealed no significant operating problems with any of the equipment including the modified secondary crusher. Material balances were within the specification of <0.5% material-unaccounted-for (MUF). Material holdup was reasonable and with minor modifications, it can be reduced still further. Process times were well within the 15-min allotted time period. However, the screener and oversize crusher were operated for the full 15 min to reduce residual material on the screen surface.

The size distribution of crushed products from the various types and configurations of H-327 graphite elements indicated no significant differences. However, the crushed product from H-451 graphite elements displayed a tendancy to be somewhat coarser. The UNIFRAME products generally met the tentative acceptance limits for primary burner feed, but the lower ranges (i.e., coarsest products) extended beyond these limits.

Crushing of scrap graphite for primary burner feed was also used to obtain further operating and crushing experience with the UNIFRAME system. Equipment continued to perform satisfactorily except material preferentially discharged into the pneumatic transport system from the equipment item closest to the product collection hopper. This condition was corrected by intermittent operation of the oversize crusher. A discharge valve

has been installed for future tests as a second corrective measure. Screener blinding continued to slowly increase throughout the tests, indicating the eventual need for a maintenance plan or alternative to correct this undesirable condition.

2.2. UNIFRAME PHASE II SYSTEM TESTS

2.2.1. Introduction

The Phase II system tests as outlined in the Activity Plan for the UNIFRAME fuel element size reduction system (AP521001, Issue D, January 4, 1977) were undertaken to provide data and observations which demonstrated the degree to which the design objectives of the UNIFRAME as a system had been met. Previous tests (Phase I individual equipment tests) had separately demonstrated the capabilities of the major equipment items (Ref. 2-1).

2.2.2. Activity

2.2.2.1. Secondary Crusher Shakedown

During the Phase I tests of the secondary crusher, problems with material holdup were encountered which required modifications to the design of the stationary jaw and the pitman wear plate (Ref. 2-1). The effectiveness of these modifications in eliminating material holdup was observed during three shakedown tests (tests SM-1, -2, and -3) in which the primary, secondary, and tertiary crushers were operated as a system without the screener and oversize crusher.

Feed for these tests was partially drilled unfueled half-length (tests SM-1 and -2) and full-length (test SM-3) scrap H-327 graphite HTGR fuel elements. The crushed product from each test was collected separately as it discharged from the tertiary crusher for subsequent screen analysis. The entire product from each test was hand screened to determine the quantity of material which was larger than 6350 μm (1/4 in.) mesh size and the

quantity of the -6350, +4750 μm (-1/4, +3/16 in.) mesh size fraction. The remaining -4750 μm (-3/16 in.) mesh fraction, constituting the bulk of the material, was split in a 12 to 1 sample splitter to obtain a suitable size sample for determination of its size distribution.

Components of the ventilation enclosure at the primary and secondary crusher levels were not installed to permit observation of the crushing operations and timing of the completion of primary and secondary crushing.

No permanent material holdup was observed in any of the three shakedown tests. However, a temporary reduction in the crushing rate occurred in test SM-1 when two fragments rode up and down with the action of the pitman for a short time and then continued to crush to completion. No tendency for material holdup in the secondary crusher was observed. A summary of the three shakedown tests is given in Table 2-1. The product size distribution data, shown in Table 2-2, are used later as a comparison to estimate the change in the product size distribution effected by the screener and oversize crusher.

2.2.2.2. System Shakedown

The screener and oversize crusher were installed and two shakedown tests (tests SM-4 and -5) were performed to observe the operation of the UNIFRAME as a system.

Feed for these tests was a partially drilled (test SM-4) and a fully drilled (test SM-5) half-length H-327 graphite HTGR fuel element. The crushed products from the screener and oversize crusher were collected separately during each test.

Components of the ventilation enclosure at the primary and secondary crusher levels remained off to permit observation of the crushing operations and timing of the completion of primary and secondary crushing.

No permanent material holdup was observed in either shakedown test. However, a temporary reduction in the crushing rate occurred in test SM-4

TABLE 2-1
PHASE II UNIFRAME SYSTEM TESTS:
PRIMARY, SECONDARY, AND TERTIARY CRUSHER SHAKEDOWN[a]

Test No.	Feed Material	Crushing Completion Times		
		Primary	Secondary	Tertiary
SM-1	Half-length H-327 graphite HTGR fuel element without fuel holes, ∿62 kg	1 min 5 s	3 min 10 s	3 min 10 s
SM-2	Half-length H-327 graphite HTGR fuel element without fuel holes, ∿59 kg	1 min 30 s	2 min 50 s	2 min 50 s
SM-3	Full-length H-327 graphite HTGR fuel element, fully drilled in one-half and partial coolant holes only in the other half, ∿110 kg	11 min 5 s	19 min 48 s	19 min 48 s

[a] Primary crusher: Close side setting, 0.053 m (2.086 in.); nip angle 14°.
Secondary crusher: Close side setting, 0.0064 m (0.25 in.).
Tertiary crusher: gap, 0.0028 m (0.1088 in.).

TABLE 2-2
TERTIARY CRUSHER PRODUCT SIZE DISTRIBUTION; PRIMARY, SECONDARY, AND TERTIARY CRUSHER SHAKEDOWN; PHASE II UNIFRAME SYSTEM TESTS

Test No.	Weight Percent of Screened Fractions (Mesh Sizes in μm)									
	+4750	-4750 +4000	-4000 +2800	-2800 +2000	-2000 +1000	-1000 + 850	-850 +425	-425 +355	-355 +250	-250
SM-1	3.0	8.7	33.5	14.7	15.1	2.9	10.1	2.0	2.3	7.7
SM-2	3.2	10.4	35.9	15.0	13.6	2.9	7.6	1.6	2.1	7.7
SM-3	3.2	8.8	36.9	15.0	13.7	3.0	7.7	1.7	2.2	7.8
Mean	3.1	9.3	35.4	14.9	14.1	2.9	8.5	1.8	2.2	7.7
Range	0.2	1.7	3.4	0.3	1.5	0.1	2.5	0.4	0.2	0.1
Avg. dev. from mean	0.1	0.7	1.3	0.1	0.6	0	1.1	0.2	0.1	0

Test No.	Cumulative Weight Percent Less Than Stated Size (Mesh Sizes in μm)									
	+4750	-4750	-4000	-2800	-2000	-1000	-850	-425	-355	-250
SM-1	100.0	97.0	88.3	54.8	40.1	25.0	22.1	12.0	10.0	7.7
SM-2	100.0	96.8	86.4	50.5	35.5	21.9	19.0	11.4	9.8	7.7
SM-3	100.0	96.8	88.0	51.1	36.1	22.4	19.4	11.7	10.0	7.8
Mean	100.0	96.9	87.6	52.1	37.2	23.1	20.2	11.7	9.9	7.7
Range	0	0.2	1.9	4.3	4.6	3.1	3.1	0.6	0.2	0.1
Avg. dev. from mean	0	0.1	0.8	1.8	1.9	1.3	1.3	0.2	0.1	0

Test No.	Breakdown by Weight Percent of Larger Mesh Fractions (Mesh Size in μm)		
	-6350	-6350 +4750	-4750
SM-1	0.12	2.16	97.72
SM-2	0.14	1.98	97.88
SM-3	0.13	2.05	97.82

when two interlocked fragments in the secondary crusher formed a bridge which continued to be chipped and worn until crushing was completed. A temporary reduction in the crushing rate also occurred in test SM-5 because of a single fragment in the primary crusher which behaved in a similar fashion to the two fragments observed earlier in test SM-1.

Since the Phase I screener tests had demonstrated that optimum motion generator settings resulted in some residual material on the screen surface (Ref. 2-1), the screener and oversize crusher were restarted and operated for an additional 10 min after original shutdown in test SM-4. A summary of the results is given in Table 2-3. The small quantity of material which discharged during the additional 10-min screening period (i.e., 0.68% of the total product) demonstrated that a total screening time of 15 min should be sufficient to reduce the residual material on the screen surface to equilibrium. Therefore, the screener and oversize crusher were operated a total of 15 min from commencement of crushing for test SM-5 and all subsequent tests. The result also indicated that the majority of screening was essentially complete shortly after completion of crushing.

A summary of the two system shakedown tests is given in Table 2-4.

2.2.2.3. Phase II System Tests

The objectives of the UNIFRAME system were defined in Design Criteria DC521001, and the system was designed to meet a majority of these objectives within the constraints of the initial budget and schedule. The Activity Plan outlined the test program which was devised to provide sufficient data and observations to demonstrate the degree to which the design objectives had been met. The major obectives of Phase II of the test program outlined in the Activity Plan are summarized as follows:

1. To observe and compare the system operation, crushing behavior, throughput rates, and product characteristics with each available type of fuel element.

TABLE 2-3
PHASE II UNIFRAME SYSTEM SHAKEDOWN, TEST SM-4

Product Distribution After 7-Min Screening Time		
Screener product	48.625 kg	85.76%
Oversize crusher product	7.691 kg	13.56%
Total	56.316 kg	99.32%
Product Distribution After 10-Min Additional Screening Time		
Screener product	0.168 kg	0.30%
Oversize discharge	0.215 kg	0.38%
Total	0.383 kg	0.68%
Total recovery	56.699 kg	100.00%

TABLE 2-4
PHASE II UNIFRAME SYSTEM SHAKEDOWN TESTS SM-4 AND SM-5[a]

Test No.	Feed Material	Crushing Completion Times	
		Primary	Secondary
SM-4	Half-length H-327 graphite HTGR fuel element without fuel holes, ∿57.3 kg	38 s	2 min 45 s[b]
SM-5	Half-length H-327 graphite HTGR fuel element, ∿42.8 kg	1 min 40 s	1 min 45 s

[a] Primary crusher: close side setting, 0.053 m (2.086 in.); nip angle, 14°.
Secondary crusher: close side setting, 0.0064 m (0.25 in.)
Tertiary crusher: gap, 0.0028 m (0.1088 in.)
Screener: motion generator, one bottom weight, 70° lead angle
Oversize crusher: gaps, 0.0016 m (0.0625 in.)

[b] All except two fragments which were crushed in 5 min 27 s.

2. To observe the system material flow and containment concepts.

The following unfueled feed materials were used in the Phase II tests:

1. Half-length H-327 graphite fuel elements (tests UE-46, -47, and -48).

2. Half-length H-327 graphite control rod elements (test UE-49).

3. Full-length H-327 graphite fuel elements (tests UE-52, -52B, -53, and -54.

4. Full-length H-451 graphite fuel elements (test UE-55).

To determine the reproducibility of the tests and the range of experimental data, three identical tests were planned for each type of feed material. Unfortunately, only single tests were possible with the control rod and H-451 graphite elements because of the limited supply of these feed materials.

One of the tests (UE-52) was repeated (UE-52B) because the system was shut down during the operation by an accidental tripping of the main switch. Crushing had begun when the accidental shutdown occurred. All components except the primary crusher restarted easily under the partially loaded condition. Due to belt slippage, it was necessary to remove all material from the primary crushing cavity and recharge it after the crusher was in operation. Because of the potential effects of this abnormal operation on product size distribution, screening efficiency, and throughput, the test was repeated to obtain data which were produced under conditions more similar to the other tests.

For observation of the primary and secondary crushing completion times, components of the ventilation enclosure in these areas remained off as during the shakedown testing. For observation of the tertiary crushing

completion times and the screener operation, a plexiglass viewport was installed in the ventilation shroud between the tertiary crusher and the screener.

The screener and oversize crusher were operated for 15 min after crushing had commenced to reduce the quantity of holdup on the screener table to an equilibrium value at the end of each test. All other components were shut down shortly after crushing was complete.

Crushed products which discharged from the screener and oversize crusher were collected separately during each test for subsequent size distribution determinations. Cleanout of the system to determine dust and material holdup was effected at the completion of all tests.

2.2.2.3.1. Equipment Operation and Test Observations. Other than the inadvertent system shutdown during test UE-52, no problems occurred with the operation of any of the UNIFRAME equipment in any of the tests.

Pertubations in the crushing rates occurred in three tests, but none resulted in cessation of crushing or permanent material holdup in any of the crushing cavities. Several graphite fragments formed a temporary bridge in the secondary crusher during test UE-53. This bridge was similar to the one observed earlier in shakedown test SM-4. In test UE-53 a single long fragment in the primary crusher was temporarily prevented from discharging into the secondary crushing cavity by the level of material in the secondary crusher. This level normally occurred in all tests because of the difference in crushing rates between the primary and secondary crusher. As the level in the secondary crusher was reduced by crushing, the fragment discharged normally. In test UE-55 a single fragment in the primary crusher temporarily rode up and down with the action of the pitman (similar to the occurrences observed in shakedown tests SM-1 and SM-5) and a temporary bridge occurred in the secondary crusher.

2.2.2.3.2. Material Balances and Material Holdup Areas. To establish material balances for each test individually, the feed materials were weighed prior to charging and the crushed products which collected separately from the screener and oversize crusher were weighed at the end of each test. At the conclusion of Phase II testing, the system was inspected and material and dust which were held up on the various components were removed and weighed to establish the total material unaccounted for (MUF). Since the system was not cleaned out after the two system shakedown tests (SM-4 and -5), the material holdup represented accumulations during a throughput which included these two tests. The results of the material balances and material accountability including identification of material holdup areas are given in Table 2-5.

Material unaccounted for in individual tests ranged from a low of 0.05 wt % to a high of 3.39 wt % of the charges. A summation of the total throughput and material recovered for all tests yielded a MUF of 0.45 wt % of the total throughput. Recovery during system cleanout was 0.26 wt % of the throughput, resulting in a final MUF of 0.19 wt % of the throughput.

No measurable material holdup was found in the primary, secondary, or tertiary crushing areas. However, as expected at the motion generator settings used, holdup did occur on the screener table (729 g or 0.10% of throughput) as was previously observed (Ref. 2-1). Within the screener housing, on the spring supports, on the slide gate valve internal mechanisms, and on the sloping surface of the ventilation shroud between the tertiary crusher and the screener, 640 g of dust (0.09% of throughput) was recovered. An additional 472 g (0.07% of the throughput) was recovered from the areas behind the two wear plates of the oversize crusher. This was also expected because of observations during Phase I individual testing of the oversize crusher (see Ref. 2-1). No other areas of material holdup were discovered.

Screen blinding of 0.9% at the end of the tests was less than expected from previous screener tests and indicated that the self-cleaning device

TABLE 2-5
MATERIAL BALANCE, UNIFRAME SYSTEM TESTS,
CONTINUOUS RUN BALANCE[a]

Test No.	Charge (kg)	Recovery (kg)	Gain (+) or Loss (-)	MUF (% of Charge)
SM-4	57.300	56.699	(-) 0.601	1.05
SM-5	42.800	42.833	(+) 0.083	0.19
UE-46	43.500	43.523	(+) 0.023	0.05
UE-47	45.000	45.585	(+) 0.585	1.30
UE-48	45.100	46.628	(+) 1.528	3.39
UE-49	43.800	43.314	(-) 0.486	1.11
UE-52	86.450	86.250	(-) 0.200	0.23
UE-52B	90.200	87.662	(-) 2.538	2.81
UE-53	86.750	86.434	(-) 0.316	0.36
UE-54	89.250	89.102	(-) 0.148	0.17
UE-55	90.500	89.408	(-) 1.092	1.21
Total	720.650	717.438	(-) 3.212	0.45

Cleanout At Conclusion of Testing

Description	Quantity (kg)	% of Charge
Holdup on screener table	0.729	0.10
Dust in screener housing	0.640	0.09
Dust in oversize crusher housing	0.472	0.07
Total	1.841	0.26

Grand Totals

Tests	Charge (kg)	Recovery (kg)	Gain (+) or Loss (-)	MUF (% of Charge)
S4-4, -5; UE-46, -47, -48, -49, -52, -52B, -53, -54, -55	720.650	719.279	(-) 1.371	0.19

[a] Screener blinded holes = 103 = 0.9%.

was successful in reducing blinding buildup with significantly large quantities of throughput.

2.2.2.3.3. Crushing Rates. Primary and secondary crushing times for the various types of fuel elements used in the Phase II tests are given in Table 2-6. Pertubations in the crushing rates as described in Section 3.2 were disregarded in the table to obtain typical rates for comparison with the rates for other types of elements. In no instance did these temporary crushing rate reductions result in a total system throughput time exceeding 15 min, including the test (UE-55) in which both primary and secondary crushing rate reductions occurred.

No significant lag between completion of the secondary and tertiary crushing could be detected and observations of the screener indicated that screening was essentially complete at that time also, except, of course, for the reduction of the normal holdup to equilibrium. Therefore, the secondary crushing completion times can be regarded as an approximation of the total system processing times.

Significant differences noted in the crushing times, from Table 2-6, are:

1. Secondary crushing times (i.e., approximate process times) were less for the half-length fuel elements than for the half-length control rod elements, possibly indicating the effect of the previously observed (Ref. 2-1) larger control rod primary crusher product on the secondary crushing rate and therefore the total process time.

2. As expected, the process times for full-length fuel elements were approximately twice those for half-length fuel elements.

3. The primary crushing and the process time for H-451 graphite was greater than for comparable size elements of H-357 graphite, indicating a difference in the crushing behavior of these types of graphite.

TABLE 2-6
CRUSHING TIMES, PHASE II UNIFRAME SYSTEM TESTS

Test No.	Crushing Time (s)	
	Primary	Secondary
Half-Length H-327 Fuel Elements		
UE-46	35	92
UE-47	55	95
UE-48	40	90
Mean	43	92
Range	20	5
Half-Length H-327 Control Rod Element		
UE-49	29	177
Full-Length H-327 Fuel Elements		
UE-52B	34	180[a]
UE-53	30[b]	205
UE-54	33	180
Mean	32	188
Range	4	25
Full-Length H-451 Fuel Element		
UE-55	75[c]	280[d]

[a] All except a minor quantity that formed a temporary bridge which crushed in 420 s.

[b] All except one long fragment which could not discharge into secondary burner due to material level.

[c] All except one piece which crushed in 210 s.

[d] Temporary bridge as in (a) which crushed in 440 s.

2.2.2.3.4. Product Distribution - Screener and Oversize Crusher. The quantities of material discharged from the screener and oversize crusher relative to the total products were studied to obtain an indication of the screening efficiencies. The product distribution for the various types of fuel elements used in the Phase II tests is given in Table 2-7. Significant differences noted from Table 2-7 are:

1. The quantity of oversize crusher product relative to the total product was slightly lower from crushing the half-length control rod element (8.82%) than it was for any of the half-length fuel elements (10.35% minimum). Similar results had been obtained with these types of elements in the Phase I screener tests, but were more pronounced [i.e., 3.7% and 13.4% (Ref. 2-1)]. Since the process times were longer for control rod elements in both phases of testing, the difference is attributed to improved screener efficiency from the lower throughput rates.

2. The quantity of oversize crusher product was also lower for H-451 graphite (13.43%) than for any H-357 graphite elements of comparable size (16.59% minimum). Again the difference is attributable to the processing time effect on screener efficiency.

3. The ranges of results for half- and full-length fuel elements overlapped sufficiently to indicate little difference in their screening efficiencies. The longer process times for the full-size elements resulted in similar throughput rates and screening efficiencies (see Section 3.4).

2.2.2.3.5. Product Size Distribution. Screen analyses were performed separately on products discharged from the screener and oversize crusher for each of the Phase II tests. Suitable size samples for analysis were obtained by reducing each product in a 12 to 1 sample splitter. From the screening results the weight percent of material in each of the screener fractions and the cumulative weight percent less than each mesh size were

TABLE 2-7
PRODUCT DISTRIBUTIONS, PHASE II UNIFRAME SYSTEM TESTS

Test No.	Oversize Crusher Product		Screener Product	
	kg	% of Total Product	kg	% of Total Product
Half-Length Standard H-327 Unfueled Graphite Fuel Elements				
UE-46	7.572	17.40	35.951	82.60
UE-47	7.697	16.88	37.888	83.12
UE-48	4.826	10.35	41.802	89.65
Mean	6.698	14.88	38.547	85.12
Range	2.871	7.05	5.851	7.05
Half-Length H-327 Unfueled Graphite Control Rod Element				
UE-49	3.819	8.82	39.495	91.18
Full-Length H-327 Unfueled Graphite Fuel Elements				
UE-52B	14.546	16.59	73.116	83.41
UE-53	14.839	17.17	71.595	82.83
UE-54	15.302	17.17	73.800	82.83
Mean	14.896	16.98	72.837	83.02
Range	0.756	0.58	2.205	0.58
Full-Length H-451 Unfueled Graphite Fuel Elements				
UE-55	12.008	13.43	77.400	86.57
Summary of All Tests				
Mean	--	14.73	--	85.27
Range	--	8.58	--	8.58

determined. To obtain an estimate of the combined screener and oversize crusher product size distributions, (i.e., system total product) composites were calculated using the screen analysis and relative proportions of the two products to the total products as shown in Table 2-7. To provide a comparison of the UNIFRAME products with the estimated primary burner feed size distribution requirements, the size distributions of the composites were recalculated assuming the material contained 17 wt % -850 μm fuel particles. The means, ranges, and average deviations from the mean were calculated for those types of fuel elements (i.e., half- and full-length H-357 graphite) on which replicate tests were made and the means and ranges were calculated for the results of all the Phase II tests. To obtain an estimate of the deviations caused by errors in the screen analysis, replicate analyses were performed on the products from test UE-48. These analyses and the earlier analyses of tertiary crusher products from the shakedown tests (SM-1, -2, and -3) provided the following information:

1. Comparison of the screener product size distributions produced by crushing various types of fuel elements.

2. Comparison of the oversize crusher product size distributions produced by crushing various types of fuel elements.

3. Comparison of the composite product size distributions produced by crushing various types of fuel elements and determination of the effect of oversize crushing on reducing the differences between the products.

4. Comparison of the expected UNIFRAME products with estimated primary burner feed size distribution requirements.

5. Estimations of the ranges and averages of results expected from crushing various types of fuel elements.

6. Estimations of the experimental errors induced by variabilities in the screen analysis.

7. Estimations of the changes in tertiary crusher product effected by screening and oversize crushing.

Comparison of Screener Product Size Distribution. Screener product size distributions obtained from crushing the various types of fuel elements are shown in Table 2-8. A graphical comparison of these results is given in Fig. 2-1. An estimate of the error introduced by the screen analysis is obtained from the replicate analysis shown in Table 2-9. Significant differences shown by these data are:

1. The screener product from crushing the half-length control rod elements differed significantly from the products of half-length fuel elements in only the -4750, +4000 μm mesh fraction. In this fraction the quantity was greater in the control rod product (12.5%) than in any of the fuel element products (10.4% maximum).

2. The screener product from crushing a full-length H-451 graphite fuel element differed significantly from the products of full-length H-357 graphite fuel elements as follows:

   a. The quantity of +4750 and -4750, +4000 μm mesh material was greater in the H-451 graphite product than in any of the H-357 graphite products (3.6% versus 0.9% maximum and 13.1% versus 8.6% maximum, respectively).

   b. The quantity of -2800, +2000 μm mesh material was less in the H-451 graphite product (13.6%) than in any of the H-357 graphite products (15.7% minimum).

   c. The ranges of values for all mesh fractions overlapped sufficiently between the half- and full-size H-357 graphite

TABLE 2-8
SCREENER PRODUCT SIZE DISTRIBUTION, PHASE II,
WEIGHT PERCENT OF SCREENED FRACTIONS

Test No.	Weight Percent of Screened Fractions (Mesh Sizes in μm)									
	+4750	-4750 +4000	-4000 +2800	-2800 +2000	-2000 +1000	-1000 + 850	-850 +425	-425 +355	-355 +250	-250
Half-Length Standard H-327 Unfueled Graphite Fuel Elements										
UE-46	0.2	10.0	39.9	14.0	14.0	2.0	8.0	2.0	2.0	8.0
UE-47	0.8	10.4	41.5	14.3	13.7	2.1	7.3	1.5	1.9	6.5
UE-48	0.5	9.0	44.0	16.7	14.1	1.9	6.4	1.2	1.5	4.7
Mean	0.5	9.8	41.8	15.0	13.9	2.0	7.2	1.6	1.8	6.4
Range	0.6	1.4	4.1	2.7	0.4	0.2	1.6	0.8	0.5	3.3
Avg. dev. from mean	0.2	0.5	1.5	1.1	0.2	0.1	0.6	0.3	0.2	1.1
Half-Length H-327 Unfueled Graphite Control Rod Element										
UE-49	0.8	12.5	41.6	16.0	13.5	2.0	5.9	1.1	1.6	5.0
Full-Length Standard H-327 Unfueled Graphite Fuel Elements										
UE-52B	0.4	8.5	42.1	15.7	13.7	2.1	7.1	1.4	2.0	7.0
UE-53	0.9	8.6	38.9	16.8	16.5	2.5	7.2	1.3	1.5	5.8
UE-54	0.4	6.9	43.2	17.4	14.6	1.9	6.8	1.3	1.6	5.9
Mean	0.6	8.0	41.4	16.6	14.9	2.2	7.0	1.3	1.7	6.2
Range	0.5	1.7	4.3	1.7	2.8	0.6	0.4	0.1	0.5	1.2
Avg. dev. from mean	0.2	0.7	1.7	0.6	1.0	0.3	0.2	0	0.2	0.5
Full-Length Standard H-451 Unfueled Graphite Fuel Element										
UE-55	3.6	13.1	38.3	13.6	14.5	2.0	6.8	1.2	1.6	5.3
Summary of All Tests										
Mean	1.0	9.9	41.2	15.6	14.3	2.1	6.9	1.4	1.7	6.0
Range	3.4	6.2	5.7	3.8	3.0	0.6	2.1	0.9	0.5	3.3

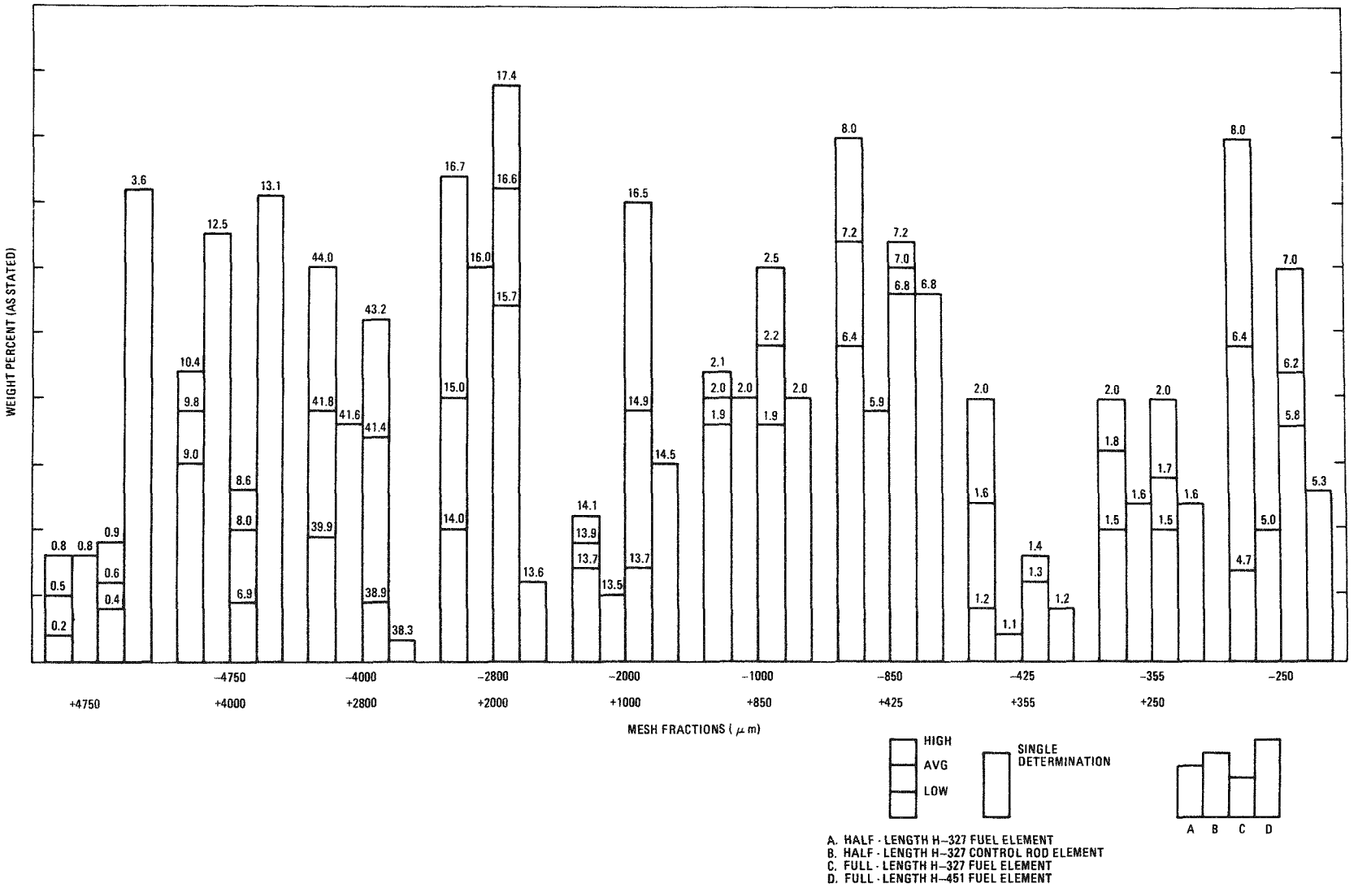

Fig. 2-1. Screener product comparison for Phase II UNIFRAME system tests, weight percent as stated

TABLE 2-9
REPLICATE SCREEN ANALYSIS OF SCREENER PRODUCT FROM TEST UE-48, PHASE II

Sample No.	Weight Percent of Screened Fractions (Mesh Sizes in μm)									
	+4750	-4750 +4000	-4000 +2800	-2800 +2000	-2000 +1000	-1000 + 850	-850 +425	-425 +355	-355 +250	-250
Half-Length Standard H-327 Unfueled Graphite Fuel Element										
1	0.5	9.1	43.6	16.8	14.0	2.1	6.4	1.2	1.6	4.7
2	0.5	8.8	44.7	16.4	13.9	1.9	6.3	1.2	1.5	4.8
3	0.5	9.2	43.8	16.9	14.3	1.8	6.4	1.1	1.5	4.5
Mean	0.5	9.0	44.0	16.7	14.1	1.9	6.4	1.2	1.5	4.7
Range	0	0.4	1.1	0.5	0.4	0.3	0.1	0.1	0.1	0.3
Avg. dev. from mean	0	0.2	0.4	0.2	0.2	0.1	0	0	0	0.1

Sample No.	Cumulative Weight Percent Less Than Stated Size (Mesh Sizes in μm)								
	+4750	-4750	-4000	-2800	-2000	-1000	- 850	-425	-355	-250
Half-Length Standard H-327 Unfueled Graphite Fuel Element										
1	100.0	99.5	90.4	46.8	30.0	16.0	13.9	7.5	6.3	4.7
2	100.0	99.5	90.7	46.0	29.6	15.7	13.8	7.5	6.3	4.8
3	100.0	99.5	90.3	46.5	29.6	15.3	13.5	7.1	6.0	4.5
Mean	100.0	99.5	90.5	46.4	29.7	15.7	13.7	7.4	6.2	4.7
Range	0	0	0.4	0.8	0.4	0.7	0.4	0.4	0.3	0.3
Avg. dev. from mean	0	0	0.2	0.3	0.2	0.2	0.2	0.2	0.1	0.1

fuel element screener products to indicate no difference in these products.

The cumulative weight percents of materials less than each stated size are given in Table 2-10 for the screener products. A graphical comparison of these results is given in Fig. 2-2. An estimate of the error introduced by the screen analysis is obtained from the replicate analyses shown in Table 2-9. Significant differences shown by these data are:

1. The total quantity of material smaller than 4000 μm mesh size was significantly less in the screener product from crushing half-length control rod elements (86.7%) than in any of the half-length fuel element products (88.0% minimum). No other significant differences were noted.

2. The total quantity of material smaller than each mesh size from 4750 μm and below was generally less in the screener product from crushing full length H-451 graphite fuel elements than in any of the full length H-357 graphite fuel element products. However, considering errors introduced by screen analysis (Table 2-9), there were only three differences which were significant: the -4750, -4000, and -2800 μm values (96.4% versus 99.1% minimum, 83.3% versus 90.5% minimum, and 45.0% versus 49.0% minimum, respectively).

3. The ranges of values for all cumulative weight percents overlapped sufficiently between half- and full-size H-327 graphite fuel element screener products to indicate no significant differences in these products.

Comparison of Oversize Crusher Product Size Distributions. Oversize crusher product size distributions obtained from crushing the various types of fuel elements are shown in Table 2-11. A graphical comparison of these results is given in Fig. 2-3. An estimate of the error introduced by the

TABLE 2-10
SCREENER PRODUCT SIZE DISTRIBUTION, PHASE II,
CUMULATIVE WEIGHT PERCENT LESS THAN STATED SIZE

Test No.	Cumulative Weight Percent Less Than Stated Size (Mesh Sizes in μm)									
	+4750	-4750	-4000	-2800	-2000	-1000	-850	-425	-355	-250
Half-Length Standard H-327 Unfueled Graphite Fuel Elements										
UE-46	100.0	99.9	89.9	50.0	36.0	22.0	20.0	12.0	10.0	8.0
UE-47	100.0	99.2	88.0	47.3	33.0	19.3	17.2	9.9	8.4	6.5
UE-48	100.0	99.5	90.5	46.4	29.7	15.7	13.7	7.4	6.2	4.7
Mean	100.0	99.5	89.5	47.9	32.9	19.0	17.0	9.8	8.2	6.4
Range	0	0.7	2.5	3.6	6.3	6.3	6.3	4.6	3.8	3.3
Avg. dev. from mean	0	0.2	1.0	1.4	2.1	2.2	2.2	1.6	1.3	1.1
Half-Length H-327 Unfueled Graphite Control Rod Element										
UE-49	100.0	99.2	86.7	45.1	29.1	15.6	13.6	7.7	6.6	5.0
Full-Length Standard H-327 Unfueled Graphite Fuel Elements										
UE-52B	100.0	99.6	91.1	49.0	33.3	19.6	17.5	10.4	9.0	7.0
UE-53	100.0	99.1	90.5	51.6	34.8	18.3	15.8	8.6	7.3	5.8
UE-54	100.0	99.6	92.7	49.5	32.1	17.5	15.6	8.8	7.5	5.9
Mean	100.0	99.4	91.4	50.0	33.4	18.5	16.3	9.3	7.9	6.2
Range	0	0.5	2.2	2.6	2.7	2.1	1.9	1.8	1.7	1.2
Avg. dev. from mean	0	0.2	0.8	1.0	0.9	0.8	0.8	0.8	0.7	0.6
Full-Length Standard H-451 Unfueled Graphite Fuel Element										
UE-55	100.0	96.4	83.3	45.0	31.4	16.9	14.9	8.1	6.9	5.3
Summary of All Tests										
Mean	100.0	99.1	89.1	48.0	32.4	18.1	16.0	9.1	7.7	6.0
Range	0	3.5	9.4	6.6	6.9	6.4	6.4	4.6	3.8	3.3

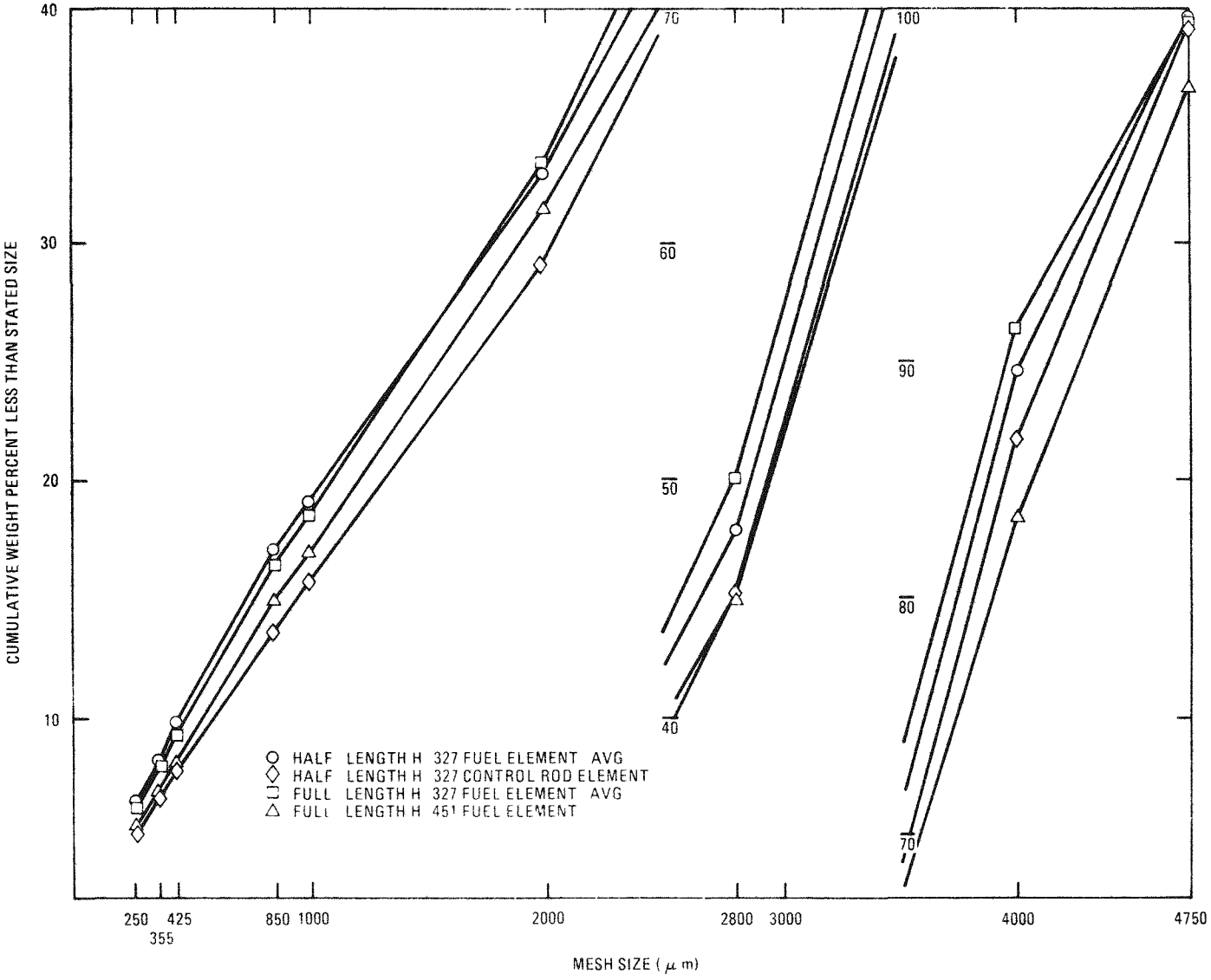

Fig. 2-2. Screener product comparison for Phase II UNIFRAME system tests, cumulative weight percent less than stated size

TABLE 2-11
OVERSIZE CRUSHER PRODUCT SIZE DISTRIBUTION, PHASE II,
WEIGHT PERCENT OF SCREENED FRACTIONS

Test No.	Weight Percent of Screened Fractions (Mesh Sizes in μm)									
	+4750	-4750 +4000	-4000 +2800	-2800 +2000	-2000 +1000	-1000 + 850	-850 +425	-425 +355	-355 +250	-250
Half-Length Standard H-327 Unfueled Graphite Fuel Elements										
UE-46	5.6	15.1	21.9	17.3	24.5	2.6	6.6	0.8	1.0	4.6
UE-47	12.3	19.9	23.0	11.6	15.5	2.1	5.9	1.0	1.3	7.4
UE-48	18.0	26.3	21.3	9.5	11.4	1.7	4.5	0.7	1.0	5.7
Mean	12.0	20.4	22.1	12.8	17.1	2.1	5.7	0.8	1.1	5.9
Range	12.4	11.2	1.7	7.8	13.1	0.9	2.1	0.3	0.3	2.8
Avg. dev. from mean	4.2	3.9	0.6	3.0	4.9	0.3	0.8	0.1	0.1	0.1
Half-Length H-327 Unfueled Graphite Control Rod Element										
UE-49	16.9	18.4	16.5	10.9	15.2	2.7	7.3	1.2	1.7	9.2
Full-Length Standard H-327 Unfueled Graphite Fuel Elements										
UE-52B	9.6	15.4	24.3	16.4	17.9	2.1	5.9	1.0	1.3	6.1
UE-53	5.7	12.0	21.4	17.3	21.6	2.6	7.9	1.4	1.9	8.2
UE-54	6.7	17.5	25.2	17.7	19.6	2.1	5.1	0.8	1.1	4.2
Mean	7.3	15.0	23.6	17.1	19.7	2.3	6.3	1.1	1.4	6.2
Range	3.9	5.5	3.8	1.3	3.7	0.5	2.8	0.6	0.8	4.0
Avg. dev. from mean	1.5	2.0	1.5	0.5	1.3	0.2	1.1	0.2	0.3	1.4
Full-Length Standard H-451 Unfueled Graphite Fuel Element										
UE-55	9.3	16.3	21.2	14.6	23.0	2.4	6.2	0.9	1.1	5.0
Summary of All Tests										
Mean	10.5	17.6	21.8	14.4	18.6	2.3	6.2	1.0	1.3	6.3
Range	12.4	14.3	8.7	8.2	13.1	1.0	3.4	0.7	0.9	4.6

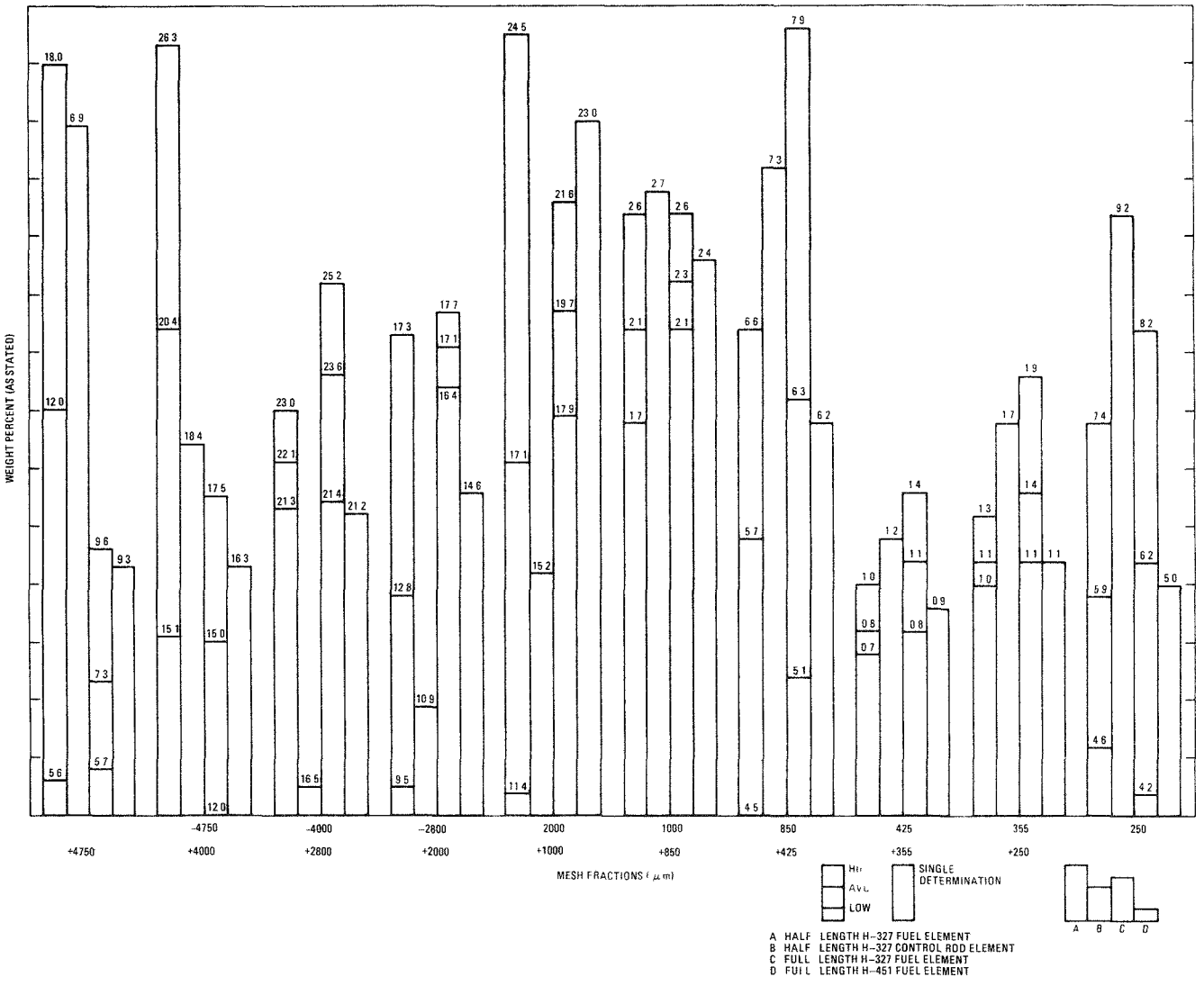

Fig. 2-3. Oversize crusher product comparison for Phase II UNIFRAME system tests, weight percent as stated

screen analysis is obtained from the replicate analyses shown in Table 2-12. The cumulative weight percents of materials less than each stated size are given in Table 2-13 and a graphical comparison of these results is given in Fig. 2-4. Significant differences shown by these data are:

1. The oversize crusher product from crushing half-length control rod elements differed significantly from the products of half-length fuel elements in only the -4000, +2800 μm mesh fraction. In this fraction the quantity was less in the control rod product (16.5%) than in any of the fuel element products (21.3% minimum).

2. The oversize crusher product from crushing full-length H-451 graphite fuel elements differed significantly from the products of full-length H-357 graphite fuel elements as follows:

   a. The quantity of -2800, +2000 μm mesh material was less in the H-451 graphite product (14.6%) than in any of the H-357 graphite products (16.4% minimum).

   b. The quantity of -2000, +1000 μm mesh material was greater in the H-451 graphite product (23.0%) than in any of the H-357 graphite products (21.6% maximum).

   c. The ranges of values for all mesh fractions overlapped sufficiently between the half- and full-size H-357 graphite fuel element oversize crusher products to indicate no difference in these products.

Comparison of Composite Screener and Oversize Crusher Product Size Distributions. The total system's product size distribution was estimated by combining the percentages of each size fraction of the screener and the oversize crusher products (from Tables 2-8 and 2-11) in proportion to the quantity found in the total product (Table 2-7). The resulting composites are shown in Table 2-14. A graphical comparison of thse results is given

TABLE 2-12
REPLICATE SCREEN ANALYSIS OF OVERSIZE CRUSHER PRODUCT FROM TEST UE-48, PHASE II

Sample No.	Weight Percent of Screened Fractions (Mesh Sizes in μm)									
	+4750	-4750 +4000	-4000 +2800	-2800 +2000	-2000 +1000	-1000 + 850	-850 +425	-425 +355	-355 +250	-250
Half-Length Standard H-327 Unfueled Graphite Fuel Element										
1	17.3	25.7	21.1	9.4	11.5	1.7	5.0	0.8	1.1	6.4
2	18.6	26.6	21.4	9.4	11.3	1.7	4.1	0.7	0.9	5.3
3	18.3	26.6	21.4	9.6	11.3	1.6	4.3	0.7	0.9	5.3
Mean	18.1	26.3	21.3	9.5	11.4	1.7	4.5	0.7	1.0	5.7
Range	1.3	0.9	0.3	0.2	0.2	0.1	0.9	0.1	0.2	1.1
Avg. dev. from mean	0.5	0.4	0.1	0.1	0.1	0	0.4	0	0.1	0.5

Sample No.	Cumulative Weight Percent Less Than Stated Size (Mesh Sizes in μm)									
	+4750	-4750	-4000	-2800	-2000	-1000	-850	-425	-355	-250
Half-Length Standard H-327 Unfueled Graphite Fuel Element										
1	100.0	82.7	57.0	35.9	26.5	15.0	13.3	8.3	7.5	6.4
2	100.0	81.4	54.8	33.4	24.0	12.7	11.0	6.9	6.2	5.3
3	100.0	81.7	55.1	33.7	24.1	12.8	11.2	6.9	6.2	5.3
Mean	100.0	81.9	55.6	34.3	24.9	13.5	11.8	7.4	6.6	5.7
Range	0	1.3	2.2	2.5	2.5	2.3	2.3	1.4	1.3	1.1
Avg. dev. from mean	0	0.5	0.9	1.0	1.1	1.0	1.0	0.6	0.6	0.5

TABLE 2-13
OVERSIZE CRUSHER PRODUCT SIZE DISTRIBUTION, PHASE II,
CUMULATIVE WEIGHT PERCENT LESS THAN STATED SIZE

Test No.	Cumulative Weight Percent Less Than Stated Size (Mesh Sizes in μm)									
	+4750	-4750	-4000	-2800	-2000	-1000	-850	-425	-355	-250
Half-Length Standard H-327 Unfueled Graphite Fuel Elements										
UE-46	100.0	94.4	79.3	57.4	40.1	15.6	13.0	6.4	5.6	4.6
UE-47	100.0	87.7	67.8	44.8	33.2	17.7	15.6	9.7	8.7	7.4
UE-48	100.0	81.9	55.6	34.3	24.9	13.5	11.8	7.4	6.6	5.7
Mean	100.0	88.0	67.6	45.5	32.7	15.6	13.5	7.8	7.0	5.9
Range	0	12.5	23.7	23.1	15.2	4.2	3.8	3.3	3.1	2.8
Avg. dev. from mean	0	4.3	8.0	7.9	5.2	1.4	1.4	1.2	1.2	1.0
Half-Length H-327 Unfueled Graphite Control Rod Element										
UE-49	100.0	85.6	66.6	49.6	38.3	22.6	19.8	12.3	11.1	9.5
Full-Length Standard H-327 Unfueled Graphite Fuel Elements										
UE-52B	100.0	90.4	75.0	50.7	34.3	16.4	14.3	8.4	7.4	6.1
UE-53	100.0	94.3	82.3	60.9	43.6	22.0	19.4	11.5	10.1	8.2
UE-54	100.0	93.3	75.8	50.6	32.9	13.3	11.2	6.1	5.3	4.2
Mean	100.0	92.7	77.7	54.1	36.9	17.2	15.0	8.7	7.6	6.2
Range	0	3.9	7.3	10.3	10.7	8.7	8.2	5.4	4.8	4.0
Avg. dev. from mean	0	1.5	3.1	4.6	4.4	3.2	3.0	1.9	1.7	1.4
Full-Length Standard H-451 Unfueled Graphite Fuel Element										
UE-55	100.0	90.7	74.4	53.2	38.6	15.6	13.2	7.0	6.1	5.0
Summary of All Tests										
Mean	100.0	89.8	72.1	50.2	35.7	17.1	14.8	8.6	7.6	6.3
Range	0	12.5	26.7	26.6	18.7	9.3	8.6	6.2	5.8	5.3

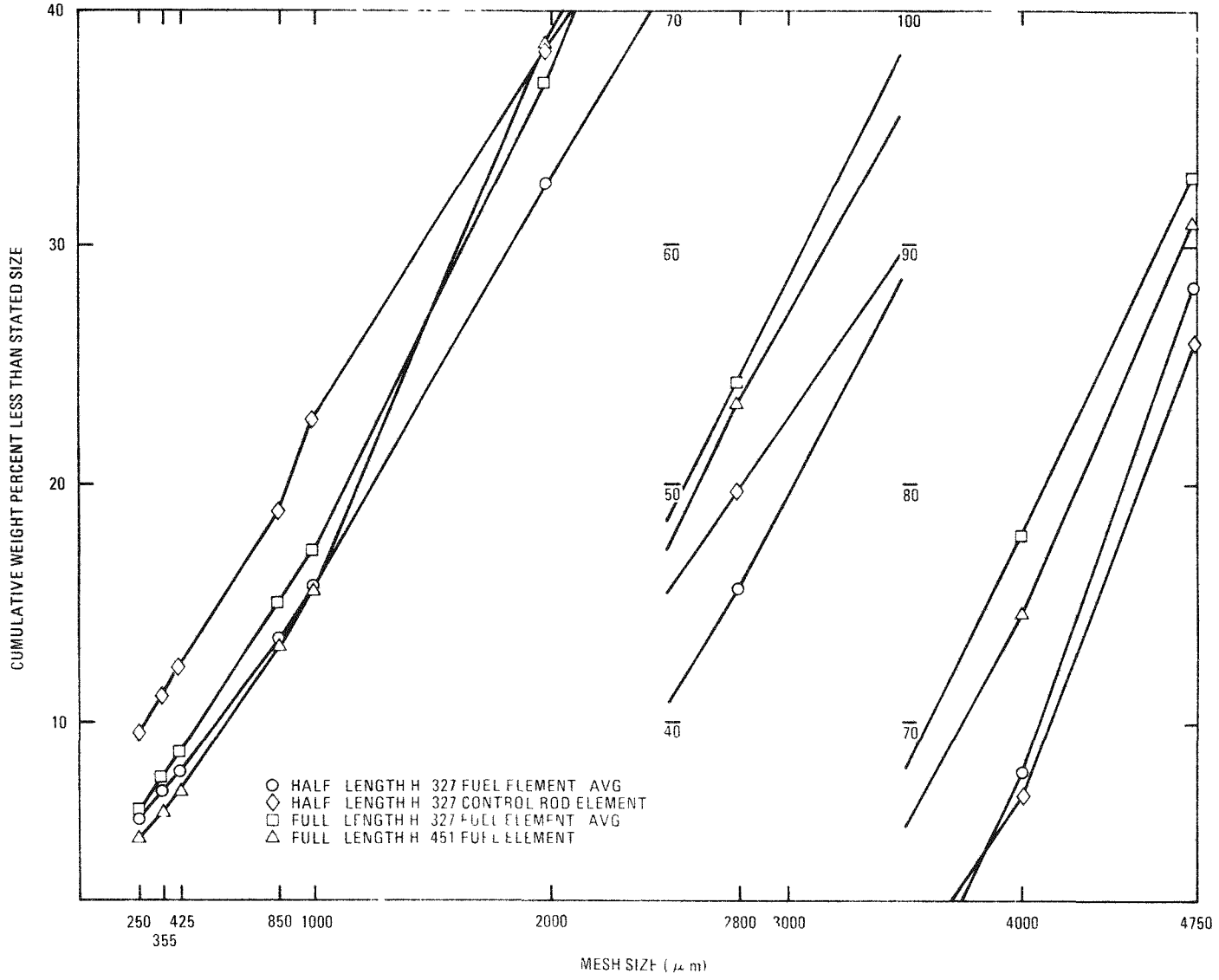

Fig. 2-4. Oversize crusher product comparison for Phase II UNIFRAME system tests, cumulative weight percent less than stated size

TABLE 2-14
COMPOSITE SCREENER AND OVERSIZE CRUSHER PRODUCT SIZE DISTRIBUTION, PHASE II, WEIGHT PERCENT OF SCREENED FRACTIONS

Test No.	Weight Percent of Screened Fractions (Mesh Sizes in μm)									
	+4750	-4750 +4000	-4000 +2800	-2800 +2000	-2000 +1000	-1000 + 850	-850 +425	-425 +355	-355 +250	-250
Half-Length Standard H-327 Unfueled Graphite Fuel Elements										
UE-46	1.2	10.9	36.8	14.5	15.8	2.2	7.7	1.7	1.8	7.4
UE-47	2.8	12.0	38.3	13.9	14.0	2.1	7.1	1.4	1.8	6.6
UE-48	2.3	10.8	41.6	16.0	13.8	1.9	6.2	1.2	1.4	4.8
Mean	2.1	11.2	38.9	14.8	15.5	2.1	7.0	1.4	1.7	6.3
Range	1.6	2.2	4.8	2.1	2.0	0.3	1.5	0.5	0.4	2.6
Avg. dev. from mean	0.6	0.5	1.8	0.8	1.2	0.1	0.5	0.2	0.2	1.0
Half-Length H-327 Unfueled Graphite Control Rod Element										
UE-49	2.2	13.0	39.4	15.6	13.7	2.0	6.0	1.1	1.6	5.4
Full-Length Standard H-327 Unfueled Graphite Fuel Elements										
UE-52B	1.9	9.7	39.1	15.8	14.4	2.1	6.9	1.4	1.9	6.8
UE-53	1.7	9.2	35.9	16.9	17.4	2.5	7.4	1.3	1.5	6.2
UE-54	1.5	8.7	40.1	17.4	15.5	2.0	6.5	1.2	1.5	5.6
Mean	1.7	9.2	38.4	16.7	15.8	2.2	6.9	1.3	1.6	6.2
Range	0.4	1.0	4.2	1.6	1.9	0.5	0.9	0.2	0.4	1.2
Avg. dev. from mean	0.1	0.3	1.6	0.6	1.1	0.2	0.3	0.1	0.2	0.4
Full-Length Standard H-451 Unfueled Graphite Fuel Element										
UE-55	4.4	13.5	36.0	13.8	15.7	2.0	6.7	1.1	1.5	5.3
Summary of All Tests										
Mean	2.2	11.0	38.4	15.5	15.0	2.1	6.8	1.3	1.6	6.0
Range	3.2	4.8	5.7	3.6	3.6	0.6	1.7	0.6	0.5	2.6

in Fig. 2-5. Significant differences shown by these data are:

1. The composite product from crushing half-length control rod elements differed significantly from the products of half-length fuel elements in only the -4750, +4000 μm mesh fraction. In this fraction the quantity was greater in the control rod product (13.0%) than in any of the fuel element products (12.0% maximum). This difference was observed in the screener products and the oversize crushing was not a factor in reducing the difference. The difference in the -4000, +2800 μm mesh fraction between the two oversize crusher products was insignificant in the composite product.

2. The composite product from crushing full-length H-451 graphite fuel elements differed significantly from the products of full-length H-357 graphite fuel elements in the same mesh size fractions as in the screener product. Oversize crushing again had little effect on reducing these differences. The difference in the oversize crusher products between the two -2000, +1000 μm mesh fractions was insignificant in the composite product.

3. Although the separate screener and oversize crusher products showed no significant differences between half- and full-length H-327 graphite fuel elements, the composite product indicated a significantly larger percentage of -4750, +4000 μm material from the half-length elements (10.8% minimum) than from the full-length elements (9.7% maximum).

The cumulative weight percent of material less than each stated size for the composites is given in Table 2-15. A graphical comparison of these results is shown in Fig. 2-6. Significant differences shown by these data are:

1. The range of values for the composite products from crushing half-length fuel elements overlapped the values from crushing

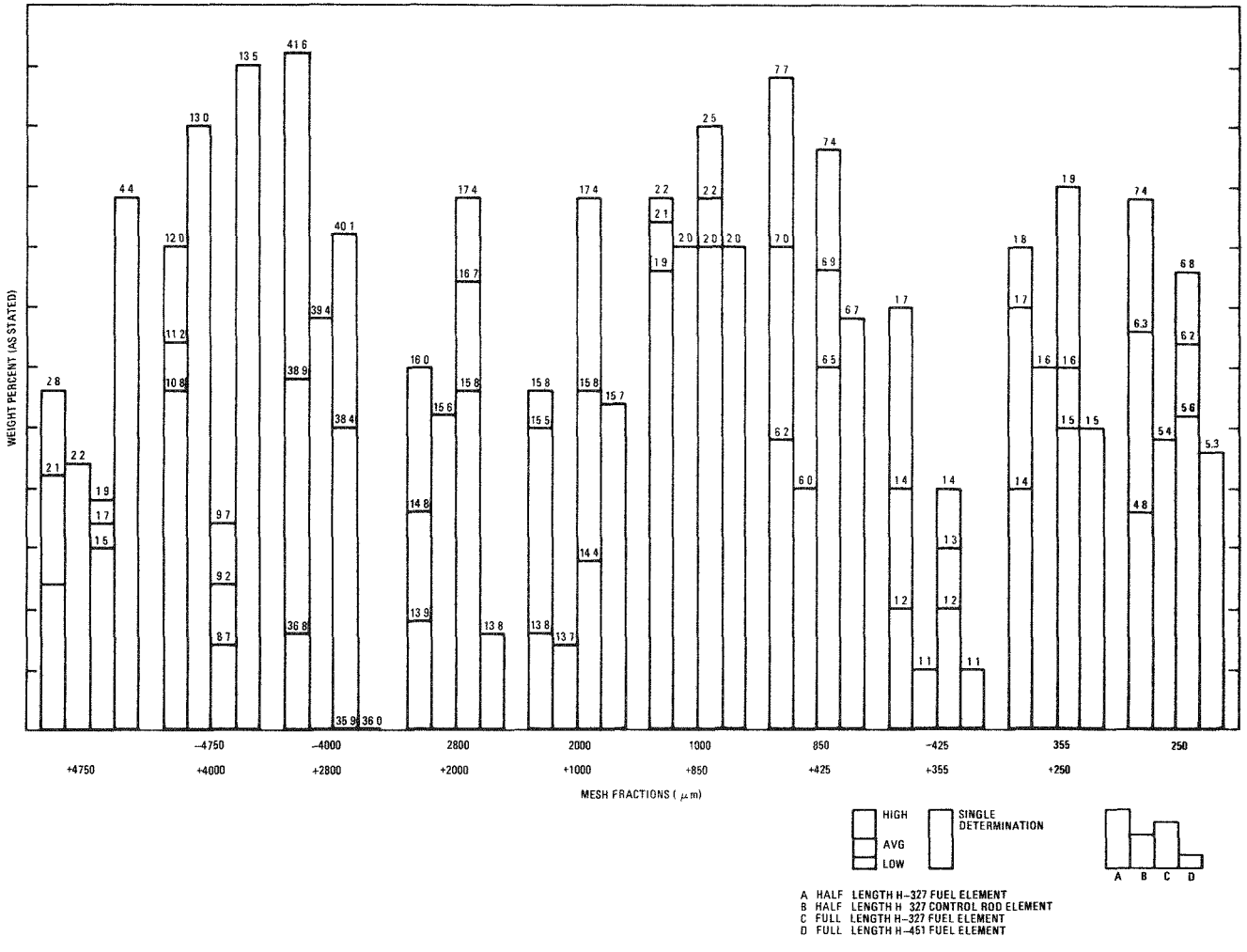

Fig. 2-5. Composite product comparison for Phase II UNIFRAME system tests, weight percent as stated

TABLE 2-15
COMPOSITE SCREENER AND OVERSIZE CRUSHER PRODUCT SIZE DISTRIBUTION, PHASE II, CUMULATIVE WEIGHT PERCENT LESS THAN STATED SIZE

Test No.	Cumulative Weight Percent Less Than Stated Size (Mesh Sizes in μm)									
	+4750	-4750	-4000	-2800	-2000	-1000	-850	-425	-355	-250
Half-Length Standard H-327 Unfueled Graphite Fuel Elements										
UE-46	100.0	98.8	87.9	51.1	36.6	20.8	18.6	10.9	9.2	7.4
UE-47	100.0	97.3	85.2	46.9	33.0	19.0	16.9	9.8	8.4	6.6
UE-48	100.0	97.7	86.9	45.3	29.3	15.5	13.6	7.4	6.2	4.8
Mean	100.0	97.9	86.7	47.8	33.0	18.4	16.4	9.4	7.9	6.3
Range	0	1.5	2.7	5.8	7.3	5.3	5.0	3.5	3.0	2.6
Avg. dev. from mean	0	0.6	1.0	2.2	2.4	2.0	1.8	1.3	1.2	1.0
Half-Length H-327 Unfueled Graphite Control Rod Element										
UE-49	100.0	97.8	84.8	45.4	29.8	16.1	14.1	8.1	7.0	5.4
Full-Length Standard H-327 Unfueled Graphite Fuel Elements										
UE-52B	100.0	98.1	88.4	49.3	33.5	19.1	17.0	10.1	8.7	6.8
UE-53	100.0	98.3	89.1	53.2	36.3	18.9	16.4	9.0	7.7	6.2
UE-54	100.0	98.5	89.8	49.7	32.3	16.8	14.8	8.3	7.1	5.6
Mean	100.0	98.3	89.1	50.7	34.0	18.3	16.1	9.1	7.8	6.2
Range	0	0.4	1.4	3.9	4.0	2.3	2.2	1.8	1.6	1.2
Avg. dev. from mean	0	0.1	0.5	1.6	1.5	1.0	0.8	0.6	0.6	0.4
Full-Length Standard H-451 Unfueled Graphite Fuel Element										
UE-55	100.0	95.6	82.1	46.1	32.3	16.6	14.6	7.9	6.8	5.3
Summary of All Tests										
Mean	100.0	97.8	86.8	48.4	32.9	17.8	15.8	8.9	7.6	6.0
Range	0	3.2	7.7	7.9	7.3	5.3	5.0	3.5	3.0	2.6

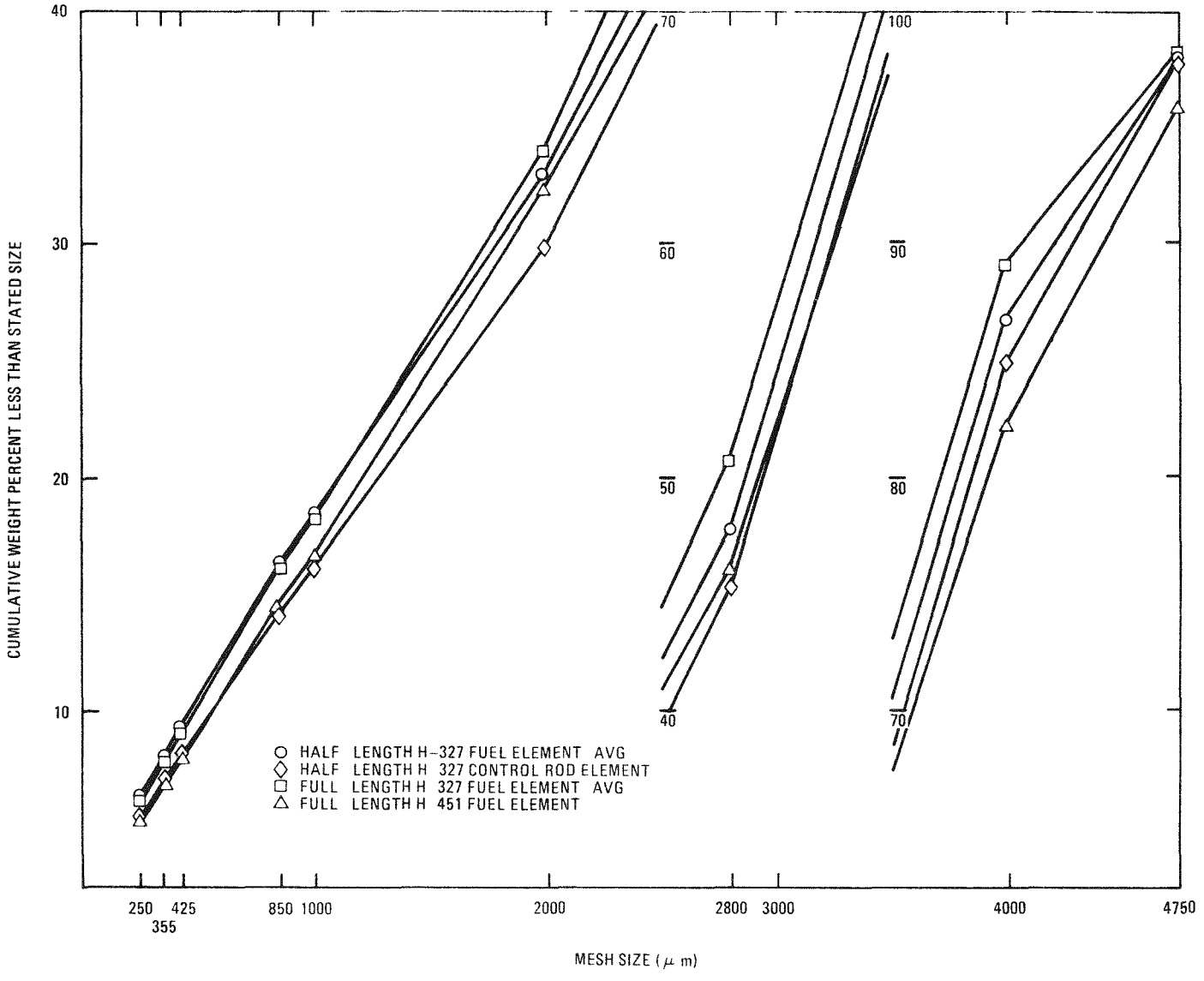

Fig. 2-6. Composite product comparison for Phase II UNIFRAME system tests, cumulative weight percent less than stated size

half-length control rod elements sufficiently to indicate no significant differences in these products. Significant differences noted in the separate screener and oversize crusher products (Tables 2-9 and 2-12) were eliminated in the combined product.

2. The composite product from crushing full-length H-451 graphite fuel elements differed significantly from those of the full-length H-357 graphite fuel elements in the same areas as in the screener products. The oversize crusher products, which showed no significant differences, had little effect in reducing the differences in the screener products.

3. The ranges of values for the composite products from crushing half- and full-length H-327 graphite fuel elements overlapped sufficiently to indicate no significant differences in these products.

UNIFRAME Product - General Conclusions. Although variations in the quantities of individual mesh size fractions of materials should occur between the different types of elements crushed, the cumulative weight percents of material less than each stated size should not be significantly different in UNIFRAME product from crushing any type of H-357 graphite element. The products from crushing H-451 graphite elements, however, should be somewhat coarser.

Comparison of Composite Screener and Oversize Crusher Products with Tertiary Crusher Products. To provide an estimation of the changes in the tertiary crusher product effected by screening and oversize crushing, the average tertiary crusher product size distribution obtained in the Phase II shakedown tests (from Table 2-2), the average composite product size distribution calculated from the Phase II test results (from Table 2-15), and the average tertiary crusher product size distribution obtained in the Phase I tests were compared. A graphical comparison of these results is shown in Fig. 2-7.

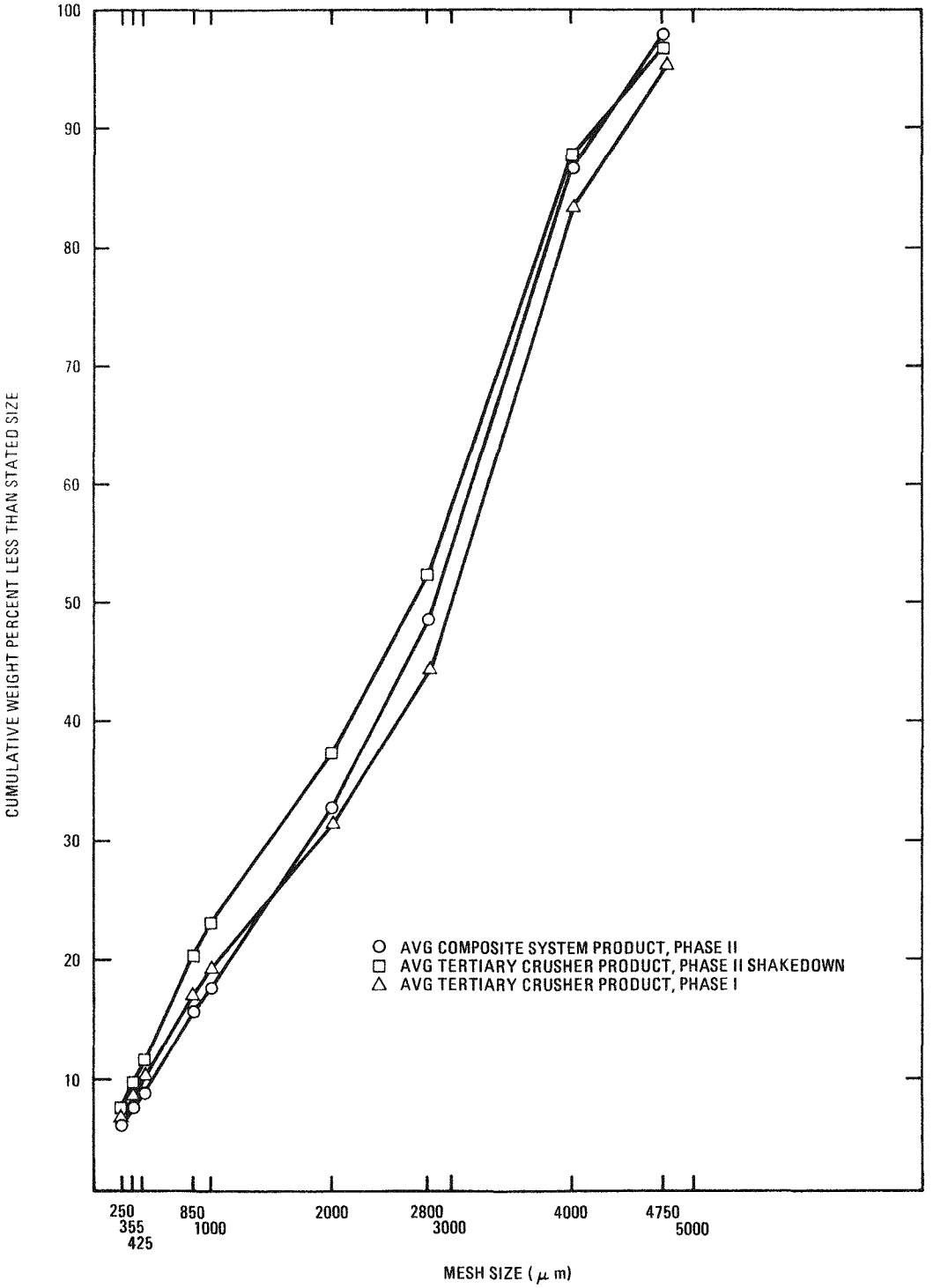

Fig. 2-7. Comparison of size distributions for products from tertiary crushing and UNIFRAME system

Due to the overlapping of the ranges of values for each of these results (not shown in Fig. 2-7), significant differences cannot be clearly established. However, certain trends do appear. A comparison of the composite system product with the Phase I tertiary crusher product shows a tendency for increased fineness in the composite product. This can be assumed to be from the effects of oversize crushing. Comparison of the composite system product with the Phase II shakedown tertiary crusher product, however, shows an opposite tendency, that is, for the tertiary crusher product to be finer. Since the shakedown tests were made with partially drilled (i.e., more solid graphite sections) fuel elements, this effect may be due to finer crushing of the more solid graphite. This is borne out by the increased times required to crush the partially drilled elements (see Tables 2-1 and 2-6) and may be an indication that a finer product and longer crushing times will result from crushing fuel-loaded (therefore more solid) elements than was observed with the unloaded elements. In any event, the effect of oversize crushing on the tertiary crusher product size distribution may be minimal.

Comparison of UNIFRAME Product with Primary Burner Feed Requirements. Cumulative weight percent of material less than each stated size obtained from the composite screener and oversize crusher products with the addition of 17 wt % -850 μm fuel particles is given in Table 2-16. A graphical comparison of these results with estimated primary burner feed size distribution requirements is shown in Fig. 2-8. From these results it can be seen that:

1. The "acceptable" burner feed curve lies within the ranges of results for UNIFRAME product.

2. The entire UNIFRAME product range is consistently within the "acceptable" limits for product greater than ∿4500 μm mesh.

3. The lower range of UNIFRAME product results is not within the "acceptable" limits for product less than 4500 μm mesh.

TABLE 2-16
SCREENER AND OVERSIZE CRUSHER PRODUCTS, COMPOSITE
WITH 17% FUEL PARTICLES (<850 μm) ADDED, PHASE II
UNIFRAME SYSTEM TESTS

Test No.	+4750	-4750	-4000	-2800	-2000	-1000	-850
Half-Length Standard H-327 Unfueled Graphite Fuel Elements							
UE-46	100.0	99.0	90.0	59.4	47.4	34.3	32.4
UE-47	100.0	97.6	87.7	55.9	44.4	32.8	31.0
UE-48	100.0	98.1	89.1	54.6	41.3	29.9	28.3
Mean	100.0	98.2	88.9	56.6	44.4	32.3	30.6
Range	0	1.4	2.3	4.8	6.1	4.4	4.1
Half-Length H-327 Unfueled Control Rod Element							
UE-49	100.0	98.2	87.4	54.7	41.7	30.4	28.7
Full-Length Standard H-327 Unfueled Graphite Fuel Elements							
UE-52B	100.0	98.4	90.4	57.9	44.8	32.8	31.1
UE-53	100.0	98.6	90.9	61.2	47.1	32.7	30.6
UE-54	100.0	98.8	91.5	58.2	43.8	30.9	29.3
Mean	100.0	98.6	90.9	59.1	45.2	32.1	30.3
Range	0	0.4	1.1	3.3	3.3	1.9	1.8
Full-Length Standard H-451 Unfueled Graphite Fuel Elements							
UE-55	100.0	96.3	85.1	55.3	43.8	30.8	29.1
Summary of All Tests							
Mean	100.0	98.1	89.0	57.2	44.3	31.8	30.1
Range	0	2.7	6.4	6.6	6.1	4.4	4.1

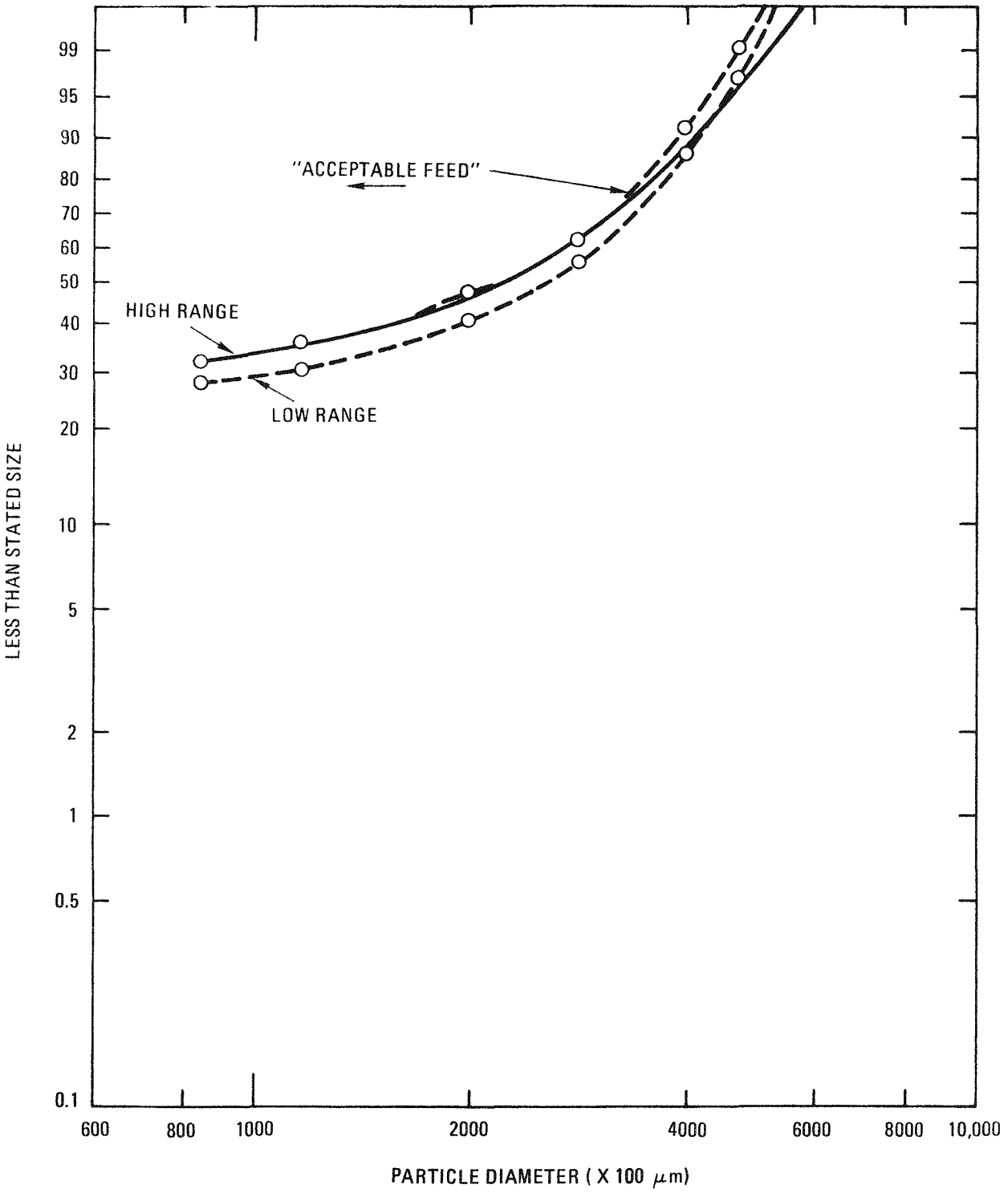

Fig. 2-8. Comparison of UNIFRAME composite high and low values with "acceptable" burner feed

4. The higher range of UNIFRAME product results is consistently within the "acceptable" burner feed limits.

2.2.2.4. Phase II Acceptance Criteria

The degree of success of each phase of the Activity Plan (AP521001) is based upon meeting certain requirements of the Design Criteria (DC521001). Acceptance criteria, defined in the Activity Plan, are based on demonstrations of performance and quantified data which prove that the requirements of the Design Criteria have been met. The following is a listing of the acceptance criteria applicable to the UNIFRAME system for the Phase II test program and a discussion of the results.

1. Material holdup: <0.5% of throughput. Results of the cleanout of the system at the end of the Phase II tests produced a recovery of 0.26% of the throughput as holdup on the various components of the system. Total MUF after cleanout was 0.19% of the throughput. Assuming the MUF was also holdup, the total holdup becomes 0.45% (see Table 2-5). These data indicate that achieving a material holdup of <0.5% is possible in the UNIFRAME system as presently designed. Identification of the holdup areas in the Phase II and future tests will provide a basis for design modifications to reduce holdup still further.

2. Throughput rate: one fuel element in <15 min. Results of the Phase II tests indicate a normal crushing time of ∿3 min for a full-length H-327 graphite fuel element and ∿5 min for a full-length H-451 graphite fuel element. Temporary material holdups in the primary and secondary crushers resulting in reduced throughput rates extended the crushing times to up to ∿7 min (see Table 2-6). These data indicate that achieving a throughput rate of one fuel element in <15 min is possible in the UNIFRAME system as presently designed. Observations during the Phase II tests indicate that charging one fuel element every 5 min with a cleanout period of ∿15 min at the end of a campaign or batch is feasible.

3. Crushed material confinement (excluding dusts): 100% to crushing and screening cavities. Observations of equipment through viewports and open ventilation areas during the Phase II tests revealed no material bypass of the crushing and screening cavities. Material balances supported this observation with 99.81% of the material accounted for. The data and observations indicate that achieving 100% material confinement to the crushing and screening cavities is possible with the UNIFRAME system as presently designed.

4. Crushed product: ≤4750 μm (≤3/16 in.) ring size with a size distribution suitable for primary burner feed. Results of screen analysis of the crushed products from the Phase II tests indicate an average of 2.2% of the product will be greater than 4750 μm (∿3/16 in.) mesh size with a maximum of ∿4.4% (found in H-451 graphite crushed product) and a minimum of ∿1.2% (Table 2-15). These data indicate that achieving a crushed product ≤4750 μm (≤3/16 in.) ring size is not possible in the UNIFRAME system without design or oparating parameter changes. However, a comparison of the ranges of UNIFRAME products with the "acceptable" primary burner feed (shown in Fig. 2-8) shows that the product consistently meets this criterion above 4500 μm.

Results also indicate that the lower range of UNIFRAME product is not within the "acceptable" limits for primary burner feed below 4500 μm (Fig. 2-8). These data indicate that achieving a crushed product which consistently meets the primary burner feed size distribution requirements is not possible in the present UNIFRAME system without design or operating parameter changes.

Meeting both of these requirements may mean redesigning or replacement of the oversize crusher and/or reducing the tertiary crusher gap. These changes could result in overcrushing and particle breakage in excess of the specified maximums, forcing a

tradeoff with burner feed requirements. The +4750 μm (+3/16 in.) material was observed earlier in the Phase I tests of the oversize crusher and the decision at that time was to reassess this requirement after further testing to determine particle breakage at the current operating perameters and after tests in the 0.40-m burner had further quantified its actual feed size requirements.

No changes are planned to the UNIFRAME system to meet these criteria until primary burner feed requirements are demonstrated and particle breakage is established.

5. Dust confinement: 100% to ventilation enclosure. The complete ventilation enclosure was not installed during the Phase II tests to permit observation of the primary and secondary crushing operations. Those components of the ventilation enclosure which were installed displayed no tendency to allow dust escape. Material balances supported this observation with 99.81% of the material accounted for. The data and observations indicate that achieving 100% dust confinement to the ventilation enclosure is possible with the UNIFRAME system. Further data will be obtained in the Phase III tests with the more easily detected radioactive fuel materials.

2.3. UNIFRAME PRIMARY BURNER FEED PREPARATION

2.3.1. Introduction

Due to the high cost and limited availability of scrap HTGR fuel elements, a large quantity of anode butt scrap graphite was purchased to provide crushed graphite feed for primary burner testing. Crushing of this graphite to prepare burner feed is also being utilized to obtain further operating and crushing experience with the UNIFRAME fuel element size reduction system prior to processing loaded fuel elements.

2.3.2. Initial Scrap Graphite Crushing Tests

Three separate crushing tests (SCRAP-1 through -3) were utilized to shake down the UNIFRAME system with scrap anode butt graphite. This graphite, as well as being of a different type, had random shapes and sizes and was expected to exhibit somewhat different crushing behavior and product characteristics than the prismatic HTGR fuel elements. In these initial tests, for comparative purposes, products were collected separately from the oversize crusher and the screener and sampled as they were in the Phase II tests with HTGR fuel elements.

Figures 2-9 and 2-10 show comparisons between the screener and oversize crusher products from scrap anode butt graphite crushing and HTGR fuel element crushing. The screener product from crushing anode graphite was not significantly different from the screener product from crushing fuel elements (Fig. 2-9). However, the anode graphite oversize crusher product was considerably finer than the product from crushed fuel elements (Fig. 2-10).

The generally smaller size of the anode graphite fragments charged was such that less primary crushing was required than for the HTGR elements. This manifested itself in a reduction of primary crushing times of ∿25% (see Table 2-17). However, because the anode graphite was solid and did not contain fuel or coolant holes as the fuel elements do, the secondary crushing times were approximately doubled (see Table 2-17). The increase in secondary crushing time resulted in lower loading rates on the screener which, coupled with the finer product, improved its efficiency. Screener product increased from an average of 85.12% of the total product when crushing fuel elements to 89.44% with anode graphite (Table 2-17).

2.3.3. Scrap Graphite Crushing

Crushing of anode graphite for primary burner feed continued with attempts to utilize the penumatic material transport system to collect the screener and oversize crusher products in the UNIFRAME product bunker.

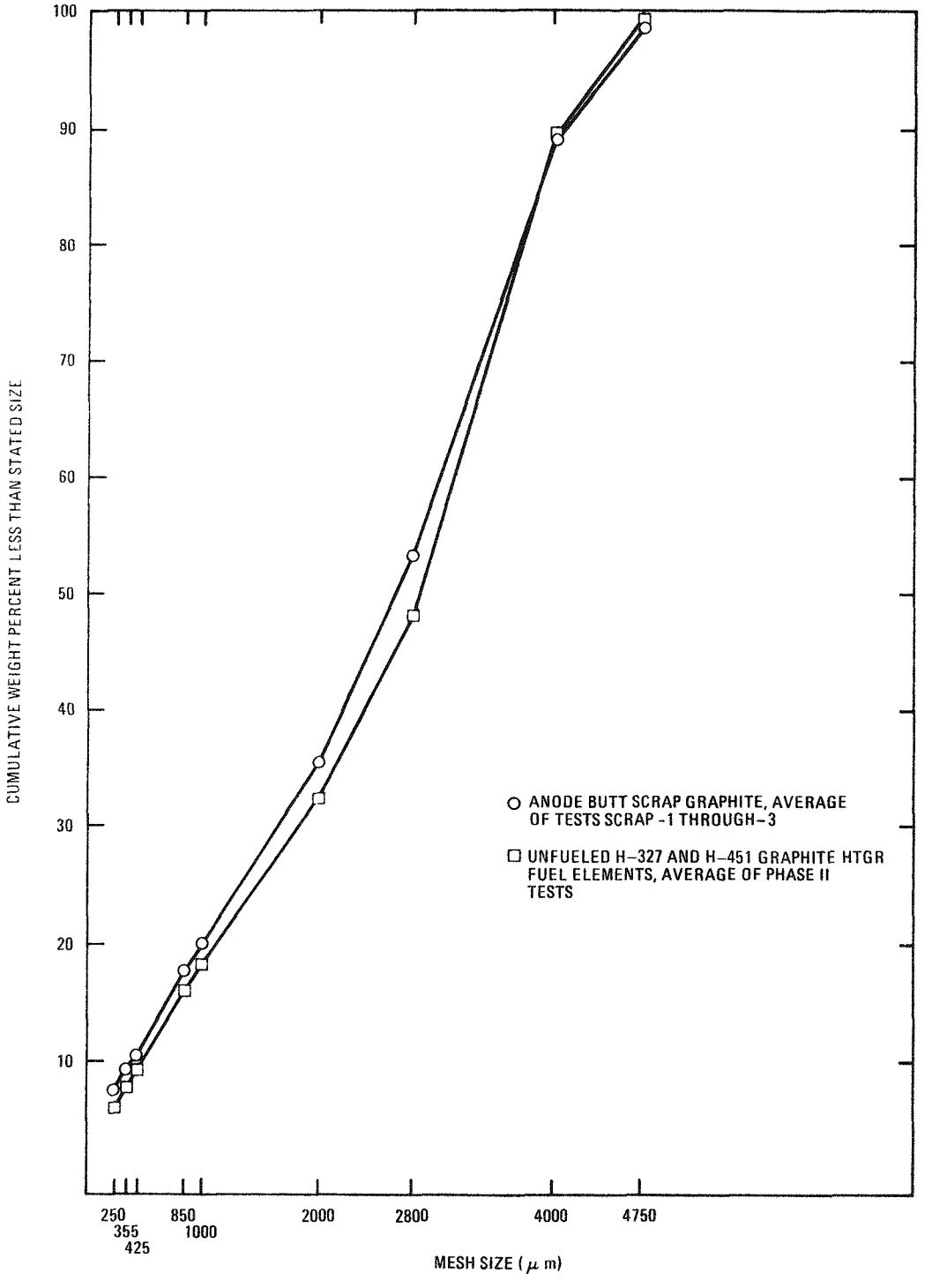

Fig. 2-9. Comparison of size distributions for UNIFRAME screener product

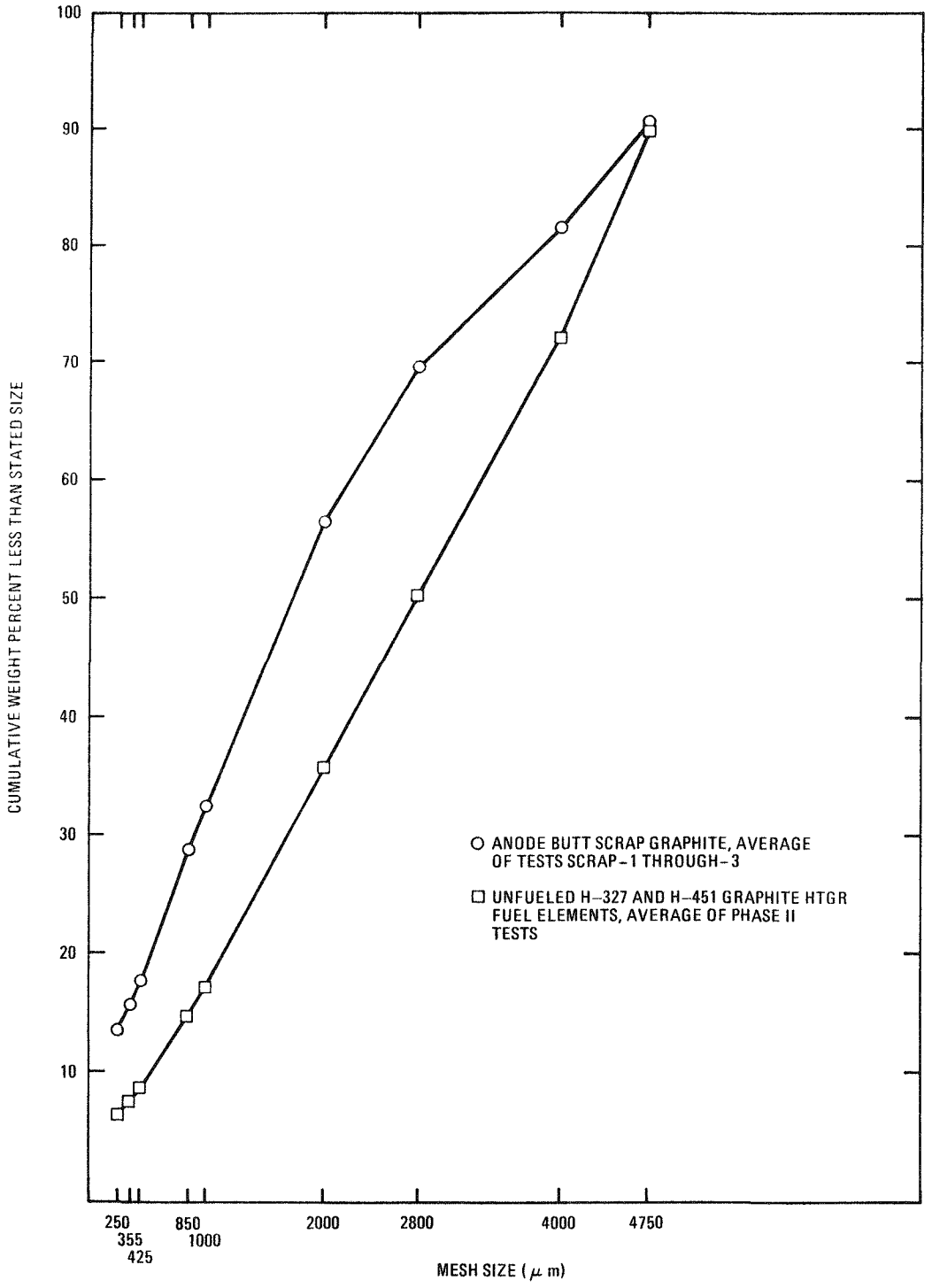

Fig. 2-10. Comparison of size distributions for UNIFRAME oversize crusher product

TABLE 2-17
COMPARISON OF CRUSHING BEHAVIOR OF HTGR FUEL ELEMENTS AND SCRAP ANODE BUTT GRAPHITE

	Half-Length Unfueled H-327 Graphite Fuel Elements				Scrap Anode Butt Graphite			
Test No.	UE-46	UE-47	UE-48	Avg	SCRAP-1	SCRAP-2	SCRAP-3	Avg
Total product, kg	43.523	45.585	46.628	45.245	44.024	44.023	44.478	44.175
% oversize crushed	17.40	16.88	10.35	14.88	5.17	11.98	14.54	10.56
% through screener	82.60	83.12	89.65	85.12	94.83	88.02	85.46	89.44
Crushing time, s								
Primary	35	55	40	43	36	29	29	31
Secondary	92	95	90	92	160	219	190	190

In the initial test (SCRAP-4) the crushed product which discharged from the screener transported well. However, crushed product from the oversize crusher did not transport at all. This was attributed to insufficient motive gas flow through the oversize crusher because increased pressure drop at the oversize crusher's product entry point to the transport line diverted the motive gas through the path of least resistance (i.e., the screener), allowing material to salt out and block the oversize crusher discharge completely (see Fig. 2-11).

Testing was continued (tests SCRAP-5 through -9) to gain experience and to make further observations on screener product discharge and transport. In all of these tests, the screener product was successfully transported to the UNIFRAME product bunker utilizing the pneumatic transport system. Because of the transport difficulties experienced in test SCRAP-3, the oversize crusher product was collected separately as in the Phase II tests and later manually combined with the screener product for size distribution analysis (see Fig. 2-12).

Comparison of the size distribution of the combined screener and oversize crusher products from these anode graphite crushing tests with the size distribution of composited screener and oversize crusher products from the HTGR graphite elements of the Phase II tests, shown in Fig. 2-13, indicated that the crushed anode graphite was generally much finer. This is probably attributable mainly to the crushing characteristics of the solid materials, and secondarily to the differences in graphites and the attrition due to transport of the screener product.

At the conclusion of the first nine crushing tests with scrap anode graphite, the UNIFRAME was partially dismantled and inspected to determine material holdup areas and to complete the material balance (see Table 2-18). At the end of these tests, the material recovered was 99.10% of the charge. Material unaccounted for was 0.90% of the charge. An additional 0.22% was recovered during cleanout of the system, resulting in a net MUF of 0.68%. This increase from the 0.19% MUF obtained in the Phase II tests

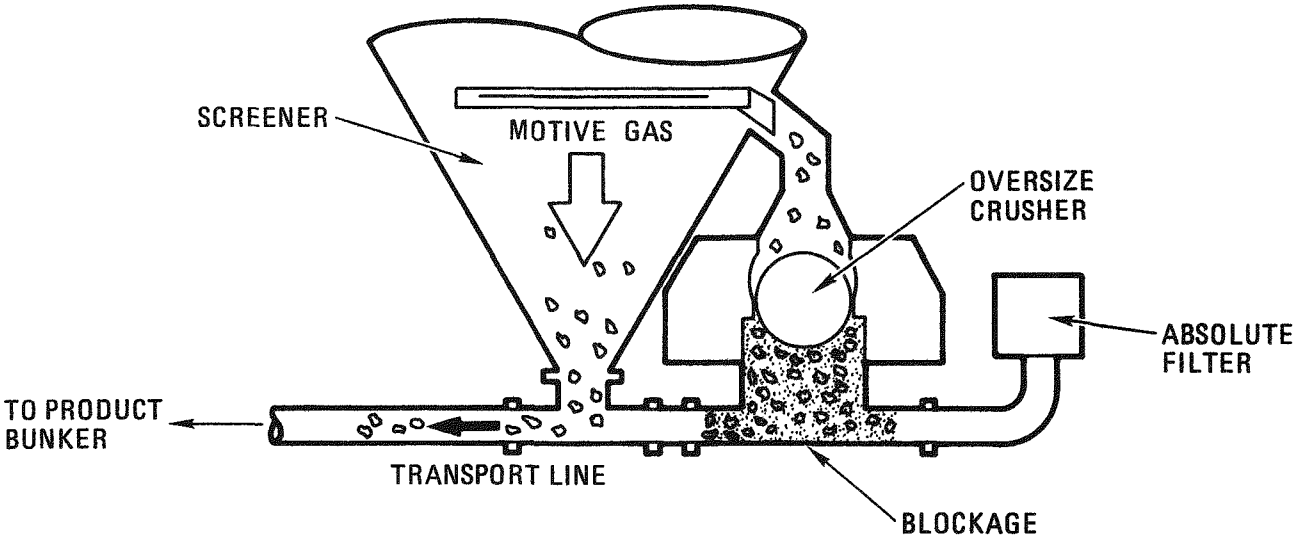

Fig. 2-11. UNIFRAME product transport line blockage, Test SCRAP-3

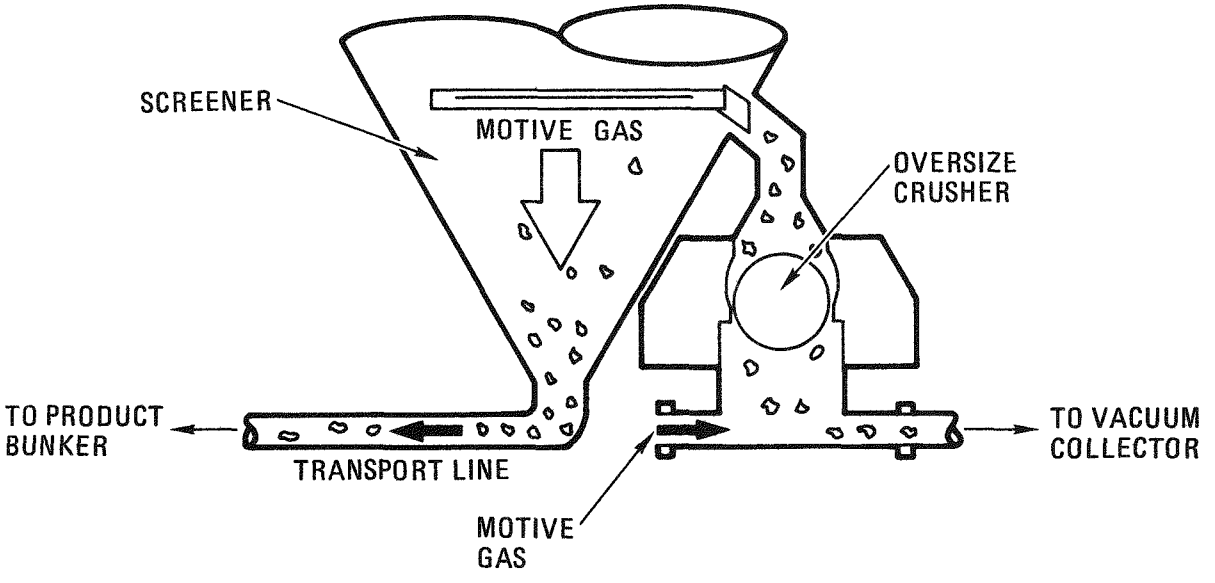

Fig. 2-12. UNIFRAME product transport arrangement, Tests SCRAP-4 through -9

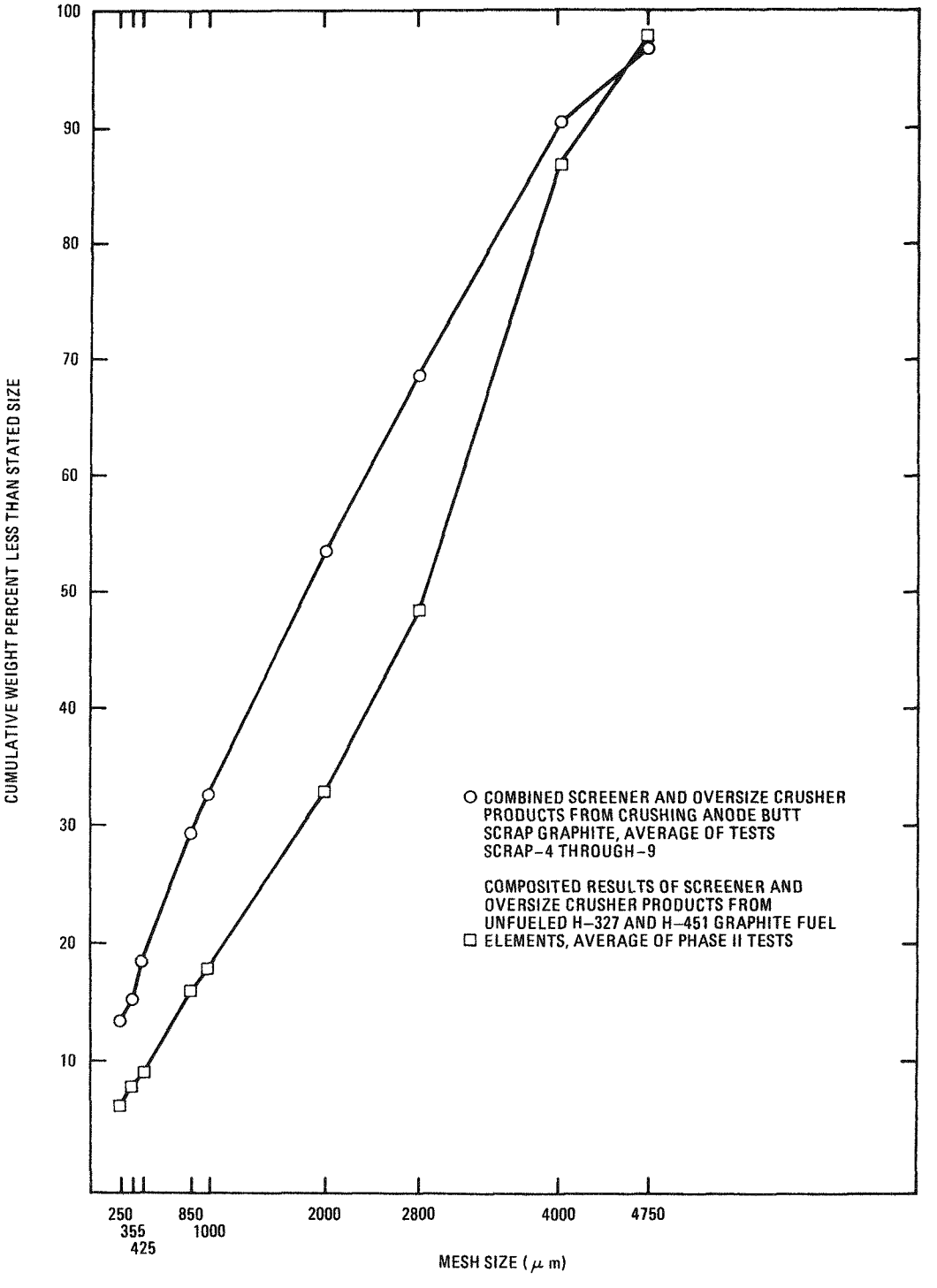

Fig. 2-13. Comparison of size distributions for UNIFRAME product

TABLE 2-18
MATERIAL BALANCE, UNIFRAME SCRAP ANODE BUTT GRAPHITE CRUSHING, TESTS SCRAP-1 THROUGH SCRAP-9[a]

Test No.	Charge (kg)	Recovery (kg)	Gain (+) or Loss (-)	MUF (% of Charge)
SCRAP-1	45.000	44.024	(-) 0.976	2.17
SCRAP-2	45.500	44.023	(-) 1.477	3.25
SCRAP-3	44.750	44.478	(-) 0.272	0.61
SCRAP-4	89.900	87.200	(-) 2.700	3.00
SCRAP-5	93.100	91.800	(-) 1.300	1.40
SCRAP-6	97.350	96.750	(-) 0.600	0.62
SCRAP-7	95.000	94.250	(-) 0.750	0.79
SCRAP-8	93.150	95.910	(+) 2.760	2.96
SCRAP-9	96.400	95.400	(-) 1.000	1.04
Total	700.150	693.835	(-) 6.315	0.90

Cleanout at Conclusion of Testing

Description	Quantity (kg)	% of Charge
Holdup on screener table	0.757	0.11
Dust in screener housing	0.527	0.08
Dust in oversize crusher housing	0.210	0.03
Total	1.494	0.22

Grand Totals

Tests	Charge (kg)	Recovery (kg)	Gain (+) or Loss (-)	MUF (% of Charge)
SCRAP-1 through SCRAP-9	700.150	695.329	(-) 4.821	0.68

[a] Screener blinded holes = 193 = 1.7%.

(see Section 2.2.2.3.2 and Table 2-5) may be due to holdup in the UNIFRAME product bunker, on its filters, and increased material handling.

At this point the number of blinded holes on the screener was again counted. The number had increased from 103 or 0.9% at the end of the Phase II tests (see Section 2.2.2.3.2 and Table 2-5) to 193 or 1.7% (see Table 2-18). Although some of the increase in blinding may be attributable to the difference between anode graphite and HTGR fuel element graphite, this result does indicate that blinding will probably increase to a point where maintenance actions are required to clear the screener.

Testing was continued (tests SCRAP-10 through -18) with studies of the effects of varying the oversize crusher's operating parameters on the pneumatic material transport of UNIFRAME products. In these tests the oversize crusher was placed so that its material discharged into the transport line downstream of the screener product discharge (the opposite of previous tests). The crushed product from the oversize crusher transported well in the initial two tests (SCRAP-10 and -11), but crushed product from the screener did not transport (see Fig. 2-14). This opposite effect from the previous observation (test SCRAP-4) was attributed to insufficient motive gas flow through the screener because increased pressure drop at the screener product transport line entry point diverted the motive gas through the new path of least resistance (i.e., the oversize crusher), allowing the screener product to salt out and block the screener discharge completely. The screener product was successfully transported at the end of each of these tests by rodding out the line blockage. From these tests and the previous observation (test SCRAP-4), it became obvious that inevitably crushed materials discharged from the equipment item closest to the product bunker would preferentially transport with subsequent blockage of the other discharge. This effect cannot be overcome by the differences in pressure drops across the equipment alone and some additional means of increasing the pressure drop needs to be utilized.

For the next test (SCRAP-12) the oversize crusher was not operated until after the secondary crushing was completed (i.e., screening essentially completed also). This allowed the pressure drop to increase across

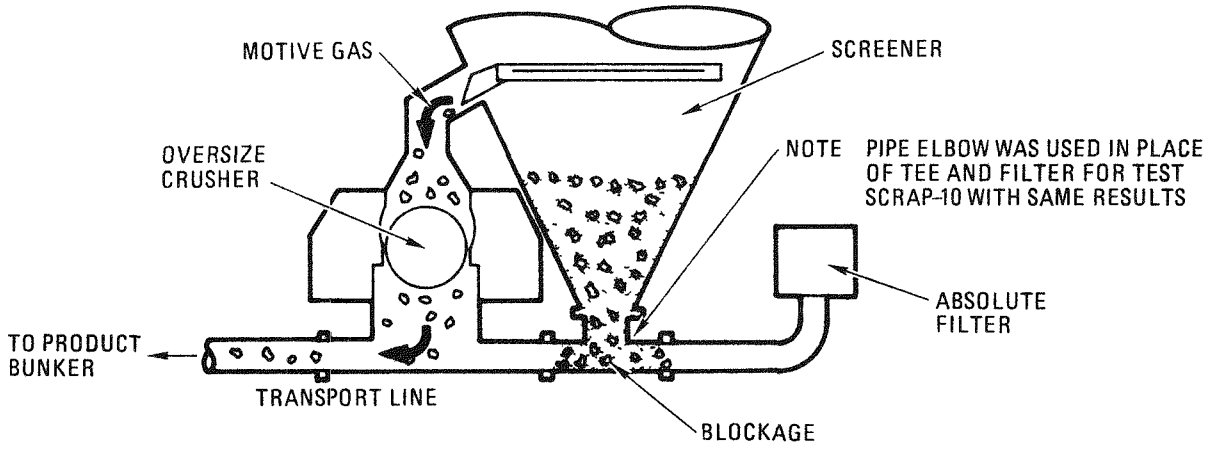

Fig. 2-14. UNIFRAME product transport arrangement for Tests SCRAP-10 through -18 showing product transport line blockage in Tests SCRAP-10 and -11

the oversize crusher, due to material backing up in the feed chute, forcing the motive gas through the screener and effecting transport. The oversize crusher was started (under full load) and its product discharged and transported well. Inspection of the system revealed no abnormal material holdup and complete material transport.

During the next several tests (SCRAP-13 through -18), the oversize crusher was operated intermittently throughout the crushing operation to allow periodic fluctuations in the pressure drop. These parameters and results are summarized in Table 2-19. Crushed product was transported from both the screener and the oversize crusher completely in every run. However, blockages occurred in transport of screener product in some tests, but transport was restarted in each case during the next shutdown cycle of the oversize crusher.

Comparison of the size distribution of crushed anode graphite from tests in which the screener product only was transported through the pneumatic transport system (tests SCRAP-4 through -9) with tests in which both the screener and oversize crusher products were transported through the pneumatic transport system (tests SCRAP-10 through -18), shown in Fig. 2-15, show that the completely transported product was finer. This is attributable to attrition due to transport. However, since the transport system was not operated at the optimum parameters (i.e., lowest transport velocity to reduce particle breakage), this effect would be reduced under optimum transport conditions.

At the conclusion of the second series of nine crushing tests (SCRAP-10 through -18) with anode graphite, the UNIFRAME was again partially dismantled and inspected to determine material holdup areas and to complete the material balance. At the end of this series, material recovered was 99.07% of the charge, and MUF was 0.93% of the charge (see Table 2-20). These results were very close to the results of the first series [i.e., 99.10% recovery and 0.90% MUF (see Table 2-18)]. An additional 0.59% was recovered during cleanout of the system, resulting in a net MUF of 0.34%.

TABLE 2-19
UNIFRAME PRODUCT PNEUMATIC TRANSPORT WITH INTERMITTENT OVERSIZE CRUSHER OPERATION

Run No.	Oversize Crusher Operating Time From Start of Crushing		Duration	Remarks
	On	Off		
SCRAP-13	3 min 30 s	4 min 0 s	30 s	No effect on screener product transport.
	5 min 0 s	5 min 30 s	30 s	
	5 min 45 s	End of test	∿9 min 15 s	
SCRAP-14	1 min 0 s	2 min 0 s	1 min	Screener product transport stopped. Restarted with crusher off.
	3 min 0 s	4 min 0 s	1 min	No effect on screener product transport.
	5 min 0 s	End of test	∿10 min	
SCRAP-15	2 min 0 s	4 min 0 s	2 min	Screener product transport stopped. Restarted with crusher off.
	4 min 30 s	5 min 30 s	1 min	Screener product transport stopped. Restarted with crusher off.
	6 min 24 s	End of test	∿8 min 36 s	No effect on screener product transport.
SCRAP-16	1 min 30 s	1 min 45 s	15 s	No effect on screener product transport.
	2 min 30 s	2 min 45 s	15 s	
	3 min 30 s	3 min 45 s	15 s	
	4 min 30 s	4 min 45 s	15 s	
	5 min 30 s	End of test	∿9 min 30 s	
SCRAP-17				Same as SCRAP-16.
SCRAP-18				Same as SCRAP-16.

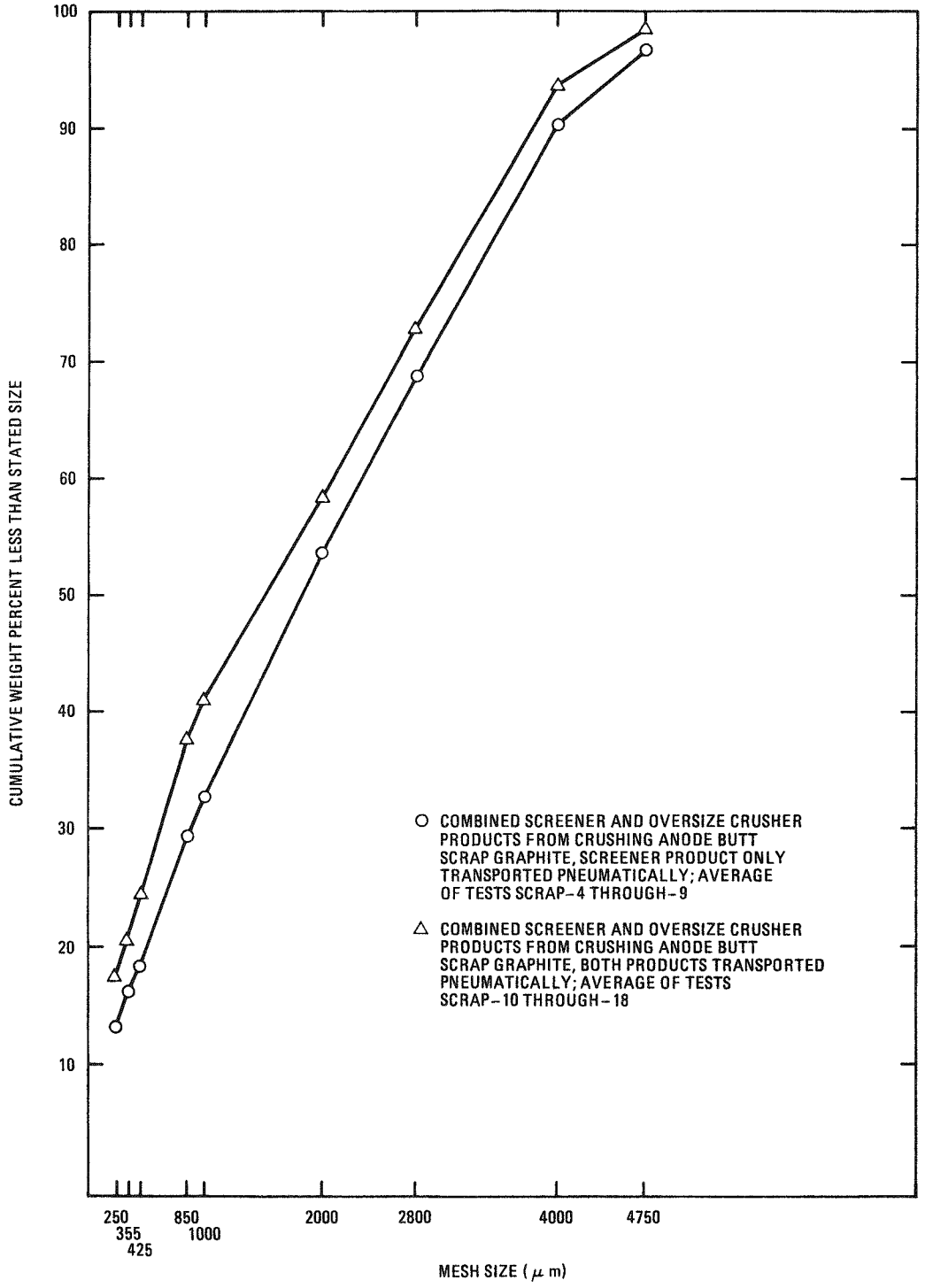

Fig. 2-15. Comparison of size distributions from crushing anode butt scrap graphite

TABLE 2-20
MATERIAL BALANCE, UNIFRAME SCRAP ANODE BUTT GRAPHITE CRUSHING,
TESTS SCRAP-10 THROUGH SCRAP-18[a]

Test No.	Charge (kg)	Recovery (kg)	Gain (+) or Loss (-)	MUF (% of Charge)
SCRAP-10	96.125	94.000	(-) 2.125	2.21
SCRAP-11	97.200	97.800	(+) 0.600	0.62
SCRAP-12	101.153	100.903	(-) 0.250	0.25
SCRAP-13	96.616	96.643	(+) 0.027	0.03
SCRAP-14	96.620	95.919	(-) 0.701	0.73
SCRAP-15	96.620	96.164	(-) 0.456	0.47
SCRAP-16	99.792	98.119	(-) 1.673	1.68
SCRAP-17	98.431	97.172	(-) 1.259	1.28
SCRAP-18	81.194	78.988	(-) 2.206	2.72
Total	863.751	855.708	(-) 8.043	0.93

Cleanout at Conclusion of Testing

Description	Quantity (kg)	% of Charge
Holdup on screener table	3.575	0.41
Dust in screener housing	0.261	0.03
Dust in oversize crusher housing	1.260	0.15
Total	5.096	0.59

Grand Totals

Tests	Charge (kg)	Recovery (kg)	Gain (+) or Loss (-)	MUF (% of Charge)
SCRAP-10 through SCRAP-18	863.751	860.804	(-) 2.947	0.34

[a] Screener blinded holes = 423 = 3.7%.

The number of blinded holes in the screener was again counted. The number had increased from 193 or 1.7% determined at the end of test SCRAP-9 to 423 or 3.7% at the end of test SCRAP-18, reaffirming the eventuality of required maintenance to clear the screener.

In the next three tests (SCRAP-19 through -21) the inner vibrating section of the screener and the oversize crusher were removed from the UNIFRAME system to observe the operation of the pneumatic transport system with material which had not been screened and in which the oversize material had not been recrushed (see Fig. 2-16). This would provide information on the capability of the transport system to handle the largest particle produced through the tertiary crushing stage of the UNIFRAME and its capability to transport without the benefit of a quasi-metered feed provided through the action of the screener at its maximum throughput.

In the first test of this series (SCRAP-19) the screener discharge stopped after approximately 1 min of crushing time and no further transport occurred. After crushing was completed the transport line was inspected and found clear. The blockage had apparently occurred at the apex of the screener outer housing. A wire was used to dislodge the obstruction and transport was resumed to completion. Examination of the product revealed several fairly large wafer-like fragments which had transported. One fragment which had passed through the 50-mm-OD, 48-mm-ID (2-in.-OD, 1.87-in.-ID) transport tubing was 64 x 32 x 2.4 mm (2-1/2 x 1-1/4 x 3/32 in.). This or similar type fragments were suspected of having produced the blockage in the screener discharge.

Prior to the second test of this series (SCRAP-20), an air jet was installed in the transport line tee at the screener discharge. During the crushing operation, the air jet was utilized to provide short blasts of 690 kPa (100-psi) air in the area where the previous blockage occurred. The jet was used when a slowdown in the flow of material to the transport line occurred and was only necessary until approximately the midpoint of the test. At this point the peak load at the discharge area was past and the jet was not required to maintain material flow.

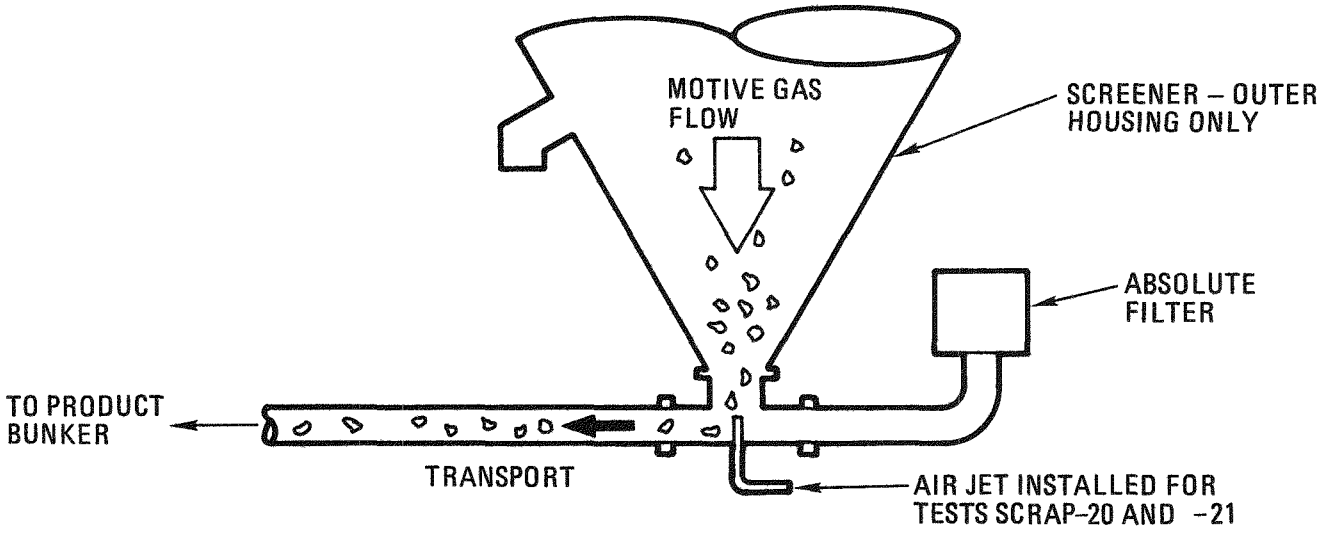

Fig. 2-16. UNIFRAME product transport arrangement for Tests SCRAP-19 through -21 and crushing of HTGR fuel element No. 1-2319

During this test (SCRAP-20) the UNIFRAME's emergency stop button was inadvertently pressed and the three crushers stopped. Primary crushing was completed and therefore start-under-load was not required. The secondary crusher restarted under this loaded condition without difficulty. The tertiary crusher was also started without difficulty under this loaded condition, both with a single roll and with both rolls operating.

During the third test of this series (SCRAP-21), the air jet was utilized only three times in short bursts during the peak loading periods of the crushing operation. Transport flow had not stopped but merely slowed at the points when the air jet was utilized, and use of the jet may not have been necessary to continue flow.

A final test was conducted without the screener and oversize crusher utilizing a full-length H-327 graphite unloaded HTGR fuel element. Transport was complete without the use of the air jet. As previously indicated, the wafer-like nature of some of the product from crushing anode graphite seemed to be the major contributor to the blockage at the apex of the screener outer housing.

In addition to providing information on the transport of "unsized" crushed product at maximum throughput, these tests provided another comparison of the size distributions of "unsized" and "sized" crushed products. Phase II results of crushing HTGR fuel graphites had indicated that the effect of screening and oversize crushing on the tertiary crusher product size distribution might be minimal (see Section 2.2.2.3.5 and Fig. 2-7). These results were further substantiated by a comparison of the product size distributions obtained from HTGR fuel element graphites which had been crushed with the screener and oversize crusher removed from the system (i.e., "unsized") with the size distributions obtained with those components in the system (i.e., "sized"). Small differences occurred in the products at or below 1000 μm and at or above 4000 μm (see Fig. 2-17). The "unsized" product contained more material ≤1000 μm. This was probably due to an increase in fines caused by attrition during pneumatic transport.

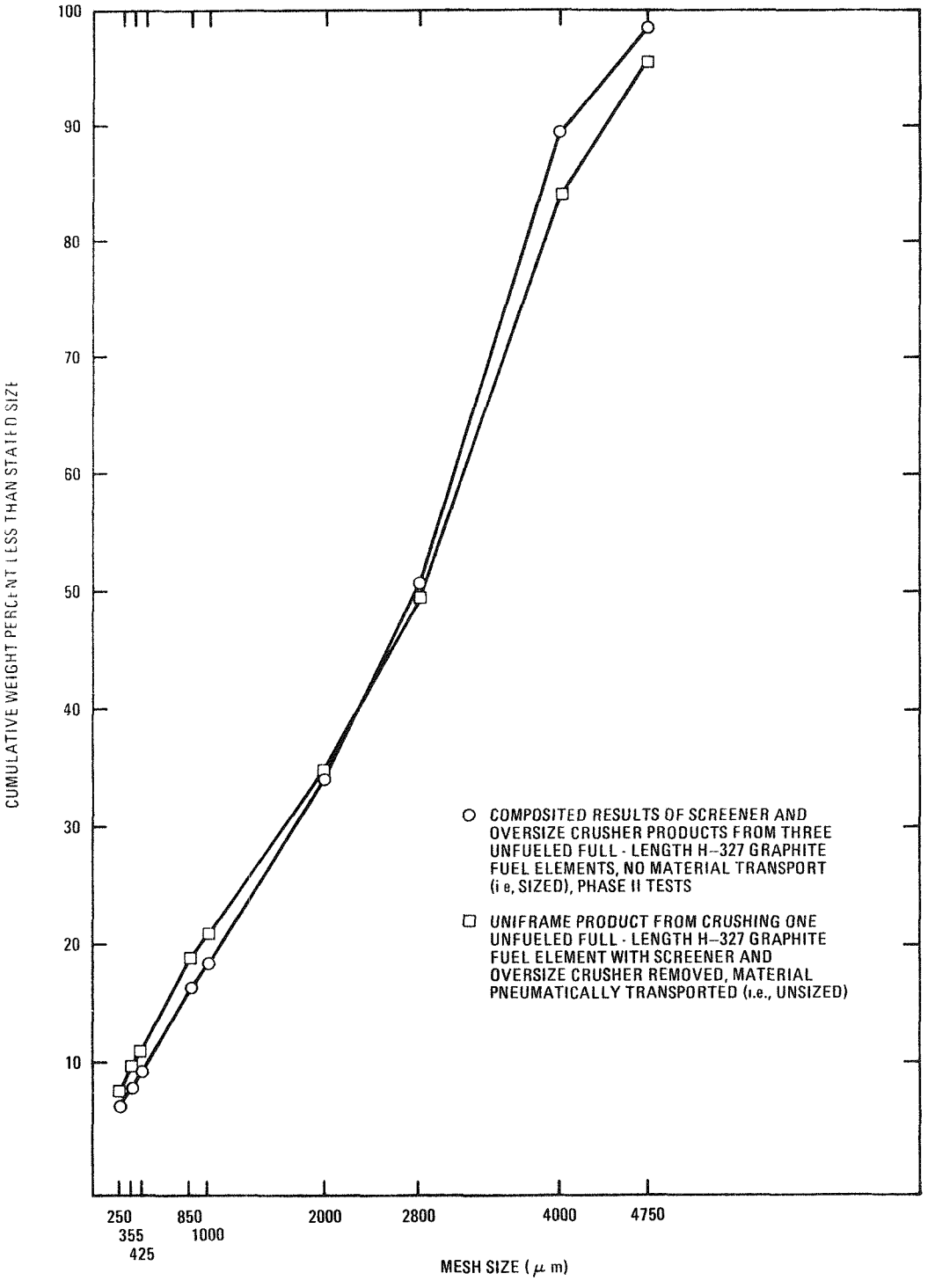

Fig. 2-17. Comparison of size distributions for UNIFRAME products from crushing H-327 graphite HTGR fuel elements

The "unsized" product contained less material ≤4000 μm (conversely, more material ≥4000 μm), an obvious effect of not removing and resizing the +4750 μm fraction with the screener and oversize crusher.

The crushed scrap anode butt graphite did not exhibit the similarities in size distributions between "sized" and "unsized" product that the HTGR graphites had. Instead, the "unsized" product was much coarser (i.e., contained less material in all sizes up to 4750 μm), demonstrating a more pronounced effect of screening and oversize crushing on the final size distribution of anode graphite. Fig. 2-18 illustrates this difference and includes size distribution results from all three of the UNIFRAME operating modes used while crushing anode graphite.

A material balance conducted at the conclusion of these four tests resulted in a MUF of 0.95% (see Table 2-21). This MUF was the highest yet attained and the cause has not been ascertained.

A slot-valve has been designed, constructed, and installed for future tests. This valve will provide a restriction in the oversize crusher discharge to the transport line and should allow control of the pressure drops and prevention of preferential transport of material from the oversize crusher. The oversize crusher and screener inner vibrating section are being reinstalled for these tests.

2.4. VENTILATION SUBSYSTEM

The shrouding for the UNIFRAME ventilation subsystem has been completed with the fabrication and installation of the upper airlock (5210071) (Fig. 2-19). This member contains an opening of sufficient size to permit entry of a whole fuel element. The opening acts as an open-faced hood with inward air flow provided by the material transport blower. Embracing the entry opening is an air sweep collar with two connections to the plant ventilation system. This provides additional ventilation protection when crushing fuel elements containing radioactive particles. Utilization of

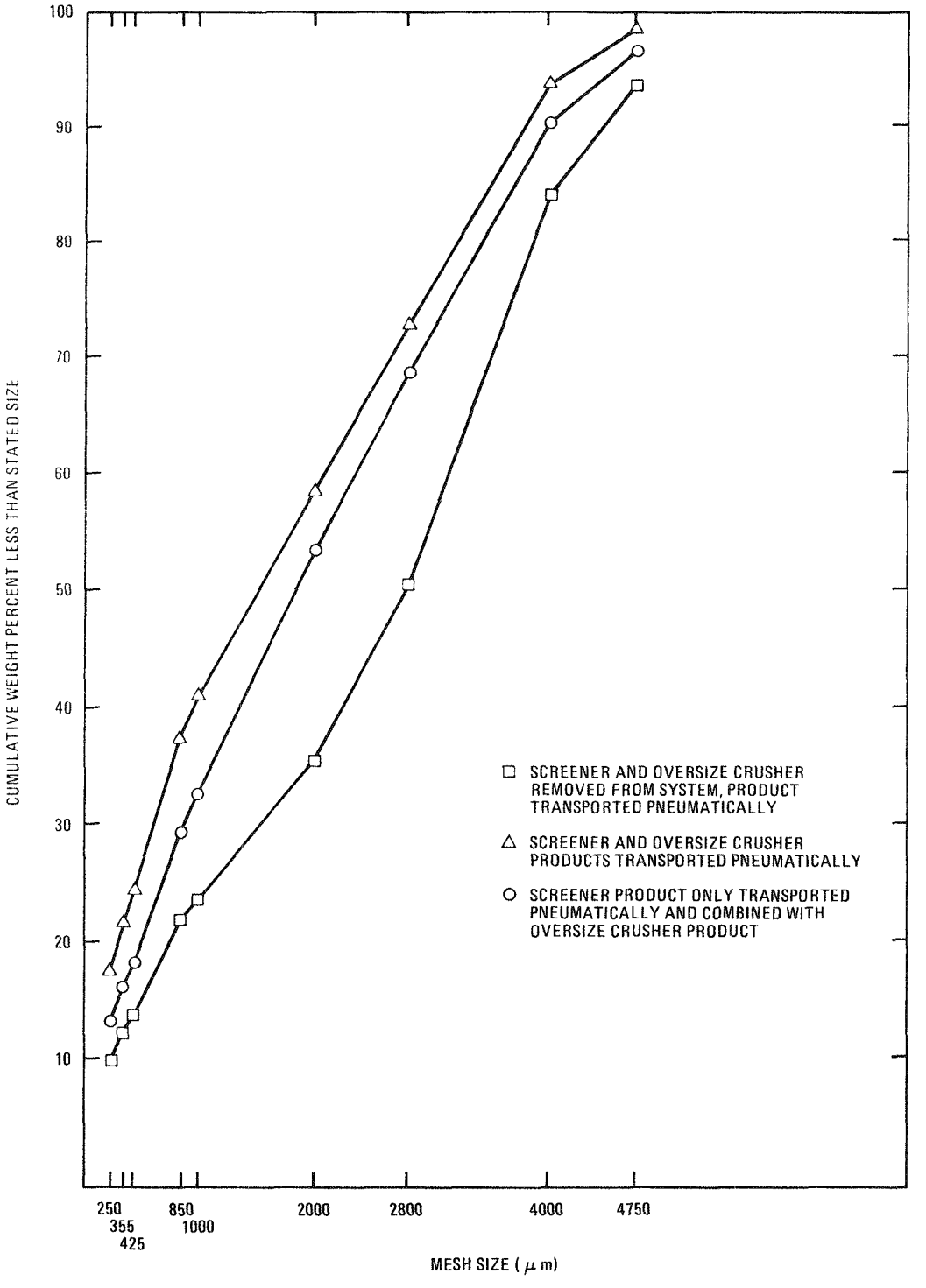

Fig. 2-18. Comparison of size distributions for UNIFRAME products from crushing scrap butt anode graphite

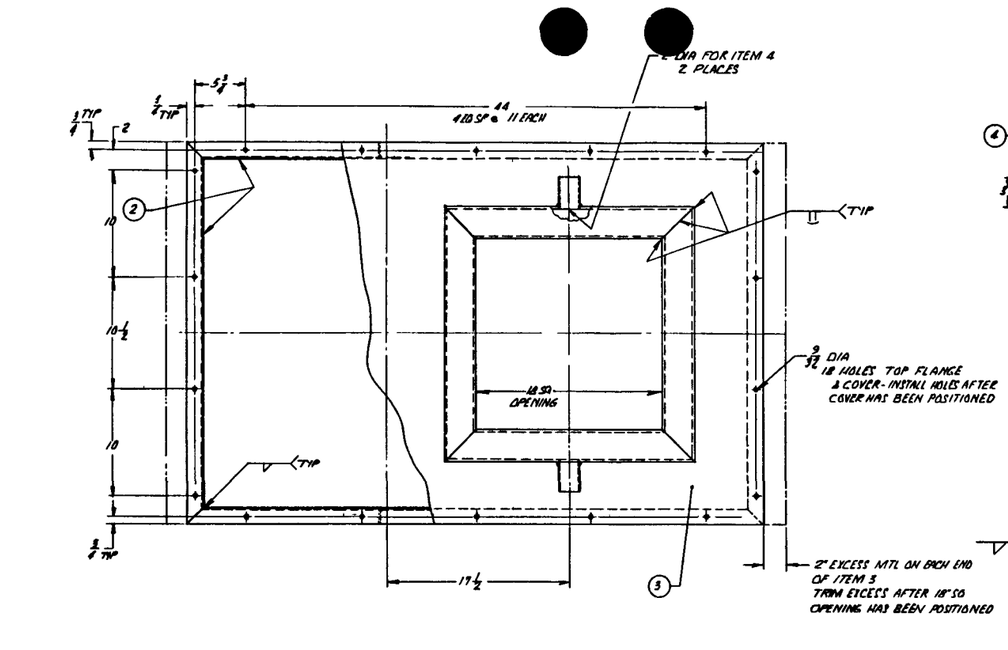

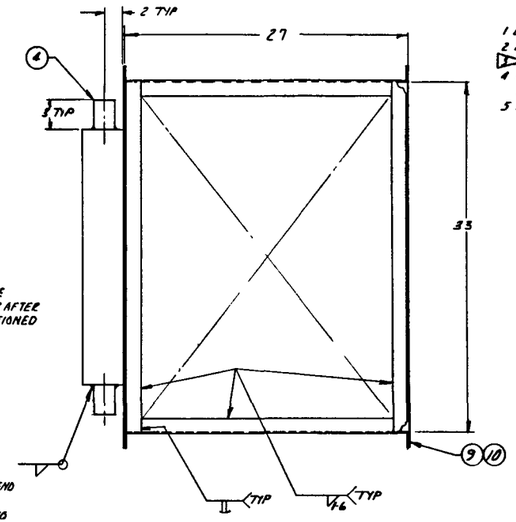

NOTES

1 DIMS & TOLERANCES PER ANSI Y14.5
2 BREAK ALL SHARP EDGES
3 SIDE & END PANELS SHALL BE STIFFENED BY CROSS BREAKING AS SHOWN.
4 ATTACH GASKET TO TOP & BOTTOM FLANGE & BEAR SURFACES USING ITEM 18 CONTACT CEMENT
5 PAINT COAT ALL EXTERIOR SURFACES

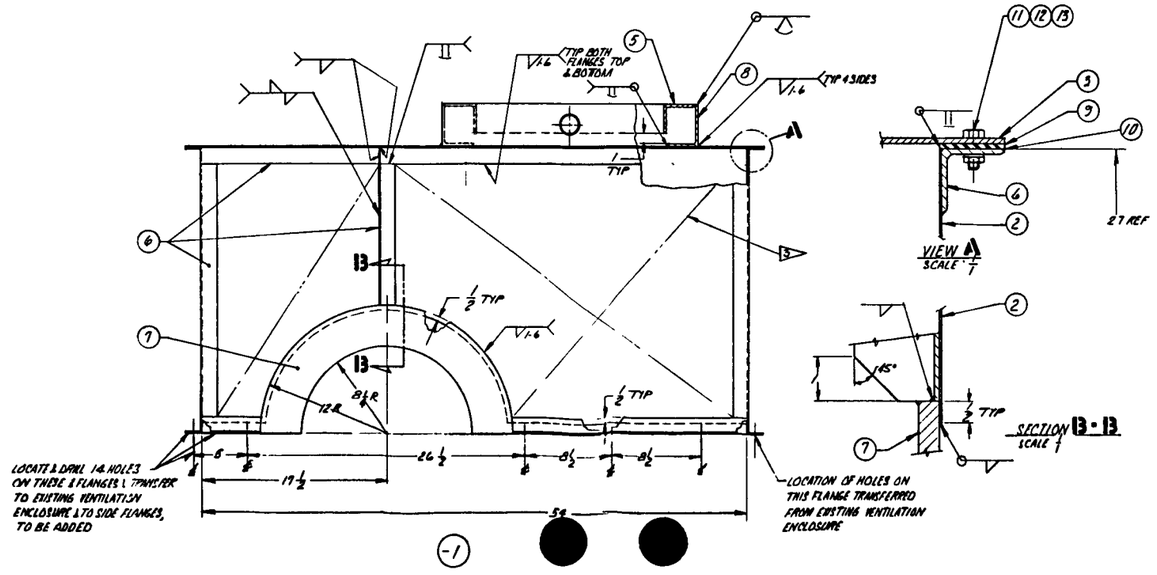

REQ'D/ASSEMBLY	ITEM	PART NO.	DESCRIPTION	MATL	
			LIST OF MATERIAL		
16	12		HEX NUT 1/4-20	STL	
16	12		LOCKWASHER 1/4	STL	
16	11		HEXHD SCR 1/4-20 x 3/4	STL	
AR	10		CONTACT CEMENT		
2	9		GASKET 1/8 THK	NEOPRENE	48 SHORE
AR	8		ANGLE 4 x 3 x 1/4	CARBON STEEL	
2	7		SIDE PLATE 1/2 THK	LOW CARBON STEEL	
AR	6		ANGLE 1 1/2 x 1 1/2 x 1/8	CARBON STEEL	
AR	5		ANGLE 3 x 3 x 1/4	CARBON STEEL	
2	4		TUBE 2 OD x .065 W	CARBON STEEL	
1	3		TOP PLATE 11/8 STK	LOW CARBON STEEL	
AR	2		SIDE PLATES 16 GA (.159)	LOW CARBON STEEL	
	1	5210871-1	UPPER AIRLOCK ASSY		

Fig. 2-19. UNIFRAME upper air lock

TABLE 2-21
MATERIAL BALANCE, SCRAP GRAPHITE CRUSHING

Test No.	Charge (kg)	Recovery (kg)	Gain (+) or Loss (-)	MUF (% of Charge)
SCRAP-19	96.616	94.349	(-) 2.267	2.35
SCRAP-20	98.050	97.080	(-) 0.970	0.99
SCRAP-21	102.895	102.950	(+) 0.055	0.05
Element 1-2319	90.493	89.737	(-) 0.756	0.84
Total	388.054	384.116	(-) 3.938	1.01

Cleanout at Conclusion of Testing

Description	Quantity (kg)	% of Charge
Dust in screener housing	0.247	0.06

Grand Totals

Tests	Charge (kg)	Recovery (kg)	Gain (+) or Loss (-)	MUF (% of Charge)
SCRAP-19 through SCRAP-21, Element 1-2319	388.054	384.363	(-) 3.691	0.95

the plant ventilation system offers a safety backup in the event of shutdown or stoppage of the material transport blower system.

2.5. STRUCTURAL SUBSYSTEM VERIFICATION

2.5.1. Instrumentation

Instrumentation to be used for the verification of the UNIFRAME structural design will provide data for the determination of the true or actual forces required to crush the fuel elements and the true response of the structure to the dynamic loading. Further uses are to establish the validity of the analytical techniques and programs used for design and to upgrade the design tools as required. Direct comparisons will be made at specific sites between the actual and the predicted levels of stress and dynamics. The regions on the structure identified as the most critical by the computer programs and the pitman toggle linkages will be examined first. The two adjusting screws (5210025-6) of the primary crusher are being equipped and calibrated as load cells to permit determination of actual crushing loads.

Simultaneous signals from the strain gages (10 channels) and the accelerometers (12 channels) will be reduced to useful stress and vibrational parameters for comparative analysis. The data processing and reduction will be automatic in response to preprogrammed instructions and will be displayed in real time by data plotters. Preliminary and exploratory data will be displayed on strip charts (12 channels) for evaluation.

The majority of the equipment for the data system is installed and will be operative in this quarter, with the programmable recording and processing equipment and the data plotter available later. Operating personnel have completed initial training on the installation and use of strain gages.

2.6. REDESIGN - CARBON-GRAPHITE BEARINGS

Preliminary investigations of carbon-graphite bearings have continued for their use in a pitman shaft pillow block as a direct replacement of the present bronze bearing and thrust washer. The carbon-graphite bearing will be tested in service without lubrication and will be evaluated for wear life and friction under UNIFRAME operating conditions. Direct comparisons can be made between the carbon-graphite bearing and a conventionally lubricated bronze bearing on the same pitman shaft.

Bearing design information and drawings of the bronze bearings have been sent to manufacturers of carbon-graphite materials for their material and design recommendations. Two manufacturers have offered specific product formulations and have submitted proposals for the replacement bearings and thrust washer.

Further action on this redesign has been deferred pending completion of the pilot plant sequential operations.

2.7. CONCLUSIONS

Phase II system tests of the UNIFRAME revealed no serious problems, and the system is being readied for testing with fuel-loaded elements. Minor differences in the coarsest UNIFRAME products and the tentative acceptance criteria for primary burner feed will be resolved using future burner and UNIFRAME tests to determine the impact of the difference.

REFERENCE

2-1. "Thorium Utilization Program Quarterly Progress Report for the Period Ending February 28, 1977," ERDA Report GA-A14304, General Atomic Company, March 1977.

3. CRUSHED FUEL ELEMENT BURNING

3.1. PRIMARY BURNER SUMMARY

Two runs were made on the 0.40-m primary burner. These runs were the initial combustion tests on the system and included in-bed fines recycle via the gas distributor cone vertex line. The results of the runs indicated that carryover of bed fuel particles and breakage of these particles in the fines recycle loop were similar to past 0.20-m burner work (4 to 6 wt % breakage of particles fed). In the 0.40-m burner system burnout of the carbon in tailburning the recycling fines was not as efficient as previously seen in 0.20-m burner work. The lack of above-bed O_2 injection in the 0.40-m burner was considered a major factor contributing to the inefficient fines tailburning. Installation of a burner penetration for the additional O_2 was therefore planned prior to further tests. Other areas which were identified as problems and were revised included (1) replacement of a fines recycle subsystem bellows with an improved design and elimination of several bellows which were found to be high risk failure areas; (2) installation of stiffer burner alignment mechanisms to replace the Peaucellier devices; and (3) a change in the outlet configuration of the fresh feed bunker outlet piping to circumvent the possibility of bridging of graphite fines. Test plans (AP524401C) for the 0.40-m burner were reviewed and restructured, based upon the results of these short-duration runs, to improve the overall system shakedown prior to planned long-duration runs.

Reassembly and inspection of the 0.40-m burner prior to the combustion tests indicated acceptable cooling air sealing by the machined graphite sliding seal and excellent sealing of the burner vessel by the reinstalled plenum clamp/seal ring.

The 0.40-m primary burner design evaluation was completed, resulting in recommendations for testing of potential design improvements on the 0.20-m primary burner.

The Diogenes high bed temperature selector problem was traced to a software problem in the system "read-only-memory" (ROM). Programming changes were made to the ROM and it was reinstalled in the Diogenese system prior to the final primary burner run in this reporting period (0.40-m Test C.1). The selector problem was not experienced in this one run, but additional runs are necessary to validate the repair and to continue automatic controller tuning which was curtailed by the ROM malfunction.

Four attempts to complete the 48-hour run on the 0.20-m burner were made in this reporting period. The initial run attempt was shut down soon after startup when the off-gas filter ΔP and the resultant system backpressure became excessive. A startup bed containing $\sim$4 wt % moisture had inadvertently been used in a shakedown run immediately prior to this initial run attempt, and the resultant condensation on the filters induced a buildup of a fines cake which could not be blown off. Filter cleaning and replacement allowed operation of increased duration in the next three tests. However, feed controller inaccuracy caused feed rates slightly in excess of burn rates and ultimately resulted in fines accumulation which exceeded the fines hopper volume. In the final run attempt, the large volume of fines was being reduced by burning in an extended fines tailburning period. A relatively short fuel particle bed reaching only the lower portion of the induction heated zone of the wall became segregated in temperature from the fines burning zone just above the bed. Ignition of a poorly mixed bed carbon layer resting on top of the short, defluidized particle bed apparently combined with the induction heater power input to cause a high localized temperature, which melted the wall (burnthrough). This required that the burner be shut down. The vessel will be repaired in conjunction with planned upgrading modifications of the fines recycle system. In addition, the capability for heating small beds will be improved and the operating procedures will be modified to exclude attempting re-ignition of beds below 650°C.

3.2. PROTOTYPE 0.40-m PRIMARY BURNER

3.2.1. 0.40-m Burner Initial Combustion Tests

3.2.1.1. Introduction

Tests B and C were the first runs on the 0.40-m primary burner involving actual combustion operation and in-bed vertex fines recycle. Hence, these runs served as the initial checkout of the burner system and resulted in identification of several mechanical areas which required revision. Further, the data obtained in this first use of vertex fines recycle on the 0.40-m burner were critical in determining fines recycle requirements in future long-term operation.

3.2.1.2. Experimental Results

The results of the successful Test B initial combustion run and the partially completed Test C are summarized below. The results are qualitative as analysis of data is not yet complete and available for presentation.

3.2.1.2.1. Test B Results. Test B operation studied the overall 0.40-m burner system response to low carbon combustion with pressurized, vertex fines recycle. A low carbon bed consisting of 85 wt % carbon coated FSV TRISO fertile particles and 15 wt % $\leq$4762 μm graphite was the startup material; additional coated particles were fed during combustion to maintain sufficient bed height for induction heated tailburning. The dual parallel pressurized hopper system was successfully used to recycle fines to the vertex during the combustion and tailburning phases of operation. The fines system operated without problems. The 0.40-m burner lower bed temperature was much more stable in response to the intermittent vertex fines flow than was experienced in 0.20-m burner work. Preliminary evaluation of the material balance indicated that the fuel particle carryover and breakage were similar to the 4 to 6 wt % experienced in 0.20-m burner vertex fines recycle runs.

The fines recycle subsystem instrumentation and the bed temperature response indicated uninterrupted material flow. The bed temperature cycling (±10°C) was less than observed on the 0.20-m burner (±50°C). The recycle mass flow rate was over 10 kg/min using 50 SLPM transport gas, a 20 to 34 kPa (3 to 5 psig) line pressure drop, and recycle hopper pressures of 69 kPa (∿10 psig).

Preliminary analysis of the Test B fines hopper contents indicates that the fuel particle breakage in feed handling, fluid bed burning, and fines recycle was greater than 3 wt %. Microscopic examination of the product bed samples after pneumatic transport revealed significant hull and oxide content, which would increase the overall breakage. Less particle holdup was observed in the 0.40-m fines hoppers (∿0.5 kg) than in the 0.20-m fines hoppers (∿2 kg), indicating that this system recycles particles more efficiently than the 0.20-m system. However, the final inventory of graphite fines was much larger (5.8 kg) than that observed with the 0.20-m (<1 kg). The remainder of the 11.8 kg total final fines hopper contents consisted of ∿5.5 kg of oxides mixed with fragments of SiC particle hulls <<355 μm. This oxide/hull content was also much larger than found in the past 0.20-m burner work. This final fines inventory occurred after an extended fines tailburning period at high fines recycle rates.

Test B was extended to obtain a heat transfer coefficient for the burned-back TRISO fertile particle bed for comparison with coefficients calculated for carbon coated particles (Test A results, Ref. 3-1). A restart and heatup of the burned-back particle bed allowed study of both transport and heatup of burned-back particles in comparison with carbon coated fuel.

Two major areas of the burner mechanical system requiring modification were identified during Test B. First, the horizontal deflection of the burner within the constraints of the Peaucellier mechanisms was unacceptable [∿9.5 mm (∿3/8 in.)]. Second, "breathing" of the unstiffened surface of the filter chamber caused surface deformations.

3.2.1.2.2. Test C Results. Test C.1 was an attempted 0.40-m burner run with a typical high carbon fresh feed bed startup and with BISO fertile/TRISO WAR fissile particles as the additional feed. The test was shut down after 6.5 hours of operation when a rupture occurred in a fines recycle bellows. The 0.15-m-ID failed bellows was in the connection between the cyclone and filter chamber discharge line and the fines hopper inlet (see Fig. 3-1). The average fines recycle hopper temperature had reached ∿440°C at the time of the bellows failure, as compared to temperatures of ≲260°C in the prior low carbon combustion Run B. The bellows collapsed when the inner sleeve impinged upon and tore the bellows wall.

The duration of the Test C.1 run attempt was sufficient to obtain heat transfer data for BISO/TRISO fresh feed and, consequently, will allow shortening the next run (to complete Test C) by ∿2 hours. Another benefit of the run was to identify additional mechanical problem areas. First, the feed bunker outlet configuration induced bridging of graphite fines. Secondly, the bellows in the 0.10-m-ID fines hopper inlet pipes were found to be distorted (see Fig. 3-2).

3.2.1.3. Conclusions and Recommendations

3.2.1.3.1. Test B Conclusions and Recommendations.

The difference between the larger final inventory of graphite fines in 0.40-m burner Test B relative to prior 0.20-m burner tests may have been due to some operational discrepancy. However, the Test B extended fines tailburning period with vertex fines recycle was similar to 0.20-m tailburns which were very successful in burning out the carbon in the recycling fines. Hence, process and/or burner configuration differences are possible explanations.

The process differences between Test B and past 0.20-m vertex recycle work include the very large oxide/hull content of the recycling fines in 0.40-m burner Test B and the fact that no above-bed source of O_2 was available on the 0.40-m burner. A maximum of ∿20 wt % oxide/hull content was

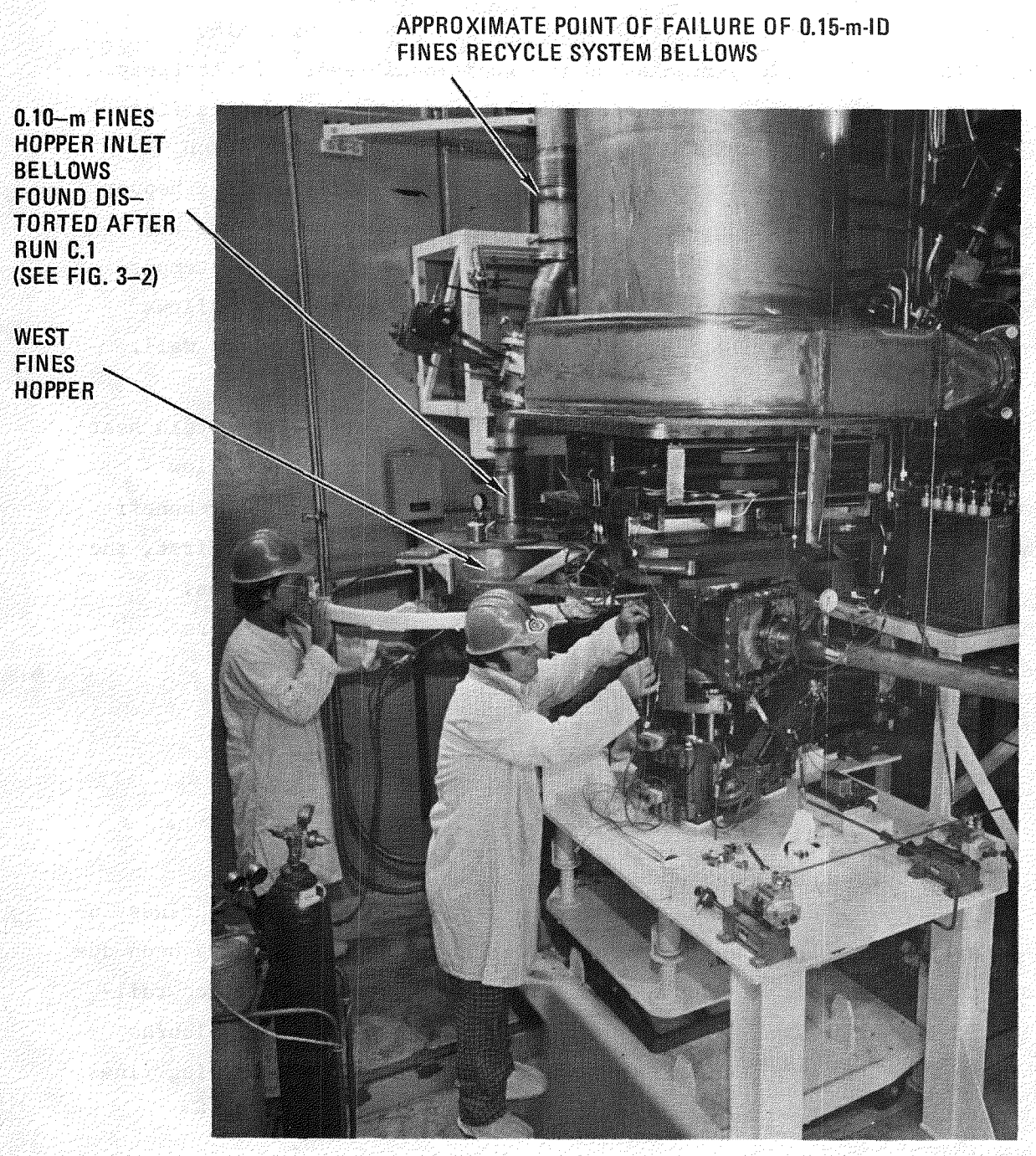

Fig. 3-1. Location of failed bellows, 0.40-m primary burner Test C.1

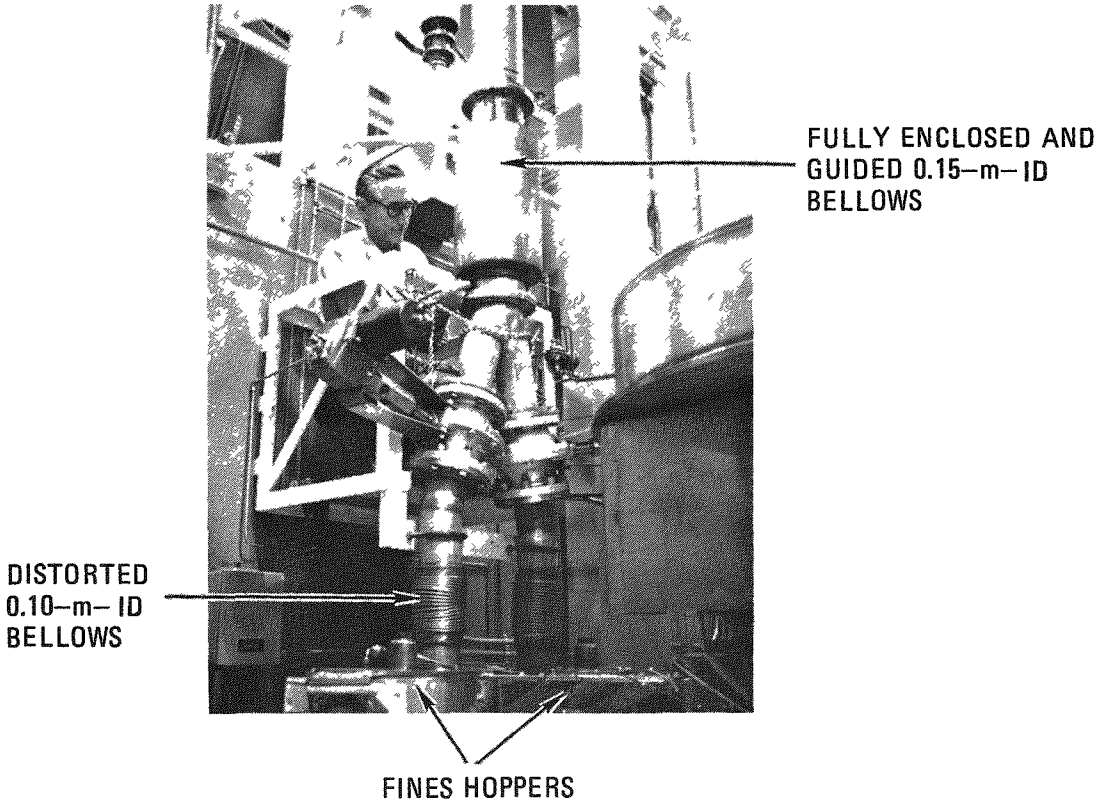

Fig. 3-2. 0.40-m primary burner fines recycle system showing 0.10-m ID distorted bellows and 0.15-m ID bellows replacement

noted in 0.20-m vertex recycle test work, as compared to the ∿50 wt % oxide/hull concentration observed in Test B. The less efficient Test B fines burnout may be associated with this higher oxide/hull concentration in that the greater mass of noncombustible fines may interfere with and limit the reaction kinetics of the recycling graphite fines. Further, the lack of above-bed O_2 throughout Test C compares to past 0.20-m work using above-bed injection of O_2 equivalent to 10 to 20 vol % of the total inlet O_2. Although this above-bed O_2 is generally not used during tailburning, its use throughout the preceeding equilibrium operation is now thought to be essential in maintaining a low fines inventory and minimizing the fines tailburning period.

Differences in the configuration of the 0.40-m burner relative to the 0.20-m burner which could affect the elutriation-burning mechanism are the lack of the above-bed gas injection in the 0.40-m burner and the relatively shorter 0.40-m length. The rapid elutriation of fines (and larger particles) in the slugging of vertex fines recycle operation may be dampened by the injection of above-bed gas perpendicular to the rising slugs. This perpendicular gas injection could destabilize the large gas bubbles that carry the solids slugs and actually shorten the height of the worst slugs. Such slug height decreases may increase the fines residence time within the burner, thereby increasing fines burning efficiency. Decreased slugs would also decrease the quantity of fuel particles carried into the recycle loop (which, in turn, would decrease particle breakage and interference of the high oxide/hull concentration in the fines). Finally, the 0.40-m overall tube length would require an extension of ∿1.6 m to match the scaled length of the 0.20-m tube. This difference may give slightly less fines residence time and slug retention in the 0.40-m burner versus the 0.20-m burner.

Summarizing Test B conclusions regarding fines recycle, the present burner configuration with vertex fines injection may be operational in planned long-term 0.40-m burner runs but may cause excessive particle breakage and accumulation of oxides/hulls. This accumulation in combination with the mass of inefficiently burning graphite fines could exceed the

capacity of the present fines recycle hoppers. These conclusions call for:

1. Installation of an above-bed burner wall penetration for O_2 injection.

2. A revision in the scope of operations planned for completion of Run C to better assess the fines system capabilities in long-term operation. This revision would change the Activity Plan (AP524401C) by altering the type of additional feed fed into the Test C startup bed from BISO/TRISO particles ($\sim$30 wt % carbon) to typical fresh feed ($\sim$85 wt % carbon) and would add the use of above-bed O_2 to the vertex recycle operation. Such operation, when continued for $\gtrsim$12 hours, should determine the long-term operability of the existing fines recycle system and indicate whether additional revisions are necessary.

3.2.1.3.2. Test C Conclusions and Recommendations. The failure of the fines recycle bellows was attributed to uneven thermal expansion due to the flow pattern of the hot fines in the piping above the bellows in combination with some initial misalignment. This caused radial movement of the inner sleeve of the bellows. A metal bellows design using a fully enclosed and guided expansion joint was procured and installed (see Fig. 3-2). Figure 3-3 shows the difference between the unguided failed bellows and the guided design installed to alleviate the inner sleeve impingement failure mode.

The bridging of graphite fines in the feed bunker outlet was thought to be due to an apparently excessive length of pipe which couples the aerated bunker outlet to the rotary feed mechanism. This pipe section (Fig. 3-4) is to be removed and the rotary valve installed directly under the knife-gate valve in the feed bunker outlet. This should avoid the packing or bridging tendency of "pockets" of fines in the graphite feed.

The distortion of the 0.10-m-ID bellows in the fines hopper inlet pipes was attributed to slippage of a hopper brace and uneven loading. These bellows are high risk failure areas based on the observed distortion

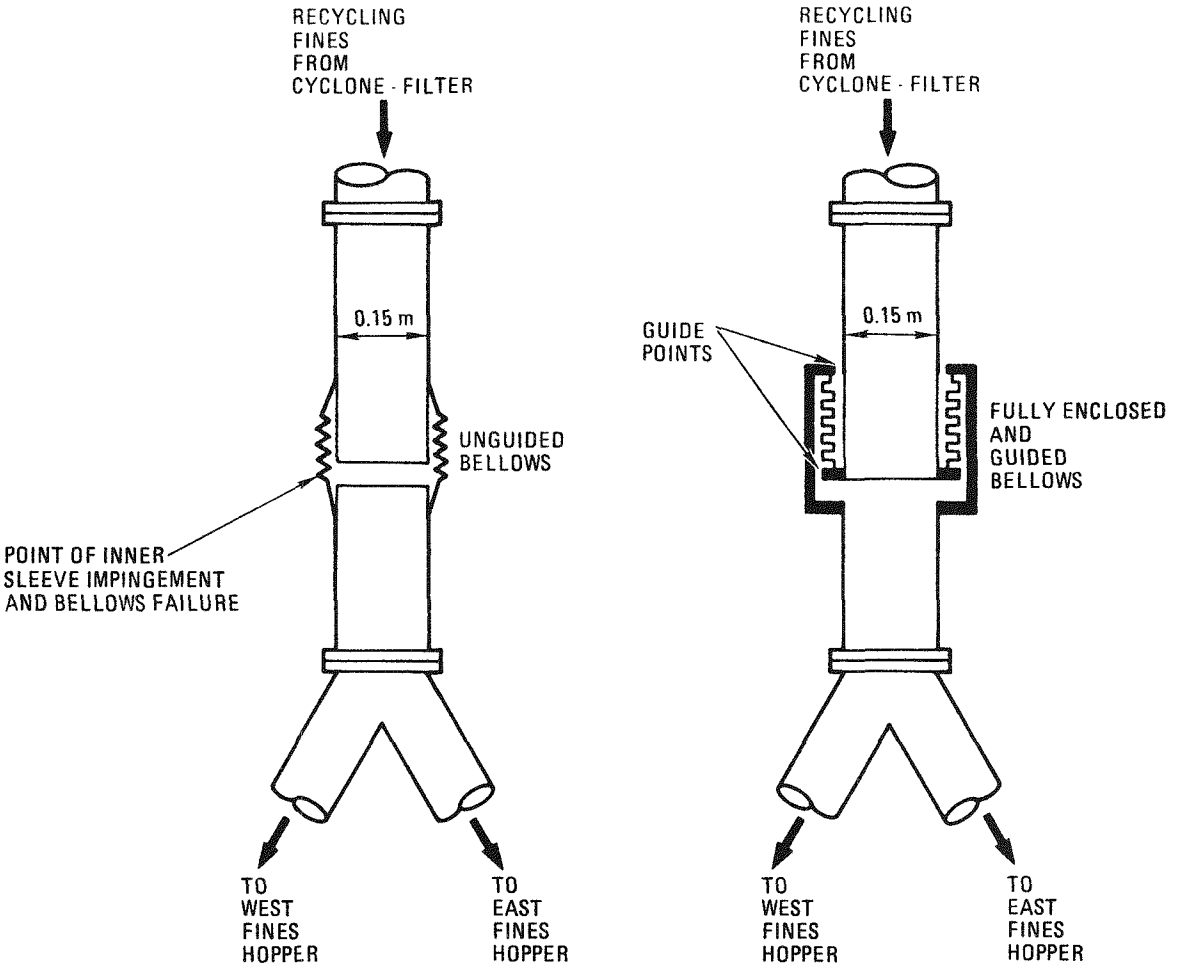

Fig. 3-3. 0.40-m primary burner unguided versus guided bellows

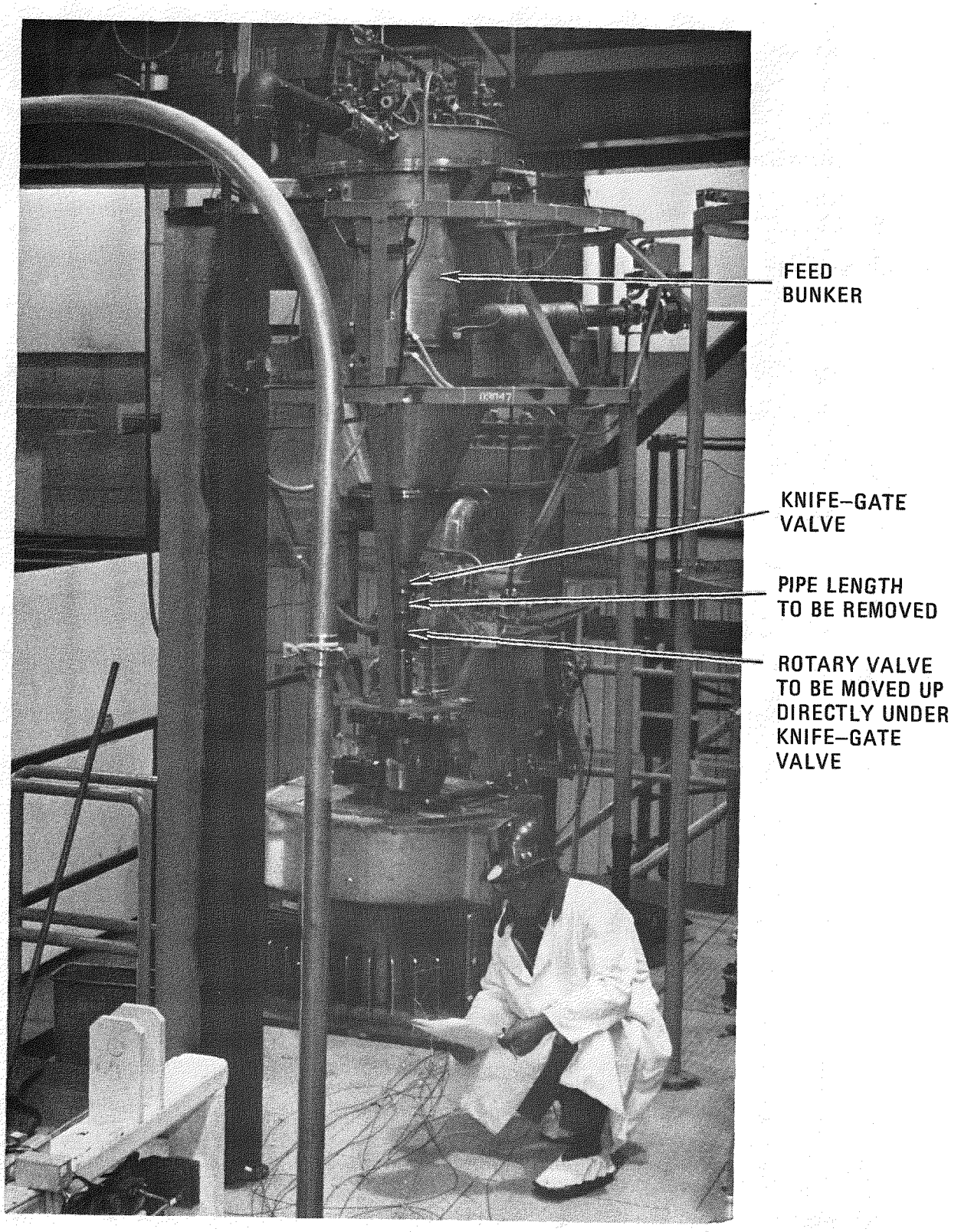

Fig. 3-4. 0.40-m primary burner showing feed bunker outlet

and the failure of the 0.15-m bellows discussed above. These bellows and the fines hopper outlet 13-mm bellows were installed for the load cell system. The load cells have not provided accurate hopper weights due to the effect of pressure surges inherent to the pressurized fines system. Hence, their high probability of failure combined with their lack of utility suggest that these bellows be replaced with rigid pipe sections. This is to be implemented.

The longer duration operation recommended for Test C in the previous section will yield operating experience with these revised mechanisms.

3.2.2. 0.40-m Primary Burner Inspection and Reassembly

3.2.2.1. Introduction

The sliding graphite cooling air seal was to be monitored for performance (Ref. 3-1). Cold testing suggested minor revisions to the seal.

The plenum chamber was to be installed and the burner leak tested prior to test B. The knife-gate product outlet valve in the plenum vertex pipe also required leak testing.

3.2.2.2. Activity

The cooling air seal was tested at room temperature with cooling air rates of 1.18 m^3/s (2500 cfm) at pressures up to 34 kPa (5 psig). The seal was also monitored during combustion operation at process temperatures.

The plenum assembly was installed and the clamp/seal ring mechanism was torqued to the specified levels. The seal ring and burner vessel were leak tested by a pressure decay test with a blind flange isolating the knife-gate product outlet valve from the pressurized vessel. The blind was then removed and the leak test repeated to analyze the leakage of the knife-gate valve.

3.2.2.3. Conclusions and Recommendations

The room temperature cooling air leak test of the sliding seal indicated that modest alterations were required to reduce the cooling air leakage to an acceptable level. Figure 3-5 and Table 3-1 identify the detected leaks, the corrective actions taken, and the results when using 1.18 m^3/s (2500 cfm) and 34 kPa (5 psig) cooling air at room temperature. Leakage during subsequent combustion tests was similar to the room temperature findings and was considered acceptable.

The burner system leak rate was $<1.14 \times 10^{-3}$ m^3/h measured over a 3-day decay test. This minimal leakage occurred through the reinstalled plenum clamp/ring seal and three other clamped blind flange areas. The subsequent leak test on the system which included the knife-gate valve indicated an ~ 0.21 m^3/h leakage as observed over a 50-min decay test. Most of this leakage was through the slide valve seats, with some leakage found through the packing of the slide stem. The leakage was considered acceptable as it represents <0.2 vol % of the 120 m^3/h nominal inlet gas flow rate.

3.2.3. 0.40-m Primary Burner Peaucellier Mechanism Replacement

3.2.3.1. Introduction

The excessive horizontal deflection of the burner in Test B called for replacement of the Peaucellier mechanisms with stiffer alignment devices (see Section 3.2.1.2.1, Test B Results). The Peaucellier mechanisms and their replacement are discussed below.

3.2.3.2. Discussion

During Run B the bottom end of the burner exhibited excessive side motion induced by the slugging behavior of the fludized bed, despite the engagement of the Peaucellier mechanisms which provide restraint against lateral movement of the burner tube (see Fig. 3-6). The end of the burner

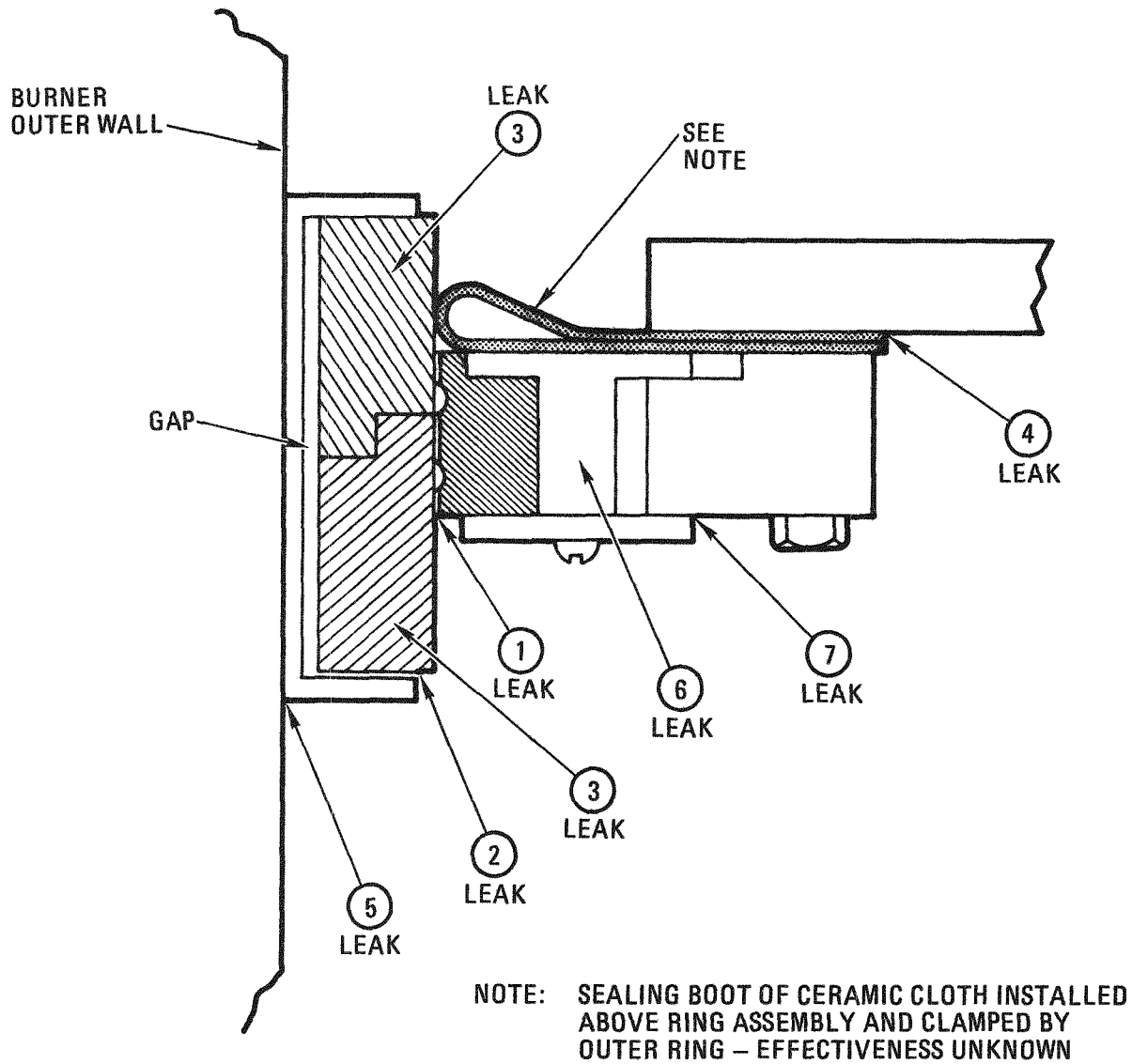

Fig. 3-5. Modified lower seal leak locations (see Table 3-1 for description of leak locations, corrective action, and room-temperature leakage)

TABLE 3-1
TESTING OF MODIFIED LOWER SEAL, 0.40-m PRIMARY BURNER

Leak No. (See Fig. 3-5)	Location	Corrective Action	Room Temp. Leakage[a]
1	Between seal elements (OD/ID leak)	Reduce outer seal circumference	Minimal
2	Between shroud and seal elements	Install ceramic cloth (SiO_2) to fill longitudinal gap	None
3	Between butt ends of inner seal segments	Install spline bridging butt ends of top members	None
4	Between gasket and mounting plate	Regasket	None
5	Between shroud and burner tube	Apply fillet of high-temperature cement	None
6	At expansion joint of seal ring assembly	Pack with ceramic cloth detained by shim clamped by clamp ring	None
7	At slipjoint between seal ring assembly elements	None feasible	Small

[a] Blower air test at 1.18 m^3/s (2500 cfm) and 34 kPa (5 psig) (burner).

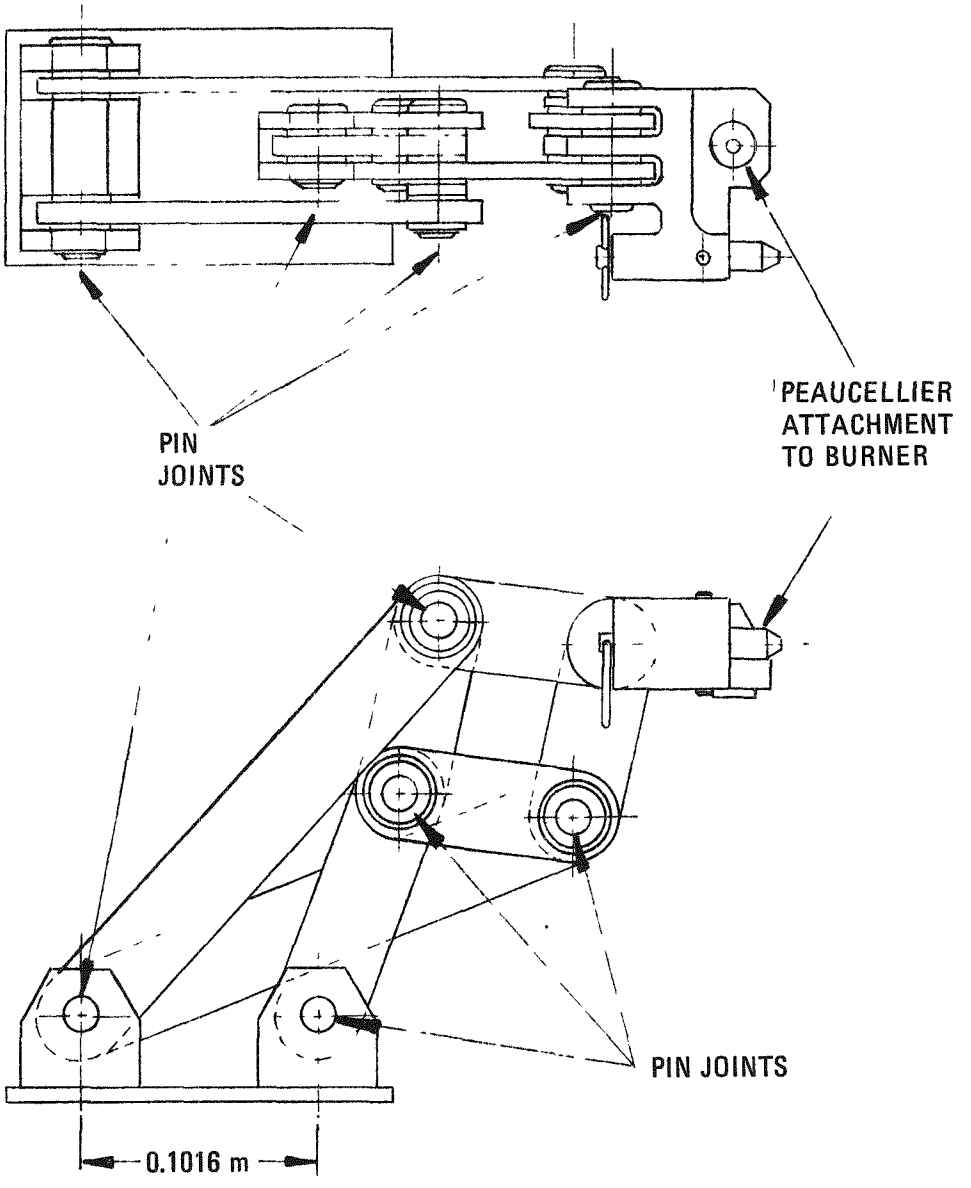

Fig. 3-6. 0.40-m primary burner Peaucellier mechanism

was observed to move an estimated 9.5 mm (0.375 in.) at maximum displacement, whereas the structural platform to which it is attached appeared not to deflect. From post-test examination it was concluded that the stack-up of tolerances in the multiple pin joints amplified by the particular arrangement of linkages permitted the observed deflection to occur. This degree of motion would be detrimental to the lower sliding seal between the burner and the shroud and had to be eliminated. Two solutions were considered.

1. Rework of the existing Peaucellier mechanisms to reduce the lateral deflection.
2. Replacement of the Peaucellier mechanisms with simpler single-bar linkage.

The reason for adopting the Peaucellier cell was that it provides theoretically perfect straight line guidance as the bottom of the burner grows downward. As shown in Fig. 3-7, the maximum theoretical horizontal deflection which results from using a 250 mm (9.83 in.) long single link connection is 0.7 mm (0.028 in.).

3.2.3.3. Conclusions and Recommendations

The 0.7-mm horizontal deflection was acceptably small and consequently the simpler and less expensive single linkage was selected over a more costly precision remachining and reassembly of the existing Peaucellier cells. The new connecting linkage design is shown in Fig. 3-8 and the installation is shown in Fig. 3-9.

3.2.4. 0.40-m Primary Burner Wall Penetrations

3.2.4.1. Introduction

The recommendation for an above-bed penetration for O_2 injection was discussed previously (see Section 3.2.1.2.1, Test B Results). Successful application of a bed level sensor in the 0.20-m burner (see Section 3.3.4,

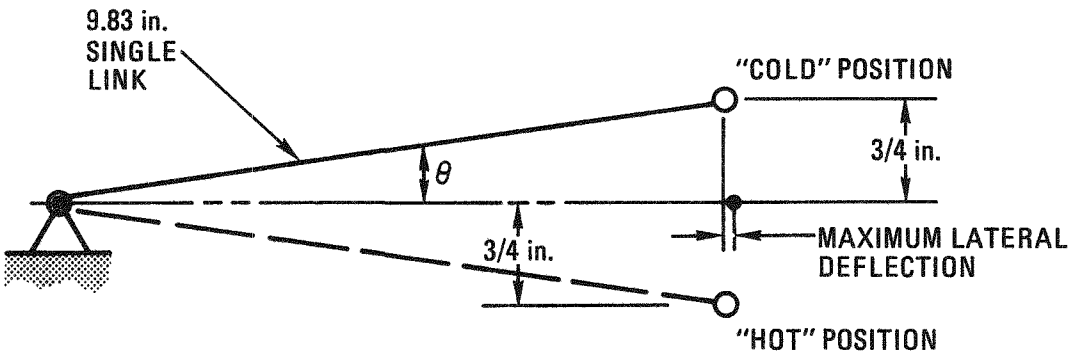

$$\theta \simeq \frac{0.75}{9.83} = 0.076 = 0.076 \left(\frac{180}{\pi}\right) \simeq 4.35^\circ$$

$$\begin{aligned} \text{MAXIMUM LATERAL DEFLECTION} &= 9.83\,(1 - \cos\theta) \\ &= 9.83\,(1 - \cos 4.35^\circ) \\ &= 0.028 \text{ in. } (0.7 \text{ mm}) \end{aligned}$$

Fig. 3-7. Side deflection of single guide link

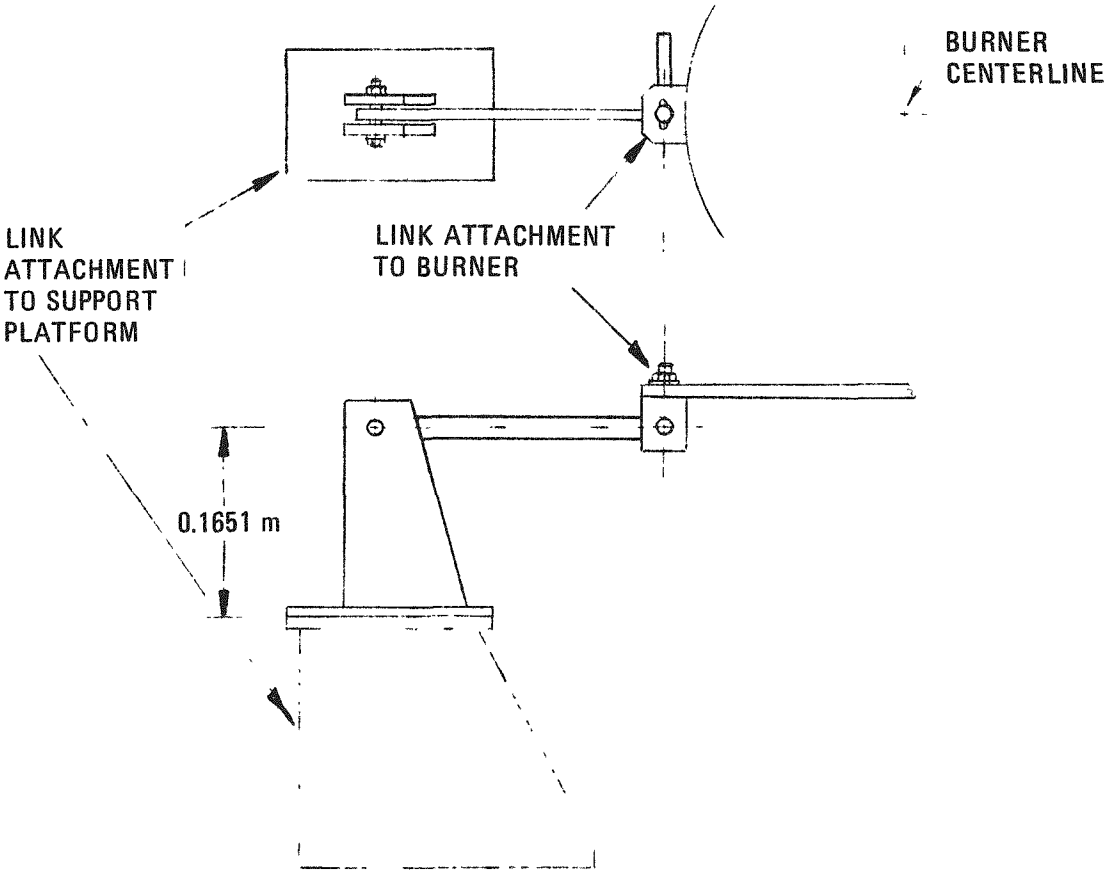

Fig. 3-8. 0.40-m primary burner connecting link

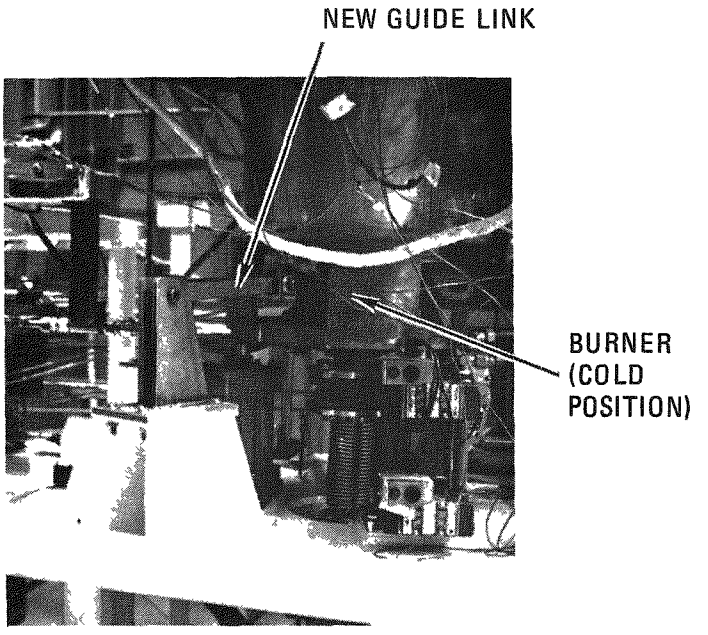

Fig. 3-9. 0.40-m primary burner showing new guide linkage

0.20-m Primary Burner Bed Level Sensor) suggested that a similar sensor in the 0.40-m burner would be beneficial. The penetrations for the above-bed O_2 and for the bed level sensor are discussed below.

3.2.4.2. Discussion

Designs for the addition of a mid-reactor gas line and a level sensing probe to the 0.40-m burner are shown in Fig. 3-10. The studded bosses welded to the burner wall are Hastelloy X and are identical for both penetrations. The mid-reactor gas line through the shroud is a stainless steel braided bellows to allow for differential thermal expansion between the shroud and the vessel. The shroud penetrations are 88.9 mm (3.5 in.) diameter stainless steel tubes.

3.2.4.3. Conclusions

The shroud penetrations are sized so that the shroud can be swung open from the hinge points with the mid-reactor gas line and the level probe instrument line connected to the vessel.

The penetrations not only provide the capability of above-bed O_2 injection and level probe placement, but also allow inclusion of above-bed pressurized fines recycle if further 0.40-m burner tests with in-bed vertex recycle uield negative results.

3.2.5. 0.40-m Primary Burner System Design Evaluation

3.2.5.1. Introduction

Possible modification of the existing dry head-end cold pilot plant engineering-scale equipment to reliable and maintainable equipment that is prototypical of the HRDF design has required an evaluation of the existing equipment design. This evaluation has taken into account performance, cost, ease of implementation of changes, impact of changes on the current HRDF design, and customer (ERDA) acceptance. Feasible alternative designs have been similarly evaluated. The entire evaluation has been completed.

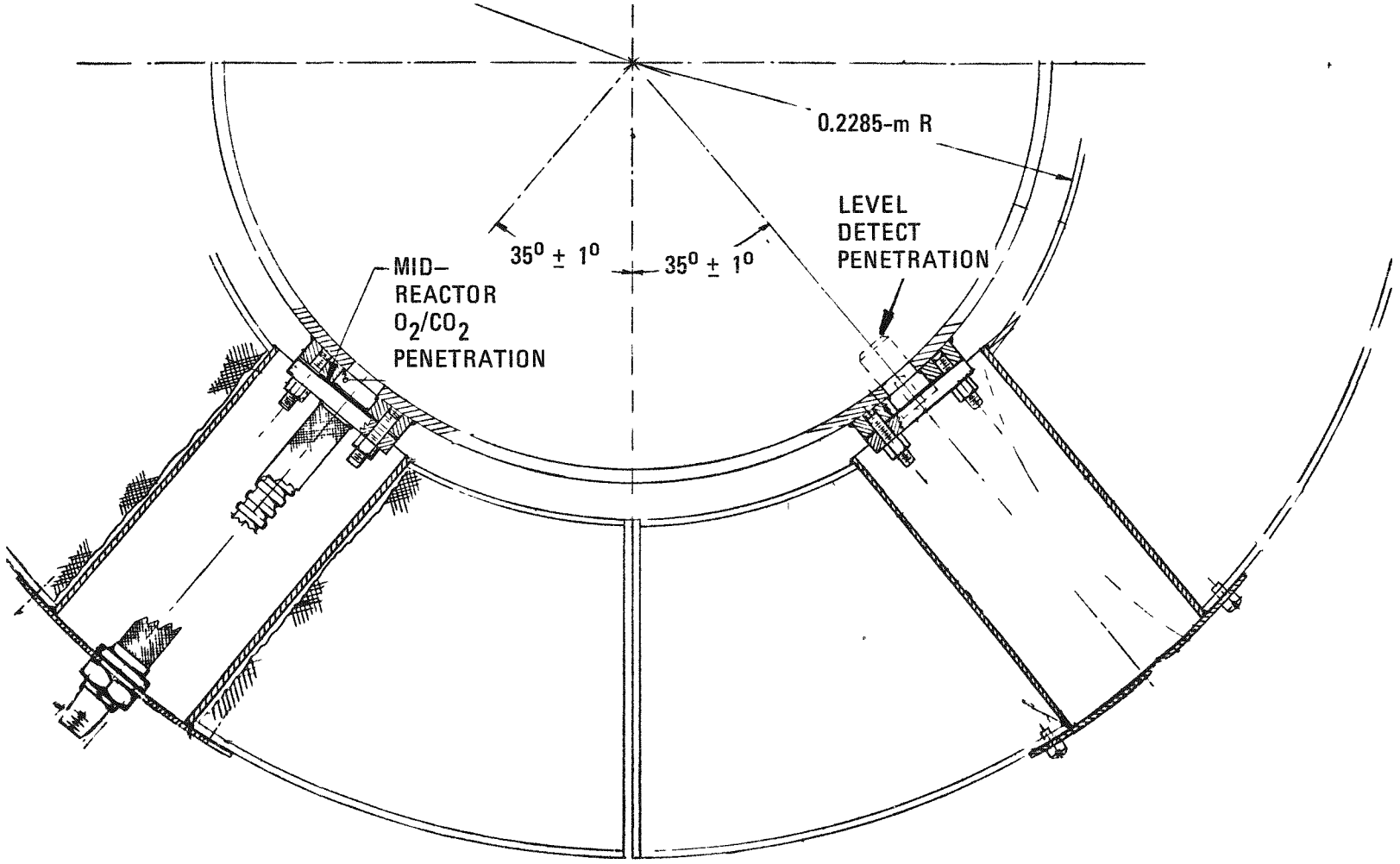

Fig. 3-10. 0.40-m primary burner wall penetrations

3.2.5.2. Activity

Thirteen features constituted the scope of the design evaluation, as follows:

1. Separability of upper and lower cooling shrouds.
2. Hinged doors on upper shroud and lower plenum.
3. Sliding seal between cooling shroud and vessel.
4. Remote disconnects (main vessel flanges and smaller flanges).
5. Concept of a coolant pressure boundary (shroud) external to the vessel.
6. Absence of recycle fines cooling capability.
7. Method of waste heat rejection from (in-cell) burner equipment.
8. Method of attachment of vessel thermocouples.
9. Method of fabrication of the susceptor.
10. Length of the burner tube.
11. Type of burner insulation used.
12. Method of heating the burner vessel and its contents.
13. Design of the insulation bonnet assembly.

For each of these features, information was compiled in the following sequence:

1. Technical evaluation of the existing system design.
2. Analysis of the existing system costs.
3. Selection and technical evaluation of alternative system designs.
4. Analysis of alternative system costs.
5. Comparison of the existing and alternative systems based on value engineering techniques.

Based on this information, design options for each of the thirteen features were selected to give the best "performance" (operability, maintainability, reliability, compliance with design criteria and technical specifications, licensability, etc.). Another set of options was selected to give the best "value" (ratio of performance and installed cost). These options are listed in Table 3-2.

The options given in Table 3-2 were evaluated and selected independently without consideration of interfacing with any of the other features. However, to consider the effect of the best designs in each case on the whole system, two integrated burner system design concepts that constitute the best "composites" of design options were developed. One concept represents the "best value" composite but may include inherent, relatively high development risks of failure to achieve design objectives (Table 3-3). The other concept represents the "minimum risk" composite but may result in only modest improvements in performance or cost (Table 3-4).

3.2.5.3. Conclusions and Recommendations

The following conclusions and recommendations are made:

1. This evaluation has led to recommendations for the parallel development of two integrated design concepts for a prototype primary burner system. One concept utilizes the existing burner heating and cooling subsystems but simplifies a number of other features associated with remote maintenance and burner operation; this concept involves minimum development risk to achieve design objectives. The other concept modifies the heating and cooling subsystems and also eliminates or simplifies a number of other features associated with heating, cooling, remote maintenance, and burner operation. The modified heating subsystem uses hot gaseous carbon dioxide and direct-contact heating of the burner contents; the modified cooling subsystem uses an internal gas-cooled heat exchanger. This second integrated design concept

TABLE 3-2
BEST OPTIONS FOR DESIGN FEATURES

Design Features	"Best Value" Option	"Best Performance" Option
1. Cooling shroud separability	Eliminate induction coil; use single, full cooling shroud	(a)
2. Hinged doors on:		
a. Upper shroud	a. Eliminate upper shroud	(a)
b. Lower plenum	b. Eliminate plenum or (a)	(a)
3. Sliding seal between burner and cooling shroud	Use welded shroud (integral with vessel)	Use bellows-loaded face seal
4. Remote disconnects		
a. Main vessel flanges	a. Relocate lower flange to a cooler zone	(a)
b. Smaller flanges	b. Use modified Tri-Clover clamps	(a)
5. Method of cooling burner	Use internal heat exchanger	(a)
6. Recycle fines cooling capability	(a)	Cool and/or redesign rotary valve. Design other components for high temperature.
7. Method of waste heat rejection	Cool the equipment rejecting heat to cell	Cool the equipment rejecting heat to cell
8. Method of vessel thermocouple attachment	Spring-loaded thermocouples	(a)
9. Method of fabrication of susceptor	?	?
10. Burner length	(a)	Provide an enlarged section at the top of the burner
11. Type of burner insulation	Fiber insulation	(a)
12. Method of heating burner	Hot gas (CO_2) preheat	(a)
13. Type of bonnet assembly	(a)	(a)

(a) Existing design (engineering-scale primary burner).

TABLE 3-3
"BEST VALUE" INTEGRATED BURNER SYSTEM DESIGN CONCEPT

Method of Cooling Burner - Internal Heat Exchanger

- Eliminate external shroud
- Eliminate hinged doors
- Eliminate sliding seal
- Eliminate insulation bonnet assembly

Method of Heating Burner - Hot Gas (CO_2) Preheat

- Eliminate induction heating system
- Eliminate susceptor
- Use cheaper external insulation (fiber) to reduce heat loss to cell only

Remote Disconnects

Main vessel flanges:

- Eliminate top flange and remote clamp (0.46 m)
- Relocate lower 0.36-m remote flange to cooler zone below distributor
- Eliminate 0.36-m swing-bolt connection

Smaller flanges:

- Eliminate Grayloc disconnects
- Use modified Tri-Clover clamps

Miscellaneous Features

- Add cooling jackets to cyclone, off-gas filter, and fines hopper
- Cool or redesign fines rotary valve for higher temperature
- Use spring-loaded thermocouples on vessel tube
- Use existing burner length. If tests confirm unacceptably high particle carryover, add an enlarged section to the top of the burner.

TABLE 3-4
"MINIMUM RISK" INTEGRATED BURNER SYSTEM DESIGN CONCEPT

Method of Cooling Burner - Existing System

- Retain external shroud
- Modify external shroud design to provide for single shroud (similar to HETF design). Alter maintenance procedures for removal of burner and induction coil.
- Eliminate hinged doors
- Eliminate sliding seal
- Retain existing "unitized" insulation bonnet assembly

Method of Heating Burner - Existing System

- Retain induction heating subsystem
- Retain susceptor (investigate methods of fabrication for HRDF burner)
- Use fiber (WRP-X) insulation for induction heating coil

Remote Disconnects

Main vessel flanges:

- Eliminate top flange and remote clamp (0.46 m)
- Relocate lower 0.36-m remote flange to cooler zone below distributor
- Eliminate 0.36-m swing-bolt connection

Smaller flanges

- Eliminate Grayloc disconnects
- Use modified Tri-Clover clamps

Miscellaneous Features

- Add cooling jackets to cyclone, off-gas filter, and fines hopper
- Cool or redesign fines rotary valve for higher temperature
- Use spring-loaded thermocouples on vessel tube
- Use existing burner length. If tests confirm unacceptably high particle carryover, add an enlarged section to the top of the burner.

offers the potential for maximum cost reduction, simplicity of design, and ease of fabrication, but involves significantly greater risk. Therefore, it must be studied in more detail and tested in existing smaller-scale pilot plant equipment before implementation as part of the prototype primary burner system (see Section 3.3.3, 0.20-m Primary Burner Equipment Design Modifications). Methods of heating and cooling the prototype primary burner and its contents should be determined before any other prototype design features are selected.

2. Cooling the burner with an internal heat exchanger (vertical array of parallel tubes) may be feasible from a process point of view but involves considerable risk at this time. Nevertheless, this concept warrants further evaluation to verify feasibility. The following aspects of this concept must be evaluated in detail before a final decision is made:

   a. Process-side ΔP (must be acceptably low).

   b. Effects of the tubes on slugging, mixing, and other dynamic characteristics of the fluidized bed.

   c. Means of supporting the tubes and the mechanical effects of the tubes, their supports, and inlet/outlet CO_2 piping on stresses, vibration, bending, erosion, etc. The effect of process-side SO_2 and other gases on the corrosion of tubes and other internal components.

   d. Effects of tubes in the upper section of the burner on fines burning efficiency, elutriation, agglomeration, and particle breakage.

   If a more detailed evaluation indicates this concept is still feasible, then it should be tested in both the 0.20-m cold glass-ware and 0.20-m primary burners. Based on three experiments with each burner, the cost of implementing this concept on the proto-type 40-m primary burner is estimated to be approximately $59,000

(includes exempt and nonexempt direct labor charges for design, engineering, installation, and testing and the cost of small-scale heat exchangers for the 0.20-m cold glassware and 0.20-m primary burners).

3. Hot gas (CO_2) heating of the burner may also be feasible but also involves considerable risk at this time. Nevertheless, this concept warrants further evaluation to verify feasibility. The following points concerning this alternative design should be evaluated in more detail:

   a. Controllability.

   b. Heatup time [must be compatible with the HRDF operating cycle and production (availability) requirements].

   c. Effects of the hot gas on the startup bed, including attrition, particle breakage, elutriation, etc.

   d. Mechanical effects of the hot gas on the vessel and any internals, including any internal cooling tubes, i.e., stress, vibration, erosion, etc.

   This concept should be tested on the 0.20-m primary burner if further evaluation looks promising. The implementation cost of this concept on the prototype 0.40-m primary burner is estimated to be approximately $56,000 (includes excempt and nonexempt direct labor charges for design, engineering, installation, and testing and the cost of a hot CO_2 delivery system for the 0.20-m primary burner).

4. If both internal heating and cooling prove to be feasible, then design features 1, 2, 3, 9, and 13 in Table 3-2 should be eliminated from the prototype burner design. If these major concepts are not feasible, then the integrated burner system design concept presented in Table 3-4 should be developed.

5. The top vessel flange (0.46-m Grayloc remote clamp) should be eliminated from the prototype burner design. The lower 0.36-m remote flange should be relocated to a cooler zone below the distributor. The 0.36-m Grayloc swing-bolt connection should be eliminated, and the 0.038-m Grayloc remote disconnect on the vertex line should be moved from inside to outside the distributor assembly, as in the HETF primary burner design.

6. Efforts should be initiated to modify Tri-Clover (or equivalent) clamps as substitutes for the existing smaller Grayloc connections (0.13 m and under).

7. Spring-loaded thermocouples should be installed and tested on the 0.20-m primary burner. Particular attention should be given to their reliability and accuracy.

8. Current studies to find and test feasible ways to provide recycle fines cooling capability for the 0.20-m primary burner should be completed and evaluated in conjunction with HRDF requirements for waste heat rejection. The prototype cyclone and off-gas filter should be designed for temperatures of 750°C (1382°F) and 700°C (1292°F), respectively, if jacket cooling of this equipment is not a feasible way to provide fines cooling.

9. An enlarged section should be added to the top of the existing 0.40-m primary burner if future tests of the existing burner indicate unacceptable particle carryover.

10. Ways of handling and installing fiber insulation such as WRP-X on the outside of the burner should be investigated and implemented once the method of heating the prototype primary burner has been established.

11. Remote maintenance fixtures should be evaluated in light of the results and recommendations of this study.

12. Future design evaluation studies of the 0.40-m primary burner should include the following three areas:

    a. Location of recycle fines injection into the burner using a gravity hopper rotary valve recycle fines system, especially side entry (above-bed) versus a dip tube (above-bed discharge).

    b. Feasibility of the HETF primary burner distributor, including the rectractable plug, expansion bellows seal, and relocated lower remote flange.

    c. Feasibility of a gravity-pneumatic pulse solids feeder similar to that used successfully on the 0.10-m and 0.20-m secondary burners (as a substitute for the existing star valve feeder). Although such a feeder has been tested extensively without success on the 0.20-m cold glassware and 0.20-m primary burners, there is a greater chance for successful operation in the larger (0.40 m) primary burner system.

3.3. 0.20-m PRIMARY BURNER

3.3.1. 0.20-m Primary Burner Automation Studies

3.3.1.1. Introduction

Automation of the burner system using the Diogenes process control computer was specified for module 7 of the Activity Plan (AP524301B). Preliminary results of the automation work and control philosophy were discussed in Ref. 3-1. Additional modifications and fine tuning of the automatic control system have since been made, but extensive studies were curtailed by a problem with the Diogenes system.

3.3.1.2. Discussion

Preliminary results of the automation study indicated that the postulated automation philosophy (Ref. 3-1) can control the primary burner in the initial heatup, in the O_2 ramp used during startup, and in the major

steady-state portion of the run. However, in additional testing, it has continued to be necessary to use manual override during the unstable phase of operation both following fresh feed startup and during the final fines tailburning process. This override consists of manually controlling the O_2 flow and/or cooling air flow rates, with all other functions remaining on automatic control.

The Diogenes control system has generally been satisfactory in performing its assigned control functions except for an intermittently erroneous temperature signal from the "high bed temperature selector." This function is normally used to scan the axial bed temperature profile and to provide a high-temperature signal to several other controllers. This erroneous signal briefly activates the induction heater and deactivates the cooling air. In doing this, the cooling air blower will cycle on and off; if this occurs often enough, the blower switch contactor will overheat and fail. The selector problem has hampered studies of fine tuning automatic controls. The reason that the high select channel randomly selected a low temperature was traced to a software problem in the system "read-only-memory" (ROM). Programming changes were subsequently made to the ROM and it was reinstalled in the Diogenes system. To date one run has been made with this corrected function (0.40-m primary burner Run C.1) and the high select problem was not experienced.

3.3.1.3. Conclusion and Recommendations

The Diogenes high bed temperature selector will be checked closely in future tests both on the 0.20-m and 0.40-m primary burners. Proper functioning of the selector will allow continuing fine tuning studies on the remainder of the automatic control system in an effort to reduce the requirement for periods of partial manual control.

Modifications to control philosophy should include scanning of the axial susceptor and vessel wall temperature profiles for maximum temperature inputs to the induction heater control system. This would better serve to minimize the possibility of overheating the vessel during abnormal operating conditions.

3.3.2. 0.20-m Primary Burner Operating Cycle Test Runs

3.3.2.1. Introduction

A 48-hour run was called for in the Activity Plan (AP524301B) as the completion of module 7 automation work. This run was planned to study the automation system in long-duration operation and also to study the proposed primary burning operating cycle. Four attempts to complete this run were made in this reporting period.

3.3.2.2. Discussion

As reported in Ref. 3-1, the initial 48-hour run attempt was terminated after 12 hours due to several mechanical problems: (1) overheating and failure of the cooling air blower switch contactor caused by the erroneous Diogenes controller signal (see Section 3.3.1.2), (2) jamming of the bed product removal valve in a partially opened position, and (3) a break in the system off-gas line. A series of three short runs was made to test system repairs and modifications prior to making another 48-hour run attempt. All of the repaired items performed acceptably.

The second 48-hour run attempt demonstrated a much smoother startup period due to the use of a longer oxygen ramping time and earlier initiation of fines recycle. However, problems with feed flow from the main feed hopper limited operation to use of a low capacity, backup feed system. The run was terminated after 12 hours when attempts to correct the flow problem in the main feed system were unsuccessful. The problem with the main feeder resulted when blockage of the off-gas system filters increased backpressure throughout the burner system. Increased gas leakage up through the hopper outlet prevented material flow from the aerated hopper. The cause of the off-gas filter blockage was traced to the previous checkout run in which the inadvertent use of wet graphite feed during startup was thought to have caked the filters.

Prior to attempting a third 48-hour run, several small leaks in the fresh feed hopper were sealed in order to increase its allowable operating

pressure. In addition, the off-gas filters were blown back for 4 hours, after which the filter blockage appeared to have been eliminated. A short test run followed which resulted in no apparent problems with either system. However, the product dump ball valve again failed to operate satisfactorily. A high-temperature knife-gate valve and bellows were substituted and successfully tested in a subsequent heatup and dump test.

A third 48-hour run attempt was made which demonstrated much smoother operation of the fresh feed system. However, plugging in the off-gas filter system was again experienced and operation was terminated after 15 hours. The entire off-gas filter system was disassembled and inspected before making modifications to the blowback control system and installing new filters and CO_2 purge lines in the filter vessel. When a fourth 48-hour run attempt resulted in the same general results, it was suspected that the excessive fines generation and accumulation experienced were due to an excessive fresh feed flow rate. Generally, it is desirable to match the feed flow rate with the burn rate such that fines accumulation does not increase appreciably and exceed the capacity of the recycle equipment. The desired feed flow rate requires operation of the feed rotary valve at a very low rpm, and hence, throughput is characteristically erratic.

The fifth and final 48-hour run attempt was performed at a reduced feed flow rate relative to previous runs. Predictably, this resulted in operation of much longer duration than previous runs. However, identical problems with the off-gas filter system plugging were eventually experienced, which indicated that poor feed flow rate control resulted in an average flow rate higher than expected. If feed flow rate is accurately metered, then excessive fines accumulation should not occur. Previous runs of shorter duration and limited feed supplies resulted in no appreciable fines accumulation and in complete fines inventory burnout.

The majority of the fertile BISO/fissile TRISO particles used in these runs were the large, dense BISO particles which generally exhibit poorer fluidization and bed mixing characteristics than the less dense TRISO particles. Segregation of bed material in the fifth run attempt was such that a relatively short bed of BISO particles (<100°C) occupied the lower

bed while a layer of burning graphite existed above. In an effort to burn some of the excessive fines inventory, fresh feed flow was terminated, after which the main source of combustion consisted of recycling fines. Bed carbon content gradually decreased, as did the bed height, since no additional fuel particles were being fed. Operation at these conditions characteristically exhibits significant above-bed fines burning and thermal cycling which is best controlled by frequent variation of oxygen flow rate to the bed. During a part of this thermal cycle, the oxygen flow rate was decreased to counteract intense fines burning on top of the bed and a rapidly rising temperature. The top bed temperature subsequently peaked and began to decrease, whereupon the automatic control system initiated induction heating of the bed once a low temperature set point was reached.

At this point, the relatively short, segragated bed reached only the lower portion of the induction heated zone. Ordinarily, the induction heater susceptor axial temperature profile is such that the peak temperature is located near the middle of the susceptor. As the susceptor continued to heat the vessel wall, oxygen flow rate to the burner was increased to counteract the rapidly decreasing bed temperature (<750°C). This resulted in an increased burning intensity in the poorly mixed bed carbon zone, further increasing the local vessel temperature. Hence the maximum wall/susceptor temperature (hot spot) was located here. Since the induction heater was automatically controlled by a thermocouple higher up the susceptor where the peak temperature is normally located, the vessel hot spot was undetected by the automatic control system and the induction heater remained on. Shortly thereafter the vessel became overheated and a burnthrough resulted. The exact location of the vessel failure is shown in Fig. 3-11.

3.3.2.3. Conclusion and Recommendations

The test failure which occurred in the final 48-hour run attempt identified several required design modifications which will be incorporated during reconstruction. The capability for heating small beds will be improved, as will the capability of the automatic control system to detect and react to unforeseen abnormal operating situations.

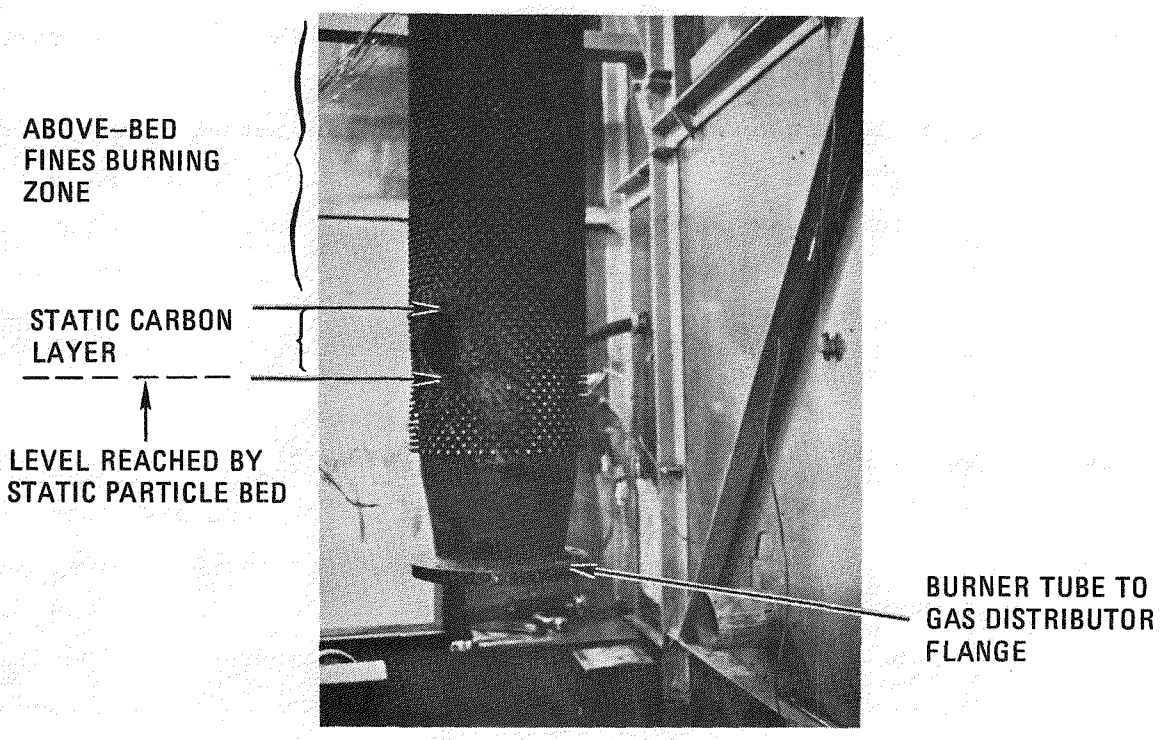

Fig. 3-11. 0.20-m primary burner burnthrough

Operating procedures will be modified to exclude attempting re-ignition of beds at low temperatures (<650°C).

The burner vessel and susceptor must be repaired. This procedure is being investigated and will be done simultaneously with planned upgrading of the gravity fines recycle system.

3.3.3. 0.20-m Primary Burner Equipment Design Modifications

3.3.3.1. Introduction

Following the final 48-hour run attempt, the 0.20-m primary burner was disassembled in preparation for future design modifications.

3.3.3.2. Discussion

The ruptured section of the vessel wall will be repaired by replacement with an approximate 0.30-m length of pinned tubing. In addition to repairs to the vessel, the susceptor design will be reevaluated. Particular emphasis will be given to the feasibility of modifying the configuration of the heating system to improve heating beds of smaller height. Also, the use of a fluidization gas preheater should improve the ability of the system to heat small beds of material. The tests with the gas preheater will allow analysis of recommendations made in Section 3.2.5, 0.40-m Primary Burner System Design Evaluation.

Concurrent with repairs to the vessel and modifications to the heating system, the fines recycle system will be redesigned, based on previous test results, to allow final verification of the above-bed recycle system. These modifications will include the insulation and cooling capability necessary for proper temperature control of the recycling fines to maintain <500°C fines temperature at the rotary valve. The fresh feed and fines hoppers will be redesigned and replaced in conjunction with these other repairs and modifications.

3.3.3.3. Conclusions and Recommendations

Several potential problem areas have been identified in recent 0.20-m primary burner tests. These will be investigated with special emphasis on modifying equipment design and operating procedures to accommodate the effects of abnormal operating conditions.

One of the goals associated with future operation of the 0.20-m primary burner is an investigation of the effects of the induction heater, gas preheater, and fines cooling design modifications on the process. The design modifications under consideration include: (1) an induction heater design which allows heating smaller bed heights and perhaps yields a more isothermal axial wall temperature profile, and (2) the potential of an inlet gas preheater to provide backup heating of small beds and its potential to completely replace the induction heating concept. In addition, the planned tests of external cooling of the off-gas piping and cyclone should be made to study circulating fines temperature control <500°C.

The 0.20-m primary burner rebuild should be completed by the first part of FY-78.

3.3.4. 0.20-m Primary Burner Bed Level Sensor

3.3.4.1. Introduction

A need to determine a discrete bed level in the primary burner to back up the bed ΔP indication initiated a program to develop such a sensor. A dual element probe (Ref. 3-1) was constructed and has since been modified and tested.

3.3.4.2. Discussion

A mechanical problem was encountered with the level sensor reported in Ref. 3-1. The U-shape sensing element became entangled with the burner

thermowall during a testing run and was broken. A new sensor, shown in Fig. 3-12, was designed. This sensor consists of a single element probe in a 6.35-mm stainless steel tube. The sensor was installed through the mid-reactor fines recycle penetration and extended down into the vessel adjacent to the burner wall. The lower 0.1524 m of the probe was offset to move the sensing leads out 0.0508 m from the burner wall.

3.3.4.3. Conclusions

Several burner runs have been made with this new design and excellent results have been obtained. No mechanical or electrical problems have been encountered. This design is recommended for future application.

3.3.5. 0.20-m Primary Burner High-Temperature Rotary Fines Valve Design

3.3.5.1. Introduction

The 500°C recycling fines temperature limitation imposed by the vendor-supplied fines rotary valve has initiated studies concerning cooling the fines in off-gas piping (see Section 3.3.3., 0.20-m Primary Burner Equipment Design Modifications and also Ref. 3-1). An alternative to cooling the fines would be a valve design that could withstand the $\lesssim$800°C expected equilibrium temperature of the recycling fines. Such a valve design is discussed below.

3.3.5.2. Discussion

The design of a high-temperature rotary fines valve developed by GA is illustrated in Fig. 3-13. The valve is made of 316 stainless steel with the exception of the rotor seal block which is Grey or Nodular cast iron. The 1000-hour rupture strength of 316 stainless steel is shown in Fig. 3-14.

Previous rotary valves dispensing fines have had trouble with seal leakage. In this design the shaft seals are a carbon ribbon pack and are

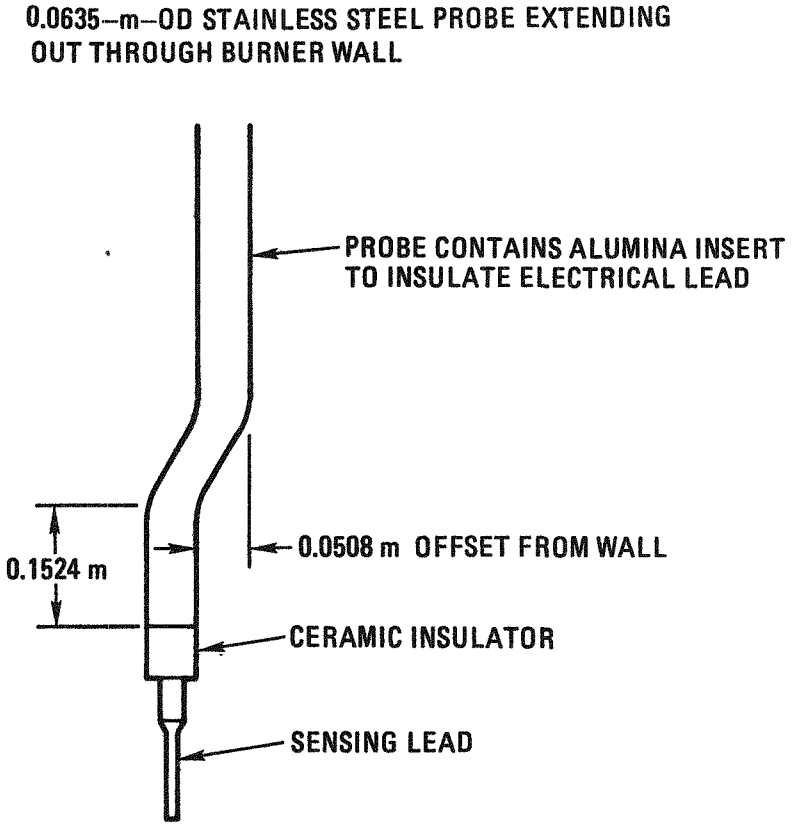

Fig. 3-12. Primary burner bed level sensor

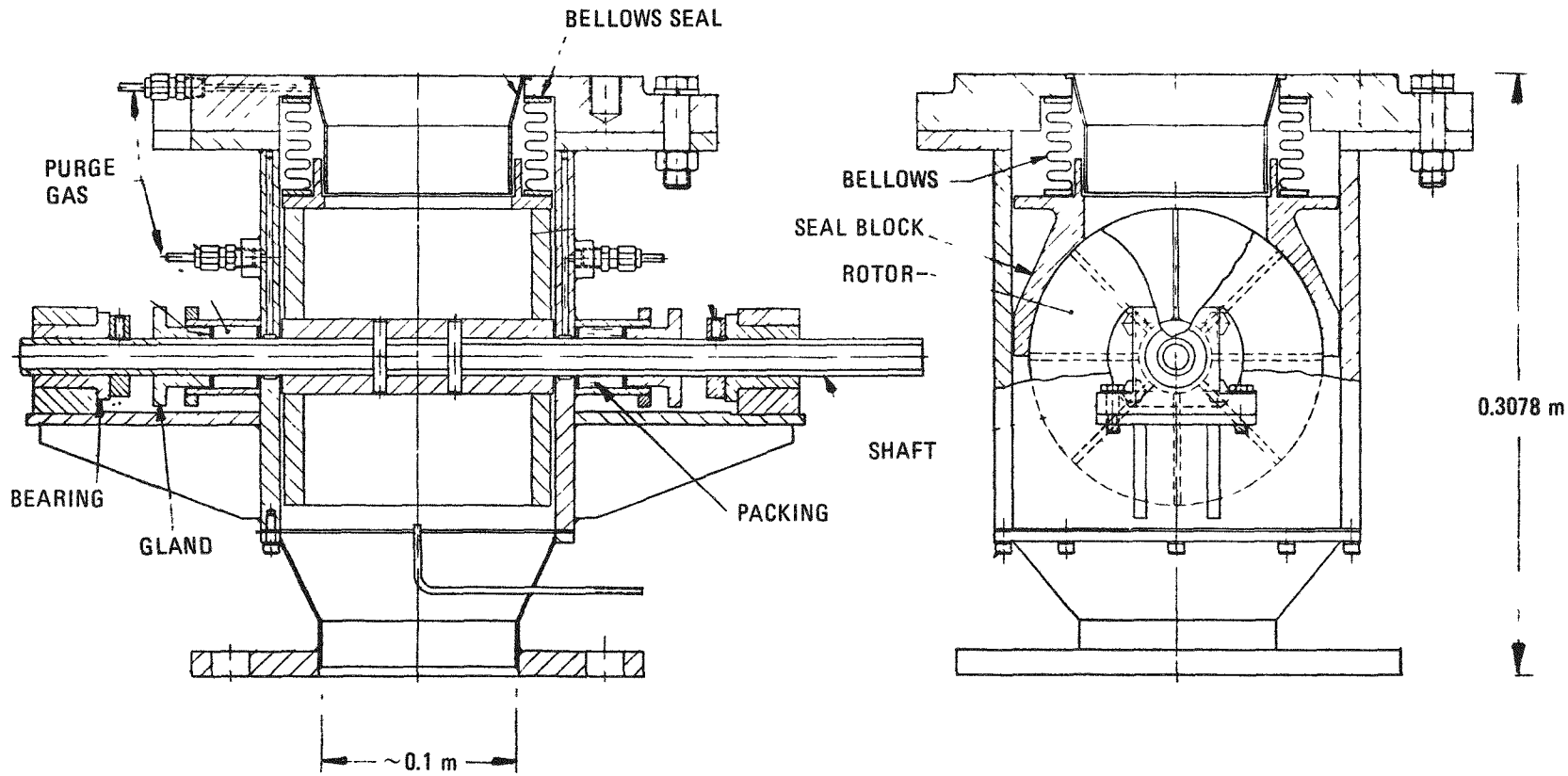

Fig. 3-13. High-temperature rotary fines valve

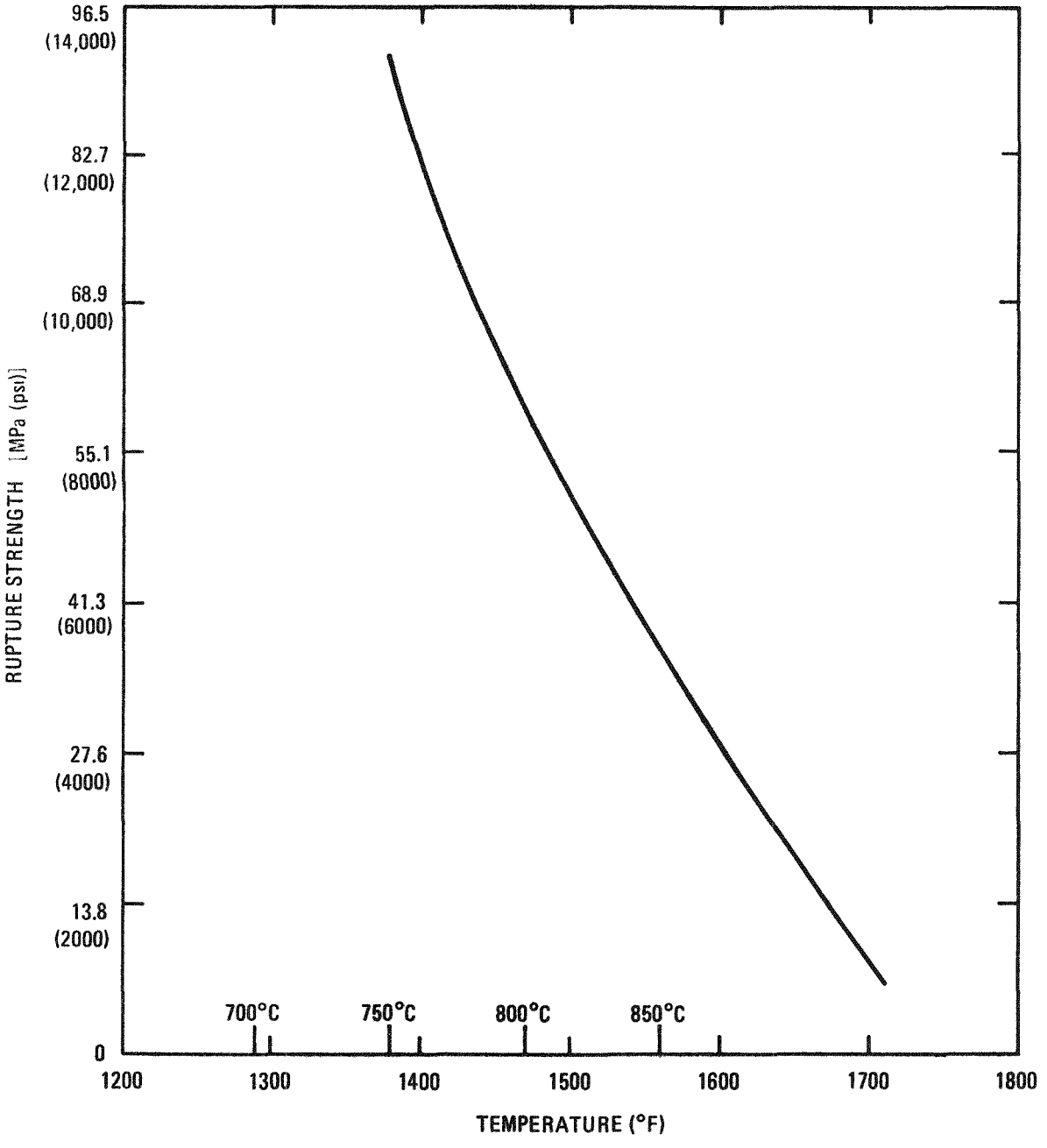

Fig. 3-14. 1000-hour rupture strength of 316 stainless steel

purged with CO_2 to prevent entry of fines into the seal. The cast iron seal block employs a stainless steel bellows as the moving seal. The design utilizes the pressure difference as well as the bellows spring rate to keep positive contact between the seal block and the rotor.

The carbon shaft bearings are outboard from the valve body so that they will operate at a reduced temperature. The hollow shaft will allow shaft cooling or purge gas to the rotor pockets if this proves to be necessary.

3.3.5.3. Conclusions and Recommendations

Since the stresses in all parts of the valve are very low and the shaft and seals are capable of being cooled, it is expected that the valve will operate with recycling fines temperatures up to 800°C. It is therefore recommended that the valve be fabricated and tested in future 0.20-m burner work.

REFERENCE

3-1. "Thorium Utilization Program Quarterly Progress Report for the Period Ending February 28, 1977," ERDA Report GA-A14304, General Atomic Company, March 1977, pp. 3-1 to 3-36.

4. PARTICLE CLASSIFICATION, CRUSHING, AND BURNING

4.1. SUMMARY

Four burner runs were made on the 0.20-m secondary burner to complete a parametric study of process variables. The last three runs were made in quick succession over a 17-hour period. Each test used 60,000 g of crushed FSV TRISO fertile fuel particles as feed. Acceptance criteria were fully met in each burner run. Overall system operability was excellent.

Analysis of the parametric study led to recommending the following values for process variables:

1. Fluid bed superficial velocity should be reduced from 0.90 to 0.80 m/s during the main burn period.
2. Ignition temperature should be lowered from 700° to 600°C.
3. Fluid bed temperature should be dropped from 900° to 850°C during the main burn period.
4. Filter blowback frequency should be reduced from 2 cycles/min to 1 cycle/min.
5. Fluid bed superficial velocity should be lowered to 0.45 m/s by the end of the tailburning period.

A design evaluation is in progress to examine possible modifications to upgrade 0.20-m secondary burner equipment design. Thirteen features are being evaluated against alternative designs, with a value analysis approach being used for ranking the existing design and alternate approaches.

The 0.10-m secondary burner was used to burn 12 kg of crushed FSV TRISO fissile fuel particles. This was the first time this type of

particle had been processed in the reprocessing pilot plant. Operations were quite smooth and trouble free and all acceptance criteria were met.

Air classifier work was deferred this quarter to allow completion of burner milestones. Preparations are under way for implementing the air classifier operations detailed in the Activity Plan.

The fertile roll crusher processed 240 kg of FSV TRISO fertile fuel particles and 15 kg of WAR TRISO fissile depleted uranium fuel particles. During the FSV particle crushing, a bearing ran low on grease and overheated; it will be replaced and the greasing method will be re-evaluated. No wear on the roll faces has been detected after processing over 500 kg of TRISO coated fuel particles. Crusher body side plate localized wear has been significantly reduced by the insertion of B_4C (boron carbide) inlays at the apex of the roll cavity.

Bearing preloads were optimized on the fissile particle crusher to yield constant roll gap during crushing while minimizing roll torque requirements. Actual roll gap settings were also optimized at 280 μm (0.011 in.), yielding complete fuel particle breakage while maximizing average product size. At present, 15 kg of FSV TRISO fissile depleted uranium fuel particles have been processed through the fissile roll crusher.

4.2. 0.20-m SECONDARY BURNER

4.2.1. Introduction

During the past 3 months, four burner runs have been made to finish experimental work on a seven-run parametric study of the following burner process variables:

1. Bed ignition temperature.
2. Bed operating temperature.
3. Bed superficial velocity.
4. Filter blowback rate.

The Operating Procedure (OP524701) and Activity Plan (AP524701) were followed throughout these four burner runs except where noted. Automated control was used during each run. Three of these runs were accomplished in quick succession over a 17-hour period. All of these runs were very smooth and trouble free.

Graphs depicting feed and product size distributions, fluidized bed and off-gas filter temperatures, off-gas composition, and inlet gas flows and pressure drops are shown in Figs. 4-1 through 4-17.

4.2.2. 0.20-m Secondary Burner Experimental Runs

4.2.2.1. Run 6 (Figs. 4-1 Through 4-5)

In Run 6 the off-gas filter blowback rate was increased to 3 cycles/min from the baseline of 2 cycles/min. The ignition temperature was lowered to 550°C following success in Run 5 at 600°C.

Feed consisted of 60,000 g of crushed TRISO fertile FSV type fuel particles.

Fluid bed heatup time to 550°C was 35 min. An inlet oxygen ramp was used leading to a pure O_2 inlet stream during main burning. At this low ignition temperature a 2-min spike of 5% off-gas O_2 was noted. The automatic bed temperature control overshot the set point, reaching 920°C and cycling twice before damping out. Control is achieved using cooling air modulation. Manual startup transient cooling air control will be used in the future, with subsequent automatic control following initial stable operation.

The filter pressure drop reached a maximum of 4 kPa at 770°C. The main burning period lasted for 50 min followed by inlet flow changes to 60% O_2 after off-gas CO decreased to zero. The filter temperature was 630°C when O_2 began to appear in the off-gas. During the final tailburning, off-gas O_2 content went through a short peak of 30% before decreasing to 20%.

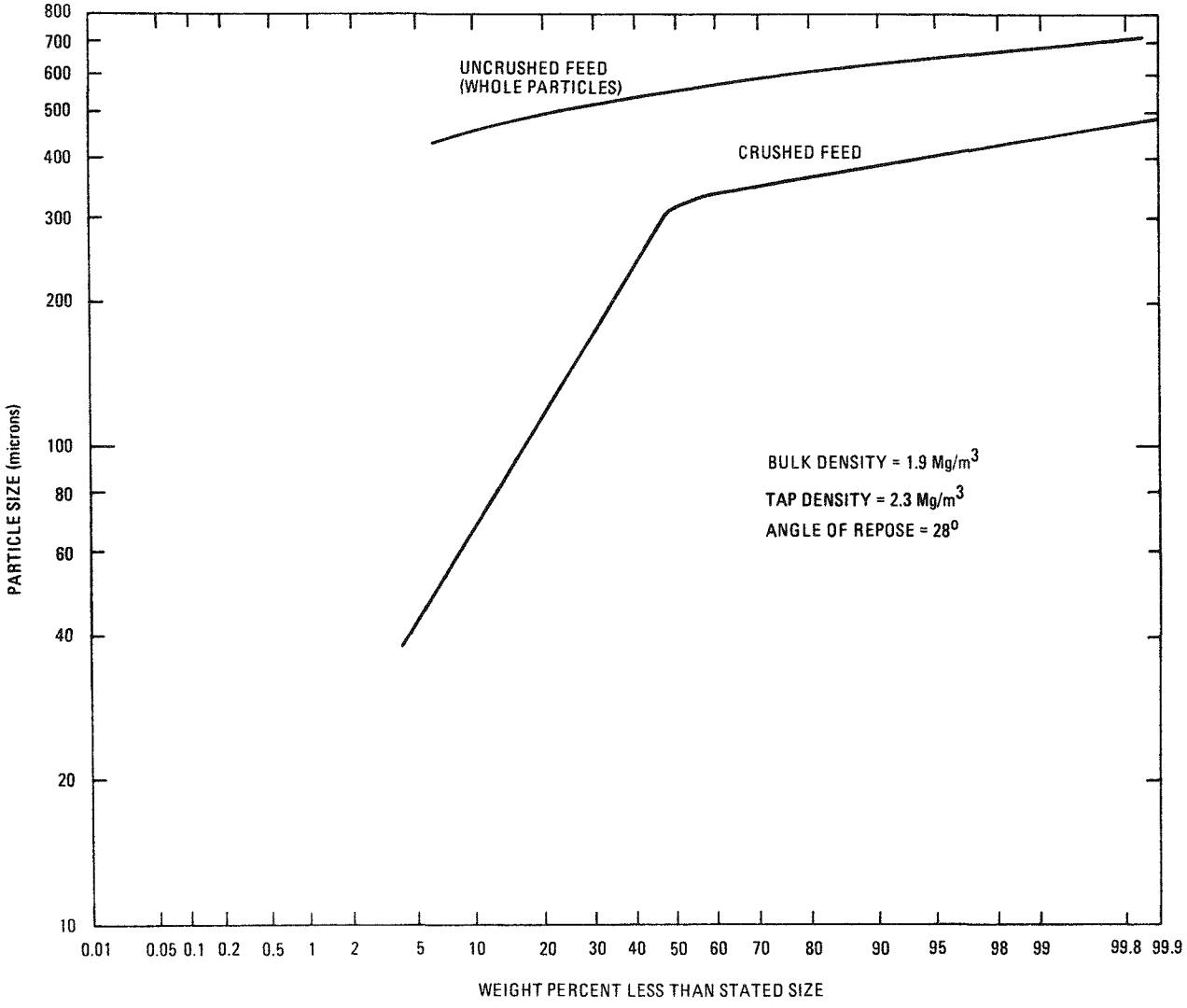

Fig. 4-1. Feed size distribution, 0.20-m secondary burner Runs 6 through 9

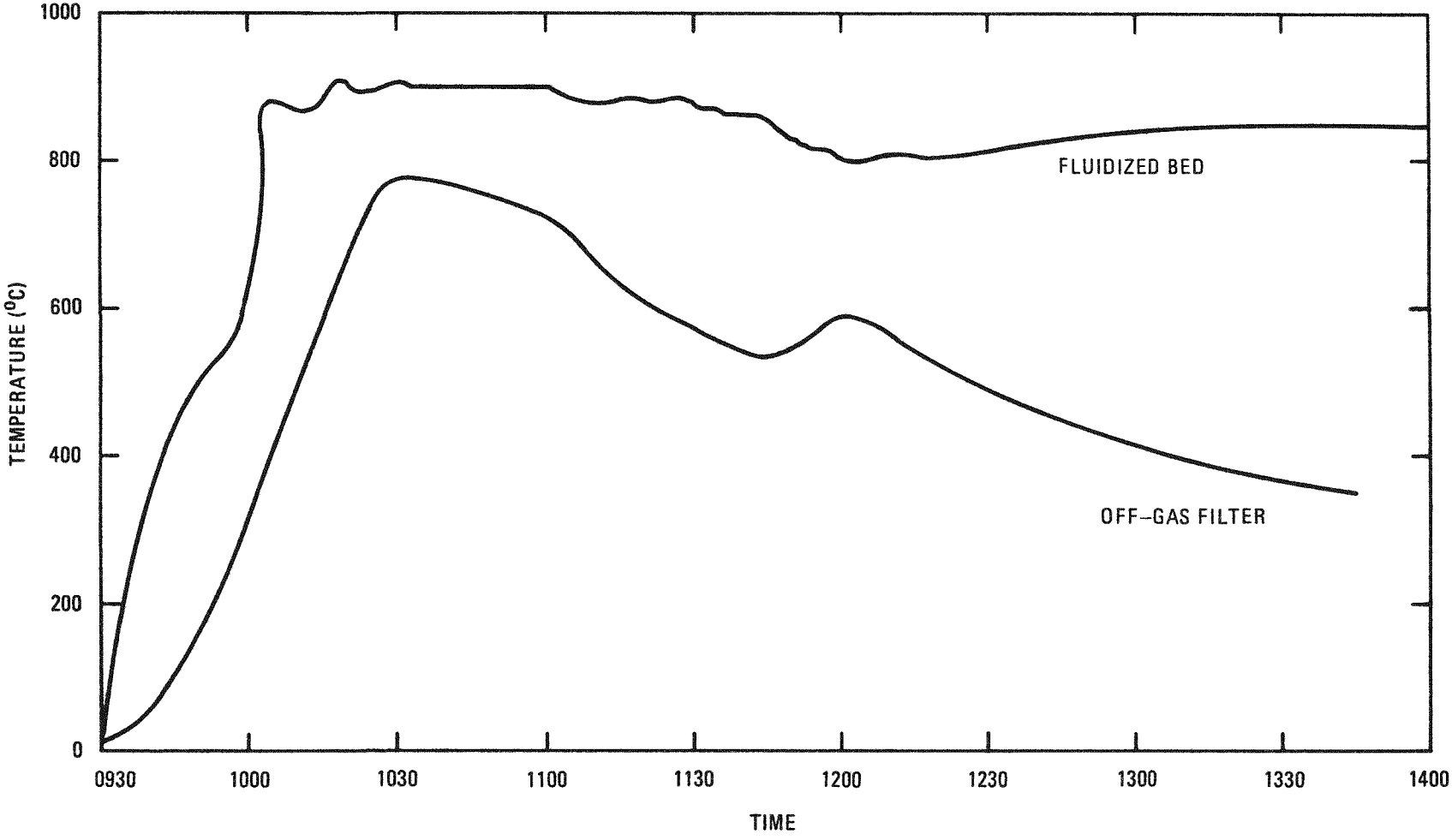

Fig. 4-2. Fluidized bed and off-gas filter temperature, 0.20-m secondary burner Run 6

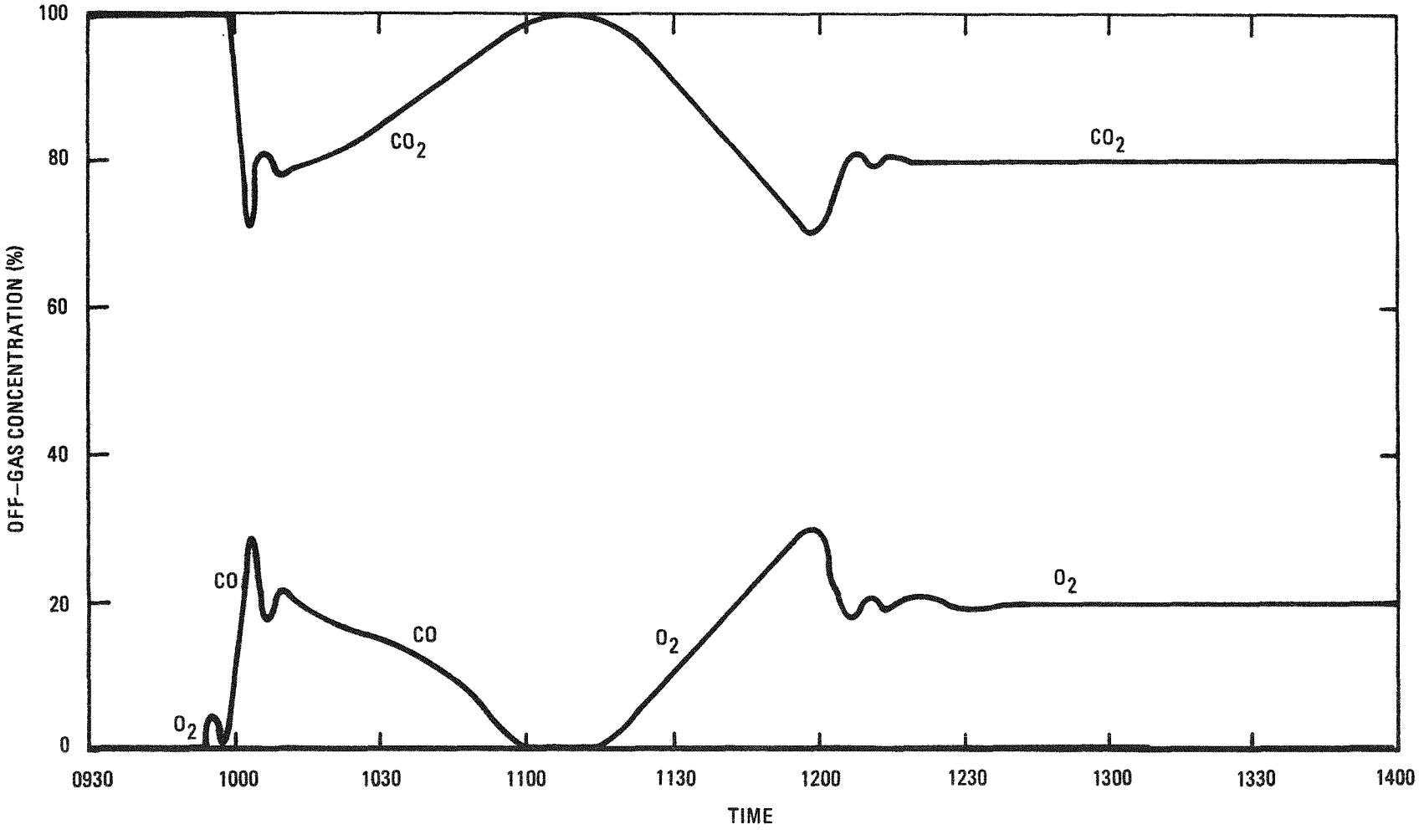

Fig. 4-3. Off-gas composition, 0.20-m secondary burner Run 6

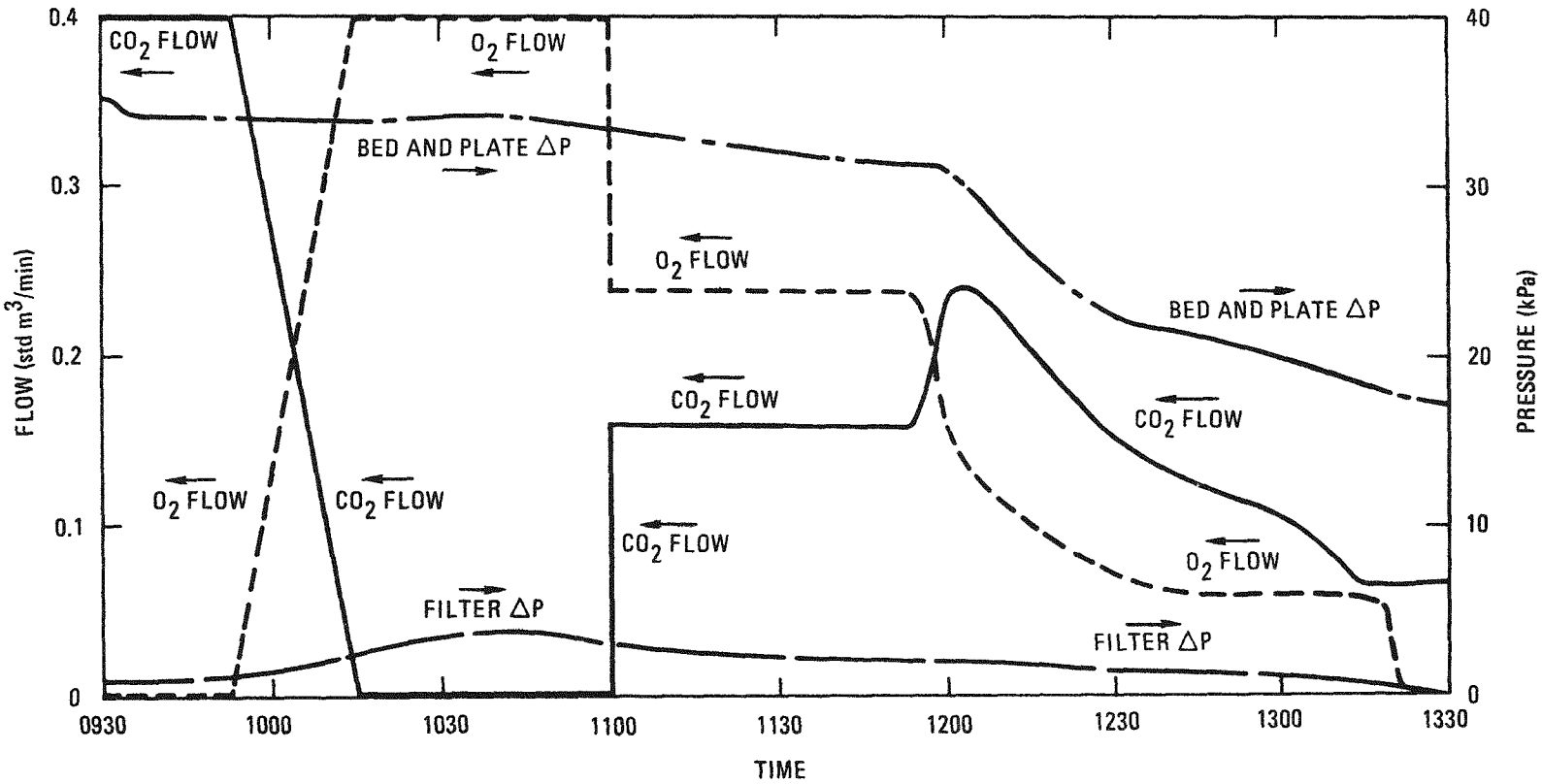

Fig. 4-4. Inlet gas flows and pressure drops, 0.20-m secondary burner Run 6

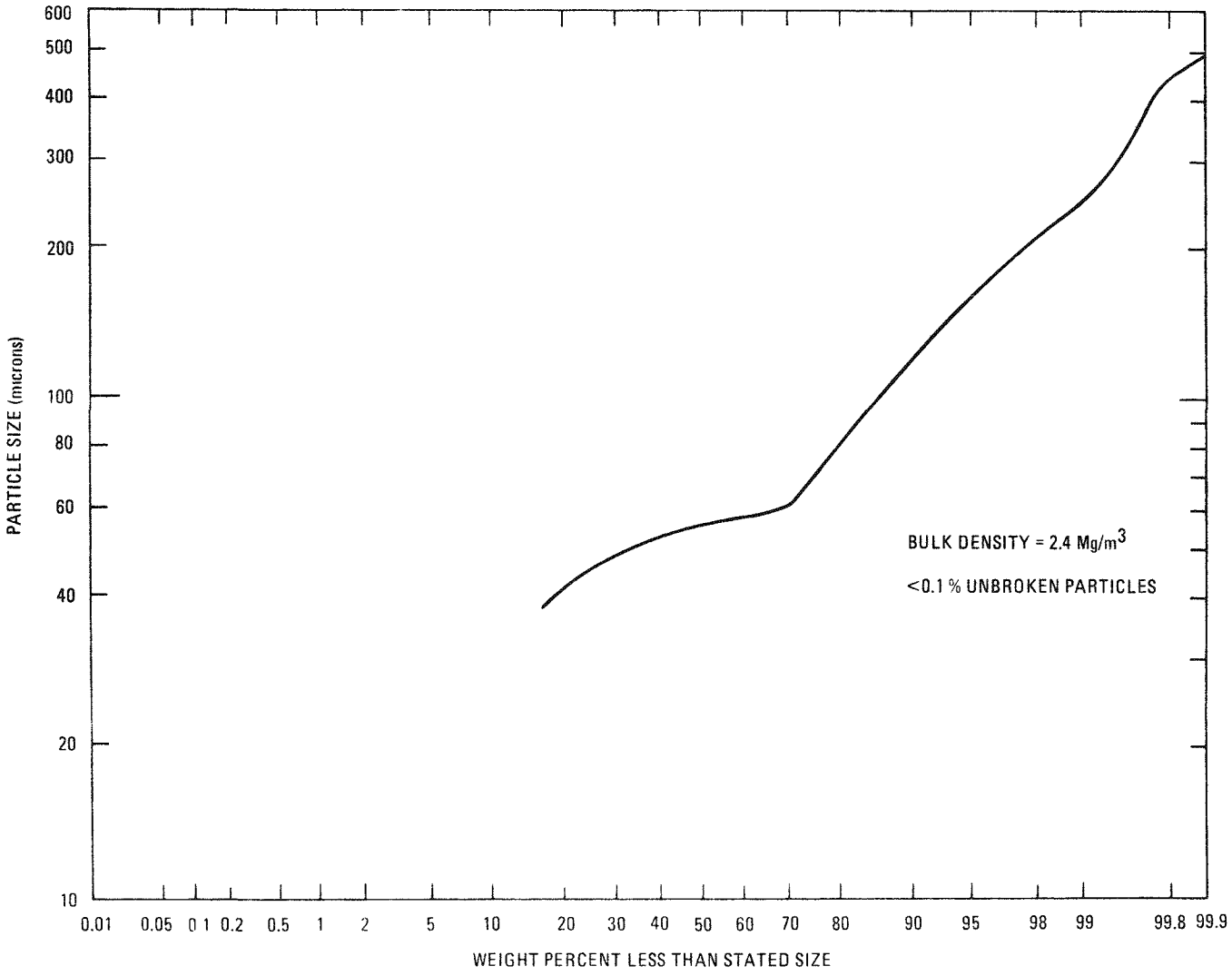

Fig. 4-5. Product size distribution, 0.20-m secondary burner Run 6

Bed temperature was held at ≥800°C and the total flow was lowered to 0.32 m/s to help carbon fines return to the bed for final combustion.

Pneumatic transport was accomplished by discharging product intermittently through the product removal valve so as not to overload the vacuum-pneumatic transport system. A 32-g heel was left on the distributor plate, which amounts to an acceptably low 0.07% of the total product. Product carbon content was an equally acceptable 0.75%. This is the lowest carbon content yet attained, giving strong impetus to using low-velocity tailburning.

4.2.2.2. Run 7 (Figs. 4-6 Through 4-9)

This was the first run of the three-run series. The off-gas filter blowback rate was lowered to 1 cycle/min from the baseline of 2 cycles/min. All other variables were at the baseline levels.

Feed material in each of these three final runs was 60,000 g of crushed FSV TRISO fertile fuel particles. Fifty minutes were required to induction heat the fluid bed to 700°C, followed by a 20-min period of ramping inlet O_2 to 100%. The bed temperature was held manually at 900°C initially, followed by automatic temperature control for the balance of the run. The peak off-gas filter pressure drop was 3.5 kPa at 775°C.

During tailburning, the total flow was dropped to 0.46 m/s while keeping off-gas oxygen levels at 20%. Product transport was carried out after cooling the bed to 100°C. Intermittent opening of the product removal valve prevented overloading the vacuum pneumatic transport line. This product removal technique was used in all of these final three burner runs. An enlarged capacity transport system is currently being procured, based on data gathered in the previous quarter.

Product carbon content was 0.6 wt %.

4.2.2.3. Run 8 (Figs. 4-10 Through 4-13)

In this second run of the three-run series, the only variable changed was the bed temperature, which was dropped to 875°C during the main burning period.

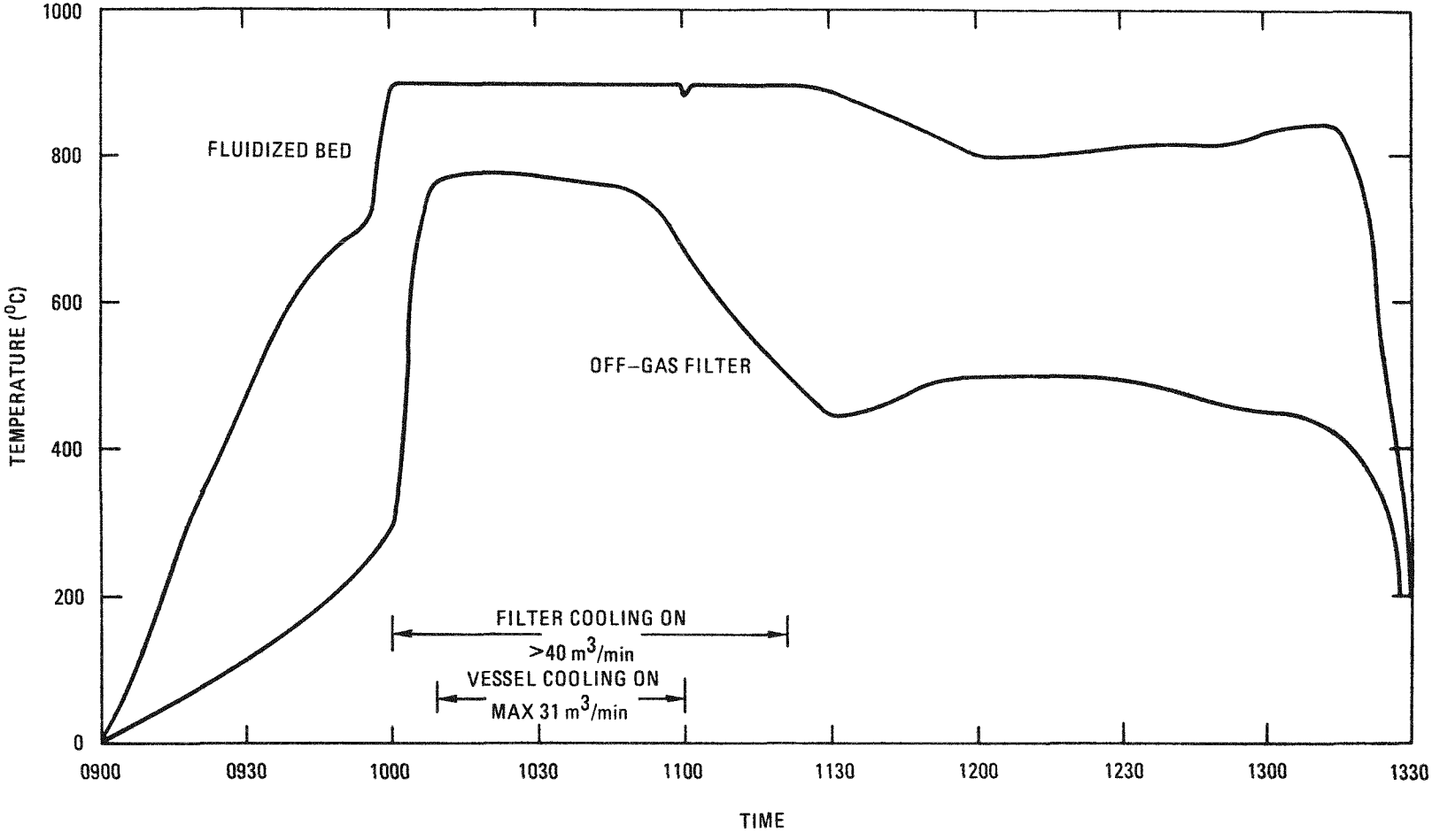

Fig. 4-6. Fluidized bed and off-gas filter temperature, 0.20-m secondary burner Run 7

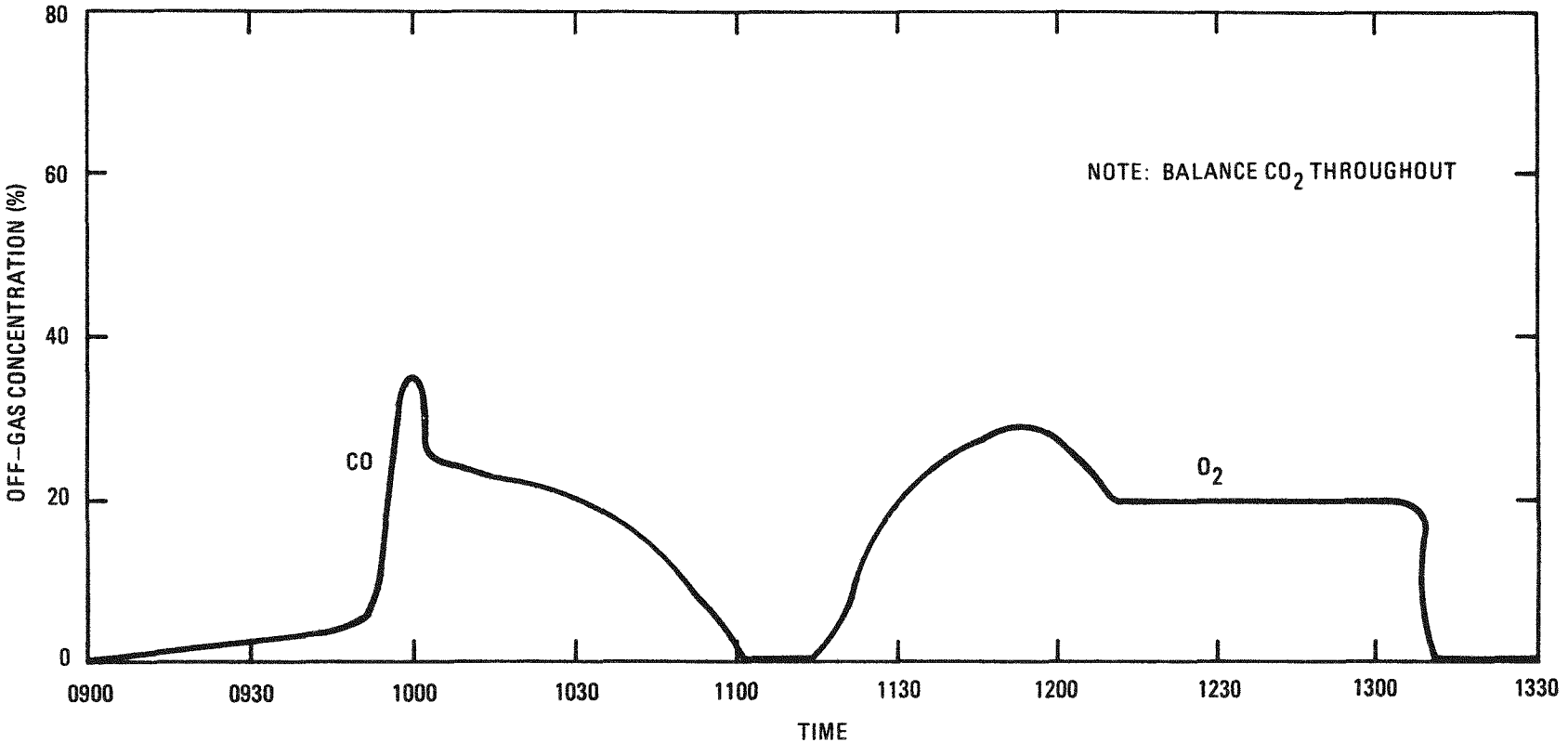

Fig. 4-7. Off-gas composition, 0.20-m secondary burner Run 7

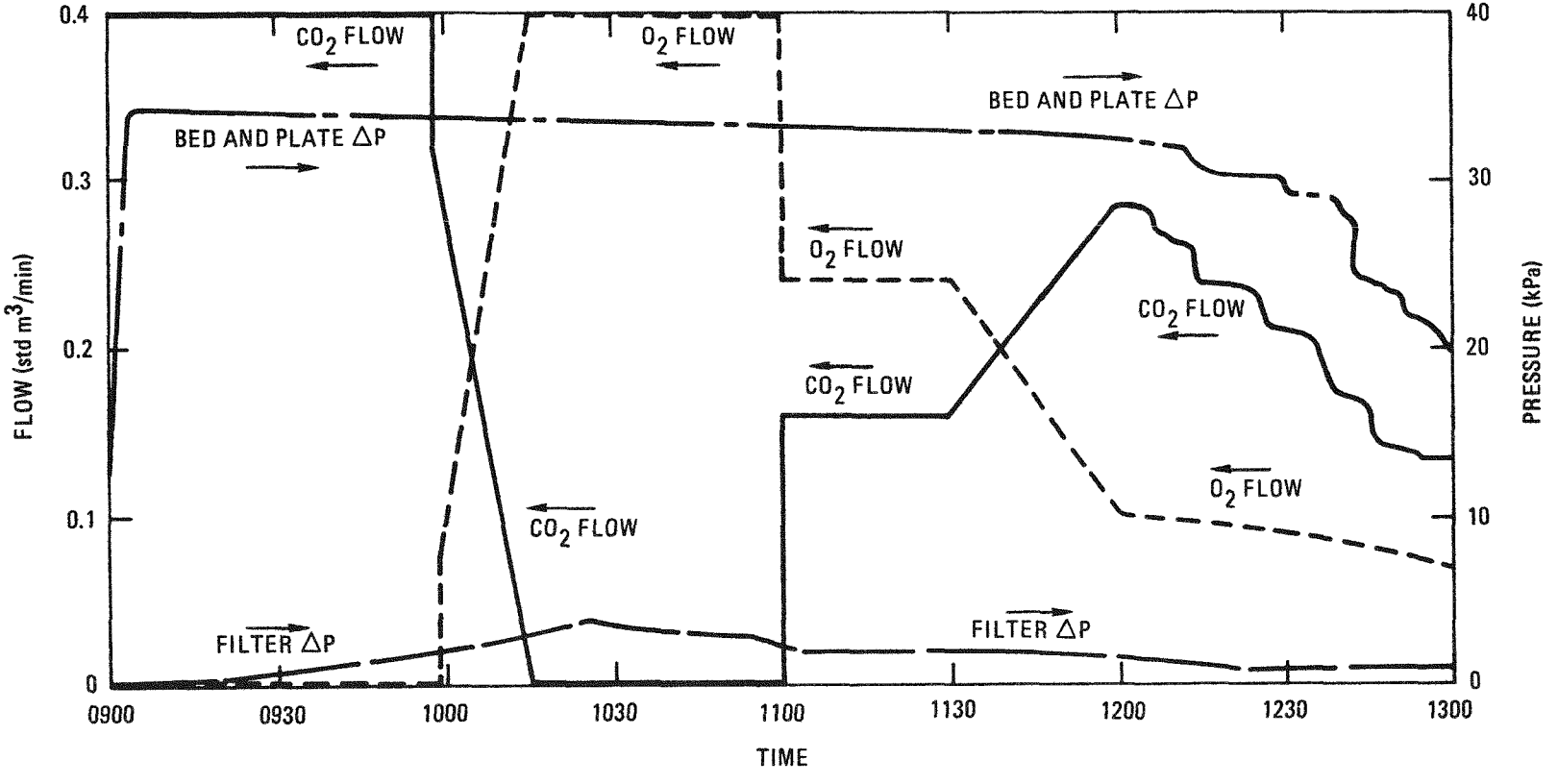

Fig. 4-8. Inlet gas flows and pressure drops, 0.20-m secondary burner Run 7

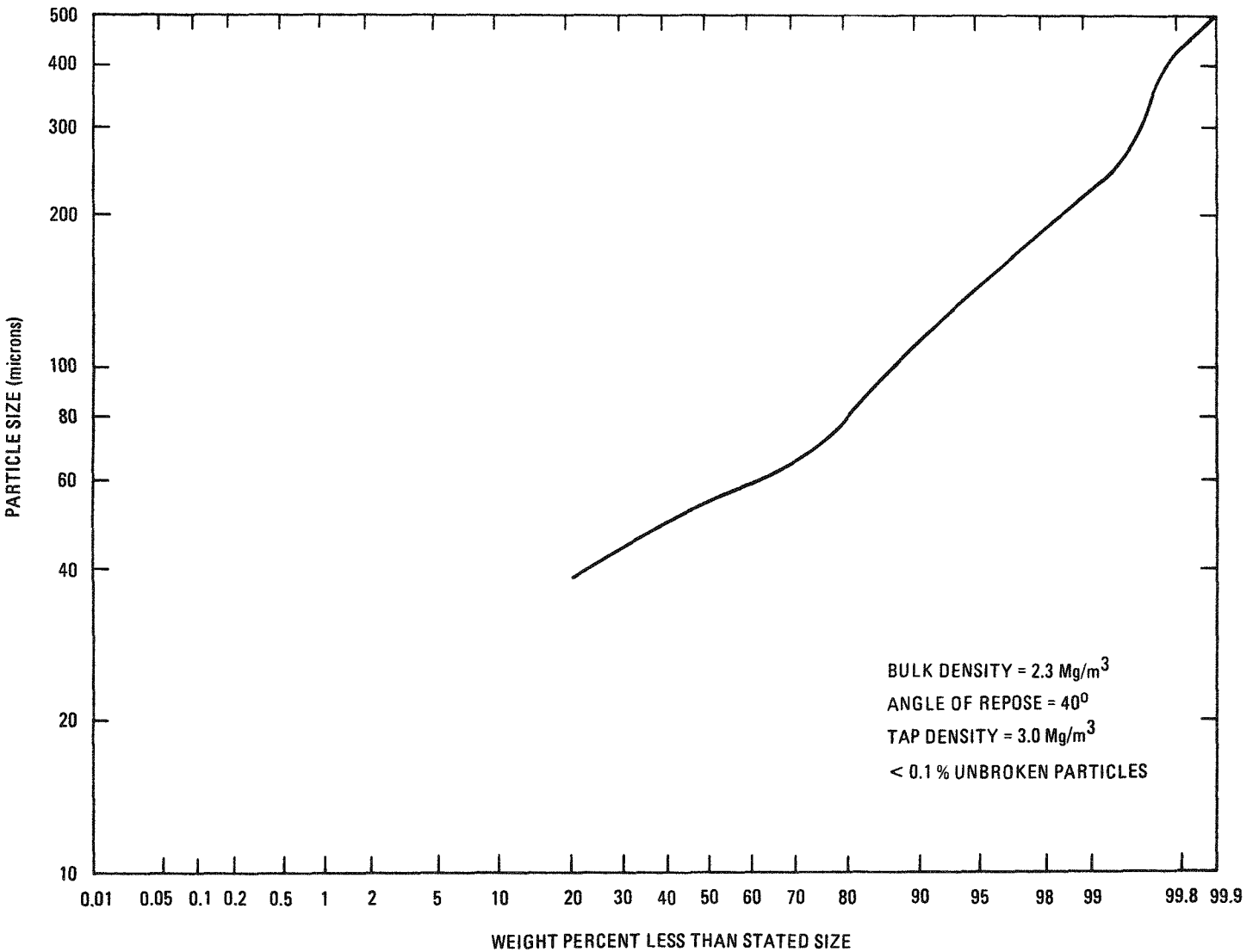

Fig. 4-9. Product size distribution, 0.20-m secondary burner Run 7

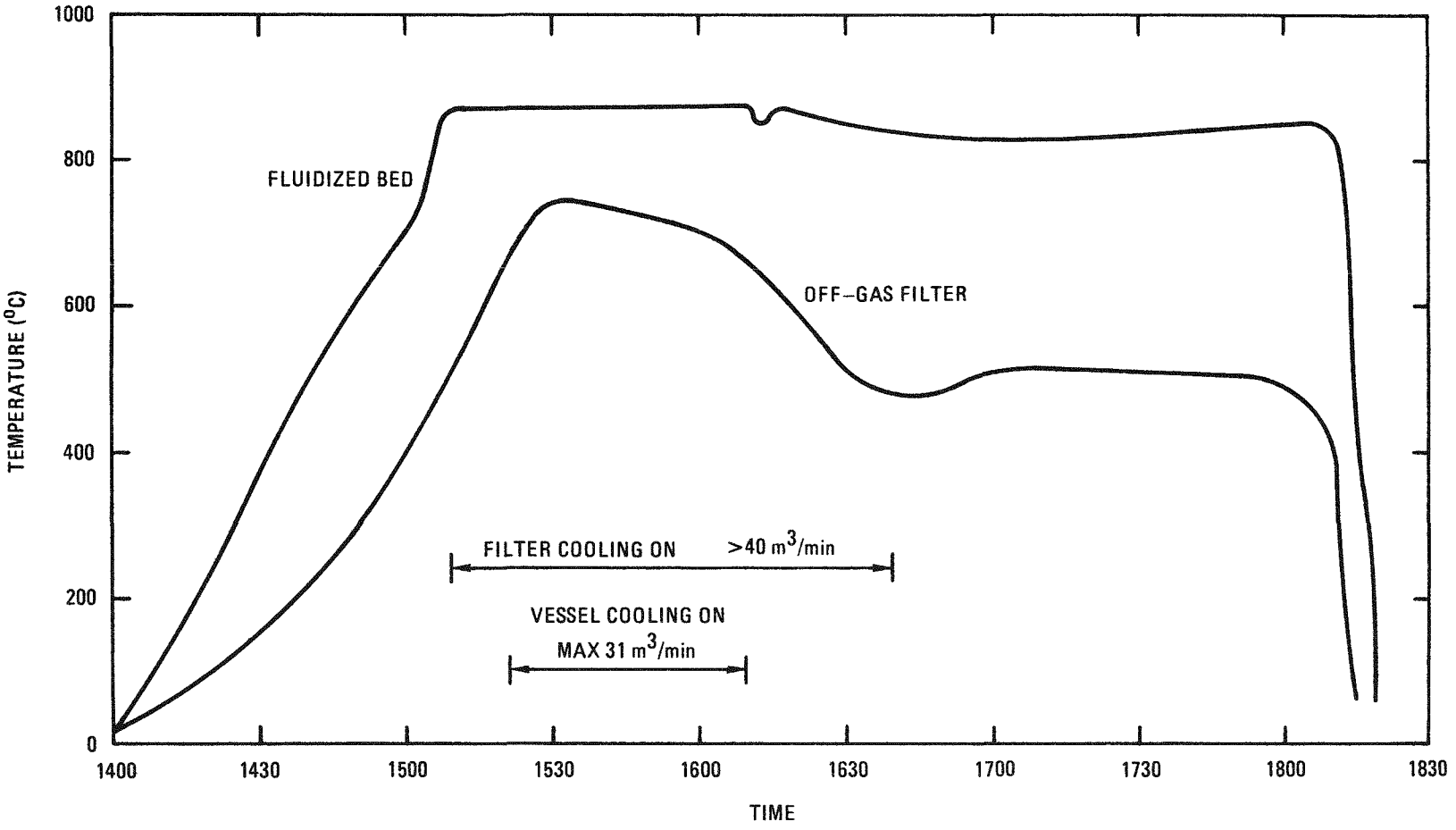

Fig. 4-10. Fluidized bed and off-gas filter temperature, 0.20-m secondary burner Run 8

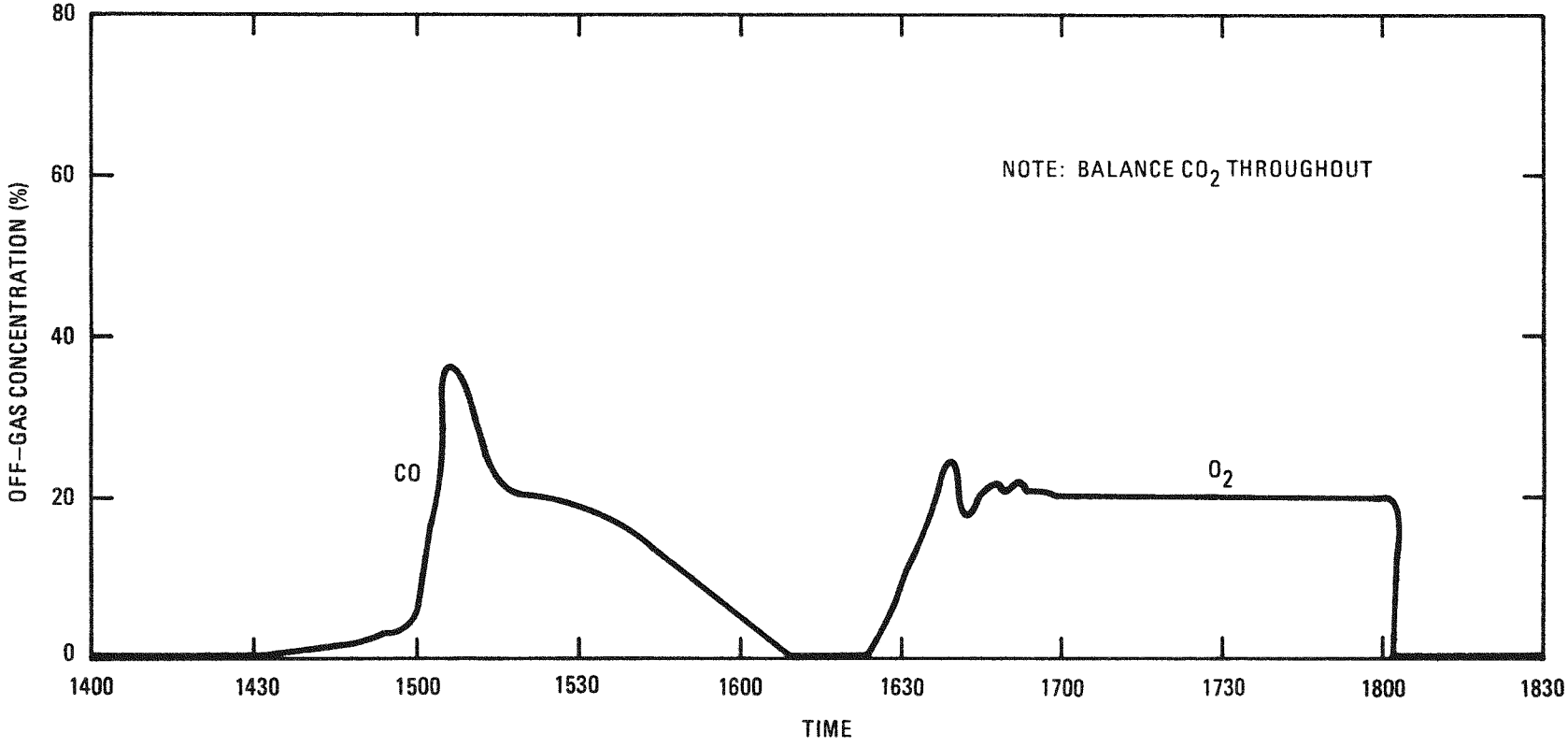

Fig. 4-11. Off-gas composition, 0.20-m secondary burner Run 8

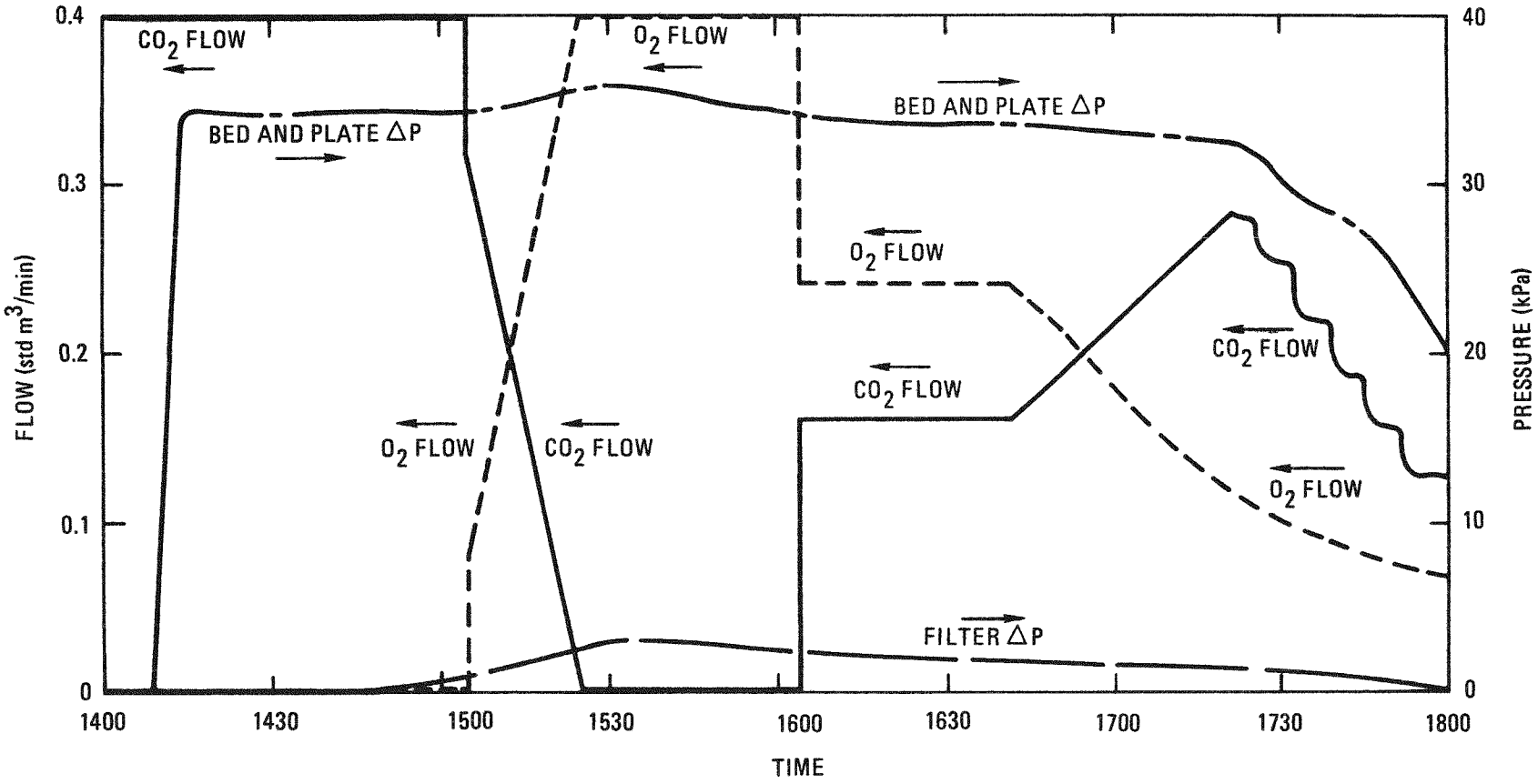

Fig. 4-12. Inlet gas flows and pressure drops, 0.20-m secondary burner Run 8

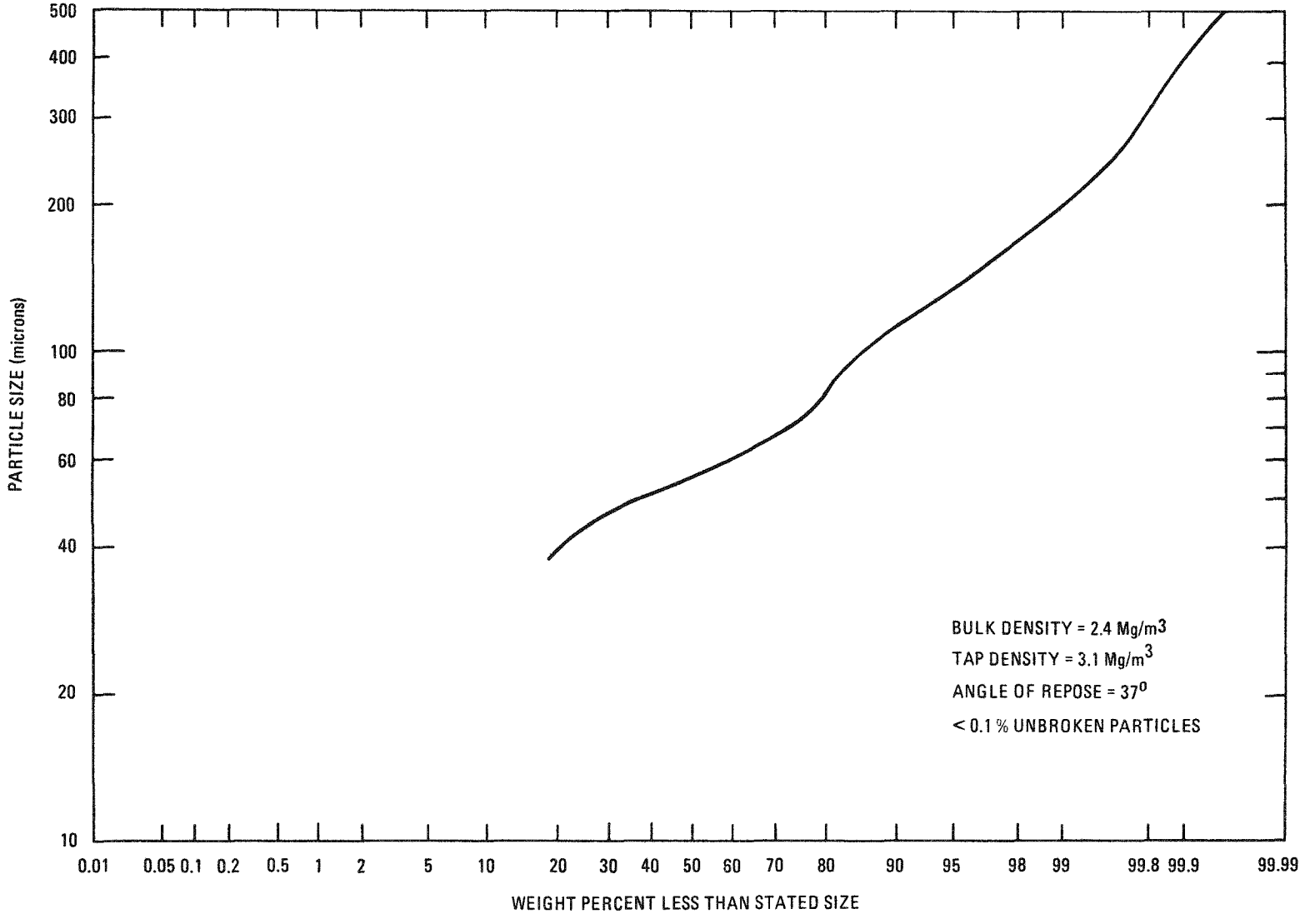

Fig. 4-13. Product size distribution, 0.20-m secondary burner Run 8

Ignition was at 700°C, following a 55-min fluid bed heatup period. The cooling air requirement was 25 m^3/min during the initial 30 min of the run, as compared with a 20 m^3/min air flow when using a 900°C bed temperature set point. Otherwise, the burner was very stable, as in previous runs.

The peak off-gas filter pressure drop was 3 kPa at 740°C. Inlet flow was dropped to 0.45 m/s by the end of final tailburning. Off-gas O_2 levels were controlled at 20% during tailburning. The product carbon content was 0.5 wt %.

4.2.2.4. Run 9 (Figs. 4-14 Through 4-17)

This final run was to test operations at a bed temperature of 850°C. The bed was ignited at 650°C following 40 min of heatup. The cooling air requirement was elevated to 33 m^3/min during the first portion of main burning and rose from this level to over 38 m^3/min. The off-gas filter pressure drop reached a high of 2.5 kPa at 660°C. The total gas flow was lowered to 0.49 m/s by the end of the tailburning period. The product carbon content was 0.5%.

4.2.2.5. Acceptance Criteria

Activity Plan AP524701 details ten acceptance criteria for the parametric study as listed below. All of these criteria were fully met.

1. No feed or product line blockage.
2. Feed time less than 15 min.
3. Product removal time less than 30 min.
4. Bed heatup in 1 hour; ability to idle at 800°C.
5. Cooling system keeps bed within 25°C of set point.
6. Control systems function properly.
7. Distributor plate functions properly.
8. Filter pressure drop <7.5 kPa.
9. No appreciable leaks or cracks.
10. No shroud frame deformation.

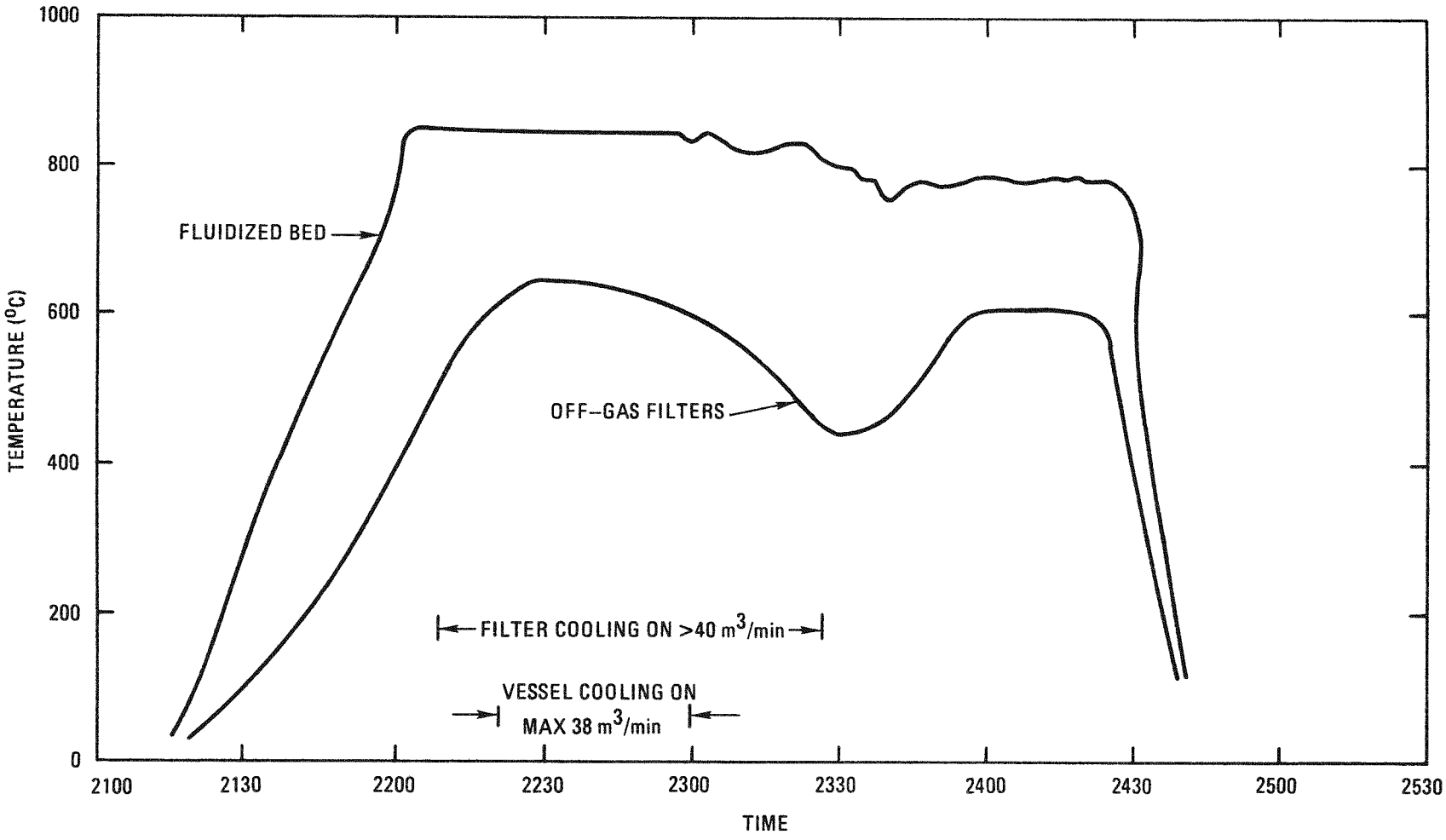

Fig. 4-14. Fluidized bed and off-gas filter temperature, 0.20-m secondary burner Run 9

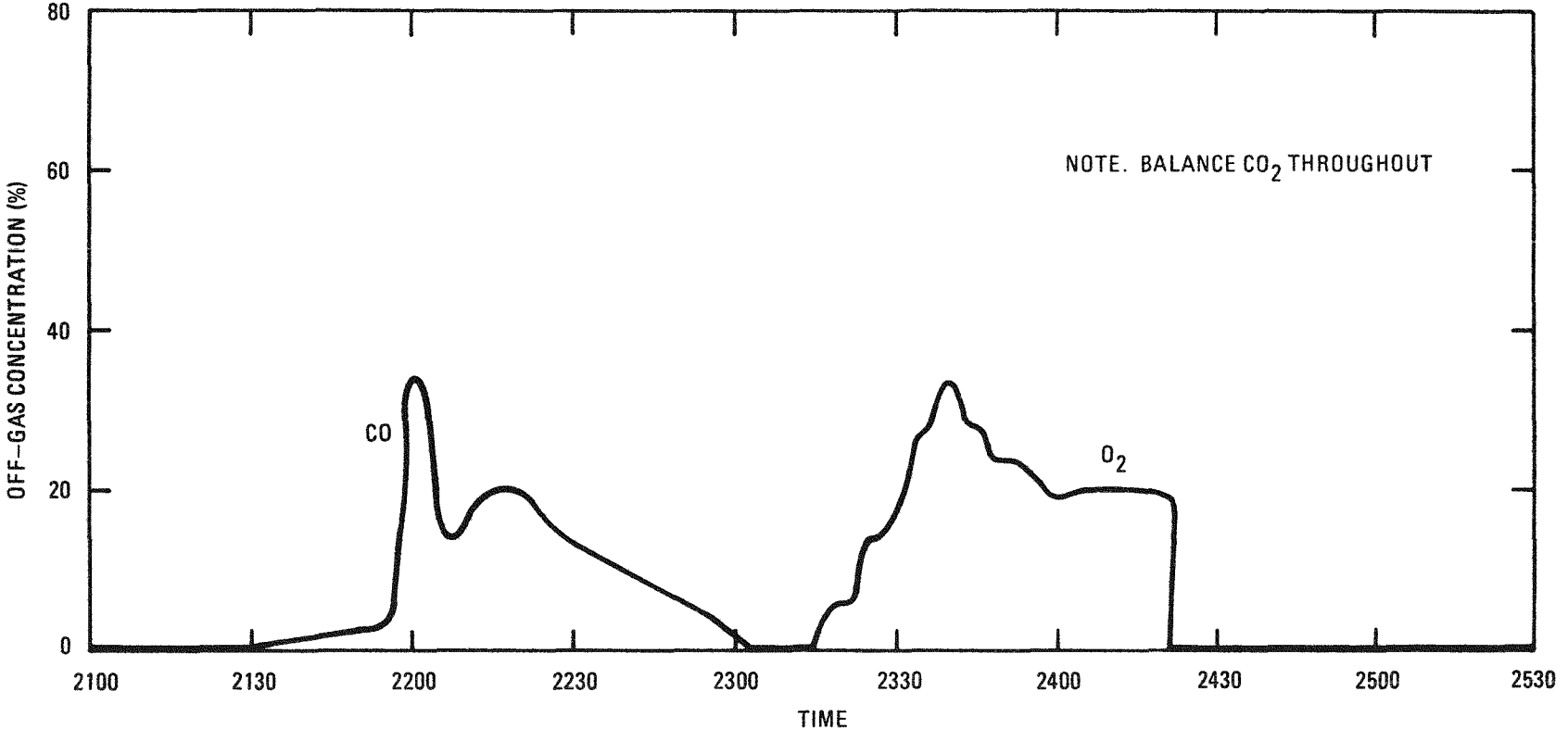

Fig. 4-15. Off-gas composition, 0.20-m secondary burner Run 9

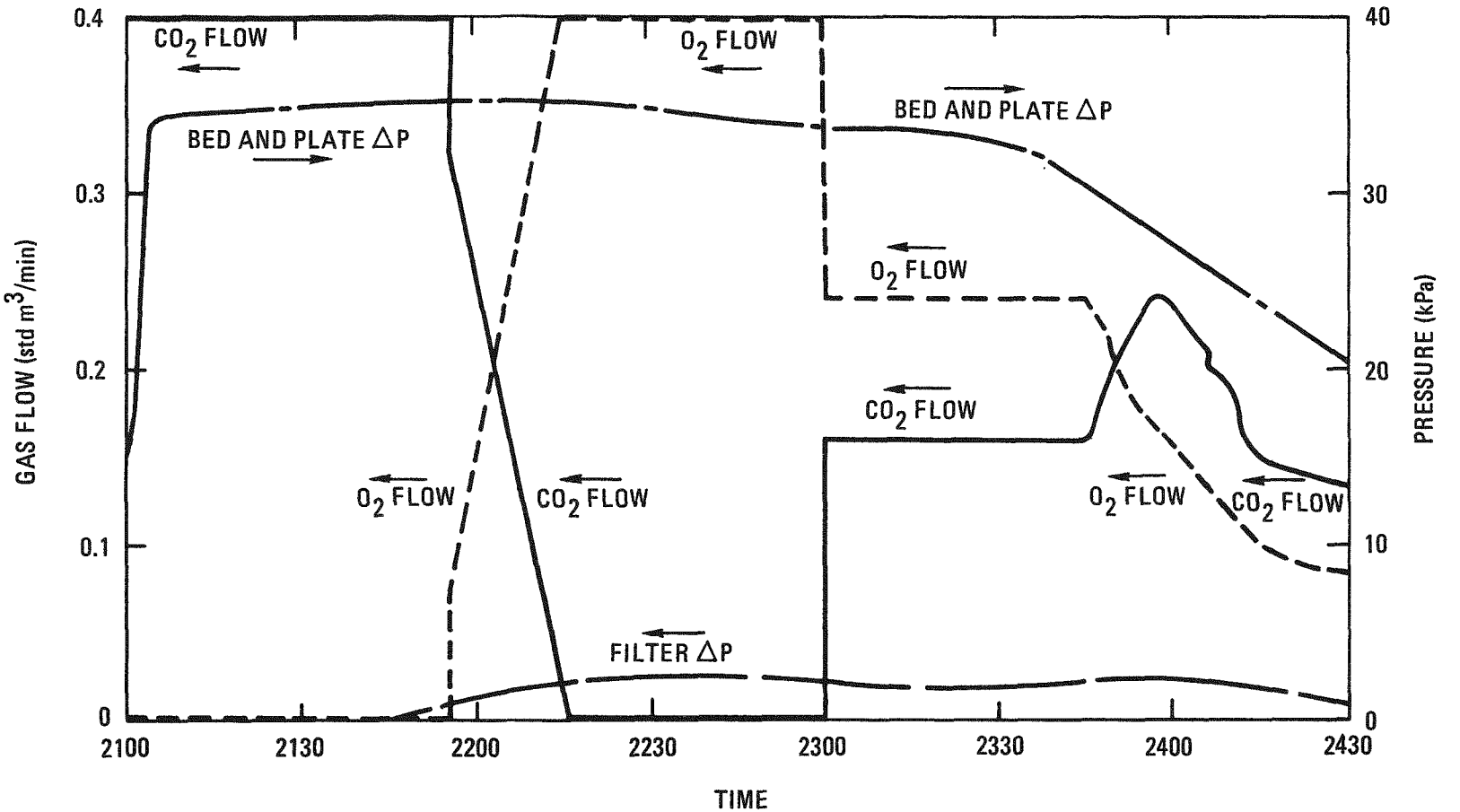

Fig. 4-16. Inlet gas flows and pressure drops, 0.20-m secondary burner Run 9

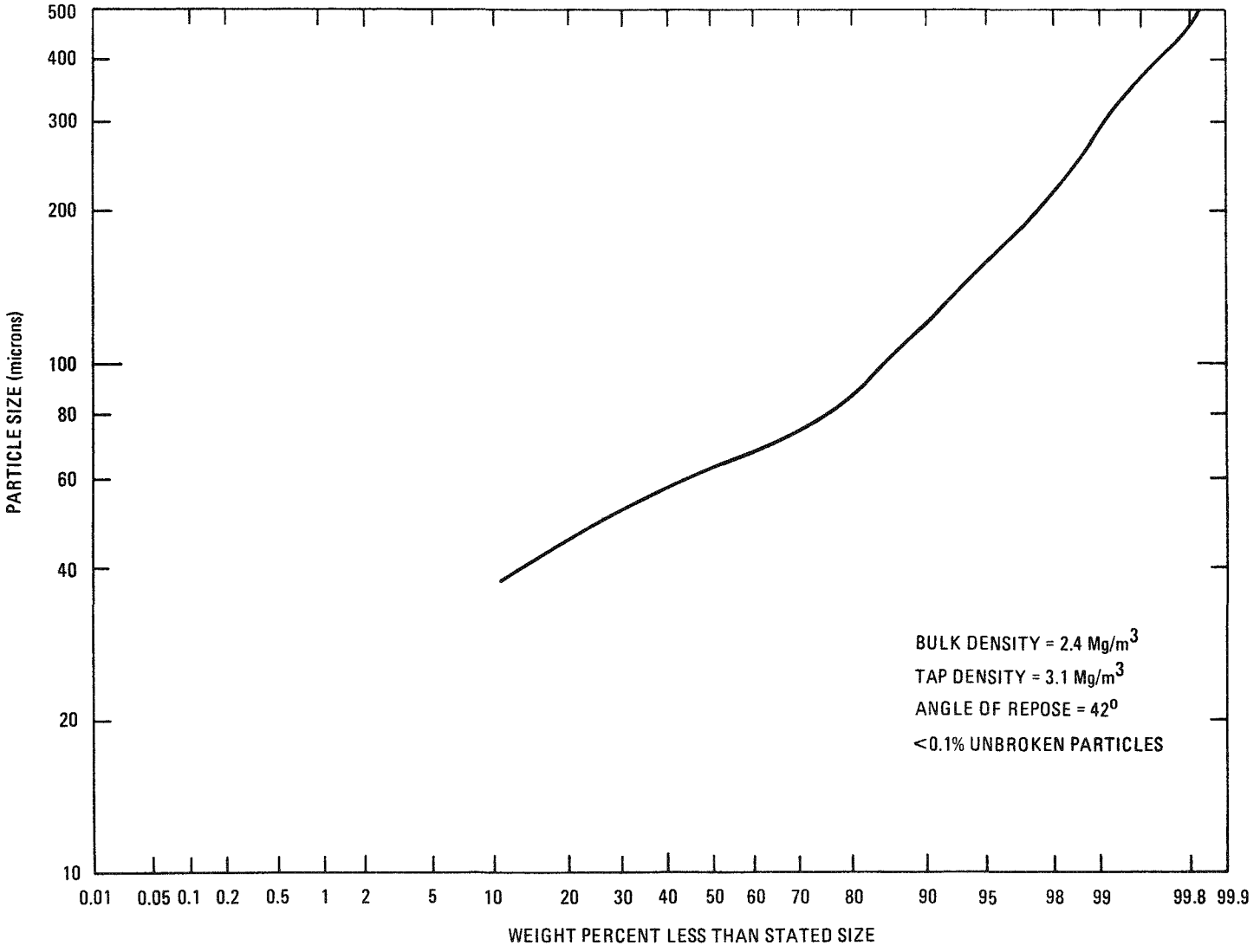

Fig. 4-17. Product size distribution, 0.20-m secondary burner Run 9

4.2.3. Evaluation of Parametric Study

Burner process variables were manipulated to yield insight to burner operation and to help optimize burner cycle efficiency.

4.2.3.1. Superficial Velocity Study

The effect of superficial velocity variation was studied in Runs 3 through 5. The superficial velocity was set at 0.90 m/s (the nominal value), 0.80 m/s, and 1.00 m/s for Runs 3, 4, and 5, respectively. Table 4-1 shows the effect of these varying flow rates on the cooling air requirement, filter temperature, and batch time reduction as a percent change from the nominal case. It can be seen that the 0.80 m/s flow rate uses less cooling air (19% less than the 1.00 m/s case), has less than half the off-gas filter pressure drop, and has an 80°C lower off-gas filter temperature. These are important benefits considering that only a 4% increase in total batch time from the 1.00 m/s case is necessary. It is therefore recommended that the inlet gas flow in future operations be 0.80 m/s.

4.2.3.2. Ignition Temperature Study

The ignition temperature was investigated in Runs 3, 4, 5, and 6 by igniting at 700°, 650°, 600°, and 550°C, respectively. Table 4-2 shows the effect on off-gas oxygen detected during startup and on the time to induction heat to the given temperature. Decreasing the ignition temperature reduced the heatup time except from 650° to 600°C where a lower superficial velocity in the former test led to equalization of the heatup times. It is desirable to reduce the heatup time while not venturing into the region where initial O_2 ramped in bypasses the bed. This gives rise to the possibility of a CO-O_2 explosion since CO is always present during startup.

It is therefore recommended that the ignition temperature in the future should be 600°C to both minimize heatup time and to preclude formation of an explosive off-gas mixture.

TABLE 4-1
EFFECTS OF VARYING BURNER SUPERFICIAL VELOCITY

Run No.	Superficial Velocity (m/s)	Peak Cooling Rate (m^3/min)	Maximum Filter ΔP (kPa)	Maximum Filter Temperature (°C)
3	0.90	32.0	3.5	775
4	0.80	29.5	2.3	720
5	1.00	36.2	5	800

TABLE 4-2
EFFECTS OF VARYING BURNER IGNITION TEMPERATURE

Run No.	Ignition Temperature (°C)	Heatup Time (min)	Startup O_2 Spike
3	700	80	No
4	650	45	No
5	600	45	No
6	550	35	Yes - 5% for 3 min

TABLE 4-3
EFFECT OF VARIATIONS IN OFF-GAS FILTER BLOWBACK FREQUENCY

Run No.	Frequency (cycles/min)	Peak Filter Pressure Drop (kPa)	Peak Filter Temperature (°C)
3	2	3.5	775
6	3	3.5	775
7	1	3.5	775

4.2.3.3. Filter Blowback Frequency Study

Increasing and decreasing the off-gas filter blowback frequency was done in three burner runs to minimize the filter pressure drop and temperature. As shown in Table 4-3, the surprising result is that no difference in peak filter pressure drop or temperature was noted. Work on the 0.10-m secondary burner had predicted a 20% decrease in pressure drop at the higher blowback rate and a corresponding increase at the lower rate. This simply did not prove to be true. The lower blowback frequency of 1 cycle/min is therefore recommended.

4.2.3.4. Bed Temperature Study

The effect of lowering bed temperature from 900°C to 875° and 850°C was studied in three burner runs. The major effects, as shown in Table 4-4, were a high cooling air requirement and a lower peak filter temperature at reduced bed temperatures. Coupling this with safer operation at lower temperatures favors the 850°C bed temperature.

The recommendation is to run the bed at 850°C while realizing that an ∿20% higher cooling air flow will be required during 1 hour of the 5-hour cycle.

4.2.3.5. Superficial Velocity During Tailburning

Superficial velocity during tailburning was not included in the original Activity Plan but was investigated as a means to lower the final bed carbon content. Figure 4-18 shows the relation between the superficial velocity during tailburning and the product carbon content.

A definite trend is noticed in these data, indicating that lower velocity at the end of the run allows more carbon fines to enter the fluid bed where they can be consumed.

The present Design Criteria DC524701 requires less than 2.0 wt % burnable carbon content in the burner product. Input from dissolution test

TABLE 4-4
EFFECTS OF VARYING BED TEMPERATURE

Run No.	Bed Temperature (°C)	Peak Cooling Air Required (m^3/min)	Peak Filter Temperature (°C)
3	900	32	775
8	875	34	740
9	850	>38	660

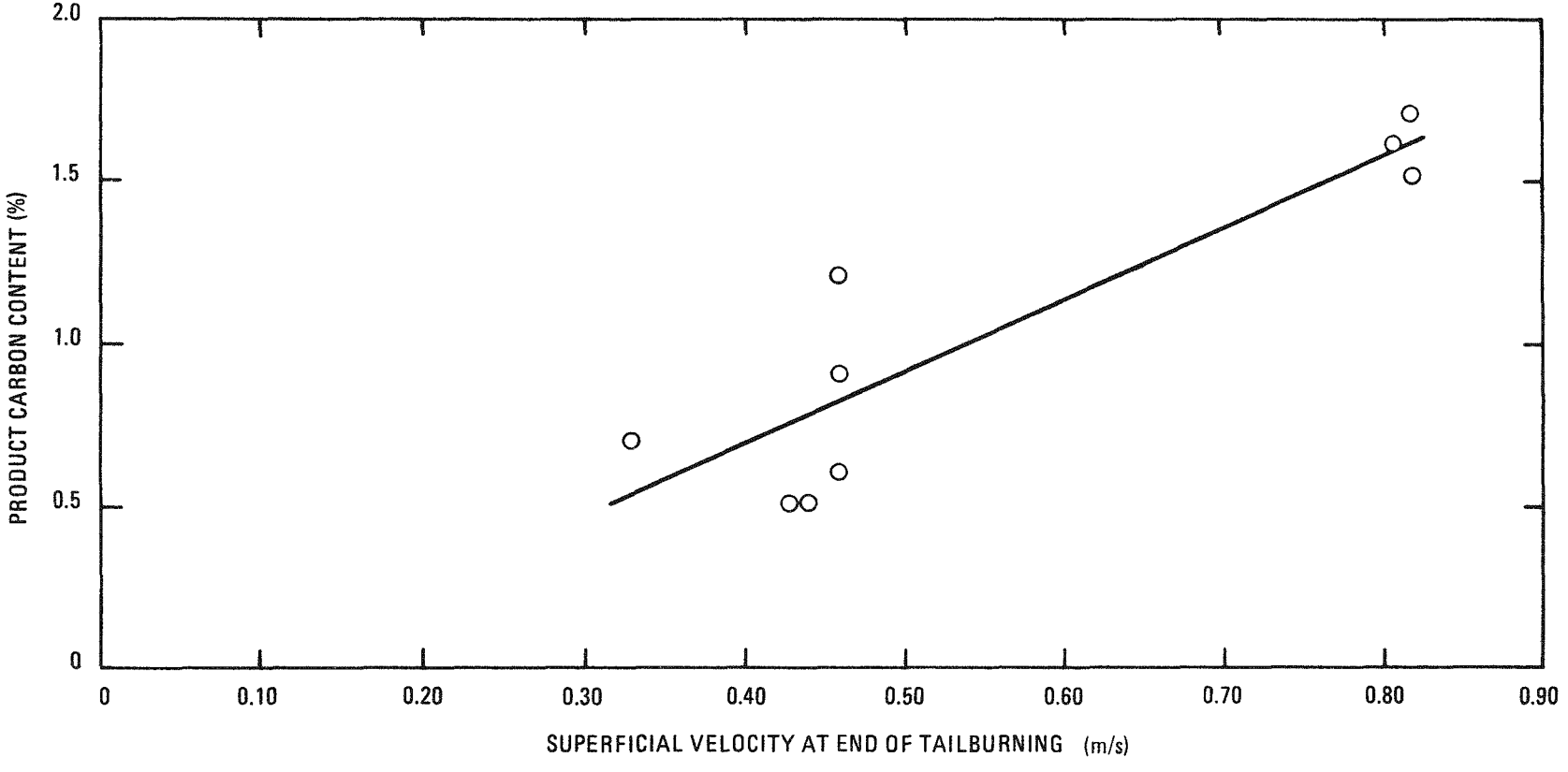

Fig. 4-18. Effect of tailburning superficial velocity on product carbon content

results will finally dictate the maximum carbon content. Until that time, the burner will be operated to ensure that the product will contain no more than 1.0 wt % burnable carbon. This requires a superficial velocity during tailburning of no more than 0.45 m/s.

4.2.4. 0.20-m Secondary Burner Design Evaluation

4.2.4.1. Introduction

Possible modification of the existing dry head-end cold pilot plant engineering-scale equipment to provide reliable and maintainable equipment that is prototypical of the HRDF design requires an evaluation of the existing equipment design. This evaluation considers the performance, maintainability, and cost of the existing system and of feasible alternative designs. Such an evaluation was initiated for the 0.20-m secondary burner system during this quarter and is nearly complete. At this point 13 significant features of the existing burner system have been evaluated, and alternative designs for these features have been considered. Ten of these 13 features are concerned with various aspects of process equipment design or manufacturing, and the other three features involve remote maintenance requirements.

4.2.4.2. Activity

The following activities were completed during the quarter and comprise approximately 85% of the design evaluation effort planned for the 0.20-m secondary burner system:

1. Technical evaluation of the 13 features of the existing design with respect to how they satisfy current requirements pertaining to ease of installation, operability, maintainability, etc.
2. Analysis of the costs of these selected features of the existing design, including labor and materials to manufacture, assemble, and install them in the burner system.

3. Selection and technical evaluation of alternative design features, using the technique of value engineering.

4. Analysis of the costs of the alternative design features.

Table 4-5 lists the 13 design features under evaluation, their basic functions, and the alternative designs being considered for each of these features. In general, at least two alternatives have been selected for cost analysis with each design feature.

4.2.4.3. Conclusions

The cost differentials of the alternatives are being developed prior to comparison with the present design and selection of the preferred design. The merits of each alternative are being evaluated not only individually but in conjunction with the other alternatives in order to achieve compatibility of the 13 features in an integrated prototype design concept. The key features that will influence the selection of the prototype design concept are the methods of heating and cooling the burner vessel and its contents.

4.3. 0.10-m SECONDARY BURNER

4.3.1. Crushed FSV Fissile Particle Burning

4.3.1.1. Introduction

At present there are 16.5 metric tons of fissile fuel particles in the Fort St. Vrain HTGR core. In anticipation of the eventual operation and refueling of the FSV reactor, there is the task of oxidizing crushed irradiated FSV fissile particles as part of the fuel reprocessing flowsheet. Toward that end, the Activity Plans for both the 0.10-m and 0.20-m secondary burners call for at least one run for each burner using a batch of unirradiated, crushed FSV fissile particles. These particle batches were made for practice prior to FSV fuel production and contain depleted, rather than enriched, uranium.

TABLE 4-5
0.20-m SECONDARY BURNER SYSTEM PRESENT DESIGN FEATURES AND ALTERNATIVES

Design Feature	Basic Function	Alternative Designs
1 Separability of upper and lower cooling shrouds	1 Allows removal of vessel, coil, and shroud	1(a) Use single removable shroud with sliding seals (b) Use integral welded shroud with bellows (c) Use single nonremovable shroud, welded at the ends, with sliding seal for thermal expansion
2 Remote disconnects on burner vessel	2 Allows removal of vessel, distributor, and/or in-vessel filters	2 Eliminate middle 0.20-m remote flange Relocate the lower 0.15-m remote flange to a cooler zone below distributor (HETF secondary burner design)
3 External vessel cooling shroud	2 Transfers heat	3(a) Use internal heat exchanger (gas-cooled tubes) (b) Use direct gas (internal) cooling
4 Method of heating the burner (induction heating subsystem)	4 Increases (bed) temperature	4(a) Blow hot gaseous CO_2 through burner bed (b) Blow hot gaseous CO_2 through external cooling shroud (c) Use (a) and (b) together
5 Method of thermocouple attachment to vessel	5 Sense temperature	5(a) Use spring-loaded thermocouples (b) Use tube-skin thermocouples
6 Method of fabrication of susceptor	6 Transfers heat	6(a) Use centrifugal casting (b) Use forging (c) Use nonmagnetic stainless steel
7 Type of burner insulation (current: ceramic)	7 Reduce heat transfer	7(a) Use moldable fiber, e.g., WRP-X (b) Use dry fiber blanket, e.g., FIBERFRAX
8 Insulation bonnet assembly	8 Allows separation for maintenance	8(a) Use unitized design (existing 0.40-m primary burner) (b) Replace bonnet with two-piece insulation assembly (c) Use single large insulated enclosure

TABLE 4-5 (Continued)

Design Feature	Basic Function	Alternative Designs
9 Upper cap assembly	9 Resist pressure/support weight	9 Eliminate filter plenum chamber. Provide external blowback system (HETF secondary burner design)
10 Solids feed entry (existing: side entry)	10 Transport flow	10 Use top entry
11 Product removal valve	11 Resist pressure/control flow	11(a) Use HETF primary burner product removal valve (b) Eliminate product removal valve; elutriate product out the top with a "push-pull" system
12 Separability of induction coil, susceptor and insulation	12 Transfer heat	12 Use integral construction of coil, susceptor, and insulation
13 Uncontrolled gap between susceptor and vessel tube	13 Permit expansion	13(a) Provide an integral shroud (b) Provide a single removable shroud with spacers

The purpose of the 0.10-m burner run(s) was to provide any trouble-shooting required prior to using the larger 0.20-m burner. A 0.10-m burner run has been completed which was very smooth and trouble free. The second portion of Activity Plan AP524601 was completed and all acceptance criteria were completely met. Single-batch operation on the 0.20-m secondary burner will conclude FSV fissile particle work as that run will use the balance of the available material.

4.3.1.2. Burner Operation

Feed material was prepared using the fissile particle roll crusher. The size distribution is shown in Fig. 4-19. The average surface area to volume ratio diameter, d_{sv}, was 93 μm. The bulk density was 1.5 Mg/m^3 and the tap density was 1.9 Mg/m^3. The angle of repose measured 29°. The material composition was 23% ThC_2, 6% UC_2, 42% SiC, and 29% C.

The crusher motor current draw was 6.3 amp or 560 W with 30-rpm roll speed. The crushing rate was 45 kg/h. The crusher stalled momentarily on initial crushing, but restarted after manual assistance.

The batch of 12 kg was introduced to the burner through the gravity pneumatic feeder system over a 3-min period. The batch was fluidized with 0.10 std m^3/min CO_2 and induction heated over a 70-min period to an ignition temperature of 650°C. Figures 4-20, 4-21, and 4-22 show the bed and off-gas filter temperatures, the O_2 and CO_2 gas flow rates and the fluid bed and off-gas filter pressure drops, and the off-gas concentrations, respectively.

Ignition was effected by raising the inlet O_2 flow to 60% while the total flow remained at 0.10 std m^3/min. No oxygen was detected in the off-gas. Earlier experiments with FSV fertile particles had precluded the use of over 70% inlet O_2 concentration in order to eliminate the possibility of small agglomerate formation in the distributor plate region.

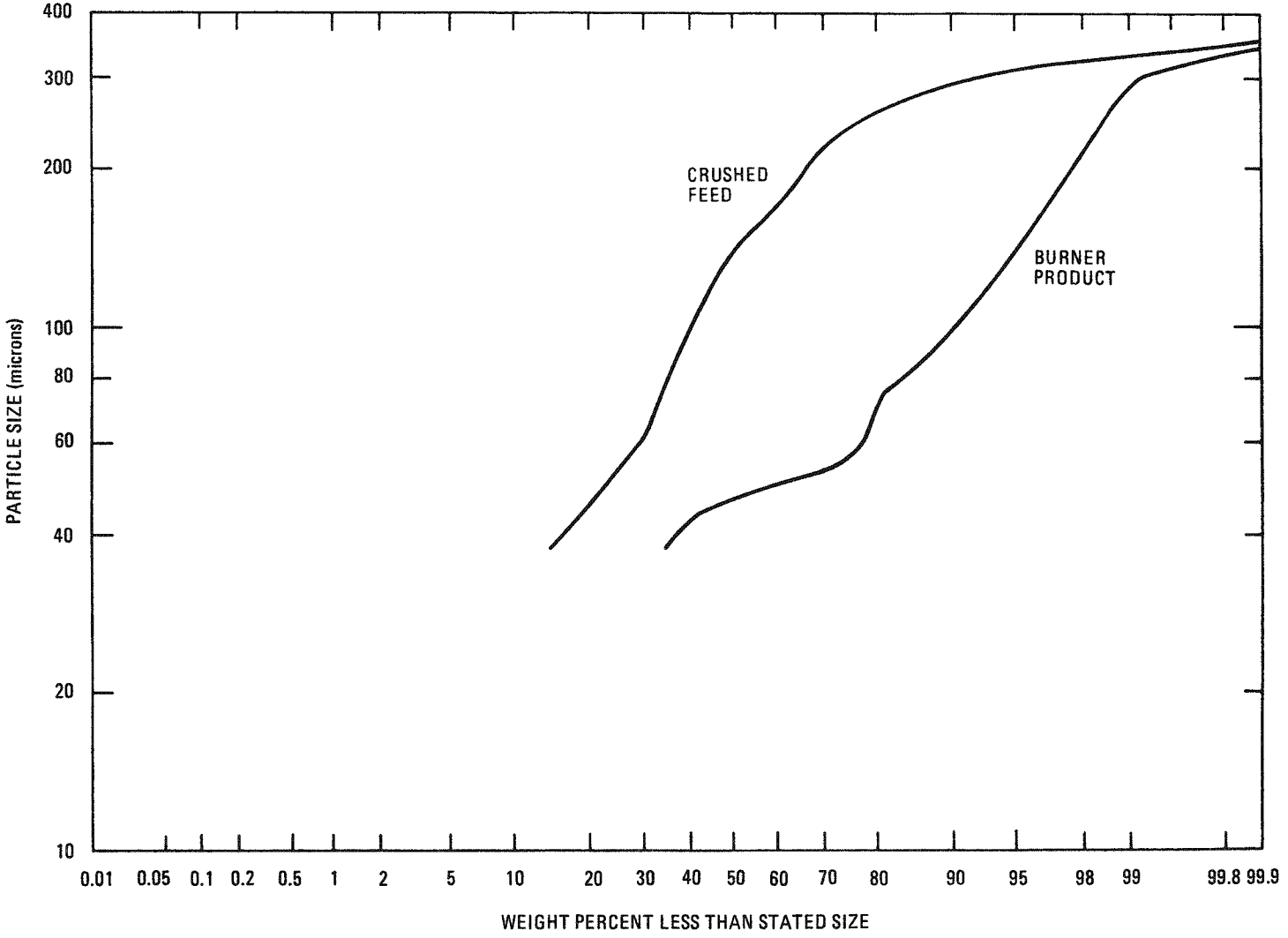

Fig. 4-19. Feed and product size distributions, 0.10-m secondary burner, FSV fissile particle Run 1

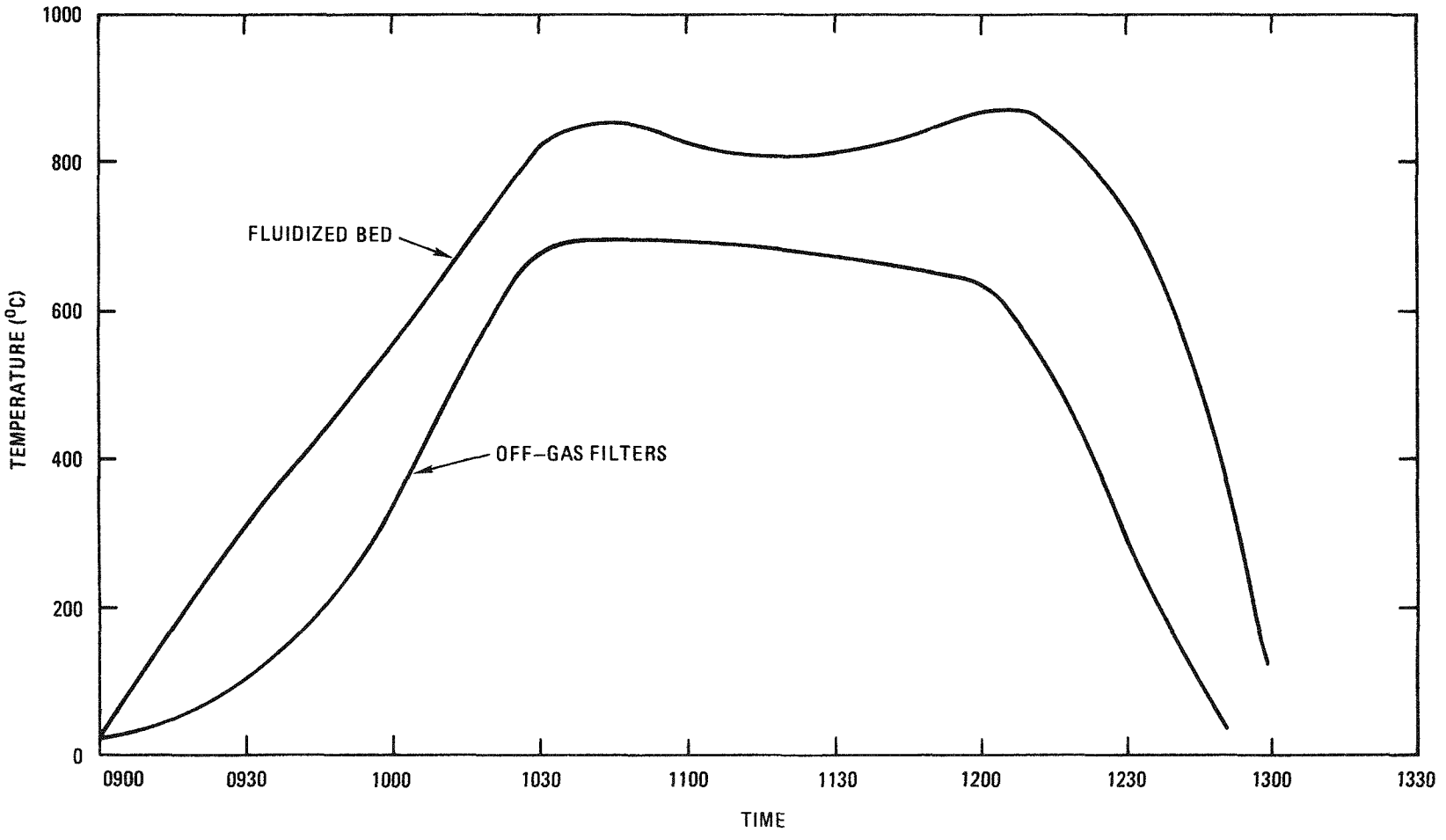

Fig. 4-20. Fluidized bed and off-gas temperatures, 0.10-m secondary burner, FSV fissile particle Run 1

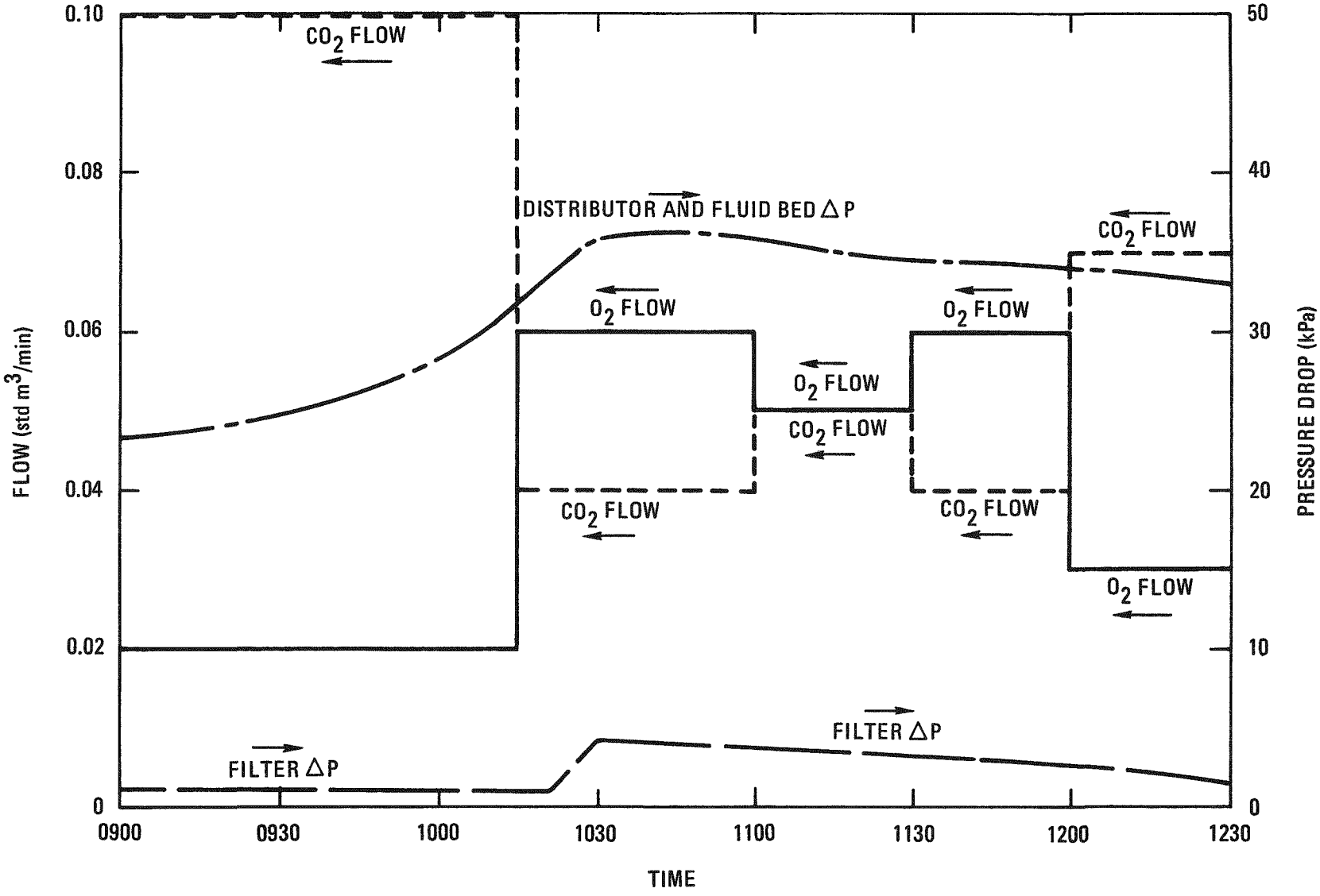

Fig. 4-21. Inlet gas flows and pressure drops, 0.10-m secondary burner, FSV fissile particle Run 1

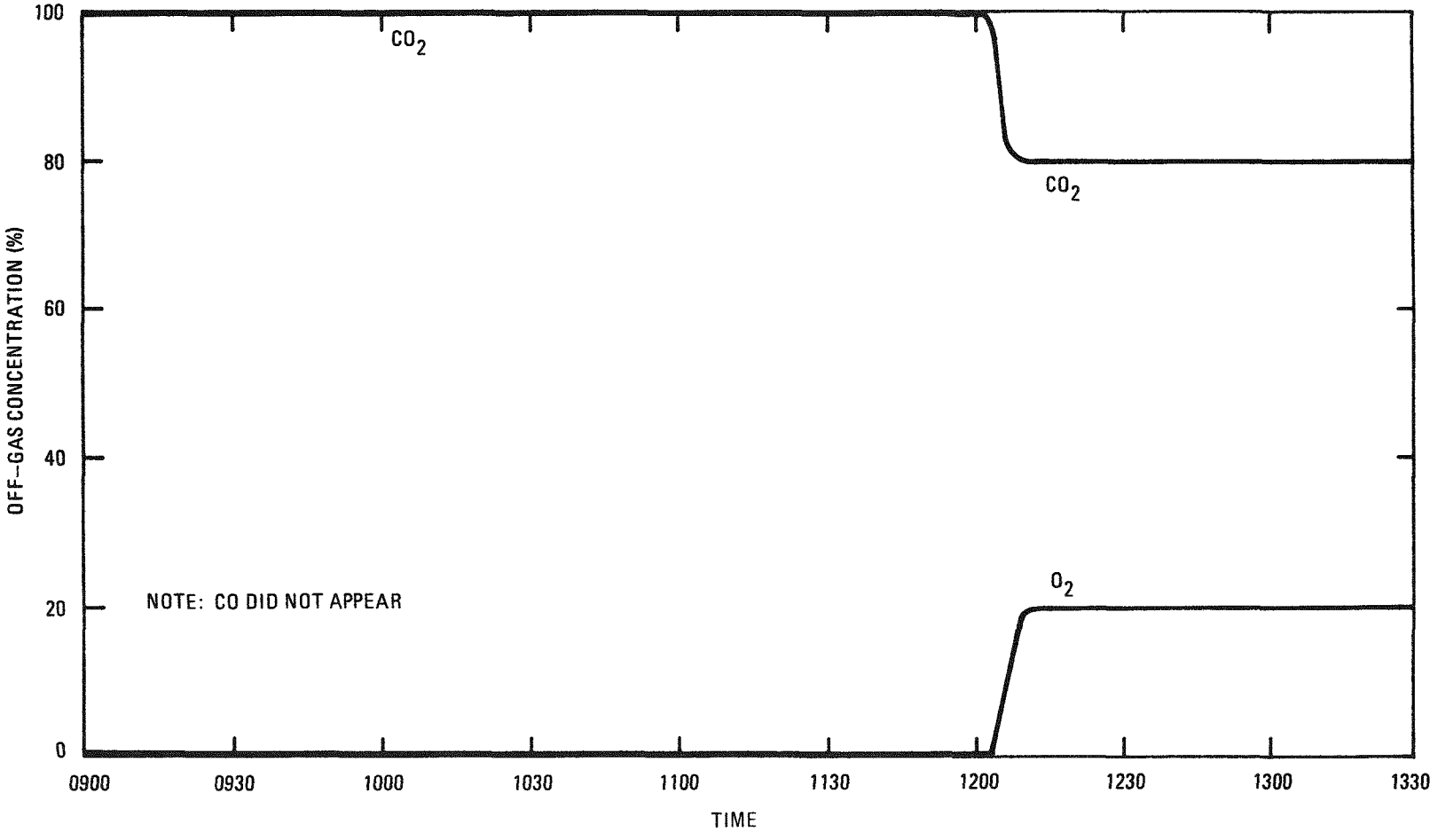

Fig. 4-22. Off-gas composition, 0.10-m secondary burner, FSV fissile particle Run 1

Process heat generated by combustion and induction heating the burner wall to 900°C yielded a fluid bed temperature of 850° to 880°C. Complete combustion was realized at this temperature. An interesting phenomenon is that the off-gas never contained carbon monoxide; this is a dramatic change from the up to 30% CO observed during crushed FSV fertile particle combustion. Fluidization was also very different with a lack of significant slugging. Bed pressure drop fluctuations were never more than ±0.75 kPa throughout the run. In addition, off-gas filter fines loadings were very reasonable with peak filter pressure drops of 4 kPa. Cooling air was not required during the entire burner run.

After 115 min of burning, oxygen utilization efficiency dropped abruptly from 100% to 0% over a 10-min span. The oxygen front had penetrated the bed only after consuming all available carbon. The burner was then switched to pure CO_2 operation and allowed to cool to <100°C prior to product removal. Pneumatic transport of the product as it exited through the side-mounted product removal valve was trouble free. Subsequent burner lower spool piece removal showed that 100% burner cleanout had been realized; there was not even any dust left on the distributor plate.

Product analysis gave a size distribution as shown in Fig. 4-19. The bulk density was 2000 kg/m^3 and the tap density was 2600 kg/m^3. The angle of repose measured 44°. The product burnable carbon content was 0.2%.

Because this was a very stable, trouble free run in comparison with other secondary burner runs, it has been recommended that preparations proceed to make a batch 0.20-m secondary burner run.

4.4. PARTICLE CRUSHING

4.4.1. FSV TRISO Fertile Particle Crushing

During the past quarter, the fertile particle crusher has been used for preparing feed for four burner runs on the 0.20-m secondary burner. The total throughput was 240 kg. The gap setting was 480 μm, and the roll

speed was between 36 and 44 rpm. The crushing efficiency was >99.9% in each run.

During the last portion of the last crushing test, a roll bearing overheated and caused the motor to overheat and stall. The bearing was found to be low on grease. After cleaning and regreasing, the bearing functioned for the remainder of the run but was in poor condition. The crusher will be disassembled and examined to determine the cause of bearing failure.

The localized wear in the crusher body side plates has continued. Inserts of tungsten carbide composites K703 and K68 were tested simultaneously crushing 150 kg of material. Both tungsten carbide inserts exhibited improved wear resistance, with the K703 proving to be the best material to date.

The K68 insert was removed and replaced with a solid ceramic material, boron carbide (B_4C), which has outstanding hardness (2750 Knoop) compared with tungsten carbide (1800 Knoop). Particle crushing was continued with the crusher equipped with the new B_4C insert and retaining the previously installed K703 insert for continued wear information. The crusher has not been disassembled since refitting with the new insert. There has been no evidence or indication of additional wear since the restarting of crushing.

Table 4-6 compares the various test materials used in the crusher body side plates and the wear test results from crushing silicon carbide coated fuel particles.

The fertile crusher rolls were decontaminated and examined by Quality Assurance for evidence of wear after crushing approximately 500 kg of material. The roll surfaces were inspected by a recording surface analyzer which scans the surface for finish or roughness and for contour change. Roll diameters were measured in 20 places and compared with previous measurements. No positive definable trends in wear of the roll crushing faces were noted after crushing the 500 kg of silicon carbide coated material.

TABLE 4-6
SIDE BODY WEAR DATA, FERTILE PARTICLE CRUSHER

Material	Source and Type	Hardness[a] R_C	Hardness[a] R_A	Abrasion Resistance[b]	Observed Wear	Crusher Throughput	Comments
Tool steel	AISI D2	57	79	13 to 14	Slot, 0.3 mm (0.012 in.) deep x 0.6 mm (0.025 in.) wide	150 kg	As designed
Chromium oxide, plasma spray	Metco 136F - repair	74	89	Unknown	100% removed	60 kg	No binder
Tungsten carbide, plasma spray	Metco	60	81	Unknown	>90% removed	60 kg	Best plasma spray product - cobalt binder
Tungsten carbide, plasma spray	Metco	53	78	Unknown	100% removed		Comparison material - cobalt binder
Tungsten carbide, and chromium oxide, solid ceramic	Kennametal K703 - insert	80	92	760	Slot, 0.1 mm (0.0044 in.) deep x 0.6 mm (0.055 in.) wide	150 kg	Cobalt binder, best material to date
Tungsten carbide, solid ceramic	Kennametal K68 - insert	>80	93	300	Slot, 0.2 mm (0.0073 in.) deep x 0.7 mm (0.028 in.) wide		Cobalt binder
Boron carbide, solid ceramic	Norton Co. B_4C insert	2750 Knoop[c]		Unknown[d]	Under test[e]	180 kg	None

[a] From vendor data, except D2 tool steel which was hardness tested.

[b] Abrasion resistance equals unity divided by volume loss with dry silica sand - Kennemetal data.

[c] For comparison, solid tungsten carbide = 1880 Knoop and solid silicon carbide = 2480 Knoop.

[d] Material used in sand blast nozzles.

[e] Product continues to be acceptable after crushing.

4.4.2. Demonstration of FSV Fissile Fuel Particle Crushing

Phase II of Activity Plan AP520001 for the fuel particle crusher has been successfully completed. The nominal roll crusher gap required to maximize both crushing efficiency and crushed particle size was 250 μm (0.010 in.).

When initially received, the roll crusher nominal gap was 230 μm (0.009 in.). This was changed to a nominal 330 μm (0.013 in.) gap for the first crushing tests by switching appropriate rolls. A 200-g sample of FSV fissile particles (see Fig. 4-23 for size distribution) was processed at that time. Approximately 50% of the particles were uncrushed; therefore, a smaller roll gap [280 μm (0.011 in.)] was assembled.

At this gap setting, a study was done on the rotating roll torque versus roll gap to establish the correlation between radial bearing preload and the crushing gap between the rolls. The radial preload of a tapered roller bearing is created by the relative axial position of the inner and the outer bearing elements or races acting on the conical surfaces of the tapered rollers. The amount of radial preload is increased as the two races are brought more closely together. In the particle crusher, these relative positions are regulated by shims which position the outer bearing race. Thinner shims produce higher preloads.

During this study, shim thicknesses were varied 25 or 50 μm (0.001 or 0.002 in.) and the bearing preloads were measured by rotating each independent roll in the assembled crusher at a constant speed using a calibrated torque wrench and mating the rolling torque. The roll gap was gauged by manually roll reducing a solid, tin-lead, soft solder wire [S/N 60, 787 μm (0.031 in.) diameter]; accurately measuring the resultant ribbon thickness in three places; and averaging the results.

Figures 4-24 and 4-25 show the results of the preload study for each of the rolls in the crusher assembly. It should be noted in each figure that a rolling preload torque of 80 to 90 in.-lb is required to eliminate

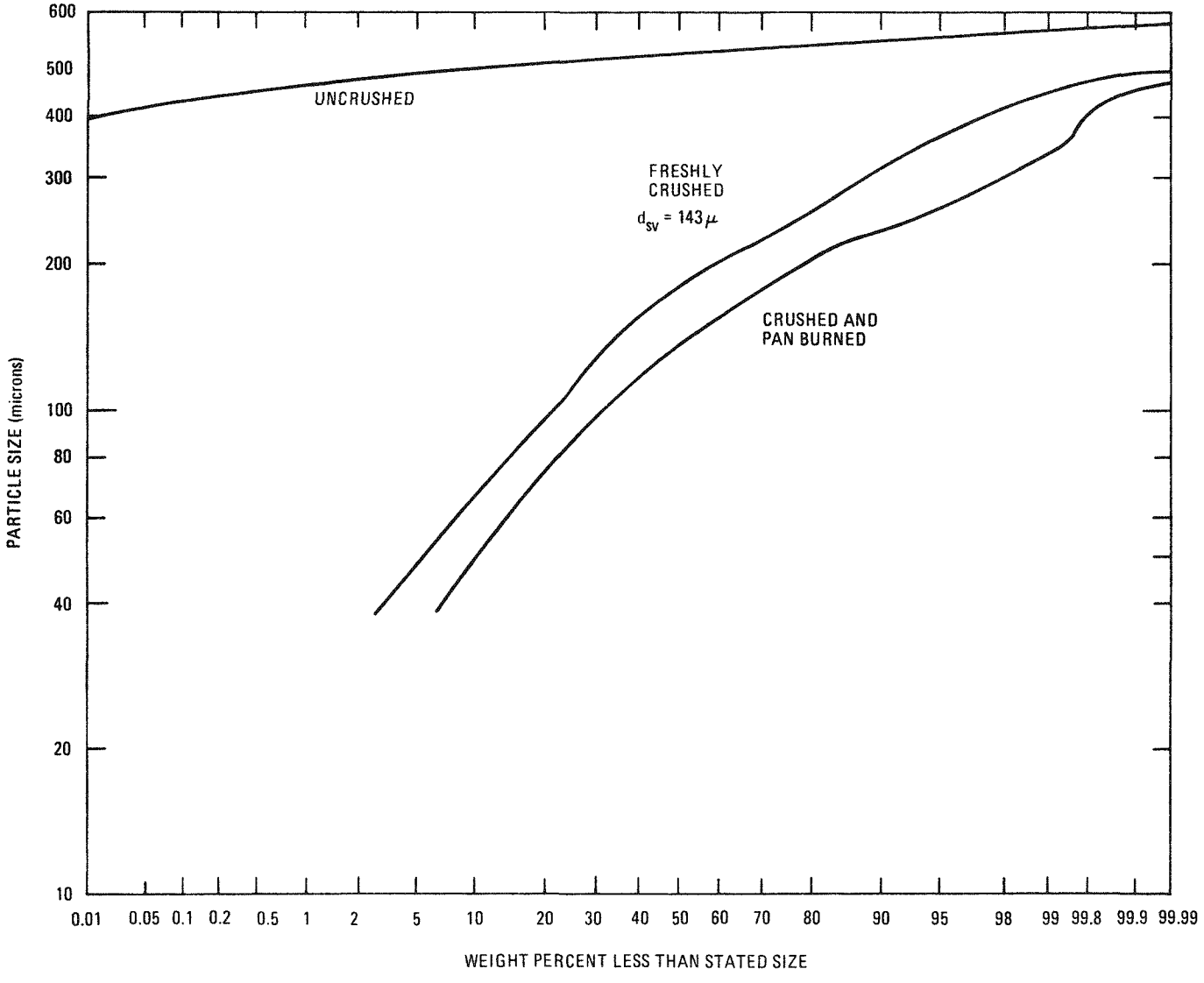

Fig. 4-23. Feed and product size distributions, FSV fissile particle crusher

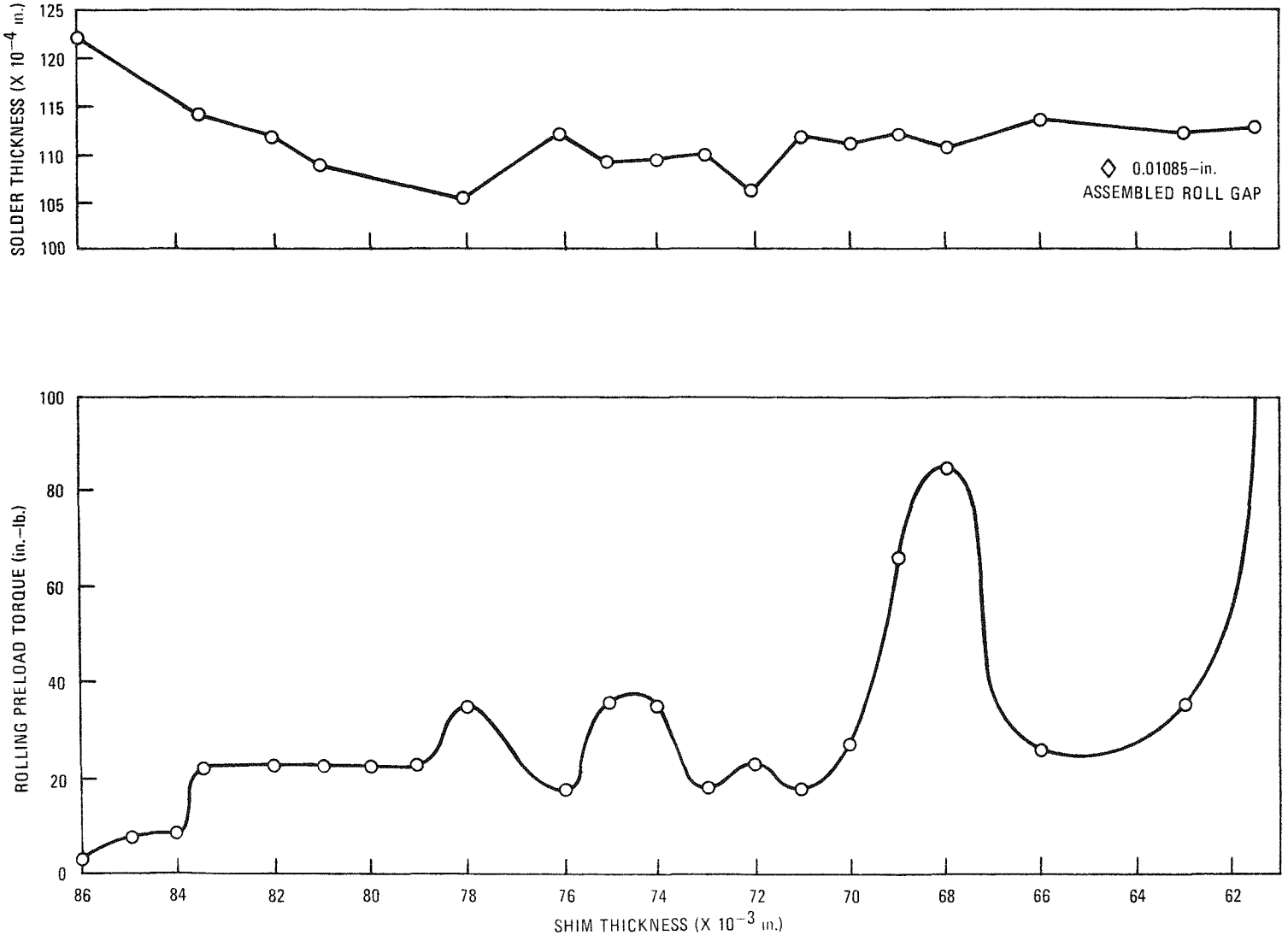

Fig. 4-24. Preload torque and solder thickness versus shim thickness, roll 5211011-13, S/N 4340-5

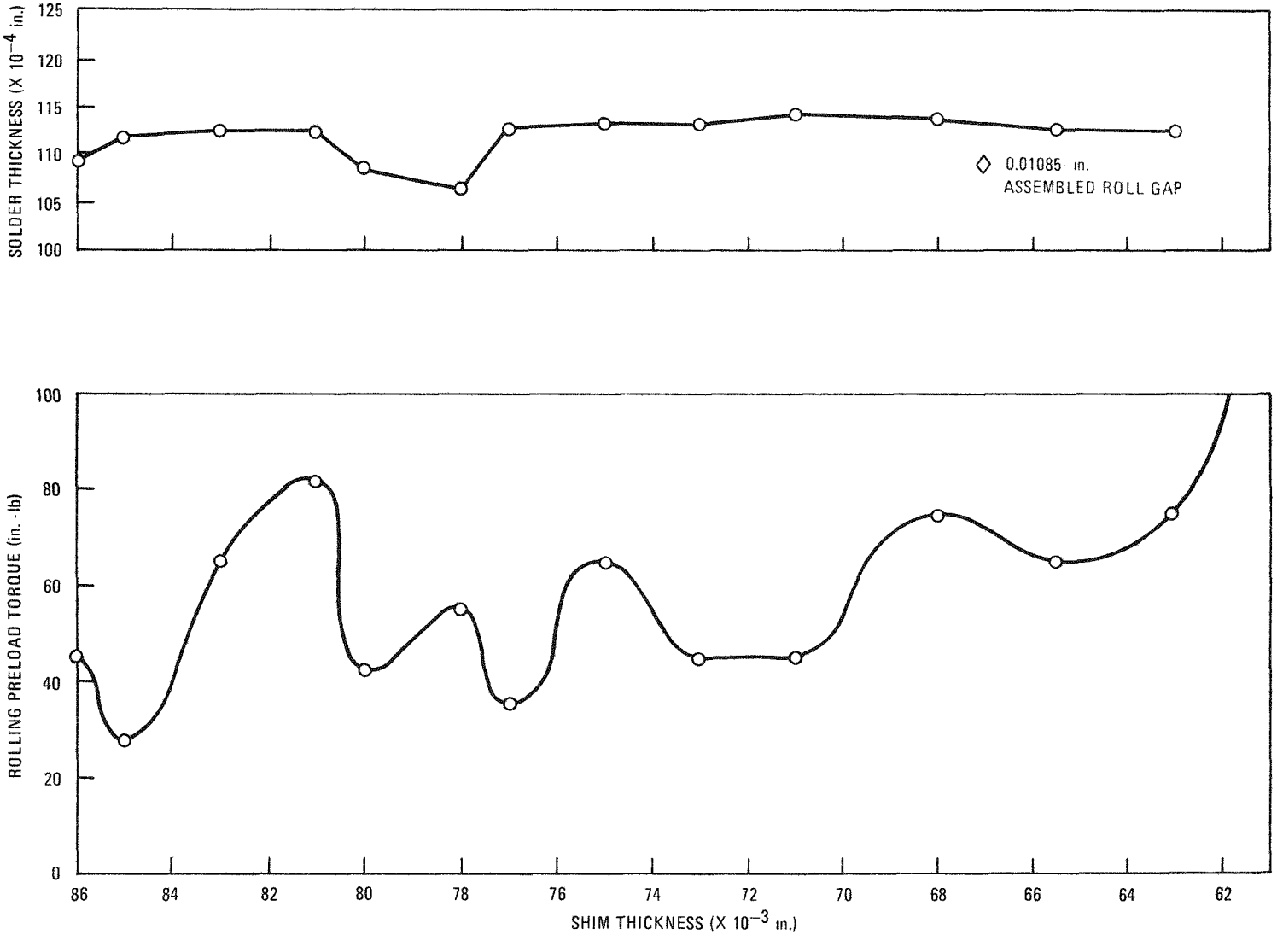

Fig. 4-25. Preload torque and solder thickness versus shim thickness, roll 5211011-10, S/N 4340-2

variances in the preload created by bearing seating, etc. However, viewing the changes in solder thickness with shim thickness, it would appear for both rolls that a preload of 40 in.-lb torque would produce a constant and consistent roll gap of from 280 to 292 μm (0.0110 to 0.0115 in.). The preload selected for future particle crushing was 90 in.-lb although this may prove to be too high for satisfactory bearing life.

Referring to Figs. 4-24 and 4-25, it can be seen that repeatable roll gap measurements can be made using proper preload shimming and 787 μm (0.031 in.) diameter solid solder. These gap measurements were consistent to within 13 μm (0.0005 in.) and were only 13 to 18 μm (0.0005 to 0.0007 in.) higher than the crusher roll gap calculated from inspection data for this crusher.

A 100-g sample of FSV fissile particles was processed yielding ∿3% uncrushed particles. The roll gap following crushing was again 280 μm (0.0110 in.) using the solder strip. Thicker solder [3302 μm (0.13 in.)] was then used. This was extruded to 330 μm (0.013 in.). Since the smallest fuel particle was 300 μm (0.0116 in.) and ∿3% were uncrushed, it is reasonable to assume that the gap during highly loaded crushing conditions is greater than the 280 μm (0.0110 in.) measured with the small solder strip. The large solder strip results tend to confirm this, as the larger strips are a definite load on the rolls when extruded through the rolls.

The rolls were again changed to yield a nominal 250-μm (0.010 in.) gap. The roll torque was adjusted to 90 in.-lb. The gap as measured by the 787 μm (0.031 in.) solder was 250 μm (0.010 in.) while the thicker 3302 μm (0.13 in.) solder yielded a 305 μm (0.012 in.) gap. The resulting crushing efficiency with 200 g of particles was 100%.

The size distribution of these fully crushed FSV fissile fuel particles is shown in Fig. 4-23. The product angle of repose was measured as 43°. The bulk density was 1.4 Mg/m^3 and the tap density was 1.8 Mg/m^3. The throughput of the material was 80 kg/h at 43 rpm roll speed. Start under load was achieved. Normal power draw at 43 rpm roll speed with choke feed conditions is 522 W.

A burner run will be made on the 0.10-m secondary burner using FSV fissile particles processed through the roll crusher using a nominal 250-μm roll gap.

4.4.3. Demonstration of LHTGR WAR Fissile Fuel Particle Crushing

Phase III of Activity Plan AP520001 for fuel particle crushing has been successfully completed using WAR (weak acid resin) type TRISO coated fissile fuel particles burned back to the SiC coating. Depleted uranium was used in the manufacture of these fuel particles as they were made in the developmental fuel production pilot plant. The particles contained 22% $UC_3O_{0.5}$, 32% carbon, and 46% SiC.

The size distribution is shown in Fig. 4-26. Inspection of Fig. 4-26 shows that ∿6 wt % of the fuel particles are less than 500 μm (0.0197 in.). Previous experience has shown that setting the roll crusher gap slightly larger than the smallest particles to be crushed will result in high crushing efficiencies (>99%) while minimizing overcrushing. A roll pair was available to give a 495-μm (0.0195 in.) roll gap, as measured by the 3175 μm (0.125 in.) solid solder technique. This gap was used and gave 100% crushing efficiency, with a size distribution after crushing as shown in Fig. 4-26. The crusher roll speed was 36 rpm with 250 W required by the motor during crushing. The material throughput was 920 g/min.

Pertinent properties of the crushed particles were as follows: angle of repose = 22°, bulk density = 1.1 Mg/m^3, and tap density = 1.4 Mg/m^3.

The material was then tray-burned in a muffle oven to burn away the carbon inner coatings and to convert the uranium to U_3O_8. Size analysis after tray burning is shown in Fig. 4-26. The material properties were: angle of repose = 34°, bulk density = 1.3 Mg/m^3, and tap density = 1.6 Mg/m^3

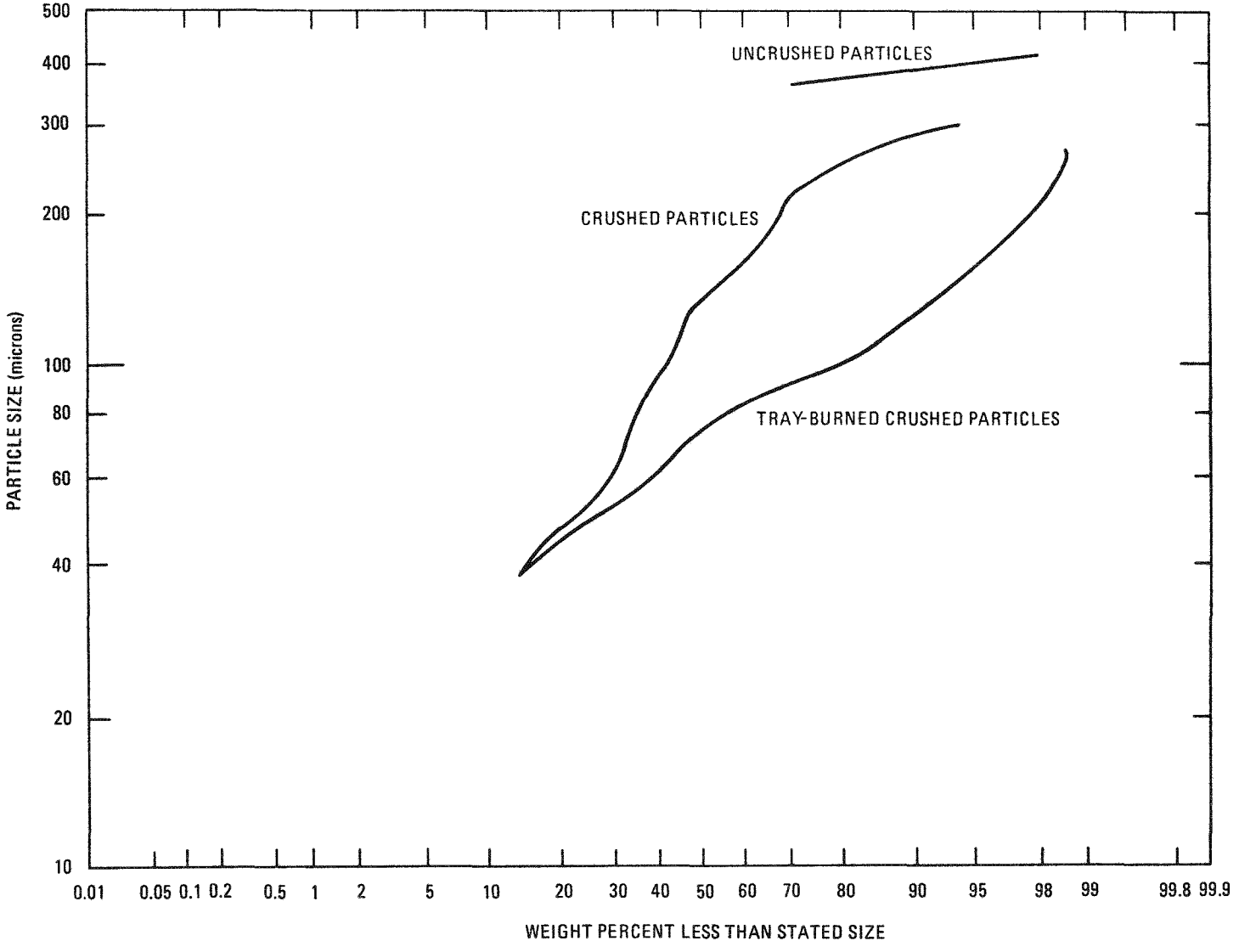

Fig. 4-26. Size distributions, crushed WAR particles

No inert gas was used or needed during the crushing tests. A slight warming of the material was noted initially (about 5°C) but this heat soon dissipated.

Start under load was achieved with 100 g of fuel particles.

Burning tests of crushed WAR particles in the 0.10-m secondary burner are planned for completion prior to the end of the fiscal year. No problems are foreseen in handling the material as processed by the roll crusher. The high SiC content (46% as compared to 22% for FSV fertile particles) will add a large degree of safety to the burner operation since it serves as inert fluidizing media.

5. AQUEOUS SEPARATION

5.1. SUMMARY

The design of the engineering-scale dissolver-centrifuge system is approximately 75% complete. Procurement of the major vessels (i.e., dissolver, repulp tank, product tank, and Thorex tank) is under way. The continuous, vertical Sharples P-850 centrifuge is ready for final testing and inspection with delivery scheduled for June. The purchase of instrumentation and the modification of the pilot plant for the new system will be initiated during the next quarter.

The first pilot plant heel dissolution run has been completed. Some difficulty was experienced with heat transfer through the settled layer of BISO particles.

5.2. ENGINEERING-SCALE DISSOLUTION

5.2.1. Large Engineering-Scale Dissolver-Centrifuge System

5.2.1.1. Introduction

The next step in the development of dissolution-centrifugation for HTGR reprocessing is the design of the engineering-scale dissolver-centrifuge system. This system, together with the future insols dryer, will be incorporated into the engineering-scale cold pilot line, thereby completing the demonstration of sequential operation of the HTGR head-end reprocessing.

Included in the system are feed and product tanks, a dissolver and condenser, a centrifuge, and a repulp tank. Specifically, data will be provided on the dissolution of Fort St. Vrain (FSV) and reference TRISO and BISO fuels, on the separation of the mother liquor from the undissolved solids, and on the repulping of the solids for better recovery of the heavy metal nitrates. Later in the program, solids drying will be added and equipment to demonstrate remote maintenance of selected components will also be added.

5.2.1.2. System and Equipment Design

5.2.1.2.1. System Design. Figure 5-1 is a process flow diagram for the dissolver-centrifuge system. The system interfaces upstream with the secondary burner system and the particle classification system and downstream with the feed adjustment and solvent extraction systems. Feed materials are transferred to the dissolver feed hoppers via pneumatic transport lines from the secondary burner product bunker and from the BISO particle storage bunker. Manual filling of the dissolver feed hoppers is also possible from a transfer can.

The physical arrangement of the system is shown in Figs. 5-2 through 5-4. Figure 5-2 shows a plan view of the system including the Thorex tank, potassium fluoride and aluminum nitrate storage tanks, dissolver vessel, BISO and product ash hoppers, repulp tank, centrifuge, and product tank. Figures 5-3 and 5-4 show system elevation views.

5.2.1.2.2. Equipment Design.

Dissolver. The dissolver is a Type 304L stainless steel vessel with a jacketed conical bottom and a jacketed cylindrical section. Steam is applied to the cone to heat the contents of the vessel and assist the nitrogen sparge in agitation. For cooling, water is run through the cylinder jacket.

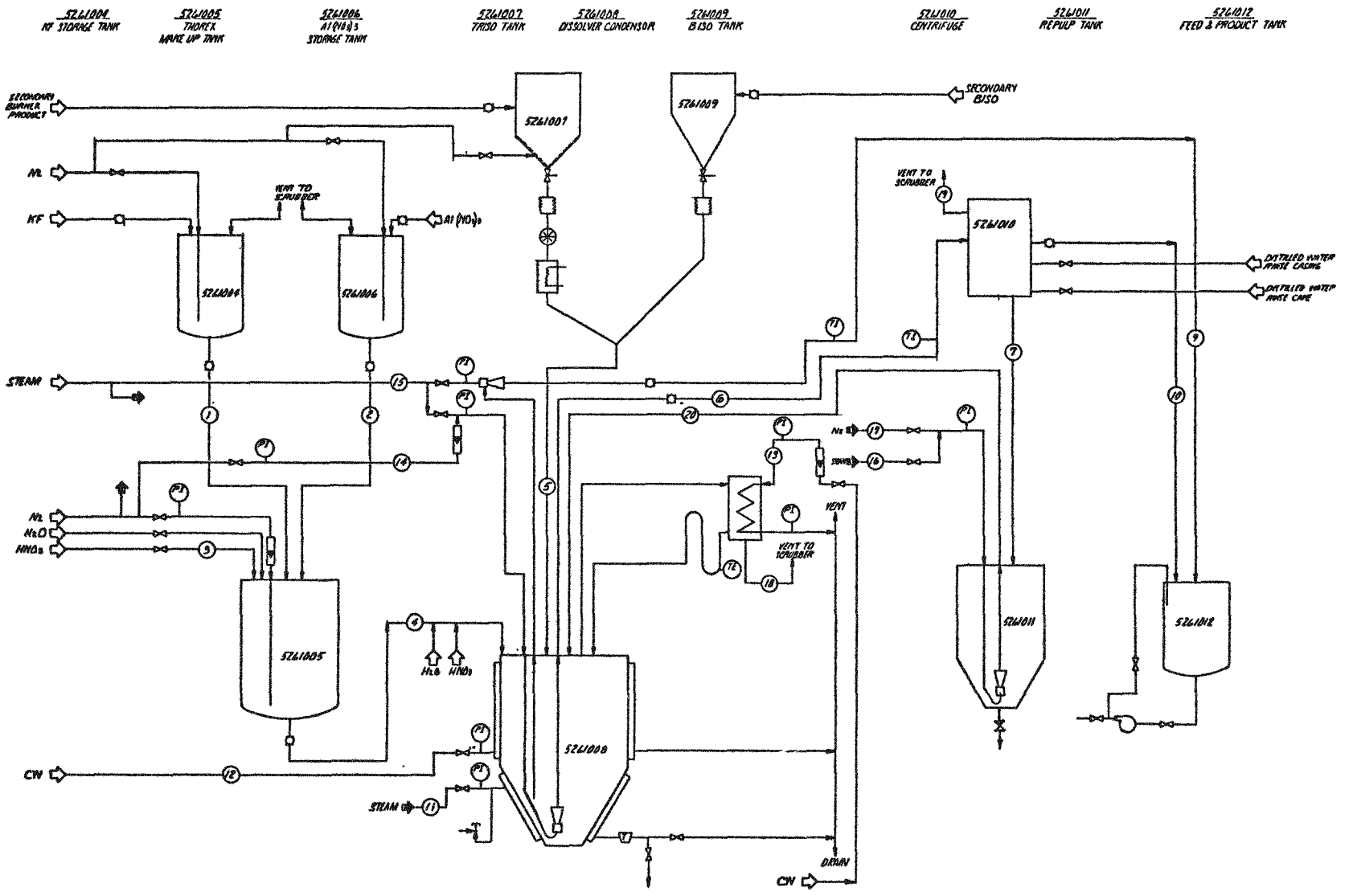

Fig. 5-1. Process flow diagram for large-scale dissolver-centrifuge system

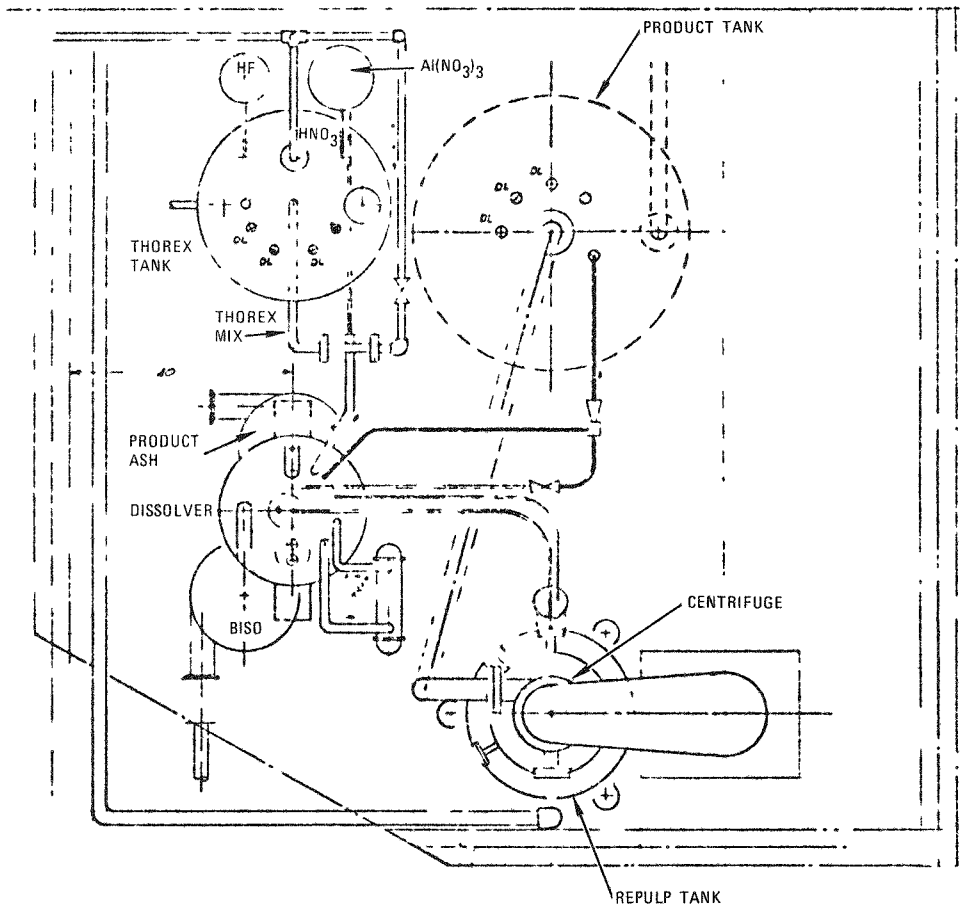

Fig. 5-2. General arrangement of dissolver-centrifuge system - plan view

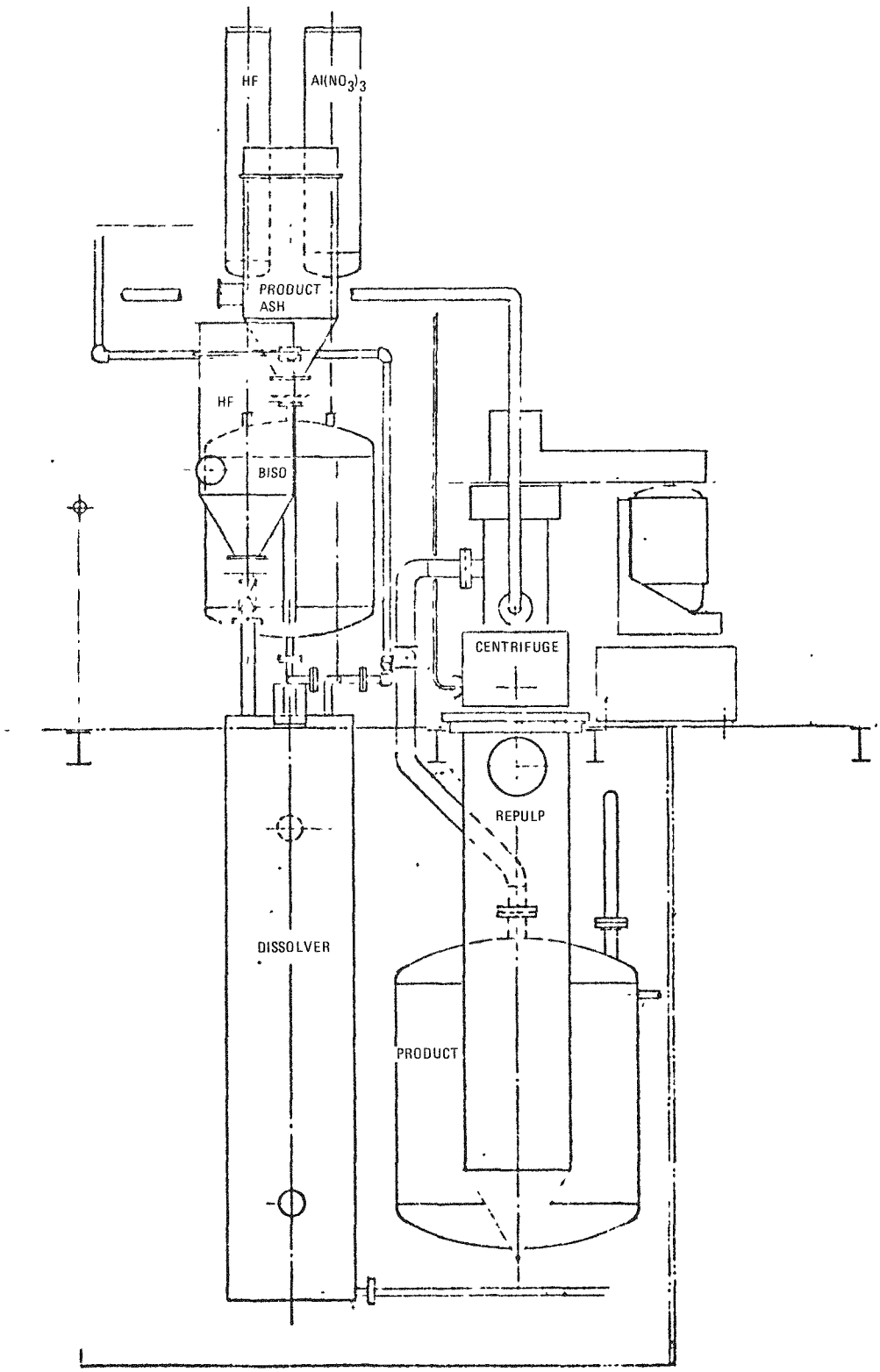

Fig. 5-3. General arrangement of dissolver-centrifuge system - elevation looking east

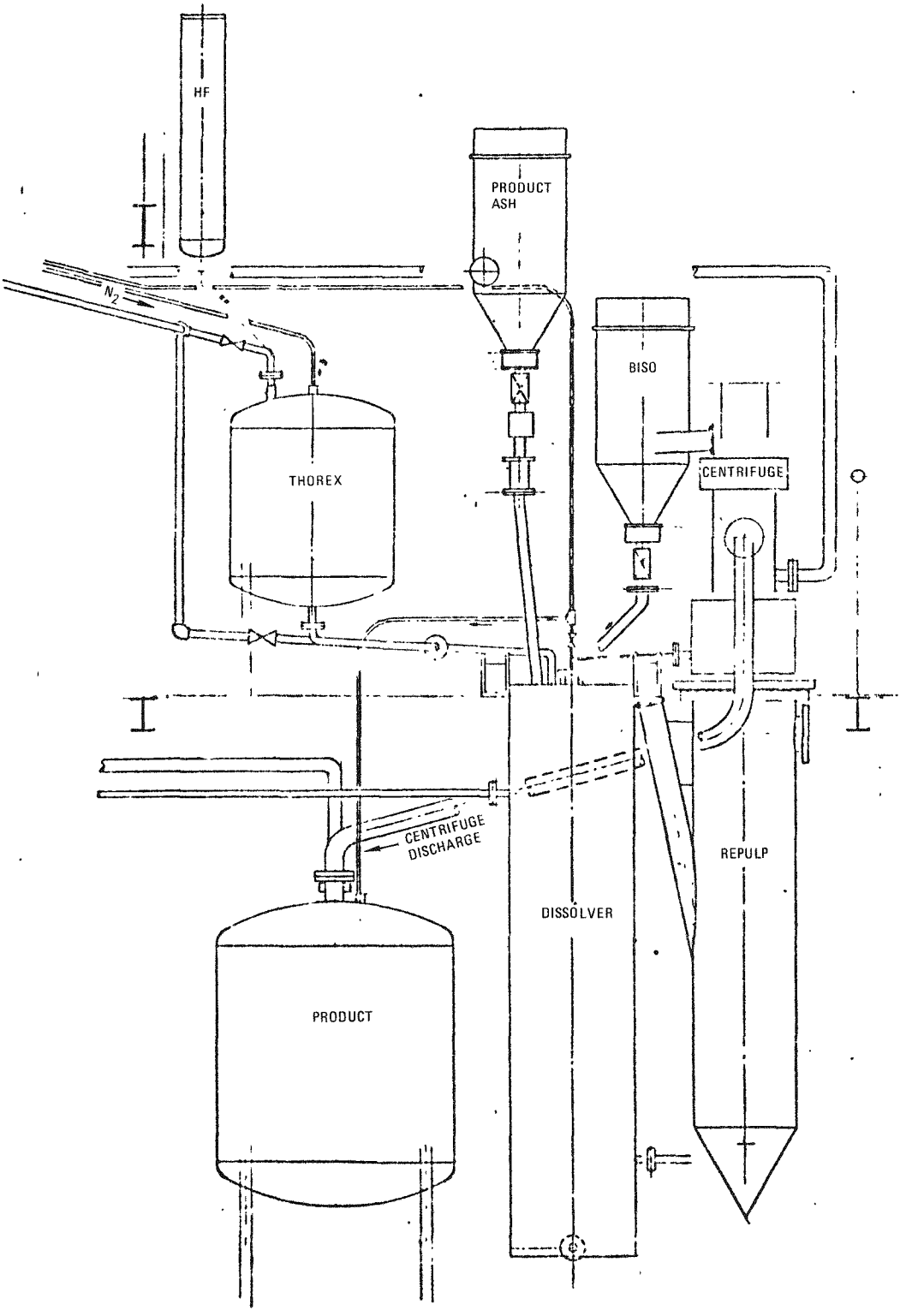

Fig. 5-4. General arrangement of dissolver-centrifuge system - elevation looking south

Figure 5-5 shows the dissolver vessel, which has a capacity of 400 liters (106 gal). It has a 90-degree conical bottom to enhance steam jet transport. A steam jacket surrounds the cone and a cooling water jacket surrounds the main part of the vessel, which is a 0.50-m (20 in.) pipe. Internal baffles are used in the cooling jacket to increase heat transfer. The vessel is designed for 620-kPa (90 psig) pressure in the steam jacket and 410-kPa (60 psig) pressure in the cooling water jacket. The vessel is an ASME Code, Section VIII, Division 1, approved vessel.

The dissolver feed hoppers are located above the dissolver and are equipped with load cells for material accountability. The secondary burner product ash will be metered into the dissolver by a rotary valve to control the rate of dissolution of burned WAR fissile particles. Thoria fuel particles will be fed in batches.

Feed lines to the dissolver consist of heated tubes for gravity solids addition. Distilled water, Thorex solution, and nitric acid are transferred via gravity from their storage tanks to the dissolver. All process and instrument lines penetrate through the top of the dissolver. In thoria particle operation, the product mother liquor can be decanted from the solid heel with a steam jet and transferred to the product tank. For removal of slurries there is a submerged steam jet which will transfer the contents to the centrifuge.

Samples may be withdrawn from the dissolver with a gas lift sampler. Corrosion coupons will be placed below the liquid level and in the vapor space.

Instrumentation includes thermocouples to monitor the temperature of the dissolver solution, steam, and cooling water. Flowmeters and/or indicators are placed on inlet gas and liquid lines. The level and specific gravity will be monitored by nitrogen-purged dip legs and manometers.

Condenser. The dissolver vents to the off-gas system through a type 304L stainless steel condenser. The condensate is returned to the dissolver through a loop seal.

The cooling water to the condenser is instrumented for flow and temperature measurement. The reflux liquid temperature can be measured and the liquid sampled.

Centrifuge. The solids will be separated from the mother liquor by means of a vertical, continuous centrifuge mounted on a frame. A single-speed motor is used, and the bearings are lubricated by a recirculating lube system. At points where erosion is likely to occur, a wear resistant material (Colmonoy 6) is used. The wetted surfaces (by vapor and liquid) are made of type 316 stainless steel.

Figure 5-6 shows a schematic of the operation of the vertical centrifuge. The features and advantages of the Sharples P-850 centrifuge have been previously reported in Ref. 5-1. The slurry is fed via steam jet to the feed section of the centrifuge (bottom entry). As the solids are being scrolled away from the liquid, wash water can be added. After separation, the solids fall by gravity from the bottom of the unit and a casing rinse flushes the solids into the repulp tank. The mother liquor is discharged at the top of the bowl and flows by gravity to the product tank. The casing is vented to the off-gas system.

Repulp Tank. The repulp tank is connected directly to the bottom of the centrifuge. The solids fall from the centrifuge outlet into the repulp tank. The wash water is either pumped or transferred by gravity. The solids are mixed with the rinse solution by gas sparge. The slurry is then transported back to the dissolver via a submerged steam jet.

Figure 5-7 shows the repulp tank, which is suspended from and bolted to the flange on the bottom of the centrifuge. The centrifuge is mounted to a structural supporting deck. This 0.38-m^3 (100 gal) tank has a conical

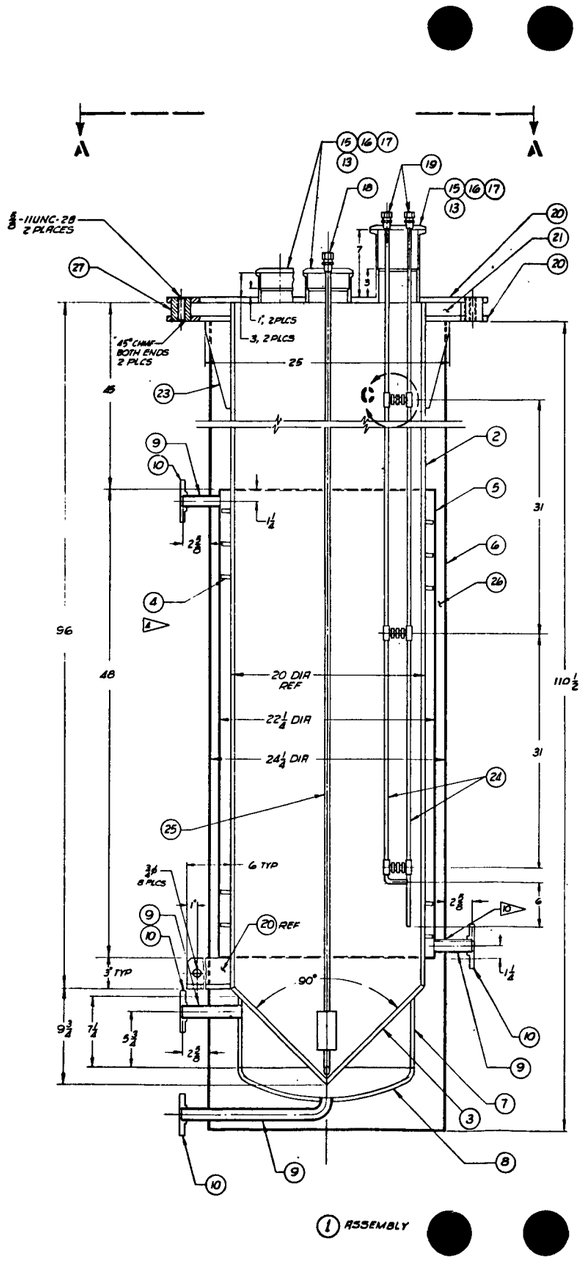

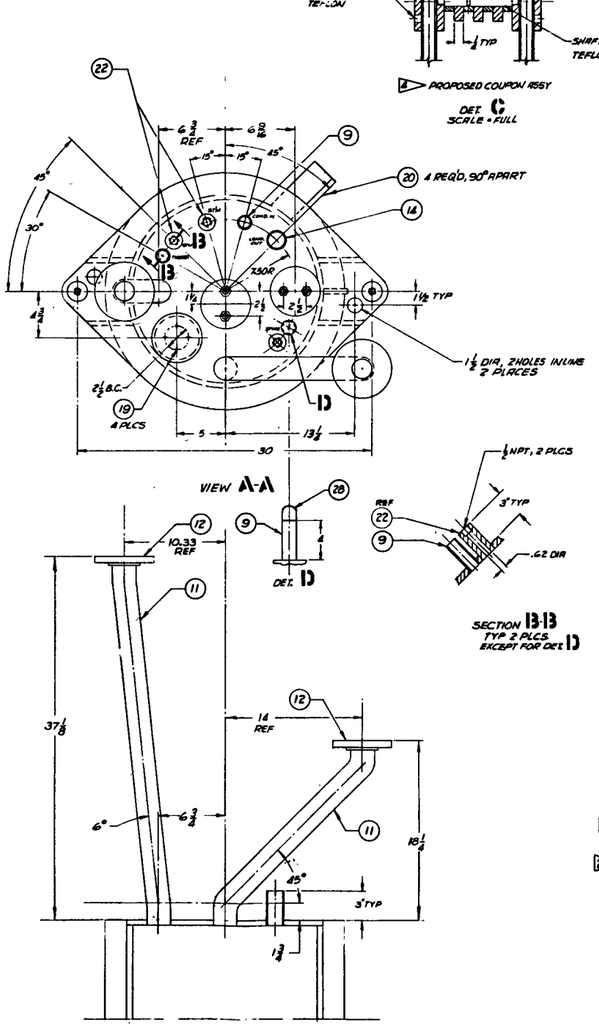

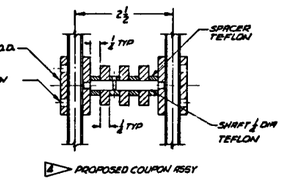

SECTION 13-13
TYP 2 PLCS EXCEPT FOR DET D

NOTES:

1. SOURCE: GYROLOK DIV, HOKE INC., CRESSKILL, N.J.; LOCAL; CASTLE CONTROLS INC. LA HABRA, CA.
2. SOURCE: TQI-CLOVER DIV, LADISH CO. RENOSHA, WISCONSIN
3. SOURCE: NRD REFRACTORY PRODUCTS MT. PROSPECT, ILL.
4. SEE COG ENGINEER FOR DESIGN CRITERIA
5. ALL WELDED CONSTRUCTION U.O.S.
6. ROD WILL SUPPLY THE FOLLOWING ITEMS:
   1) AIR LIFT SAMPLE ASSY, ITEMS 19 & 24
   2) STEAM JET ASSY ITEMS 18 & 25
7. ALL MATERIALS IN VESSEL WELDMENT TO BE 304 L, EXCEPT FOR INSULATION JACKET, ITEM 6
8. DESIGN CONDITIONS:
   DISSOLVER VESSEL, -0.4 PSIG TO +13 PSIG 170°C (338°F)
   CONTENTS, * 500 LBS MAX
   CORROSION ALLOWANCE .075 INCHES
   STEAM JACKETS 30 PSIG STEAM 170°C (338°F)
9. DESIGN & STAMP PER ASME SECTION VIII DIV 1, CORROSION TEST PER ASTM A-262-70
10. MAKE PROVISION FOR EXPANSION BETWEEN INSULATION JACKET & PENETRATIONS
11. ROD TO SUPPLY INSULATION AFTER VESSEL INSTALLATION ON PLATFORM
12. ALL MATERIAL THICKNESSES SHOWN IN B/M ARE APPROX. ONLY & SUBJECT TO DETAIL DESIGN CALC.
13. TOLERANCES TO BE ASSIGNED IN ACCORDANCE WITH FABRICATORS STANDARD MANUFACTURING PRACTICES

REQ'D/ASSEMBLY	ITEM	PART NO.	DESCRIPTION	MATL
1	28		CAP, WELDING 1"	SST
1/R	27		ROUND 2" DIA	SST
1/R	26		INSULATION (REMOVABLE)	
1/R	25		TUBE 1/2 O.D. x .042 WALL	SST
1/R	24		TUBE 3/8 O.D. x .032 WALL	
2	23		FLAT 5/8 x 2 1/2	
2	22		ROUND 1 1/2" DIA	
4	21		FLAT 5/8 x 1 1/2	
1/R	20		ANGLE 3 x 3 x 1/2	
6	19	GCM6-316	CONNECTOR, MALE 3/8"	
2	18	GCM8-316	CONNECTOR, MALE 1/2"	
3	17	13MHHVM	CLAMP - SCH 5	
4	16	14WLMV	FERRULE - WELD ON TYPE	
3	15	16RMV	CAP 4" SCH 5	
1/R	14		PIPE 1 1/2" SCH 40	
1/R	13		PIPE 4" SCH 40	
2	12		WELDING FL. 150# SOC. TYPE 6"	
1/R	11		PIPE 2" SCH 40	
3	10		WELDING FL. 150 SOC. TYPE 1"	
1/R	9		PIPE 1" SCH 40	
1	8		ELLIPTICAL DISH 18"	
1	7		STEAM JACKET, 18 PIPE	
1/R	6		INSULATION SHELL 20&9 (OD)	
1/R	5		WATER JACKET	
1/R	4		BAFFLE	
1	3		CONE	
1	2		BODY 20" PIPE	
	1		ASSEMBLY	

LIST OF MATERIAL

Fig. 5-5. Dissolver vessel

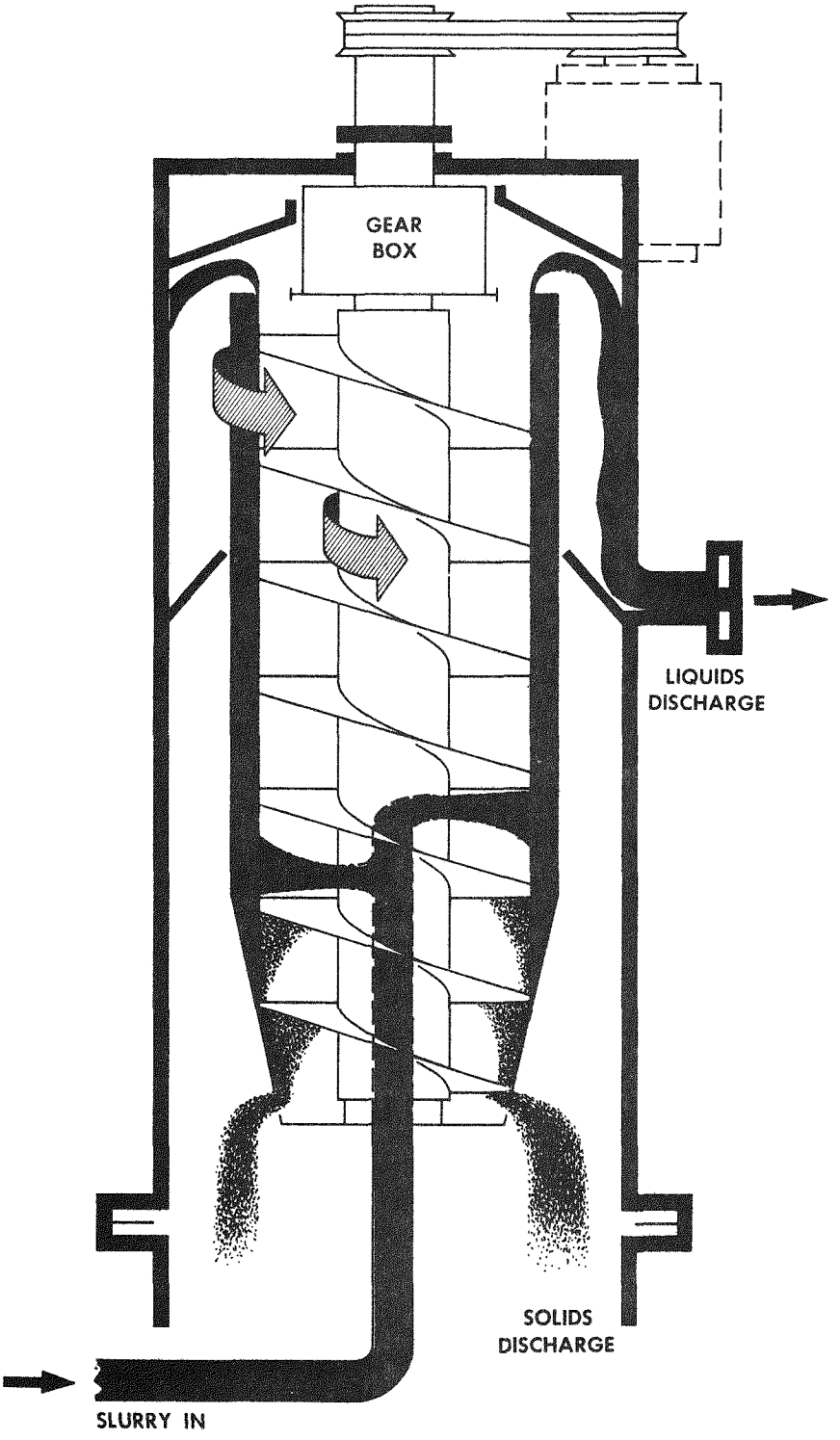

Fig. 5-6. Operation of a continuous vertical centrifuge

bottom to enhance steam jet pickup. The steam jet and air lift sample legs are removable through a 0.1 m (4 in.) pipe which is welded to the side of the vessel at an angle of 12 degrees to the vertical. This provides for top removal of the steam jet and air lift sample, which would otherwise be obstructed by the centrifuge above. The repulp tank also contains an inspection port, an overflow pipe, and dip tubes.

Feed and Product Tanks. The Thorex and product tanks are freestanding, type 304L stainless steel, cylindrical tanks with dished bottoms. They have a bottom drain, with all other penetrations coming into and out of the top. A gas sparge is used to mix the contents. All tanks are vented to the off-gas system.

5.2.2. Pilot Plant Heel Dissolution

5.2.2.1. Introduction

Heel operation takes advantage of the rapid dissolution rate during the first portion of leaching of ThO_2 kernels. By interrupting the normal cycle before complete dissolution is achieved, it may be possible to shorten the combined dissolution time for several batches. For sol-gel ThO_2 kernels, the point of interruption appears to be about 60% to 80% dissolution. To pinpoint the optimal parameters, a series of eight test segments were planned to be carried out in bench-scale glassware and 0.13-m and 0.20-m pilot plant dissolvers. Segments 1 through 3 will establish the operating parameters. Segments 4 and 5 will verify these parameters using the centrifuge to separate the heel from the product. Segments 6 through 8 will investigate steam jet decanting of the mother liquor from the heel. To date, segments 1 and 2 have been completed.

5.2.2.2. Results

As previously reported (Ref. 5-1), based on the results of test segments 1 and 2, a threefold increase in the rate of dissolution using

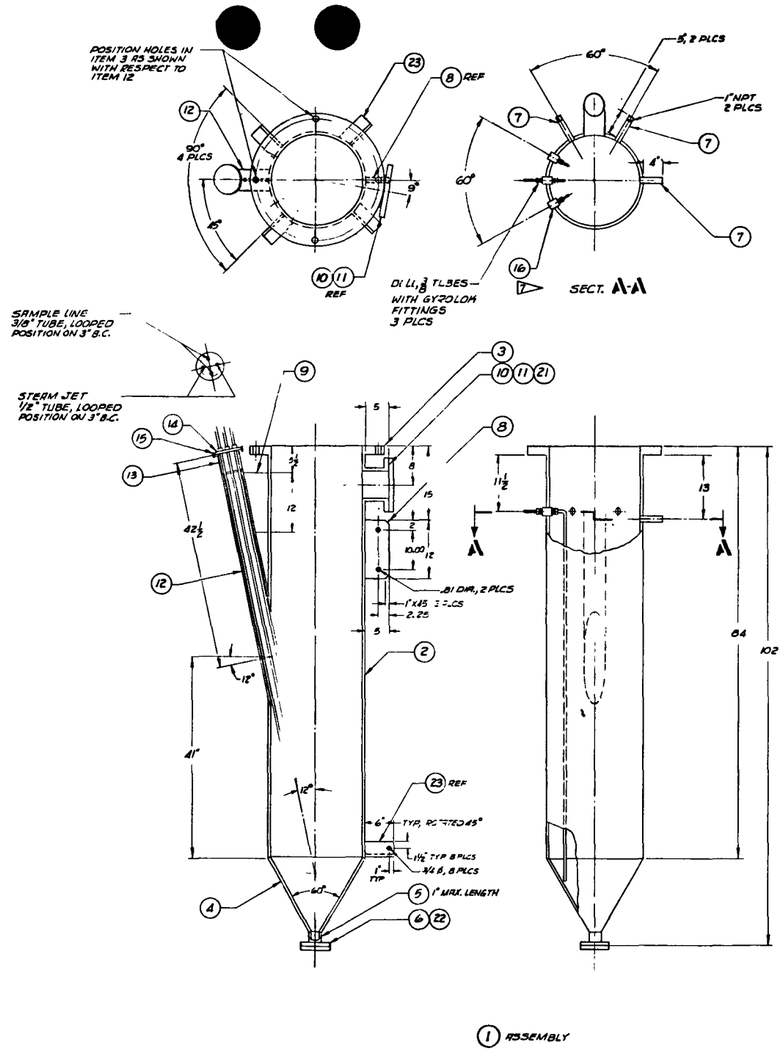

(1) ASSEMBLY

NOTES

1. SOURCE: GYROLOK DIV., HOKE INC., CRESSKILL, N.J., LOCAL; CASTLE CONTROLS INC., LAWNDALE, CA.
2. SOURCE: TRI-CLOVER DIV., LADISH CO. KENOSHA, WISCONSIN
3. ALL WELDED CONSTRUCTION U.O.S.
4. ROO WILL SUPPLY THE FOLLOWING ITEMS; 1. AIR LIFT SAMPLE ASSY 2. STEAM JET ASSY
5. ALL MATERIALS IN VESSEL WELDMENT TO BE 304L
6. DESIGN CONDITIONS; REPULP TANK PRESSURE, -0.4 PSIG TO 15 PSIG " " TEMP 50°C (122°F)
7. 1/2 NPT. IN ITEM 16, BOTH ENDS
8. MATERIAL THICKNESSES IN ACCORDANCE WITH ASME B+PV CODE, SECT. VIII DIV. 1 NO CODE STAMP REQD.
9. ALL WELDERS & MATERIALS TO BE QUALIFIED IN ACCORDANCE WITH SECT. IX OF THE ASME B+PV CODE.
10. CERTIFICATIONS TO BE SUBMITTED FOR ALL MATERIALS.
11. CORROSION TEST PER ASTM A-262-70
12. ALL MATERIAL THICKNESSES SHOWN IN B/M ARE APPROX. & SUBJECT TO DETAIL DESIGN CALC.
13. TOLERANCES TO BE ASSIGNED IN ACCORDANCE WITH FABRICATORS STANDARD MANUFACTURING PRACTICES

	4	23		ANGLE 3×3×1/2	SST		
	1	22		FLANGE, BLIND 2"			
	1	21		FLANGE, BLIND 6"			
	9/16	20		TUBE 3/8 O.D. × WALL			
	9/16	19		TUBE 1/2 O.D. × WALL			
	6	18	GRB-316	REDUCER 3/8".			
	6	17	BCM8-316	CONNECTOR, MALE 1/2"			
	3	16		ROUND 1 1/2 DIA X 3" LG.			
	1	15	13MNHM	CLAMP, SCH 5			
	1	14	16A1V	CAP, SOLID END 8"			
	1	13	16NLMV	FERRULE - WELD ON IPS SCH 5			
	9/16	12	8	PIPE 8" SCH 40			
	9/16	11		PIPE 6" SCH 40			
	1	10		FLANGE 6", 150# SOC. WELD			
	9/16	9		FLAT 1/2" × 6"			
	9/16	8		FLAT 1" × 6"			
	9/16	7		PIPE 1" SCH 40			
	1	6		FLANGE 2", 150# SOC. WELD			
	1	5		PIPE 2" SCH 40			
	1	4		CONE 1/2" WALL			
	1	3		FLANGE, 20", 150# LAP TYPE			
	1	2		BODY 20" PIPE			
		1		ASSEMBLY			
		ITEM	PART NO.	DESCRIPTION	MATL		
REQD/ASSY'D QTY				LIST OF MATERIAL			

Fig. 5-7. Repulp tank

heel operation instead of batch dissolution was estimated. A 40% heel for sol-gel ThO_2 dissolution with a 5-h dissolution time was selected for segment 3 tests in the 0.13-m dissolver.

To date, one run with the 40% sol-gel ThO_2 heel has been made in the 0.13-m dissolver, which was down for maintenance during the last quarter. With the normal 0.5 m^3/h (18 SCFH) sparge rate in the dissolver, sufficient agitation by sparging was not obtained before solution boiling. As a result, the ThO_2 kernels formed a layer at the bottom, preventing good heat transfer and superheating the dissolver solution at the bottom cone to 150°C without much indication of boiling action. By increasing the sparge rate to the maximum setting of 0.9 m^3/h (32 SCFH), the dissolver temperature was brought down to 135°C. Only after 2 to 3 h of dissolution did the indicated temperature return to normal (125°C).

Methods to increase the degree of agitation of the very dense ThO_2 kernels ($\sim$10 Mg/m^3) are being evaluated. It was observed in the bench-scale conical (glassware) dissolver that air sparging would not promote sufficient mixing of the kernels. Gas bubbles would simply bypass or channel through the layer of kernels. Even at boiling temperature, the degree of agitation of the kernels was at best minimal, especially in the early portion of dissolution when a large amount of ThO_2 kernels settled on the conical bottom. In the next run, the Thorex solution will be brought to boiling before feed dump in an attempt to avoid the superheating problem due to insufficient agitation.

REFERENCE

5-1. "Thorium Utilization Program Quarterly Progress Report for the Period Ending November 30, 1976," ERDA Report GA-A14214, General Atomic Company, December 1976.

6. SOLVENT EXTRACTION

6.1. SUMMARY

Three solvent extraction feed adjustment runs (Runs 28, 29, and 30) were completed during the quarter. The purpose of these runs was to examine the use of formic acid to aid in the semicontinuous denitration of thorium solutions in the feed adjustment step. The solutions used for feed were representative of the leacher product solution. Several difficulties developed in the operation of the feed adjustment system during these runs. In particular, the capacity of the off-gas system was inadequate when formic acid was used to enhance denitration. These runs were useful in identifying modifications which were required to permit successful operation under conditions of significant evolution of gases.

Five solvent extraction runs were completed during the quarter. Three runs (Runs 61, 64, and 65) simulated a plutonium partition column in the first cycle of the HRDF thorex flowsheet (see Section 6.3.1, Fig. 6-2). The Robatel centrifugal contactor and the five pulsed columns in the solvent extraction pilot plant were used.

Several operating problems were encountered in the plutonium partition runs. The low flow rates of the scrub streams created most of the problems. The low flow rates caused difficulty in controlling the column interfaces. Thorium losses from the 1PU system exceeded desirable levels in each of the runs. Some ZrNb decontamination was obtained in the 1PU system. However, effective decontamination was reduced as thorium losses from the 1PU system were reduced.

Two solvent extraction runs (Runs 66 and 67) were used to test the efficiency of the Robatel centrifugal contactor for uranium extraction

under a variety of conditions. (See schematic flow diagram of this operation in Section 6.3.1, Fig. 6-3.) Several flow rates were used for each of the three feed concentrations of uranium. The SEPHIS computer code was used to calculate theoretical values for the effluent streams from the operation for comparison with the data collected from the pilot plant runs.

No significant operating problems occurred in Runs 66 and 67. The operating stage efficiency of the contactor was near 100% for these runs. Typical losses from the centrifugal contactor operation were less than calculated values.

Preliminary tests have been run on ruthenium and fluoride volatility from bench-scale feed adjustment operations. Fluoride volatility averaged about 1%. However, either ruthenium tracers or a more sensitive ruthenium analytical method will be required to quantitatively measure ruthenium volatility.

A gas chromatographic method was developed for measuring the tributyl phosphate content of pilot plant solvent. The total phosphorous content of the uranium products from solvent extraction runs after steam stripping and concentration is 13 to 19 parts per million parts of uranium.

6.2. SOLVENT EXTRACTION FEED ADJUSTMENT

6.2.1. Introduction

The continuous solvent extraction feed preparation process consists of continuously feeding an acidic thorium nitrate stream to a boiler pot of boiling concentrated, acid-deficient thorium nitrate solution. Excess acid from the feed stream is boiled off (steam stripped), leaving more acid-deficient thorium nitrate in the boiler pot. The acid-deficient thorium nitrate product is continuously or semicontinuously removed from the boiler pot and is then diluted with water to prevent solidification upon cooling.

There is potential for using formic acid to provide some denitration of the feed in addition to steam stripping. A schematic of the feed adjustment system is shown in Fig. 6-1.

A continuous feed adjustment system has the advantage of providing a uniform condensate flow and composition, thereby facilitating operation of the downstream waste processing system. Also, since the solvent extraction process is inherently continuous, there is an additional incentive to have a continuous feed adjustment step for the dilute, intercycle thorium stream.

Bench-scale demonstration of the feasibility of the process for continuous feed adjustment has been completed. Pilot plant testing is being done (1) to determine necessary equipment items for commercial-scale operation, in particular, for the difficult task of concentrated product removal, and (2) to determine scale-up effects from the bench-scale work. Reference 6-1 discusses feed adjustment work with formic acid on the bench scale.

6.2.2. Results

The feed concentrations are given in Table 6-1. The feed concentration which was used in Runs 28, 29, and 30 was typical of the solution expected as leacher product. Table 6-1 also contains the typical steady-state concentrations of the distillate and product streams. Due to the brevity and upsets of Runs 28 and 29, steady-state operation was not achieved. Conditions near steady state were achieved in Run 30.

6.2.3. Discussion - Run 28

Run 28 was the first run in which formic acid was added to the evaporator/stripper. The purpose of the formic acid was to aid in the denitration of the thorium nitrate solution.

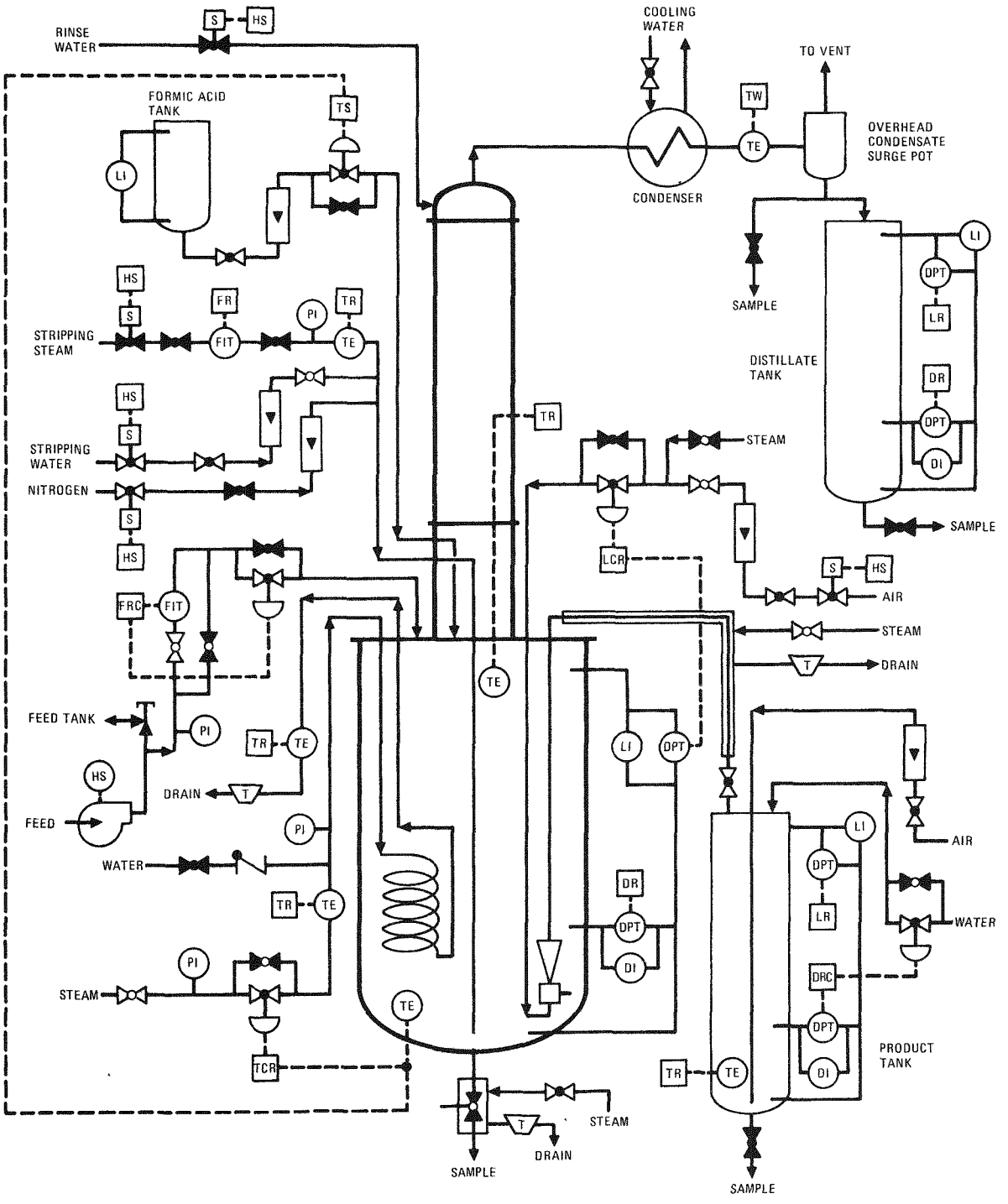

Fig. 6-1. Piping and instrumentation diagram for continuous feed adjustment equipment

TABLE 6-1
COMPOSITION OF TYPICAL STREAMS AT STEADY STATE FOR RUNS 28, 29, AND 30

Stream	H^+ (M) to Th (M) Ratio	H^+ (M)	Th (M)	Al (M)	F^- (M)
Feed	5	5	1.0	0.15	10^{-4} to 0.1
Distillate	--	~3	$<10^{-4}$	$<10^{-3}$	$<2 \times 10^{-3}$
Concentrated Product (After dilution)	~0.5	0.8	1.8	0.25	5×10^{-4}

The hydrogen ion to thorium mole ratio in the feed was about five. The mole ratio in the evaporator/stripper in Run 28 was about 1.5. The formic acid which was added in this run had essentially no effect since it was added to the tower. Therefore, the formic acid did not react with the bottoms solution in the evaporator/stripper because it was not mixed with it. Formic acid with a concentration of about 23M was used for these tests.

An inadvertent addition of a large slug of formic acid to the evaporator/stripper caused the vessel to pressurize. The reaction of formic acid with the nitrate solution produced carbon dioxide and oxides of nitrogen. Enough formic acid was added in the large slug so that the quantity of reaction gases produced exceeded the capacity of the off-gas system.

In Run 28 no packing was present in the tower on the evaporator/stripper. As a result most of the formic acid which was added to the tower was carried through the overhead condenser into the distillate. The formic acid and the nitric acid contained in the distillate reacted in the distillate storage tank, but at a much slower rate compared to the evaporator/stripper due to the reduced temperature.

The evaporator/stripper was shut down for modifications to increase efficiency for the formic acid operaton.

6.2.4. Discussion - Run 29

Prior to Run 29 the following modifications were made on the evaporator/stripper system:

1. Packing was added to the tower of the evaporator/stripper. This packing was 0.013 m (0.5 in.) ceramic Intalox saddles. The purpose of the packing was to provide contact area for the formic acid - nitric acid reaction and to prevent carryover of the formic acid into the distillate.

2. The off-gas line from the tower to the condenser was changed to a larger diameter. This change was made to reduce a potential flow restriction and to reduce a potential cause for vessel pressurization.

3. The addition point of the formic acid was lowered from the tower to near the bottom of the evaporator/stripper vessel. This change was made to provide mixing and reaction of the formic acid with the solution in the vessel.

4. The bypass valve around the control valve for formic acid addition was eliminated. Elimination of the bypass prevented potentially large relative volumes from being inadvertently added to the evaporator/stripper.

In Run 29, the contents of the evaporator/stripper were brought to boiling. The boiloff capacity was tested with the packing in the tower and the new off-gas line. No problems developed under operational conditions expected of the feed adjustment step for the leacher product.

The addition system for formic acid was tested using water as the test solution. No flow was obtained through the gravity feed system due to inadequate hydraulic characteristics.

6.2.5. Discussion - Run 30

Prior to Run 30, the addition point of the formic acid was raised from near the bottom of the vessel to near the normal interface of the liquid and vapor in the vessel. The formic acid addition system was tested with water under normal boiling conditions. No water flow was obtained by gravity feed through the formic acid system due to marginal hydraulics.

A small metering pump was installed on the formic acid addition system. This pump had a variable control setting which permitted operating

in a range from zero to about 30 milliliters/min. The pump and formic acid addition system were tested with water with the evaporator/stripper operating under normal conditions. Good control of the flow from the formic acid tank to the evaporator/stripper was obtained under these conditions.

After successful testing of the metering pump with water, formic acid was added to the head tank. Formic acid was added to the evaporator/-stripper while operating near normal boilup conditions for only 25 min when the vessel pressurized. The operation was shut down.

The evaporator/stripper was started up and returned to normal steady-state operation prior to the introduction of additional formic acid. The formic acid addition was started at a low rate of about 5 milliliters/min. An addition near this rate was continued for about 1.3 hours before instability in the evaporator/stripper developed and the formic acid flow was stopped. The instability was symptomatic of pressurization and consisted of wide fluctuations in the readout of the liquid level and specific gravity instrumentation. The run was completed without further formic acid additions.

The instability in the evaporator/stripper was caused by the evolution of carbon dioxide and oxides of nitrogen which exceeded the off-gas capacity of the system. It is also possible that foaming may have developed in the evaporator/stripper due to contamination of the feed. A layer of crud was present with some of the feed.

Changes made to alleviate the operating problems discussed here will be discussed in future reports.

6.3. SOLVENT EXTRACTION

6.3.1. Introduction

Runs 61, 64, and 65 simulated a plutonium partition column in the first cycle of the HRDF Thorex flowsheet (Fig. 6-2). The centrifugal contactor and the five pulsed columns in the solvent extraction pilot plant

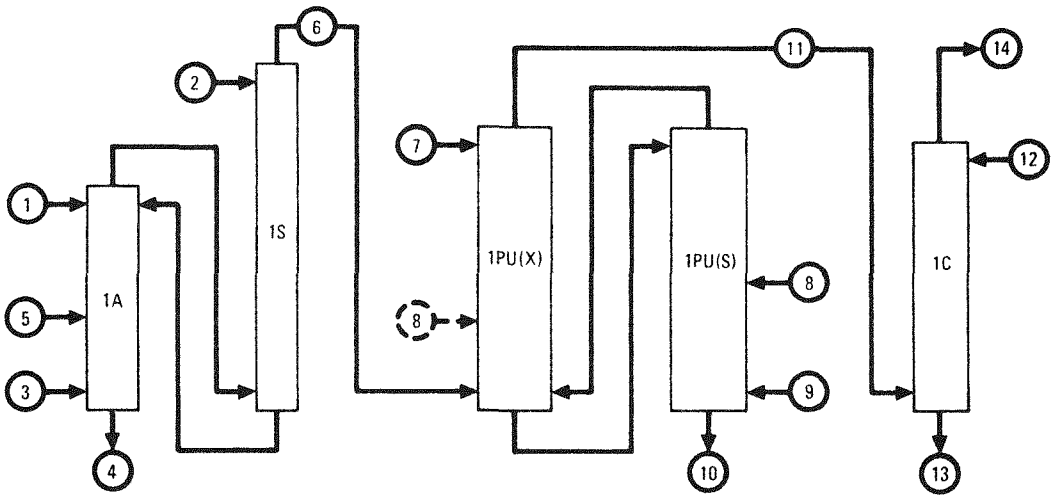

Column Stream	Stream No.	Relative Flow	Composition U (g/ℓ)	Th (g/ℓ)	HNO_3 (M)
1AF	1	100	14	348	<1.0
1AS	2	190			1.0
1AX	3	1200		(30% TBP)	
1AW	4	320			
1AA	5	30			13.0
1SP	6	1200	1.2	29	
1PUX	7	125			1.0
1PUA	8	9			13.0
1PUS	9	120		(30% TBP)	
1PUW	10	135			
1PUP	11	1320	1.1	26	
1CX	12	1200			0.01
1CP	13	1200	1.2	29	
1CW	14	1320		(30% TBP)	

Fig. 6-2. Pu partition flowsheet, solvent extraction Runs 61, 64, and 65

were used for these runs. Uranium and thorium were coextracted in the centrifugal contactor. One column was used for scrubbing, two columns for the Pu partitioning, one for costripping, and one for solvent washing. The Pu partition column was simulated by the addition of ferrous nitrate into its aqueous scrub stream. No plutonium was used in this operation.

Runs 61, 64, and 65 were used to collect efficiency and capacity data for the Pu partition system. Additional testing of this flowsheet will be required to reduce the loss of thorium during Pu partitioning.

Runs 66 and 67 were used to test the Robatel centrifugal contactor under a variety of conditions to determine its efficiency for the extraction of uranium. The solvent used was 30% TBP in NPH diluent. A schematic flow diagram for this operation is shown in Fig. 6-3. Several flow rates were used for each of three feed concentrations of uranium. The SEPHIS computer code was used to calculate theoretical values for the effluent streams from the contactor operation for comparison with the data collected from the pilot plant operation.

Two pulsed columns were also used as part of the operation. One column was used for uranium stripping and the other column was used for solvent washing.

6.3.2. Results and Discussion - Run 61

Table 6-2 contains the stream analyses and flow rates for Run 61. Table 6-3 contains the loss data and operating conditions. Table 6-4 contains the descriptions of the contactor, columns, and column cartridges.

In Run 61, flooding tests of both columns of the two-column 1PU system were conducted. The interfaces of the 1PU columns were difficult to control not only during the flooding tests, but throughout the run. The interface control problems occurred because very low aqueous flow rates are used in this flowsheet relative to the normal flow rates used in the pilot plant. The control valves are sized for the higher flow rates.

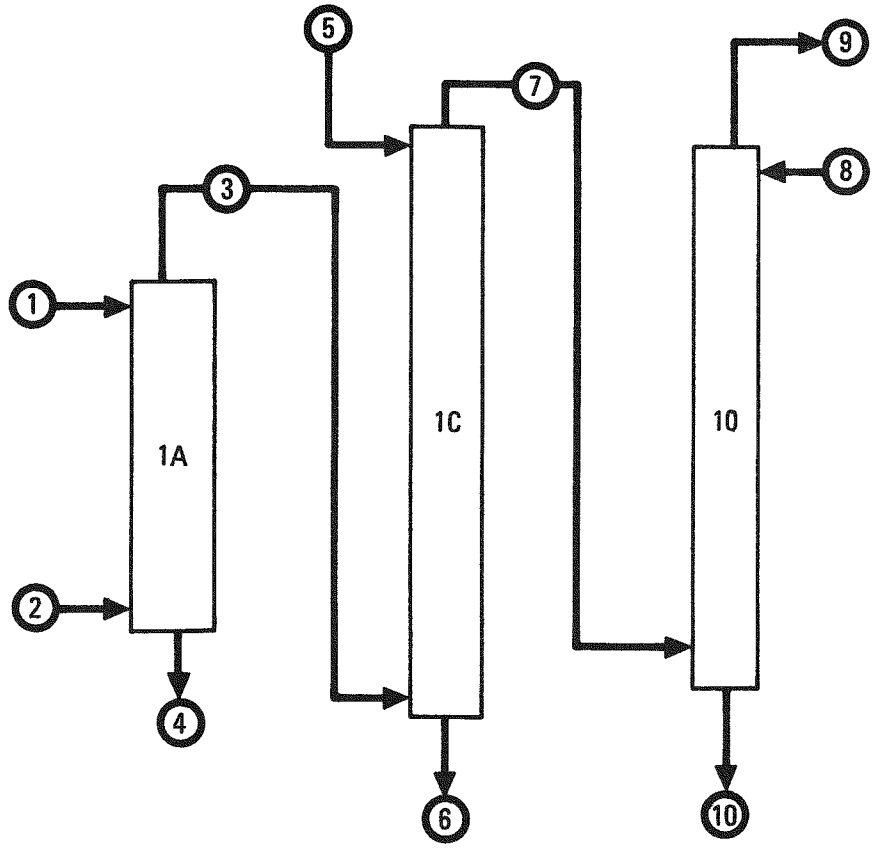

Stream	Stream No.	Composition U (g/ℓ)	Composition HNO_3 (M)
1AF	1	10-180	2.0
1AX	2	–	(30% TBP)
1AP	3	–	–
1AW	4	–	–
1CX	5	–	0.01
1CU	6	10-100	–
1CW	7	–	(30% TBP)
1OS	8	–	(0.2M Na_2CO_3)
1OO	9	–	(30% TBP)
1OW	10	–	Waste

Fig 6-3. Flowsheet schematic for Runs 66 and 67

TABLE 6-2
STREAM AND ANALYTICAL DATA, SOLVENT EXTRACTION RUN 61[a]

Stream	Stream No.	U, (g/ℓ)	Th, (g/ℓ)	HNO_3, (M)	ZrNb, (cpm)	Flow (mℓ/min)	Other
1AF	1	30.05	360.20	0.31	4.5×10^4	94	Zr = 2.5 g/l
						(83)	
1AX	3			[30% TBP]		1208	
						(1151)	
1AA	5			∿13		27	
						(31)	
1AS	2			0.96		179	
						(181)	
1PUX	7			0.26		136	Fe^{++} = 0.05 M
						(151)	
1PUS	9			[30% TBP]		83	
						(82)	
1PUA	8			∿13		8.4	
						(8.7)	
1CX	12			0.020		1315	
						(1175)	
1OS						122	Na_2CO_3 = 0.27 M
1AW	4	0.4×10^{-3}	6.2×10^{-3}	1.17	1.3×10^5		
		(0.4×10^{-3})	(5.5×10^{-3})	(1.53)	(1.1×10^5)		
1AP		0.73	39.5	0.19	7866		
		(2.19)	(64.8)	(0.34)	(9177)		
1SR		0.22	46.05	2.23	4.3×10^4		
		(0.23)	(41.80)	(2.46)	(9.8×10^4)		
1SP	6	1.58	23.4	0.19	44.4		
		(1.84)	(28.8)	(0.19)	(782.6)		
1PUP	11	1.86	22.4	0.052	-		
		(1.29)	(10.8)	(0.052)	(34.7)		
1PUW	10	-	19.49	1.07	-		
		-	(17.38)	(1.19)	164.6		
1PUR		0.24	38.93	0.82	-		
		(0.22)	(41.85)	(0.82)	(190.7)		
1PUT		0.25	23.3	0.16	-		
		(0.47)	(30.8)	(0.16)	(6.63)		
1CP	13	2.12	31.97	0.068	-		
		(1.61)	(22.93)	(0.068)	(20.7)		
1CW	14	7×10^{-4}	1.15×10^{-2}	0.012	-		
		(5×10^{-4})	(1.20×10^{-2})	(0.012)	(2.57)		
1OW		3×10^{-4}	1.4×10^{-3}	-	-		
		(3×10^{-4})	(2.0×10^{-3})	-	-		
1OO		3×10^{-4}	9×10^{-4}	-	-		
		(2×10^{-4})	(1.2×10^{-3})	-	(0.20)		

[a] The values in parentheses correspond to a second set of operating conditions.

TABLE 6-3
PERCENT LOSS, Zr DECONTAMINATION FACTOR, AND FLOODING DATA,[a] SOLVENT EXTRACTION RUN 61

Contactor	Purpose	Volume Velocity (gal/hr/ft^2)	$\bar{v}_a$ (cm/sec)	$\bar{v}_o$ (cm/sec)	Flooding Frequency [cpm (rpm)]	Continuous Phase	Aqueous to Organic Ratio	ZrNb DF Th Basis	% Loss U	% Loss Th	% Flooding Frequency	Temp (°C)
1A Centrifugal	Extraction	-	-	-	<500 rpm	-	0.248	0.63	$<10^{-2}$	$<10^{-2}$	-	28[b]
		-	-	-			(0.256)	(0.88)	(40^{-2})	($<10^{-2}$)		
1S Pulse Column	Scrub	1008	0.147	0.99	86	Organic	0.148	105	-	-	93	Ambient
		(968)	(0.148	(0.94)	(89)		(0.157)	(5.21)	-	-	(90)	
1PU(X) Pulse Column	Pu Partition	461	0.049	0.47	93	Aqueous	0.105	-	-	-	73	Ambient
		(447)	(0.055)	(0.45)			(0.122)	(8.46)	-	-	(80)	
1PU(S) Pulse Column		165	0.118	0.068	103	Aqueous	1.740		-	7.83	75	Ambient
		(176)	(0.141)	(0.072)			(1.948)		-	(8.78)	(75)	
1C Pulse Column	U-Th Costrip	842	0.480	0.47	79	Aqueous	1.02		0.03	0.04	89	46
		(778)	(0.428)	(0.45)	(83)		(0.953)		(0.02)	(0.05)	(89)	
1O Pulse Column	Solvent Wash	1027	0.101	1.06	116	Organic	0.095		-	-	69	32
		(968)	(0.081)	(1.01)	(118)		(0.080)		-	-	(70)	

(a) The data in parentheses resulted from a second set of operating conditions.

(b) Average of 1AP and 1AW stream temperatures.

TABLE 6-4
SOLVENT EXTRACTION RUNS 61, 64, AND 65: CENTRIFUGAL CONTACTOR AND COLUMN DESCRIPTION

Unit	Purpose	Diameter (mm)	Total Height of Mixing Area (m)	Other			
1A Contactor	Extraction	180	0.32	Eight Stages with 0.4 Liter Total Holdup per Stage			
				Plates			Plate Spacing (mm)
				Nozzle Direction	Hole Size (mm)	% Free Area	
1S Column	Scrub	51	6.7	Down	3.2	23	51
1PUX Column	Partition	76	5.8	Up	4.8	23	Graded[a]
1PUS Column	Partition Scrub	51	5.2	Up	4.8	23	51
1C Column	U Strip	76	4.6	Up	4.8	23	Graded[a]
1O Column	Solvent Wash	51	5.5	Down	3.2	23	51

[a] Graded cartridge is, from the bottom, 2.6 m with 100 mm spacing, 0.5 m with 76 mm spacing, and the remainder with 51 mm spacing.

In this run, the 13M HNO_3 1PUA stream was added about 2.14 m (7 ft) above the bottom of the 1PU(S) column. The purpose of this acid addition is to add salting strength to assure the extraction of the thorium present in the column. Despite the acid addition, significant thorium losses did occur.

Two other operating problems occurred. First, the 1AP system failed temporarily. This failure caused a temporary loss of flow to the 1S column. This loss of flow affected each of the downstream columns. The effects were particularly significant in the 1PU system columns. The interfaces in both columns dropped. Since the aqueous flow rate in these columns was very low, a long period of time was required to restore interfaces to their normal levels. The loss of the interfaces and the long recovery period also contributed to the thorium losses from the 1PU column.

The second problem which occurred was foaming in the top of the 1S column. The foaming was caused by the nitrogen which was used for the airlift which moves the organic stream from the 1PU(S) column to the 1S column. The foaming resulted from a very high nitrogen flow rate. The high nitrogen flow rate resulted from the loss of organic overflow from the 1PU(S) column. The loss of the organic overflow was due to the drop in the column interface.

A significant ZrNb decontamination was obtained in the 1PU system. Since the thorium loss was about 8%, a large decontamination factor for ZrNb was the expected result.

The ferrous nitrate concentration in the 1PUX stream is sufficient to chemically reduce the quantity of plutonium expected in spent HTGR fuels. The chemical reduction of plutonium from the +4 to +3 valence state assures its transfer to the aqueous phase since Pu^{+3} is virtually inextractable.

6.3.3. Results and Discussion - Run 64

Table 6-5 contains the stream analyses and flow rates for Run 64. Table 6-6 contains the loss data and operating conditions. Run 64 was similar to Run 61 except the 1PUA flow rate was doubled to produce a higher nitric acid concentration in the 1PU(S) column. Thorium losses were somewhat reduced from Run 61. However, the thorium losses were also a function of the 1PUX flow rate, which was greater near the end of the run.

The interfaces for the 1PU(X) and 1PU(S) columns were more easily controlled in Run 64 than in Run 61. However, to maintain control of the interfaces, nearly constant attention was required.

No significant ZrNb decontamination was obtained in the 1PU system in Run 64. The loss of decontamination was due to the higher nitric acid concentration in the 1PU(S) column. The nitric acid concentration in the 1PUW stream was twice as high in Run 64 ad in Run 61. The nitric acid concentration in the 1PU(S) column was increased to improve thorium extraction.

Some flooding occurred at the top of the 1S column. The occurrence of flooding was partly due to the presence of a third phase. However, the top of the 1S column is particularly susceptible to flooding even when no third phase is present.

6.3.4. Results and Discussion - Run 65

Table 6-7 contains the stream analyses and flow rates for Run 65. Table 6-8 contains the loss data and operating conditions.

Run 65 had the same basic column configuration as Runs 61 and 64. To reduce the thorium losses from the 1PU system, the 1PUA stream was added to the 1PU(X) column 2.14 m (5 ft) above the inlet point for the 1SP stream. Lower thorium losses were achieved; however, the run was interrupted by an electrical outage.

TABLE 6-5
STREAM AND ANALYTICAL DATA, SOLVENT EXTRACTION RUN 64

Stream	Stream No.	U (g/ℓ)	Th (g/ℓ)	HNO_3 (M)	ZrNb (cpm)	Flow (mℓ/min)	Other
1AF	1	16.42	330	0.67	6.26×10^5	86	
						(113)	
						(113)	
1AX	3			[30% TBP]		1104	
						(1278)	
						(1230)	
1AA	5			∿13		27	
						(29)	
						(29)	
1AS	2			0.97		183	
						(186)	
						(195)	
1PUX	7			0.26		116	Fe^{++} = 0.05 M
						(128)	
						(148)	
1PUS	9			[30% TBP]		107	
						(117)	
						(150)	
1PUA	8			∿13		18	
						(18)	
						(20)	
1CX	12			0.02		1204	
						(1159)	
						(1282)	
10S						124	Na_2CO_3 = 0.27 M
						(120)	
						(132)	
1AW	4	0.4×10^{-3}	1.22×10^{-2}	1.25	1.9×10^5		
		(1.1×10^{-3})	(1.15×10^{-2})	(0.67)	(2.2×10^5)		
		(1.0×10^{-3})	(1.38×10^{-2})	(0.77)	(2.6×10^5)		
1AP		0.64	11.3	0.30	1.1×10^4		
		(1.76)	(49.1)	(0.38)	(1.3×10^4)		
		(2.01)	(102.9)	(0.38)	(1.1×10^4)		

TABLE 6-5 (Continued)

Stream	Stream No.	U (g/ℓ)	Th (g/ℓ)	HNO_3 (M)	ZrNb (cpm)	Flow (mℓ/min)	Other
1SR		0.23	69.62	1.79	6.0×10^4		
		(0.38)	(94.03)	(1.64)	(1.9×10^5)		
		(0.30)	(86.32)	(1.64)	(1.5×10^5)		
1SP	6	1.61	26.4	0.14	716		
		(6.77)	(164.9)	(0.12)	(494)		
		(1.70)	(33.0)	(0.15)	(174)		
1PUP	11	1.52	21.5	0.08	206.2		
		(1.78)	(26.9)	(0.07)	(155.5)		
		(2.39)	(32.9)	(0.09)	(433.4)		
1PUW	10	3×10^{-4}	4.95	2.09	51.5		
		(5×10^{-4})	(17.44)	(2.64)	(379)		
		$(<2 \times 10^{-4})$	(21.24)	(2.55)	(608)		
1PUR		0.22	49.84	0.83	584		
		(0.24)	(49.34)	(0.83)	(950)		
		(0.25)	(52.68)	(0.83)	(1206)		
1PUT		0.25	22.8	-	2.75		
		(0.56)	(25.9)	-	(16.3)		
		(0.28)	(30.1)	-	(16.5)		
1CP	13	1.59	21.79	0.09	-		
		(1.58)	(21.09)	(0.09)	-		
		(1.37)	(15.51)	(0.08)	-		
1CW	14	$<2 \times 10^{-4}$	1.3×10^{-3}	0.006	195.5		
		(-)	(-)	(0.012)	(151.1)		
		(7×10^{-4})	(1.4×10^{-3})	(0.006)	(198.0)		
1OW		$<2 \times 10^{-4}$	1.6×10^{-3}	-	36.7		
		$(<2 \times 10^{-4})$	(1.4×10^{-4})	-	(27.7)		
		(2×10^{-4})	(1.7×10^{-4})	-	(47.3)		
1OO		-	-	-	0.44		
		(-)	(1.6×10^{-3})	-	(0.58)		
		$(<2 \times 10^{-4})$	(6×10^{-4})	-	(0.59)		

TABLE 6-6
PERCENT LOSS, Zr DECONTAMINATION FACTOR, AND FLOODING DATA,[a] SOLVENT EXTRACTION RUN 64

Contactor	Purpose	Volume Velocity (gal/hr/ft^2)	$\bar{v}_a$ (cm/sec)	$\bar{v}_o$ (cm/sec)	Flooding Frequency [cpm (rpm)]	Continuous Phase	Aqueous to Organic Ratio	ZrNb DF Th Basis	% Loss U	% Loss Th	% Flooding Frequency	Temp (°C)
1A Centrifugal	Extraction	-	-	-	<500 rpm	-	0.268	1.98	$<10^{-2}$	0.01	-	-
							(0.257)	(7.19)	(0.02)	(0.01)	-	-
							(0.274)	(17.6)	(0.02)	(0.01)		30[b]
1S Pulse Column	Scrub	935.6	0.150	0.906	91	Organic	0.166	35.2	-	-	∿90	Ambient
		(1064.3)	(0.153)	(1.048)	(82)		(0.146)	(88.1)	-	-	-	
		(1036.0)	(0.160)	(1.006)	(84)		(0.159)	(20.5)	-	-	-	
1PU(X) Column	Pu Partition	428.8	0.042	0.442	∿95	Aqueous	0.096	2.83	-	-	63	Ambient
		(492.1)	(0.047)	(0.509)	(∿90)		(0.092)	(0.52)	-	-	(76)	
		(493.7)	(0.054)	(0.503)	(∿90)		(0.107)	(0.40)	-	-	(76)	
1PU(S) Pulse Column		175.2	0.110	0.088	∿100	Aqueous	1.252		-	2.3	76	Ambient
		(191.2)	(0.120)	(0.096)	(∿97)		(1.248)		-	(6.8)	(78)	
		(231.2)	(0.138)	(0.123)	(∿90)		(1.120)		-	(9.6)	(84)	
1C Pulse Column	U-Th Strip	780.3	0.439	0.442	83	Aqueous	0.994	-	<0.02	$<10^{-2}$	84	42
		(825.2)	(0.423)	(0.509)	(80)		(0.831)	-	-	-	(88)	
		(860.1)	(0.468)	(0.503)	(78)		(0.929)	-	(0.05)	($<10^{-2}$)	(90)	
1O Pulse Column	Solvent Wash	970.5	0.101	0.990	118	Organic	0.102	-	-	-	∿70	
		(1101.4)	(0.098)	(1.140)	(114)		(0.086)	-	-	-		
		(1099.2)	(0.109)	(1.135)	(114)		(0.096)	-	-	-		

[a] The values in parentheses resulted from a second and third set of operating conditions.

[b] Average of 1AW and 1AP stream temperatures.

TABLE 6-7
STREAM AND ANALYTICAL DATA, SOLVENT EXTRACTION RUN 65

Stream	Stream No.	U (g/ℓ)	Th (g/ℓ)	HNO_3 (M)	ZrNb (cpm)	Flow (mℓ/min)	Other
1AF	1	18.11	342.9	0.76	4.8×10^5	101	
						(124)	
1AX	3			[30% TBP]		1133	
						(1204)	
1AS	2			0.96		193	
						(192)	
1AA	5			∿13		19	
						(41)	
1PUX	7			0.96		125	Fe^{++} = 0.05 M
						(140)	
1PUA	8			∿13		9	
						(9)	
1PUS	9			[30% TBP]		123	
						(122)	
1CX	12			0.015		1217	
						(1214)	
1OS						132	Na_2CO_3 = 0.27 M
						(128)	
1AW	4	1.0×10^{-3}	1.9×10^{-2}	1.00	1.4×10^5		
		(1.1×10^{-3})	(2.0×10^{-2})	(1.78)	(1.7×10^5)		
1AP		1.38	28.04	0.30	1.2×10^4		
		(1.86)	(43.64)	(0.44)	(1.6×10^4)		
1SR		0.19	54.09	2.16	7.1×10^4		
		(0.26)	(79.71)	(1.78)	6.8×10^4		
1SP	6	1.45	26.74	0.20	616		
		(1.65)	(30.27)	(0.14)	(2014)		
1PUP	11	1.13	24.56	0.24	121		
		(1.73)	(21.86)	(0.18)	(222)		
1PUW	10	-	4.97	1.11	4441		
		-	(4.38)	(1.33)	(5945)		
1PUR		0.151	35.90	1.34	5822		
		(0.194)	(35.96)	(1.44)	(5291)		
1PUT		0.13	25.13	0.25	-		
		(0.18)	(24.21)	(0.25)	(272)		
1CP	13	1.75	27.40	0.27	136		
		(2.02)	(24.01)	(0.25)	(156)		
1CW	14	4×10^{-4}	4×10^{-4}	0.006	13.6		
		(4×10^{-4})	(6×10^{-4})	(0.012)	(39)		
1OW		4×10^{-4}	1.8×10^{-2}	-	106		
		(1.1×10^{-3})	(3.7×10^{-2})	-	(110)		
1OO		3×10^{-4}	2.2×10^{-3}	-	6.4		
		(4×10^{-4})	(2.2×10^{-3})	-	(13.3)		

TABLE 6-8
PERCENT LOSS, Zr DECONTAMINATION FACTOR, AND FLOODING DATA,[a] SOLVENT EXTRACTION RUN 65

Contactor	Purpose	Volume Velocity (gal/hr/ft^2)	$\bar{v}_a$ (cm/sec)	$\bar{v}_o$ (cm/sec)	Flooding Frequency [cpm (rpm)]	Continuous Phase	Aqueous to Organic Ratio	ZrNb DF Th Basis	% Loss		% Flooding Frequency	Temp (°C)
									U	Th		
1A Centrifugal	Extraction	-	-	-	<500 rpm	-	0.276	3.20	0.02	0.02	-	27[b]
							(0.297)	(3.74)	(0.02)	(0.02)		(30)
1S Pulse Column	Scrub	974	0.158	0.930	90	Organic	0.170	18.95	-	-	77	Ambient
		(1015)	(0.157)	(0.988)	(86)		(0.159)	(5.62)	-	-	(55)	
1PU(X) Pulse Column	Pu Partition	446	0.051	0.503	93	Aqueous	0.995	4.68	-	-	75	Ambient
		(474)	(0.051)	(0.484)			(0.106)	(6.55)	-	-		
1PU(S) Pulse Column		180	0.102	0.101	~97	Aqueous	1.016		-	1.79	77	Ambient
		(190)	(0.115)	0.100			(1.148)		-	(1.44)		
1C Pulse Column	U-Th Strip	799	0.444	0.458	82	Aqueous	0.969	-	0.03	$<10^{-2}$	78	47
		(821)	(0.443)	(0.484)	(80)		(0.916)	-	(0.02)	($<10^{-2}$)	(80)	
1O Pulse Column	Solvent Wash	1009	0.108	1.031	116	Organic	0.105	-	-	-	~60	
		(1057)	(0.105)	(1.088)	(115)		(0.0965)	-	-	-		

(a) The values in parentheses resulted from a second set of operating conditions.

(b) Average of 1AW and 1AP stream temperatures.

During the initial startup, numerous problems were experienced. The interfaces for the 1PU(X) and 1PU(S) columns continued to be difficult to control due to the low aqueous flow rate. Other startup difficulties included flooding in the 1S column, 1PU(X) column, and 10 column. The top section of the 1S column was flooded throughout the run. The 1PU(X) column flooded while trying to establish the interface. The flood in the 10 column was dissipated after the temperature of the column contents was increased to the normal operating level.

The electrical outage caused a shutdown of all the motors on pumps and pulsers. The two phases in each column separated when the pulsing stopped. The interfaces in each of the aqueous continuous columns dropped, especially in the 1PU system. Both the 1S column and 10 column were flooded during the startup following the electrical outage. The 1S column operation was particularly difficult to recover. After the interruption, a steady-state operation was not achieved since the interfaces of the 1PU(X) and 1PU(S) columns had dropped down into the columns.

The thorium losses from the 1PU system in Run 65 were lower than in Runs 61 and 64, but the interruption of the run reduced the validity of the process sample analyses. Raising the input point for the 1PUA stream and lowering the aqueous to organic flow ratio in the 1PU system was responsible for the reduction of thorium losses.

The overall ZrNb decontamination factor in Run 65 was comparable to that achieved in Runs 61 and 64. However, the ZrNb decontamination factor in the 1PU system was greater than in Run 64. This improved decontamination factor was possible because the 1PUA flow rate was reduced. The location of the 1PUA inlet in the 1PU(X) column significantly reduced nitric acid requirements for effective thorium extraction. The reduction of the nitric acid concentration in the 1PU(S) reduced the re-extraction of ZrNb which occurred in Run 64.

6.3.5. Conclusions - Runs 61, 64, and 65

The partitioning of plutonium from thorium and uranium in the acid-Thorex flowsheet will be difficult to accomplish as shown by these experiments. Either aluminum nitrate salting will be needed in the 1PUA stream or else an additional cycle will be needed to complete the thorium-plutonium separation.

Final thorium cycle solvent extraction flowsheet tests are planned. A simulation will be made of plutonium separation from thorium by adding reductant to the 1BX, 2DF, and 2DIS streams. This preferred alternative to the system presented here would place the plutonium in the 2DW stream.

6.3.6. Results and Discussion - Runs 66 and 67

Table 6-9 contains the stream flow rates and analytical data for Run 66 and Table 6-10 contains the same data for Run 67. Table 6-11 contains loss and other calculated data. A description of the centrifugal contactor and pulsed columns is contained in Table 6-12. A comparison of pilot plant results with the results from SEPHIS code calculations is shown in Table 6-13. The high stage efficiency of the Robatel centrifugal contactor for uranium extraction was demonstrated in Runs 66 and 67.

For each aqueous feed condition, the contactor was started under conditions which produced low loading of the solvent. The flow rate of the aqueous stream was increased and/or the flow rate of the organic stream was decreased to increase the uranium loading in the organic phase. The effluent streams were sampled at each selected flow ratio after steady-state operation was achieved.

In Run 66, the 1AF concentration of uranium was too low to produce a saturated organic stream, even though a high aqueous to organic flow ratio was used. Although the extreme flow ratio was greater than the maximum recommended by the manufacturer, no operating problems occurred. Some aqueous droplets were entrained in the 1AP stream, but no measurable losses were produced in the 1AW stream.

TABLE 6-9
STREAM AND SAMPLE DATA, SOLVENT EXTRACTION RUN 66

1AF (Stream 1)			1AX (Stream 2) (30% TBP)	1AP (Stream 3)		1AW (Stream 4)	
Flow (mℓ/min)	U (g/ℓ)	HNO_3 (M)	Flow (mℓ/min)	U (g/ℓ)	HNO_3 (M)	U (g/ℓ)	HNO_3 (M)
372	10.81	1.71	328	11.25	0.231	$<10^{-3}$	1.46
327			314	10.07	0.36	$<10^{-3}$	1.35
320			273	12.04	0.36	$<10^{-3}$	1.42
422			282	14.26	0.23	$<10^{-3}$	1.48
386			207	20.04	0.27	$<10^{-3}$	1.59
376			153	28.12	0.20	$<10^{-3}$	1.60
433			87	37.45	0.20	$<10^{-3}$	1.63
466			99	46.10	0.16	$<10^{-3}$	1.66

TABLE 6-10
STREAM AND SAMPLE DATA, SOLVENT EXTRACTION RUN 67

1AF (Stream 1)			1AX (Stream 2) (30% TBP)	1AP (Stream 3)		1AW (Stream 4)	
Flow (mℓ/min)	U (g/ℓ)	HNO_3 (M)[a]	Flow (mℓ/min)	U (g/ℓ)	HNO_3 (M)	U (g/ℓ)	HNO_3 (M)
397	85.39	2.2	366	81.76	0.13	$<10^{-3}$	1.953
518	85.39	2.2	401	96.73	0.13	$<10^{-3}$	2.134
549	85.39	2.2	488	108.25	0.13	$<10^{-3}$	2.152
604	85.39	2.2	384	104.12	0.11	13.3	2.152
495	180.71	2.1	933	90.26	0.11	$<10^{-3}$	1.85
496	180.71	2.1	732	109.45	0.09	$<10^{-3}$	1.65
473	180.71	2.1	706	108.89	0.05	$<10^{-3}$	2.19
485	180.71	2.1	419	131.70	0.09	59.22	2.10
504	180.71	2.1	732	115.68	0.07	8.67	2.08
∿504	180.71	2.1	785	-	-	2.89	2.01

(a) The values for the nitric acid concentrations in the feed were calculated from a material balance based on the nitric acid concentration in the 1AP and 1AW streams. The analyses of the nitric acid had been reported as 1.43 and 1.25, respectively.

TABLE 6-11
CALCULATED LOSS AND FLOW RATE DATA, SOLVENT EXTRACTION RUNS 66 AND 67

Contactor	Purpose	Total Flow (ℓ/min)	Flooding Frequency (rpm)	Contactor Operating rpm	Aqueous to Organic Ratio	Per cent Loss, Uranium	Temp (°C)(a)
			RUN 66				
1A Centrifugal	Extraction		<500				
		0.700		1200	1.134	$<10^{-2}$	26
		0.641			1.041	$<10^{-2}$	27
		0.593			1.172	$<10^{-2}$	28
		0.704			1.496	$<10^{-2}$	29
		0.593			1.865	$<10^{-2}$	29
		0.529			2.458	$<10^{-2}$	29
		0.520			4.977	$<10^{-2}$	29
		0.565			4.707	$<10^{-2}$	29
			RUN 67				
1A Centrifugal	Extraction		<500				
	(2)	0.763		1200	1.085	$<10^{-2}$	22
	(6)	0.919			1.292	$<10^{-2}$	24
	(7)	1.037			1.125	$<10^{-2}$	24
	(8)	0.988			1.573	15.6	24
	(10)	1.428			0.531	$<10^{-2}$	25
	(12)	1.228			0.678	$<10^{-2}$	26
	(13)	1.179			0.670	$<10^{-2}$	26
	(14)	0.904			1.158	32.7	26
	(16)	1.236			0.689	4.80	27
	(17)	1.289			0.642	1.60	27

(a) Average of 1AW and 1AP temperatures.

TABLE 6-12
SOLVENT EXTRACTION RUNS 66 AND 67, CENTRIFUGAL CONTACTOR AND COLUMN CARTRIDGE DESCRIPTION

Unit	Purpose	Diameter (mm)	Total Height of Mixing Area (m)	Other			
1A Contactor	Extraction	180	0.32	Eight Stages with 0.4 Liter Total Holdup per Stage			
				Plates			Plate Spacing (mm)
				Nozzle Direction	Hole Size (mm)	% Free Area	
1C Column	U Strip	76	4.6	Up	4.8	23	Graded[a]
1O Column	Solvent Wash	51	5.5	Down	3.2	23	51

(a) Graded cartridge is, from the bottom, 2.6 m with 100 mm spacing, 0.5 m with 76 mm spacing, and the remainder with 51 mm spacing.

TABLE 6-13
COMPARISON OF 1AW AND 1AP CONCENTRATIONS BETWEEN PILOT PLANT RESULTS AND SEPHIS CALCULATIONS

Corresponding Input Stream Flow Rate [a] (mℓ/min)	Output Stream	Experimental Results		SEPHIS Eight Stage Calculation	
		U, (g/ℓ)	HNO_3, (M)	U, (g/ℓ)	HNO_3, (M)
1. 401 (1AX)	1AP	96.7	0.13	105.8	0.09
518 (1AF)	1AW	$<10^{-3}$	2.13	$<10^{-3}$	2.18
2. 488	1AP	108.3	0.13	92.4	0.16
549	1AW	$<10^{-3}$	2.15	$<10^{-3}$	2.11
3. 384	1AP	104.1	0.11	107.3	0.08
604	1AW	13.3	2.15	14.6	2.19
4. 933	1AP	90.26	0.11	92.2	0.19
495	1AW	$<10^{-3}$	1.85	$<10^{-3}$	1.84
5. 732	1AP	109.5	0.09	115.1	0.05
496	1AW	$<10^{-3}$	1.65	1.90	2.14
6. 706	1AP	108.9	0.05	114.9	0.05
473	1AW	$<10^{-3}$	2.19	$<10^{-3}$	2.14
7. 419	1AP	131.7	0.09	115.1	0.05
485	1AW	59.2	2.10	79.3	2.12
8. 732	1AP	115.7	0.07	115.1	0.05
504	1AW	8.67	2.08	4.91	2.14

[a] See Tables 6-9 and 6-10 for the concentration of uranium and nitric acid in each input stream.

In Run 67, two concentrations of uranium in the aqueous feed stream were selected for testing. Each of these feed streams was tested at several aqueous to organic flow ratios. With these feed streams, sufficient loading of the organic phase was achieved to effect losses via the 1AW stream.

The operational losses are typically less than the calculated losses because of the inaccuracy of the TBP analysis and the uncertainties in the SEPHIS code. Knowing the TBP concentration accurately is imperative because a small variation of less than 1% has a significant effect on SEPHIS calculations. The accuracy of the correlations used for the SEPHIS code has not been thoroughly tested under conditions of high solvent loading. These two factors plus random sampling error prohibit absolute determination of the stage efficiency of the centrifugal contactor.

Considerable difficulty has been experienced in obtaining a satisfactory TBP analysis of the solvent. Based on analyses, the concentration has been less than 30% TBP. However, based on the specific gravity and other tests, the concentration has been 30%. Since the analyses vary a great deal without corresponding operational explanation, the TBP analysis is suspect. A gas chromatographic technique has since reduced the error in TBP analysis (Section 6.4.2).

The one case in which the operating loss is greater than the calculated loss can be attributed to sample contamination. The 1AW sample with the uranium concentration higher than the calculated value was the first sample taken after the uranium loss of 59.22 g/liter was obtained. Some contamination of the later sample undoubtedly occurred due to residual uranium in the aqueous outlet system of the contactor.

As noted in the footnote in Table 6-10, the nitric acid concentrations in the feed streams for Run 67 were calculated based on the average 1AW and 1AP stream analyses. The analyzed values for the nitric acid concentration in feed were very low and obviously incorrect. The error in analysis presumably occurred due to the high uranium concentration. The accuracy of the nitric acid analyses for the 1AW stream was confirmed by reanalysis.

Two pulse columns were also used in Runs 66 and 67. One column was used to strip the uranium and the other to wash the solvent. No significant problems occurred with the operation of either of these columns.

6.4. BENCH-SCALE INVESTIGATIONS

6.4.1. Volatility of Ruthenium and Fluoride Ion During Feed Adjustment

6.4.1.1. Introduction

Feed adjustment steps are required in HTGR fuel reprocessing for dissolver and intercycle thorium nitrate solutions prior to solvent extraction. The purpose of the feed adjustment operation is to simultaneously concentrate thorium and reduce free nitric acid levels. As currently prescribed, feed adjustment will be used to reduce the acidity of the Thorex dissolver product solution from ∿9M in $[H^+]$ to <1M in $[H^+]$. A second feed adjustment operation will be necessary to render the thorium partition solvent extraction product acid deficient ($[-H^+]$) in order to produce feed for the second thorium solvent extraction cycle. Ruthenium and fluoride ion are potentially volatile species during feed adjustment. Ruthenium will be present in HTGR thorium nitrate reprocessing solutions as a fission product, while fluoride ion will be introduced in dissolution and solvent extraction operations. Experiments described in the present work were undertaken to study the degree of volatilization of ruthenium and fluoride ion during feed adjustment and to assess possible methods for suppressing losses due to volatilization. The work is of importance because fluroide volatility results in increased system corrosion and ruthenium volatility adds to the complexity of off-gas treatment.

6.4.1.2. Experimental and Results

6.4.1.2.1. Fluoride Volatility. An experiment was conducted to determine the fluoride loss to the overhead during batch and continuous operation with simulated Thorex dissolver solution (9M H^+, 1M Th^{+4}, 0.1M

Al^{+3}, 0.05M F^-). For the initial batch operation, 200 milliliters of dissolver solution was evaporated to a boiling point of 135°C and steam stripped to $-[H^+]$. In the continuous operation mode, diluted dissolver feed (1 part feed to 13 parts water, i.e., 200 milliliters dissolver solution to ∿2.8 liters final volume) was added to the acid-deficient boiler pot to permit long-term operation at or near acid deficiency. Overhead distillate samples were collected during the experiment, and a fluoride specific ion electrode was used to measure the fluoride content of each portion of distillate collected. The fluoride content of batch and continuous overhead samples is given in Table 6-14. Examination of Table 6-14 reveals ∿4.0 mg of fluoride total was lost to the overhead during the experiment. This represents about 1% of the total fluoride charged to the boiler pot, and approximately equal losses occurred during batch and continuous operation (2.2 mg and 1.8 mg, respectively).

The effect of boron addition on fluoride volatility was studied in the present work. The effect of boron was evaluated because boron is known to form complexes with fluoride ion and could possibly reduce boiler pot fluoride losses. An opposite effect was observed in practice, however, and fluoride losses were greater in experiments with boron added to the boiler pot. These experiments were performed by feeding simulated intercycle thorium partition product (1BT) with and without 0.2M boron to an acid-deficient boiler pot. Temperature and flow rates were maintained equal in order to have only one variable, i.e., feed boron concentration. Data for equilibrium fluoride concentrations overhead during continuous operation with and without boron are given in Table 6-15. Examination of Table 6-15 indicates the fluoride losses are about an order of magnitude greater when 0.2M boron is present in the incoming 1BT feed.

6.4.1.2.2. Ruthenium Volatility. A feed adjustment ruthenium volatilization study was performed with simulated dissolver solution. In this experiment, 200 milliliters of dissolver solution containing ruthenium in a Ru/Th weight ratio of 1.4×10^{-3} was evaporated to 135°C and steam stripped to $-[H^+]$. Samples of overhead distillates were taken for analysis

TABLE 6-14
FLUORIDE VOLATILITY DURING FEED ADJUSTMENT OF DISSOLVER SOLUTIONS, BENCH-SCALE DATA SUMMARY

Operational Mode [a]	Overhead Sample	Sample Volume (mℓ)	gF^-/Spl.Vol.(10^{-4}) [b]	Total mg F^- [b] Volatilized/Mode	% of Total F^- [b] Charged to Boiler Pot Volatilized/Mode
Batch	Evap. 1	99	13.7		
↓	Evap. 2	42	5.59		
	Stm. Str. 1	50	1.81		
	Stm. Str. 2	51	0.68	2.2 mg.	1.2
Continuous	OH 1	232	1.85		
↓	2	138	0.60		
	3	178	0.88		
	4	215	1.02		
	5	198	1.11		
	6	195	1.19		
	7	319	1.94		
	8	358	2.38		
	9	486	3.60		
	10	163	1.11	1.8 mg.	0.9

(a) Batch operation consisted of evaporating 200 mℓ of dissolver solution to 135°C, followed by steam stripping to $-[H^+]$.

Cont. operation consisted of continuous addition of 1 part dissolver solution to 13 parts water to the $-[H^+]$ boiler pot at 135°C.

(b) Determined by analysis of overhead samples.

Feed Rate = 3.85 mℓ/min; temperature = 135°C.

TABLE 6-15
FLUORIDE VOLATILITY DURING FEED ADJUSTMENT OF 1BT SOLUTION WITH AND WITHOUT BORON ADDITION - CONTINUOUS OPERATION

1BT Feed Boron Content	Overhead F^- Molarity at Equilibrium
None	6.9×10^{-5}
	6.0×10^{-5}
	4.6×10^{-5}
0.2M	2.9×10^{-4}
	3.0×10^{-4}
	3.6×10^{-4}

Conditions:

1BT Feed Rate = 3.85 mℓ/min

Temp. = 135°C

Initial Boiler Pot Acidity = -0.161M

Final Boiler Pot Acidity = -0.201M

Note: Boron loss to the overhead was calculated to be ca. 14% of the total boron charged to the boiler pot.

of ruthenium content. The Ru/Th weight ratio of 1.4×10^{-3} was chosen to represent the dissolver solution resulting from dissolution of full-burnup, 1-year, four-segment fuel and assumes complete ruthenium dissolution. A packed tower was used to prevent mechanical introduction of ruthenium into the overhead. Following batch operation, continuous feed adjustment was initiated with diluted dissolver solution (200 milliliters dissolver solution to 2800 milliliters final volume) containing 900 mg Ru (Ru/Th weight ratio = 1.9×10^{-2}). As with the batch operation, distillate samples were taken for ruthenium analysis. No ruthenium was found in any of the overhead samples taken; however, the sensitivity of the analytical procedure used (X-ray fluorescence) is inadequate for determining ruthenium at levels <20 ppm.

Data are presented in Table 6-16 for upper limit ruthenium overhead concentrations during batch and continuous feed adjustment operations. Maximum ruthenium volatilization values of <7% in the batch mode and <5.6% in the continuous mode were calculated.

6.4.1.3. Conclusions

Based on data available to date, the following conclusions were drawn:

1. Continuous feed adjustment offers no apparent advantage over batch operation with regard to the reduction of fluoride volatility. Both types of operation yielded 1% fluoride volatility.

2. Reduction of fluoride volatility by the addition of boron to the boiler pot is not feasible. The addition of boron to the boiler pot actually increased the fluoride volatilization. Corrosion rate data are needed to determine whether the boron reduces vapor space corrosion of stainless steel even though the fluoride volatility is higher.

TABLE 6-16
RUTHENIUM VOLATILITY DURING FEED ADJUSTMENT OF DISSOLVER SOLUTIONS, BENCH-SCALE DATA SUMMARY

Operational Mode [a]	Overhead Sample	Sample Volume, (mℓ)	mg Ru/Spl. Vol.	Maximum Total mg Ru [b] Volatilized/Mode	Max. % of Total Ru [b] Charged to Boiler Pot Volatilized/Mode
Batch	Evap. 1	99	1.98		
↓	Evap. 2	42	0.84		
	Stm. Str. 1	50	1.00		
	Stm. Str. 2	51	1.02	4.8	<7
Continuous	OH 1	232	4.64		
↓	2	138	2.76		
	3	178	3.56		
	4	215	4.30		
	5	198	3.96		
	6	195	3.90		
	7	319	6.38		
	8	358	7.16		
	9	486	9.72		
	10	163	3.26	49.6	<5.6

[a] Batch operation consisted of evaporating 200 mℓ of dissolver solution to 135°C, followed by steam stripping to $-[H^+]$.

Continuous operation consisted of continuous addition of 1 part dissolver solution to 13 parts water to the $-[H^+]$ boiler pot at 135°C.

[b] Determined by analysis of overhead samples.

Feed Rate = 3.85 mℓ/ min; temperature = 135°C.

3. No measurable ruthenium losses occurred during batch or continuous feed adjustments; however, the calculated upper limit values are quite high. Additional sample aliquots are being retained and will be resubmitted for atomic absorption analysis when a more sensitive ruthenium procedure is established. In the interim, tracer Ru-103 will be ordered to permit ruthenium determination at lower levels by gamma spectrometry in future samples, should this be required.

6.4.2. Gas Chromatographic Determination of Tributyl Phosphate in Normal Paraffin Hydrocarbon Diluent

6.4.2.1. Introduction

Tributyl phosphate (TBP) is the heavy metal extractant used in Thorex solvent extraction processes. An accurate analysis of TBP in normal paraffin hydrocarbon (NPH) is necessary for proper evaluation of solvent extraction performance data.

The makeup target value for TBP concentration in the process solvent is 30% by volume. A gas chromatograph was used to measure the TBP content of 20%, 30%, and 40% TBP/NPH solutions (prepared volumetrically) and a sample of process solvent from the solvent extraction pilot plant system. Resultant gas chromatographic data indicate an error of <2% absolute (30% ± 0.6% at the 30 vol % level) is achievable with the gas chromatographic method. The value measured for the TBP concentration of the process solvent was 30.5 vol %.

6.4.2.2. Experimental

The gas chromatograph was fitted with a 0.30 m x 3.2 mm column packed with 5% OV-101 (methyl silicone) on 100/120 mesh Chromasorb G. Following initial scoping tests, which demonstrated adequate separation of the

components in TBP/NPH solutions, the experimental conditions given below were established for the TBP analysis:

Sample volume = 2 μliters; helium carrier gas flow rate = 10 milliliters/min,

Initial column temperature = 150°C, time = 1 min,

Column temperature rise = 40°C/min,

Final temperature = 225°C.

A typical chromatogram obtained using instrumental conditions described above is given in Fig. 6-4. Figure 6-5 is a plot of TBP peak area obtained for 20, 30, and 40 vol % TBP/NPH solutions. A value of 30.5 vol % TBP was obtained for the process solvent sample.

6.4.2.3. Conclusions

The gas chromatographic method is applicable to a rapid determination of TBP in TBP/NPH solutions.

6.4.3. Phosphorus Separation During Concentration of Uranyl Nitrate

Work was performed during the reporting period to determine the distribution of total phosphorus during concentration of 1CU (uranium product stream) with steam stripping in recent LWR solvent extraction operations. The data are reported here for cross reference into the Thorium Utilization Program. All values reported herein were obtained following replacement of the concentrator steam stripping tower packing material (Norton Intalox saddles, nominal size = 0.0125 m) with Norton pall rings (nominal outside diameter and length = 0.016 m) in an effort to improve tower flooding characteristics. Steam stripping is currently being used in pilot plant equipment for the removal of organic phosphorus-containing compounds, e.g., tributyl and dibutyl phosphate, present in the 1CU stream as a result of solvent contact. This operation is done to clean up the uranium stream prior to recycle as feed for subsequent runs.

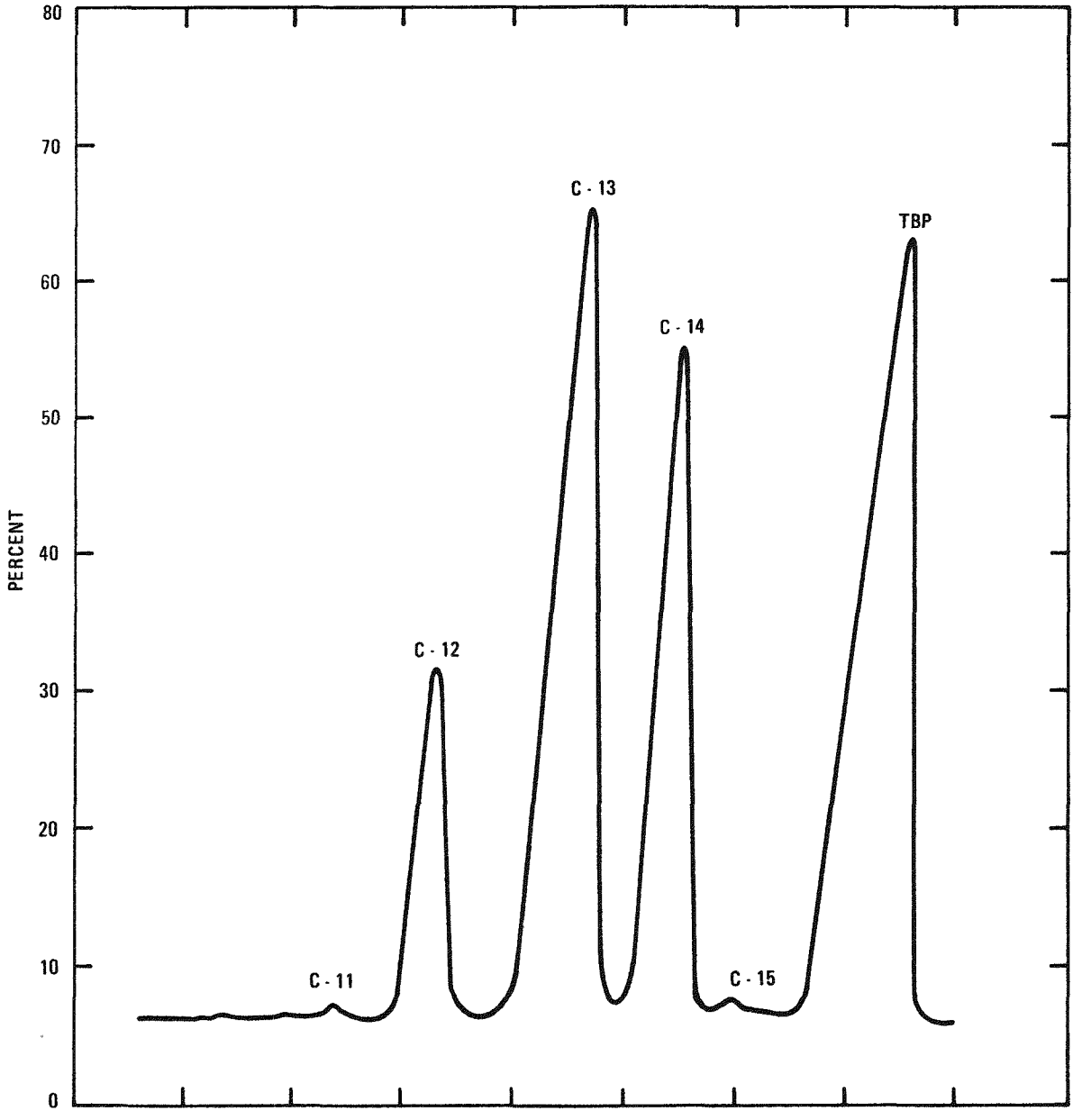

Fig. 6-4. Chromatogram of 40 vol % TBP in NPH

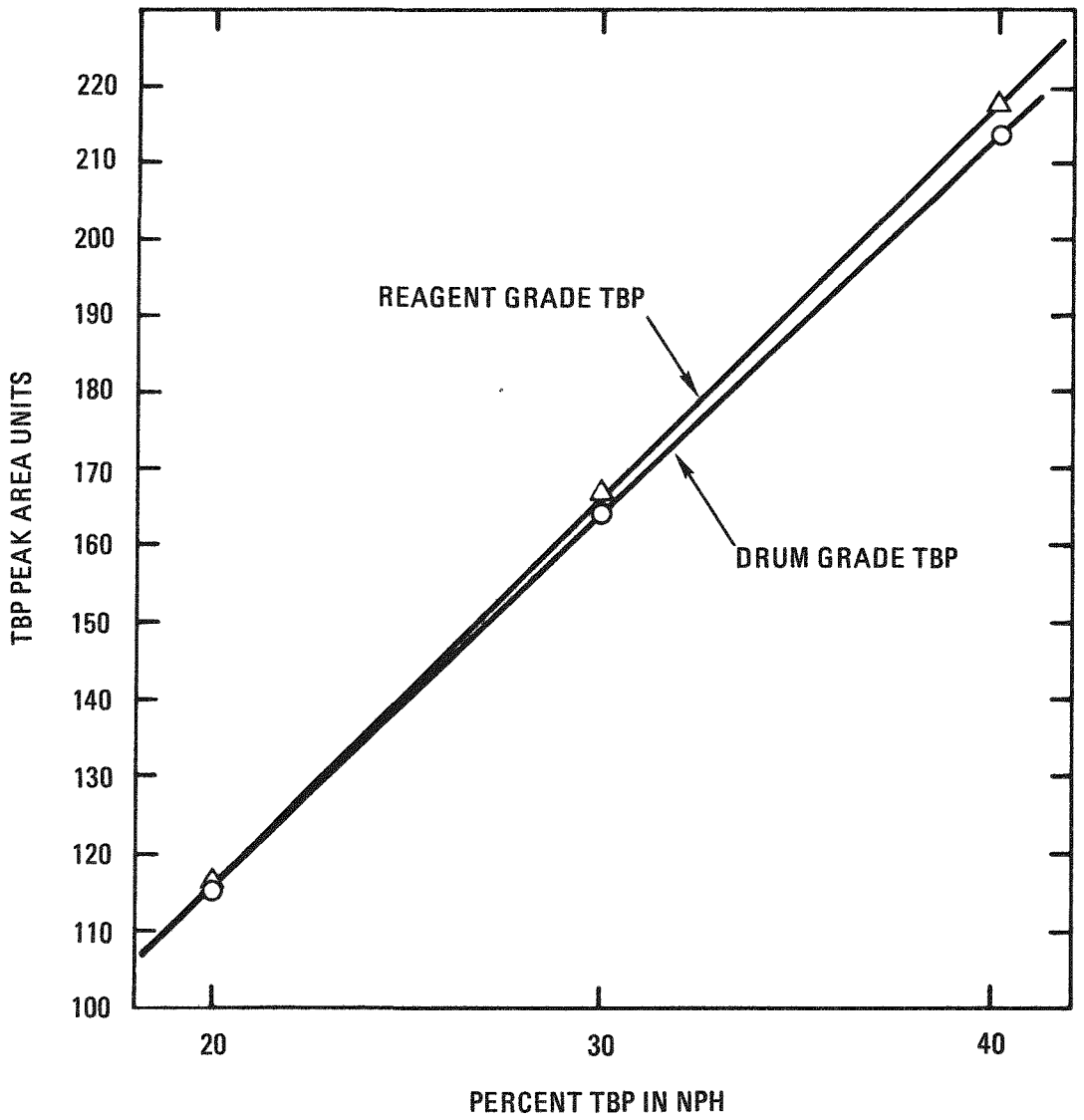

Fig. 6-5. TBP calibration plot

Details of the analytical procedure used and total phosphorus values obtained prior to the change in the concentrator packing material were reported previously (Ref. 6-2).

Data summaries for samples from three concentrator runs are presented in Table 6-17. The P/U weight ratios in Table 6-17 are slightly lower than those reported prior to the tower packing change, indicating some improvement in TBP removal with the Norton pall ring tower packing; however, total phosphorus material balances are still not greater than ∿70%. As before, the phosphorus to uranium recycle fuel specification of 200 ppm was achieved in all product samples.

6.4.4. Solvent Degradation in HTGR Fuel Reprocessing

A topical report entitled "Safety Aspects of Solvent Nitration in HTGR Fuel Reprocessing" (GA-A14372 - scheduled for publication in June 1977) was prepared during the reporting period. The major findings of the report are contained in previous quarterly reports (Refs. 6-1 through 6-4).

REFERENCES

6-1. "Thorium Utilization Program Quarterly Progress Report for the Period Ending February 29, 1976," ERDA Report GA-A13833, General Atomic Company, March 31, 1976.

6-2. "Thorium Utilization Program Quarterly Progress Report for the Period Ending February 28, 1977," ERDA Report GA-A14304, General Atomic Company, March 1977.

6-3. "Thorium Utilization Program Quarterly Progress Report for the Period Ending May 31, 1976," ERDA Report GA-A13949, General Atomic Company, June 30, 1976.

6-4. "Thorium Utilization Program Quarterly Progress Report for the Period Ending August 31, 1976," ERDA Report GA-A14085, General Atomic Company, September 30, 1976.

TABLE 6-17
PHOSPHORUS DATA SUMMARY

Sample	Phosphorus Content (µg/ml)	Uranium Content (M)	P/U Product (ppm)
	Run L-14		
1CU product	7	1.56	19
Overhead	19		
	Run L-15		
1CU product	6	1.60	16
Overhead 1	19		
Overhead composite	18		
	Run L-16		
1CU product	5	1.60	13
	19		
	14		

7. DRY SOLIDS HANDLING

7.1. SUMMARY

Progress with component and system testing continues. Installation and in-place testing of rotary feeder valves has continued with satisfactory results. A vibratory feeder has been calibrated and related improvements verified. Evaluation of different types of samplers has progressed. Three samplers have shown particularly encouraging results.

Further experimental data have been obtained for several of the transport systems. Data analyzed to date have shown close agreement between observation and prediction. The primary burner product removal system successfully transported burner product at an elevated temperature.

7.2. INTRODUCTION

The development work, as described in the Experimental Plan, is divided into several stages:

1. Cold laboratory development.
2. Hot laboratory development.
3. Cold engineering development.
4. Hot engineering development.
5. Cold prototype development.
6. Procedure development.

During the quarter, progress was made in development stage 3.

7.3. COLD ENGINEERING DEVELOPMENT (DEVELOPMENT STAGE 3)

7.3.1. Qualification Testing

The activities in the coming months will be concerned with qualification testing, which can be defined as partial verification of the design under simulated conditions, followed by complete verification during sequential operation. The testing is divided into two phases. Phase I is concerned with component testing and Phase II with system testing.

The solids handling system is divided into six subsystems (see Fig. 7-1):

Subsystem No. 1. Crusher product removal system.
Subsystem No. 2. Primary burner feed system.
Subsystem No. 3. Primary burner product removal system.
Subsystem No. 4. Particle classifier feed system.
Subsystem No. 5. Particle crusher feed system.
Subsystem No. 6. Secondary burner product removal system.

7.3.1.1. Component Qualification and Improvement

In a previous quarterly report (Ref. 7-1), a detailed description of various components of the solids handling systems was given. Progress in component testing for the current quarter has been made with feeders and samplers.

7.3.1.1.1. Feeders. Rotary feeder valves (0.05-m inlet dimension) were installed beneath the fertile and fissile classifier product bunkers. Actual in-place performance verification was established in conjunction with related system tests utilizing uncoated BISO fertile fuel particles as the feed material. A constant feed rate had to be maintained for the system tests, thus preventing the acquisition of a range of feed rates for various rotary valve rotational speeds. The feed rate of 0.23 kg/s at zero

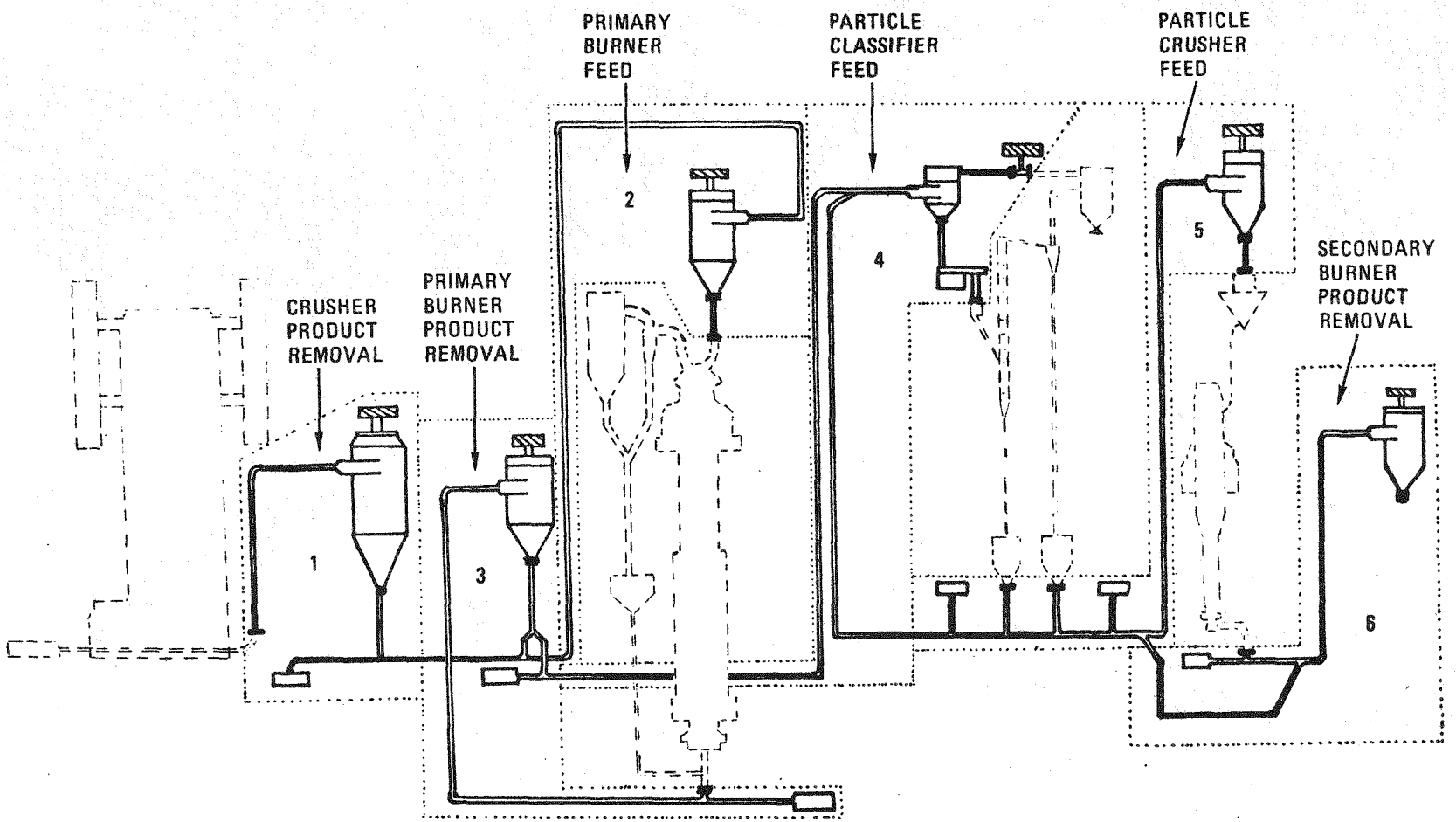

Fig. 7-1. Solids handling subsystems

rpm with a valve clearance of 4.76 mm was consistent with transport system requirements. Additional feeder calibration will take place during sequential pilot plant tests.

Preliminary tests on rotary feeder valves with an 0.010-m opening dimension were conducted to establish vane clearances and throughput capacities. Crushed graphite, steel shot, and glass beads were used as feed materials for tests to simulate actual feed materials encountered in pilot plant operations. Results of these tests are shown in Fig. 7-2.

7.3.1.1.2. Samplers. Progress was achieved in the testing and evaluation of several types of samplers.

Crusher Product Sampling. The cross-cutting sampler described in the previous quarterly report (Ref. 7-2) was acquired for use under the crusher product bunker. The sampler was tested with simulated feed material consisting of crushed graphite from UNIFRAME system tests. The size distribution of the cross-cutting sampler was repeatable and compared favorably with the size distribution as determined by a 12 to 1 split sampler, which has been used exclusively for crusher product sampling. Figure 7-3 illustrates the sampler performance as compared to the 12 to 1 split sampler using the same feed material of crushed scrap graphite from crusher test No. 18. Because of the favorable sampling performance, ease of operation, and cleanliness of the cross-cutting sampler, it has taken the place of the split sampler as the method of sampling crusher test product.

Primary Burner Feed and Product Sampling. The Model TS (tube and screw) sampler from Quality Control Equipment Company was selected for sampling primary burner feed and product materials. This sampler is designed to sample dry, free-flowing granular or powdered material which flows by gravity through vertical or sloping chutes. The TS sampler consists of a slotted tube with an internal auger, each driven by its own motor. The tube slot faces down when not in the sampling mode. During a sampling cycle, the tube rotates 180° so that the slot faces into the

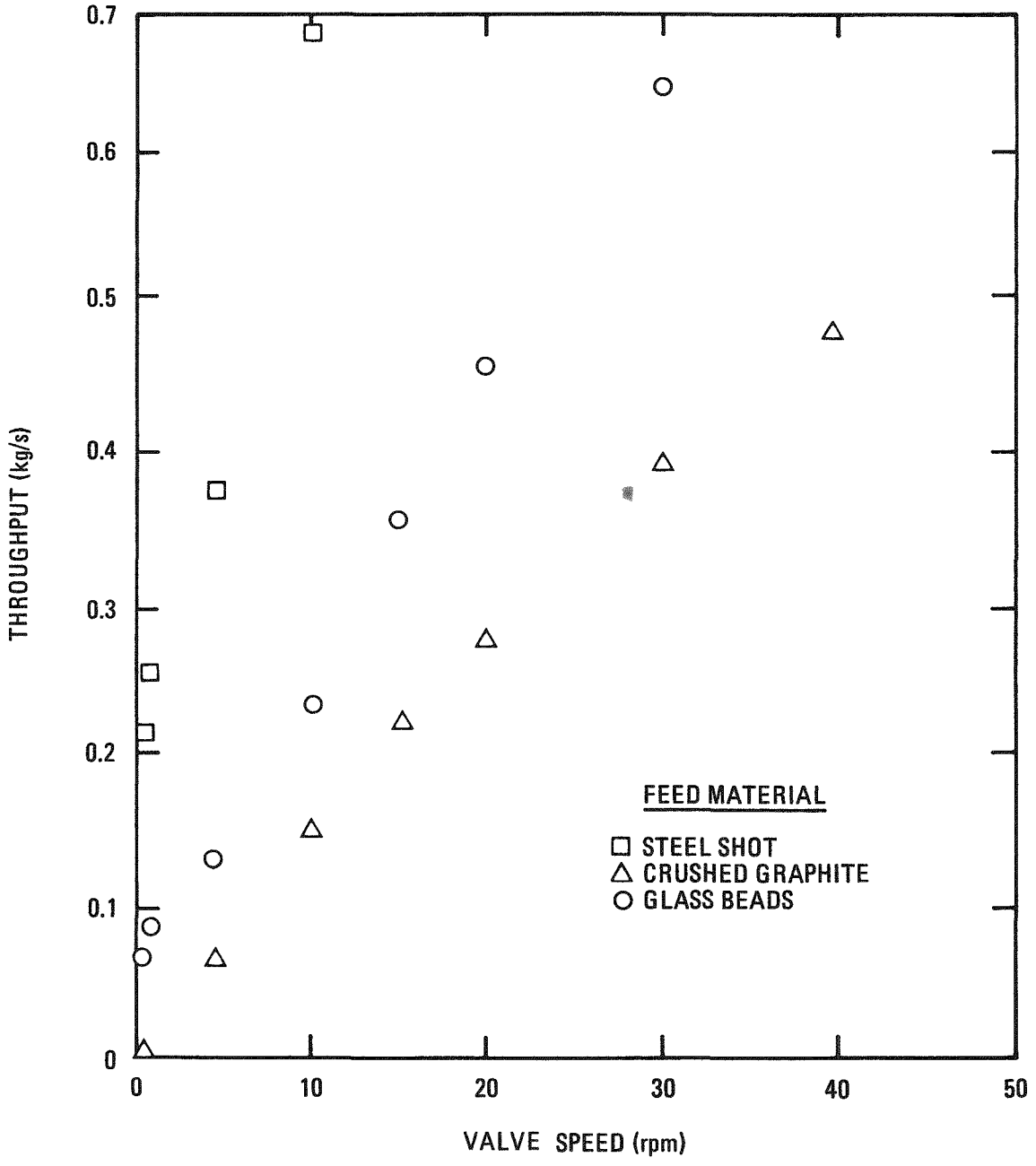

Fig. 7-2. Rotary feeder valve test results [0.010 m (4 in.) inlet]

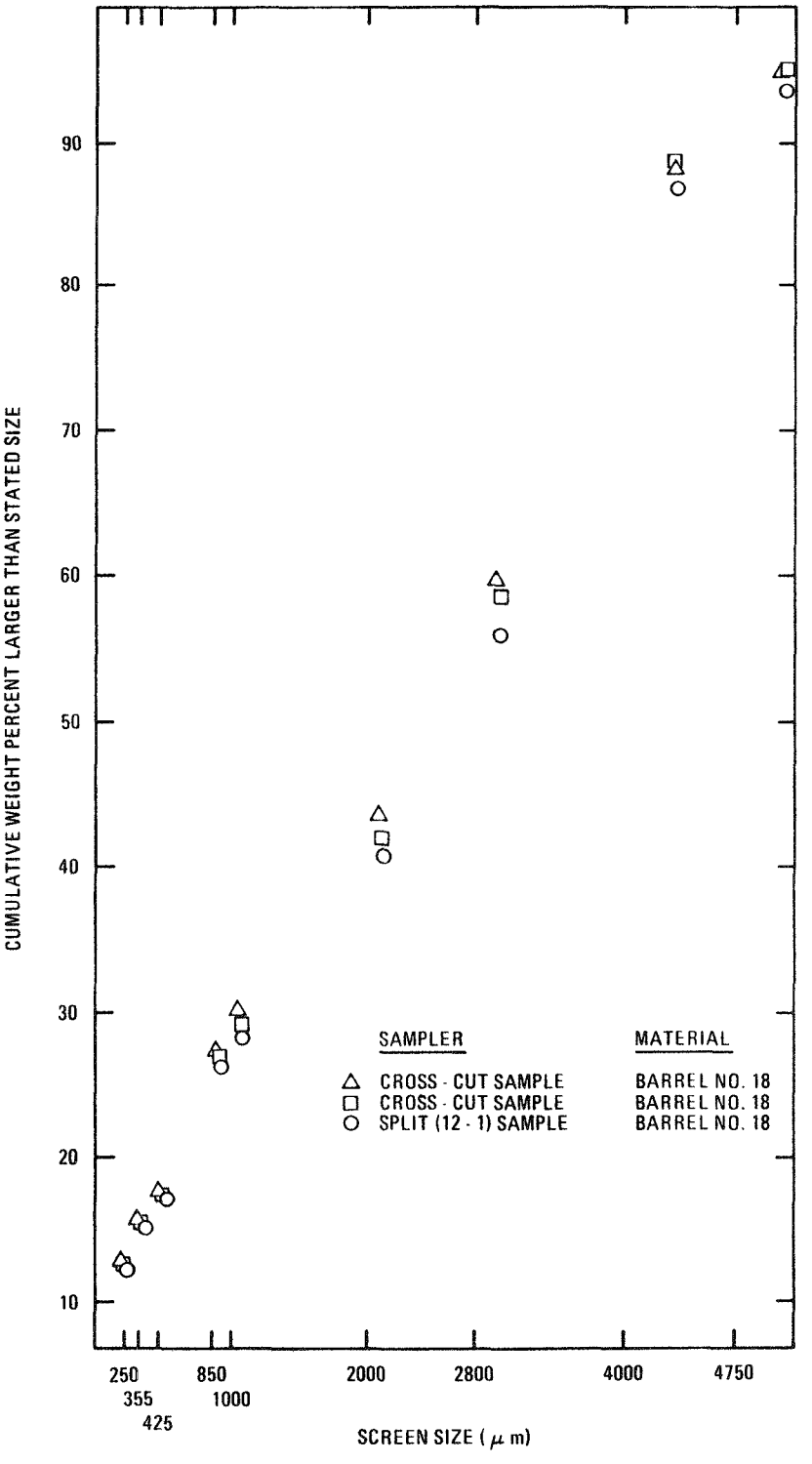

Fig. 7-3. Size distributions of samples taken by cross-cut sampler and 12 to 1 split sampler

material stream. At the same time, the auger rotates to move the sample through the tube to the discharge. This condition continues for a predetermined period, which can be adjusted to control the quantity of each sample. At the end of the sample period, the tube again rotates 180° leaving the slot facing downstream. The auger continues for a short time to assure complete sample discharge. An adjustable timer controls the frequency of sampling cycles to provide the desired total sample quantity. The TS sampler is illustrated in Fig. 7-4.

The TS sampler was tested with simulated primary burner feed consisting of crushed graphite, steel shot, and glass beads. The sample size distribution was analyzed and compared to the size distribution of the same feed material as sampled by the cross-cutting sampler. The results were favorable, as shown in Fig. 7-5.

Secondary Burner Feed Sampling. The Model RT (retractable tube) sampler from Quality Control Equipment Company was selected for sampling feed from the particle crusher prior to entry into the secondary burner. The RT sampler consists of a slotted tube with an internal auger. The tube is thrust into the material stream to collect a sample. The tube is then retracted and the sample removed by rotation of the auger. The period and frequency of the sampler are adjustable to control sample size and total quantity collected (see Fig. 7-6).

During the quarter the RT sampler was bench tested and then installed for use during secondary burner tests. The RT sampler successfully extracted grab samples during each of three secondary burner experiments.

7.3.1.2. System Qualification

7.3.1.2.1. Introduction. The goal of system qualification is to ensure that each subsystem can convey material at a rate compatible with upstream and downstream operations so that particle breakage is minimal. This involves establishing the conveying characteristics of each system by

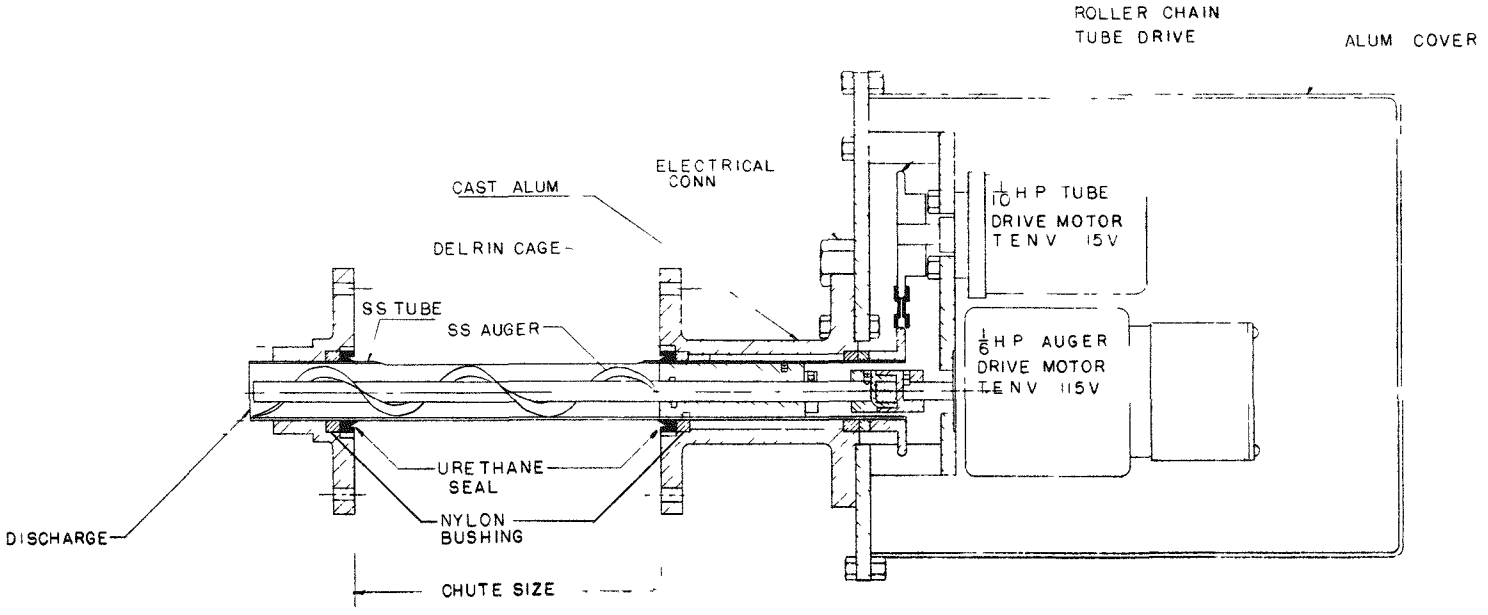

Fig. 7-4. TS (tube and screw) sampler

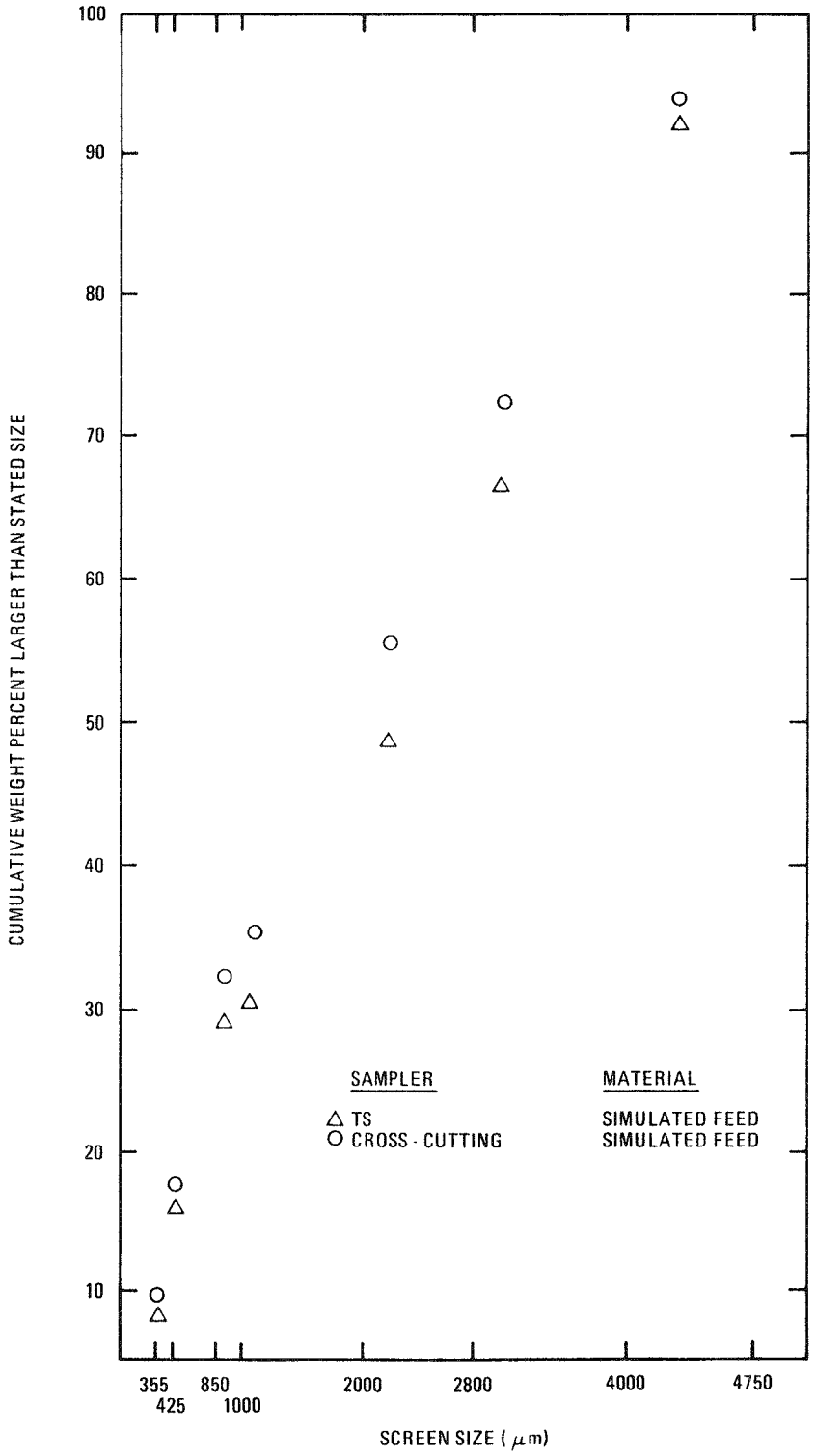

Fig. 7-5. Size distributions of samples taken by cross-cutting and TS samplers

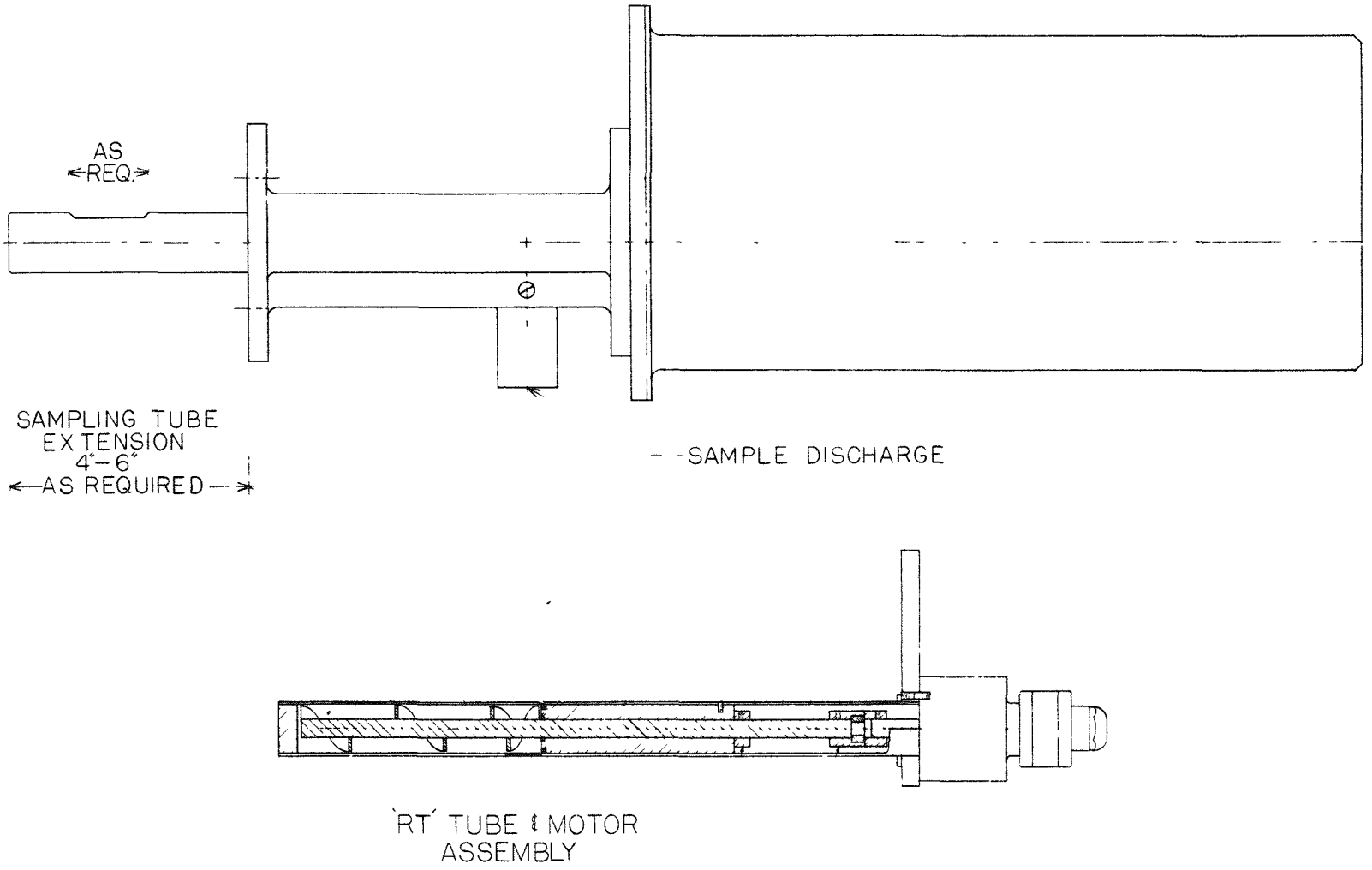

Fig. 7-6. Retractable tube (RT) sampler

measuring pressure drops at different solids flow rates over a range of gas velocities. The determination of the saltation point, i.e., where the suspension collapses and particles fill up the line, is also required. The ability to restart, after plugging the line, by use of the blower only should also be investigated.

The solids handling test rig, described in previous quarterly reports, is equipped with a variable speed blower, which is being used for system qualification. Once the optimal conditions for a given system have been determined, a fixed speed blower, suitably set, can be used.

The final part of system qualification, which is the measurement of fuel particle breakage during sequential operation, can be performed only during pilot plant operation with loaded fuel elements.

Progress with system testing is described below.

7.3.1.2.2. Crusher Product Removal System (Subsystem No. 1). The crusher product removal system tests consisted of transporting the crushed graphite product directly from the outlet of the UNIFRAME size reduction system through the transport tubing and into the crusher product bunker. The variable speed blower from the test rig was used so that transport gas velocities could be varied. The product feed rate varied due to the operating characteristics of the crushing system. The feed rate was steady enough, however, to achieve approximate correlation between predicted and observed values for system pressure drop.

The mean feed rate is determined by dividing the total weight of feed by the total transport test time. For a given feed rate, the pressure drop across the solids transport portion of the system ($P_2 - P_1$) can be calculated in relation to the transport gas velocity using the pressure drop formula published by the Engineering Equipment Users Association (EEUA) (Ref. 7-3). From previous experiments, it was found that one-half the EEUA value closely correlates with our laboratory results.

The EEUA formula is as follows:

$$\Delta P = \frac{1}{2} \rho_{ns} \bar{V}_G^2 \left(F_1 + F_2 \frac{L}{D} + F_3 N \right) + \rho_{ns} g H \quad ,$$

where ΔP = pressure difference (Pa),

ρ_{ns} = non-slip density = $\bar{\rho}_g + (F_p . 4/\pi D^2 \bar{V}_g)$ (kg/m^3),

F_p = particle flow rate (kg/s),

$\bar{V}_G$ = mean gas velocity (m/s),

$\bar{\rho}_g$ = mean gas density (kg/m^3),

L = length of conveying system (m),

H = change in elevation (m),

D = internal diameter of the conveying line (m),

F_1 = acceleration factor = 2.5,

F_2 = friction factor - $0.0127 + 2.71/\bar{V}_g^2$,

F_3 = bend factor = 0.5 for gradual bends,

N = number of bends.

The calculated pressure drop across the system can be compared to the experimental pressure drop by observing the pressure drop $(P_2 - P_1)$ for a particular velocity and feed rate.

The diagram of the piping for subsystem No. 1 is shown in Fig. 7-7. Pressures and pressure drops were measured past the inlet (P_1), at the bunker (P_2), across the in-bunker filters (ΔP_3), at the end of the system (P_4), at the inlet to the variable-speed blower (P_5), in front of the orifice plate (P_6), and across the orifice plate (ΔP_7). The temperature at the exit from the variable-speed blower was also measured.

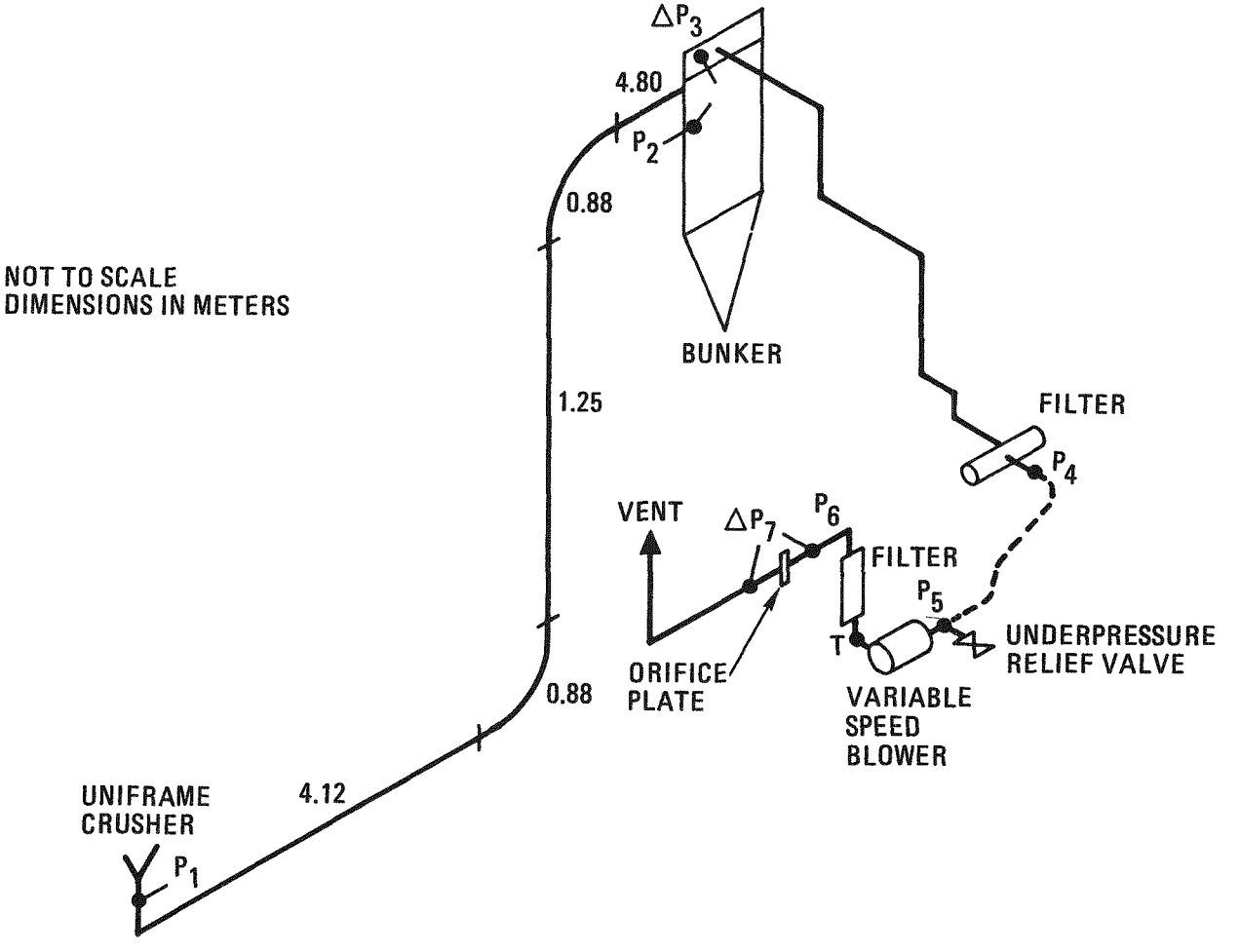

Fig. 7-7. Crusher product removal system

The inlet gas velocity is related to the orifice plate measurements by

$$V = 4.57 \sqrt{\Delta P_7} \sqrt{\frac{(T + 273)}{300} \cdot \frac{100}{(100 + P_6)}} \quad ,$$

where V is in m/sec, T is in °C, and P is in kPa.

The inlet gas velocity is averaged between ambient pressure and P_2 to obtain the mean gas velocity ($\bar{V}_G$) to provide direct comparison between predicted and observed values for the pressure drop across the crusher product removal system.

The results of one such exercise of comparing predicted to observed pressure drops in crusher product removal system tests are shown in Fig. 7-8. The average feed rate of 0.15 kg/s was used in the calculations. Correlation of observed and predicted values within ±30% is considered acceptable for pneumatic conveying of solids. The data are representative of several crusher tests utilizing scrap graphite as the feed material. Additional effort is planned to obtain more accurate solids feed rates before repeating this analysis with loaded fuel blocks during sequential operations of the pilot plant.

7.3.1.2.3. Primary Burner Feed System (Subsystem No. 2). Data were collected during operation of the primary burner feed system in support of primary burner tests. Two different types of feed materials were used: (1) simulated burner feed consisting of 81% crushed graphite, 13% coated BISO fuel particles, and 6% coated WAR fuel particles, and (2) coated TRISO fuel particles. The simulated feed mixture was used for burner startup and the TRISO fuel was used for later bed addition.

The methods of predicting pressure drop across a pneumatic conveying system were outlined in the previous section. The difference between this system and the crusher product removal system previously discussed is the system geometry. The primary burner feed system is shown schematically in Fig. 7-9.

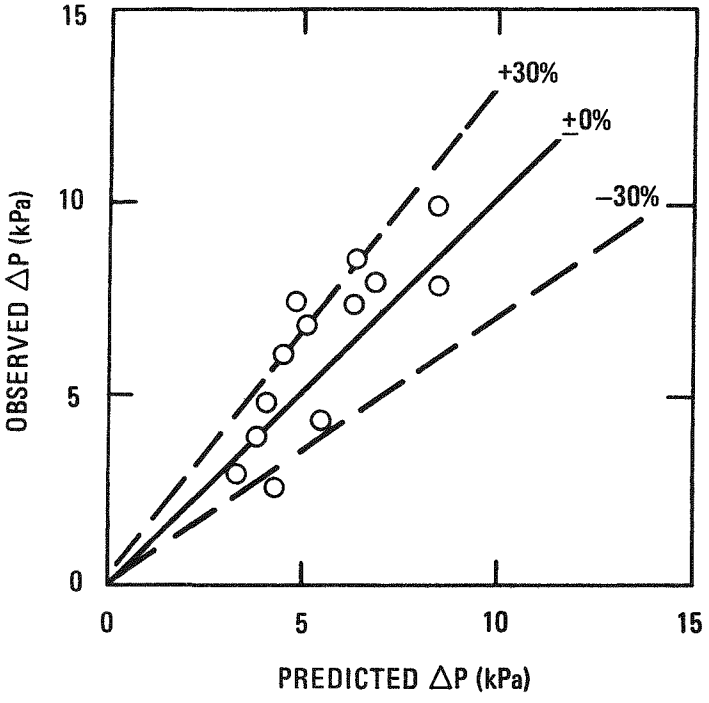

Fig. 7-8. Observed versus predicted pressure drop results for the crusher product removal system using crushed graphite fed at ≃0.15 kg/s

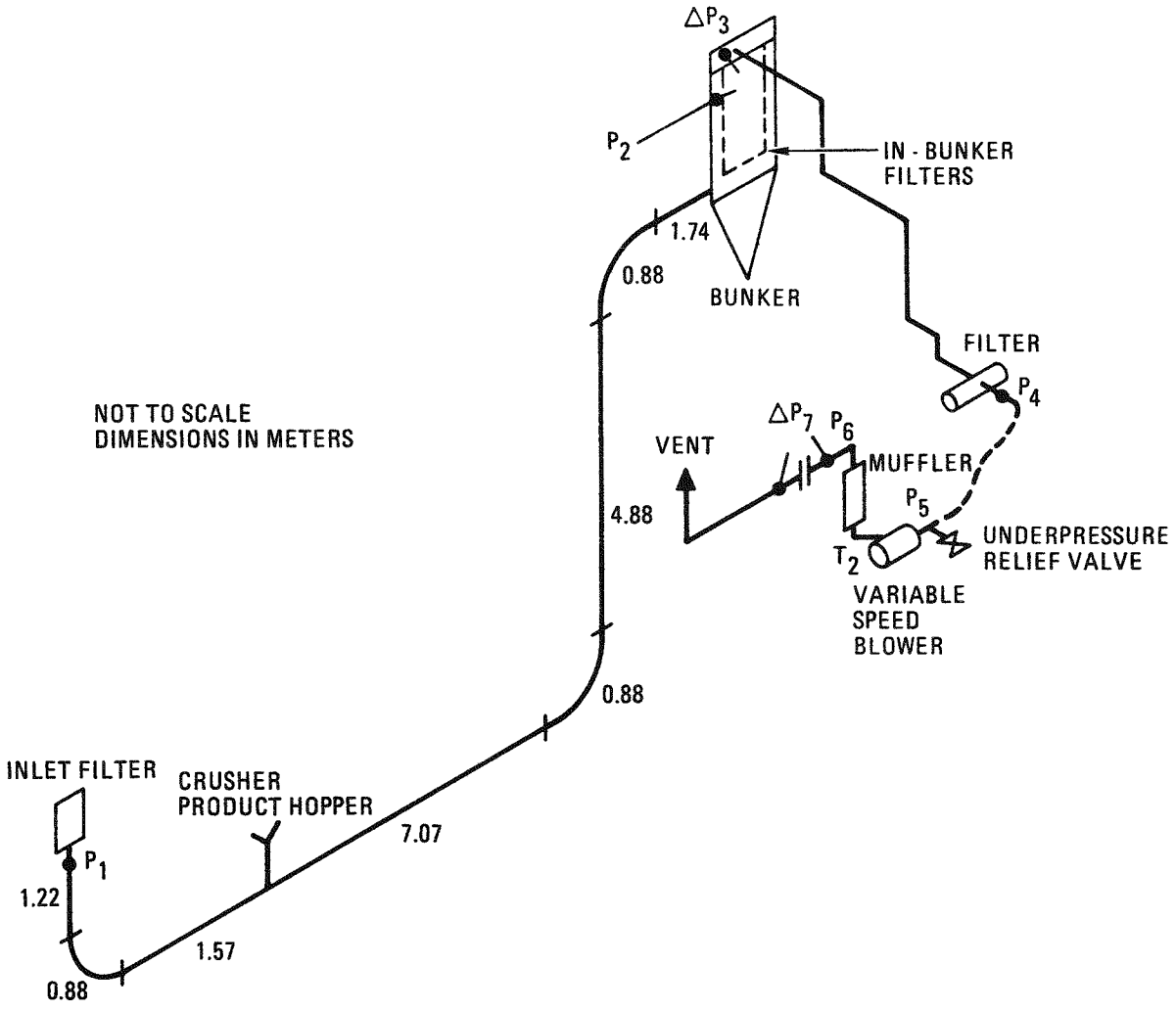

Fig. 7-9. Primary burner feed system

The experiments consisted of pneumatically conveying a known weight of feed material from an entry point beneath the crusher product bunker through the transport tubing and into the primary burner feed bunker. The feed rate was not dependent upon the operation of another system, as was the case with subsystem No. 1, enabling a more consistent feed with the average being representative of the instantaneous rate.

The conveying experiment using the simulated burner feed mixture involved feeding the mixture at 0.23 kg/s into a gas stream of average velocity ranging from 15.4 m/s (on the verge of saltation) to 30.0 m/s. Table 7-1 gives a comparison between predicted and observed values of the conveying line pressure drop ($P_2 - P_1$) over the tested range of gas velocities.

The experimental results are shown graphically in Fig. 7-10. The agreement between calculated and measured ΔP values is within ±20% except at the low-velocity end where saltation effects and instrument error begin to produce major inaccuracies.

The coated TRISO fuel particle feed experiment was conducted at 0.27 kg/s and average velocities of 22.6 to 33.4 m/s. The feed rate is considered more accurate than for the simulated feed mixture since the TRISO feed is much more homogeneous than a mixture containing a large percentage of crushed graphite, which varies greatly in particle size. The test results are in close agreement with the calculated values as shown in Table 7-2 and in Fig. 7-11.

Similar analyses will be conducted during sequential operations with actual design basis feed material to verify the prediction methods for standard pilot plant operating conditions.

7.3.1.2.4. Primary Burner Product Removal System (Subsystem No. 3). The variable position knifegate valve was installed beneath the primary burner prior to primary burner test B. The primary burner removal system

TABLE 7-1
PRESSURE DROPS FOR CONVEYING SIMULATED FEED MIXTURE
IN THE PRIMARY BURNER FEED SYSTEM

Mean Gas Velocity (m/s)	Calculated ΔP ($P_2 - P_1$) (kPa)	Observed ΔP ($P_2 - P_1$) (kPa)	Difference (Calc. - Obs.) (kPa)
30.0	9.83	10.70	-0.87
27.8	9.36	9.95	-0.59
25.3	8.51	8.46	+0.05
23.1	7.81	7.46	+0.35
20.5	7.09	6.22	+0.87
18.0	6.42	5.23	+1.19
15.4	5.87	4.48	+1.39

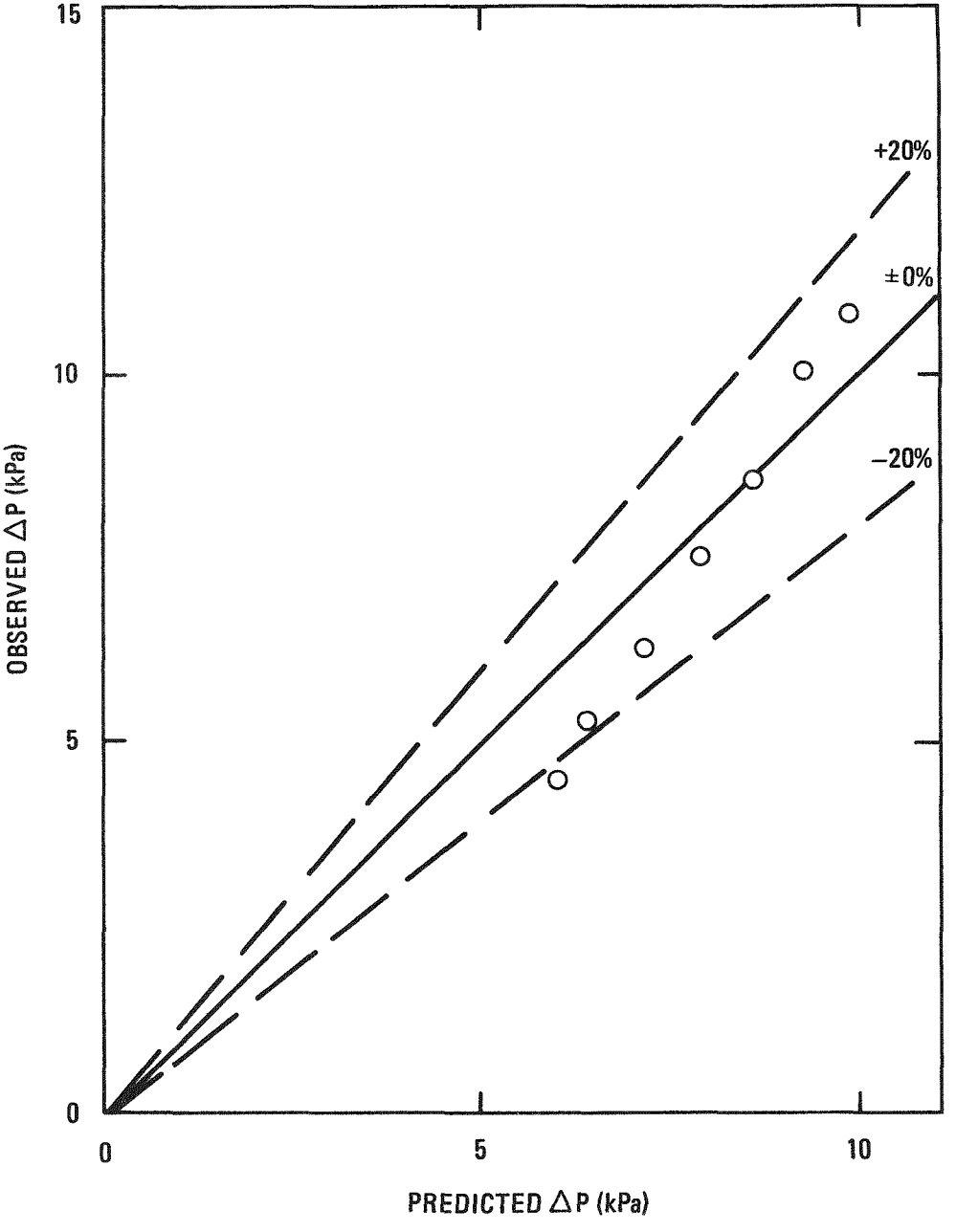

Fig. 7-10. Observed versus predicted pressure drop results for the primary burner feed system using simulated primary burner feed at 0.23 kg/s feed rate

TABLE 7-2
PRESSURE DROPS FOR CONVEYING TRISO COATED FUEL PARTICLES
IN THE PRIMARY BURNER FEED SYSTEM

Mean Gas Velocity (m/s)	Calculated ΔP ($P_2 - P_1$) (kPa)	Observed ΔP ($P_2 - P_1$) (kPa)	Difference (Calc. - Obs.) (kPa)
33.4	12.77	13.44	-0.67
31.5	11.94	12.94	-1.00
29.7	10.82	12.44	-1.62
28.3	10.80	11.45	-0.65
26.2	10.00	10.70	-0.70
22.6	8.78	9.95	-1.17

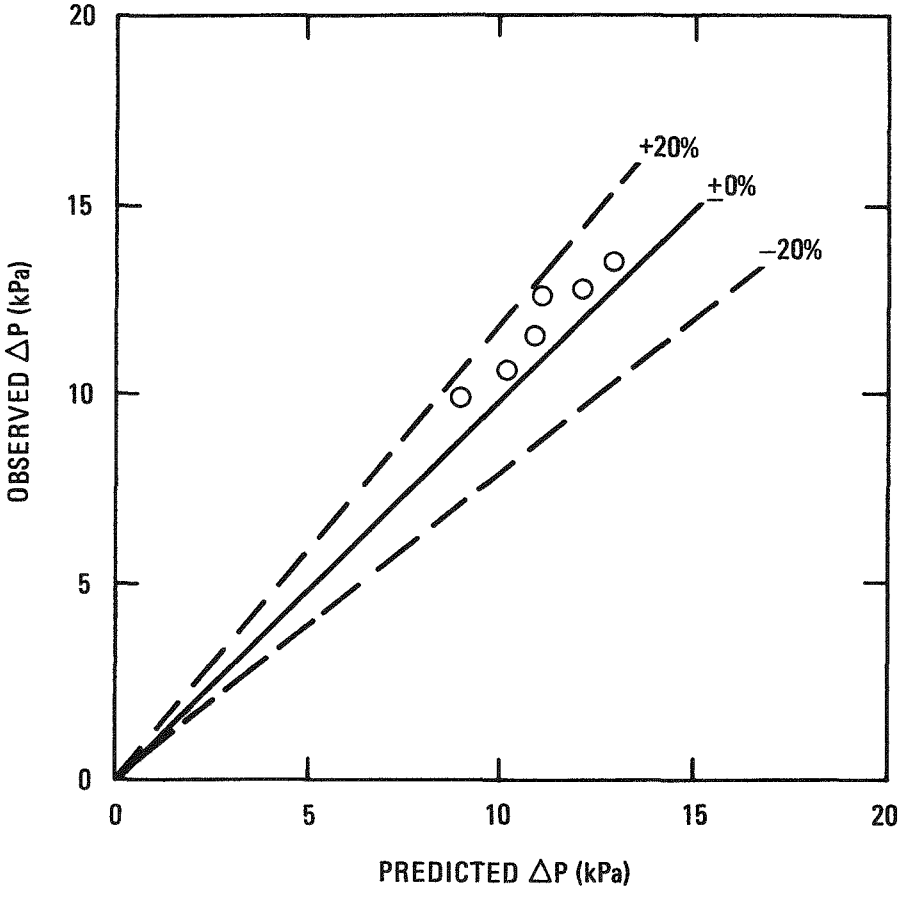

Fig.7-11. Observed versus predicted pressure drop results for the primary burner feed system using coated TRISO fuel particles fed at 0.27 kg/s

was successfully operated utilizing the variable position knifegate valve to control the feed rate. Simulated burner feed (fresh feed) was transported at ambient temperature and FSV TRISO particle burner product was conveyed both at 700°C and at ambient temperature. Particle breakage analyses for the hot and cold TRISO transport experiments are progressing in conjunction with primary burner post-test analyses.

Additional controls and instrumentation have been installed for operation of the variable position knifegate valve, eliminating the need for more than one operator during system operation. Collection of system pressure drop data and feed rate data will be attempted during subsequent primary burner tests.

7.3.1.2.5. Classifier Feed System (Subsystem No. 4). Work progressed on two portions of the classifier feed system, the primary burner product to classifier feed loop (Fig. 7-12) and the classifier recycle loop (Fig. 7-13). Uncoated fertile BISO fuel particles were used for feed material as pressure drop data were collected during pneumatic conveying across each transport loop.

Comparison of the measured data with the calculated results for the classifier feed loop is shown in Table 7-3 and Fig. 7-14. Likewise, results of the classifier recycle loop are shown in Table 7-4 and Fig. 7-15. The lesser accuracy in correlation between calculated and measured pressure drop results for the classifier feed loop is attributable to the small feed rates of 0.05 and 0.06 kg/s as compared to the 0.23 kg/s feed rate of the classifier recycle system.

7.3.1.2.6. Secondary Burner Removal System (Subsystem No. 6). Final qualification of the secondary burner removal system was accomplished during the quarter with the tests conducted on the BISO transport portion of subsystem No. 6. Uncoated BISO fuel particles were conveyed at a feed rate of 0.19 kg/s from the fertile classifier bunker to the secondary burner

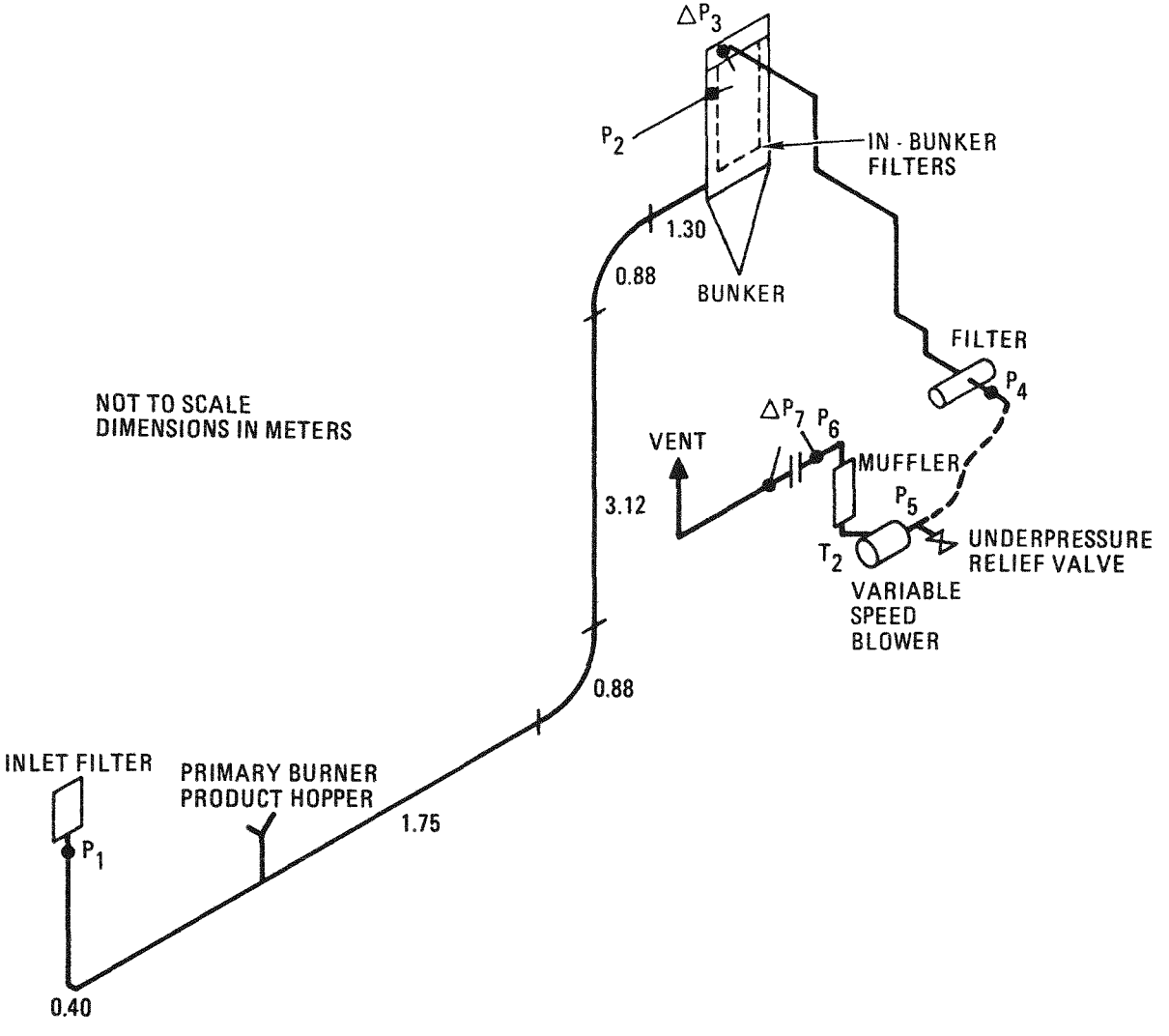

Fig. 7-12. Classifier feed system

NOT TO SCALE
DIMENSIONS IN METERS

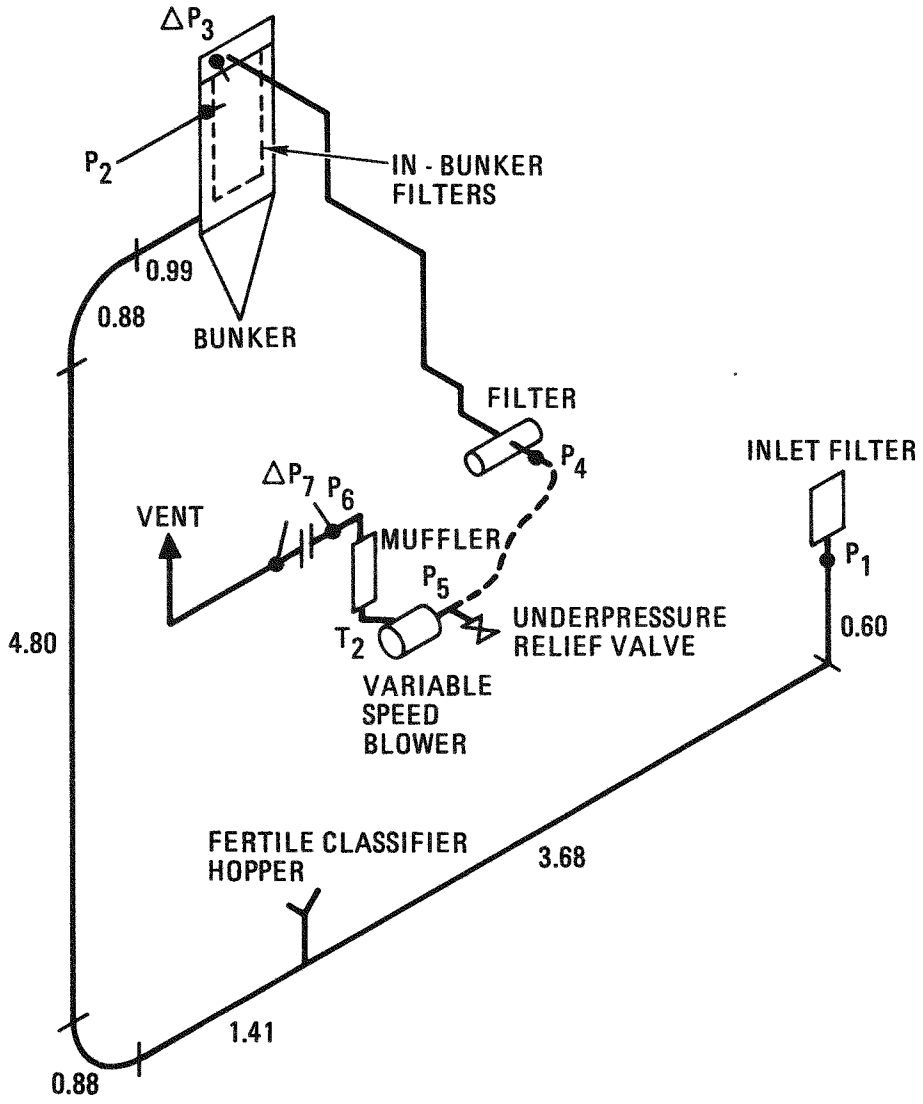

Fig. 7-13. Classifier recycle system

TABLE 7-3
PRESSURE DROPS FOR CONVEYING UNCOATED BISO FUEL PARTICLES
IN THE CLASSIFIER FEED SYSTEM

Mean Gas Velocity (m/s)	Calculated ΔP ($P_2 - P_1$) (kPa)	Observed ΔP ($P_2 - P_1$) (kPa)	Difference (Calc. - Obs.) (kPa)
28.8[a]	6.77	12.19	-5.42
26.4[a]	6.10	10.95	-4.85
24.3[a]	5.65	9.46	-3.81
22.2[a]	4.90	8.46	-3.56
21.6[b]	5.18	9.21	-4.03
19.3[b]	4.60	7.71	-3.11
17.0[b]	4.03	6.72	-2.69

[a] Feed rate = 0.05 kg/s.

[b] Feed rate = 0.06 kg/s.

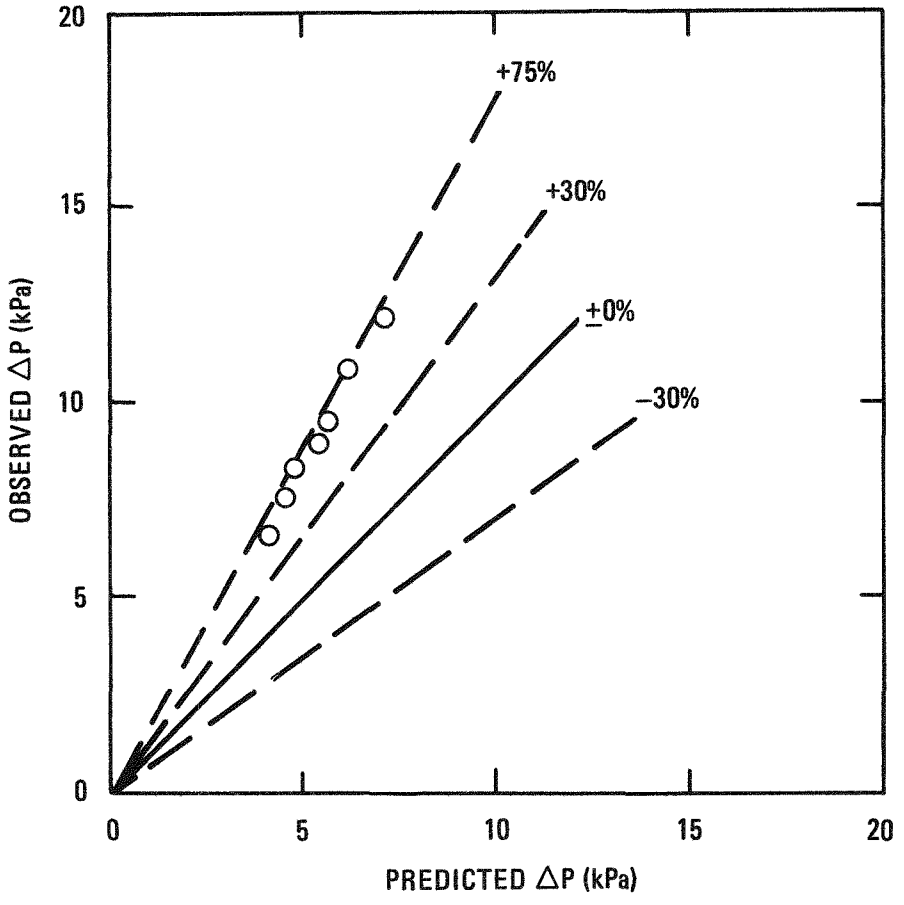

Fig. 7-14. Observed versus predicted pressure drop results for classifier feed system using uncoated BISO fuel particles fed at 0.05 kg/s

TABLE 7-4
PRESSURE DROPS FOR CONVEYING UNCOATED BISO FUEL PARTICLES
IN THE RECYCLE LOOP OF THE CLASSIFIER FEED SYSTEM

Mean Gas Velocity (m/s)	Calculated ΔP ($P_2 - P_1$) (kPa)	Observed ΔP ($P_2 - P_1$) (kPa)	Difference (Calc. - Obs.) (kPa)
26.1	15.95	21.15	-5.20
24.3	15.01	20.16	-5.15
22.2	13.98	18.66	-4.68
20.1	13.11	16.42	-3.31
20.4	8.51	6.22	+2.29

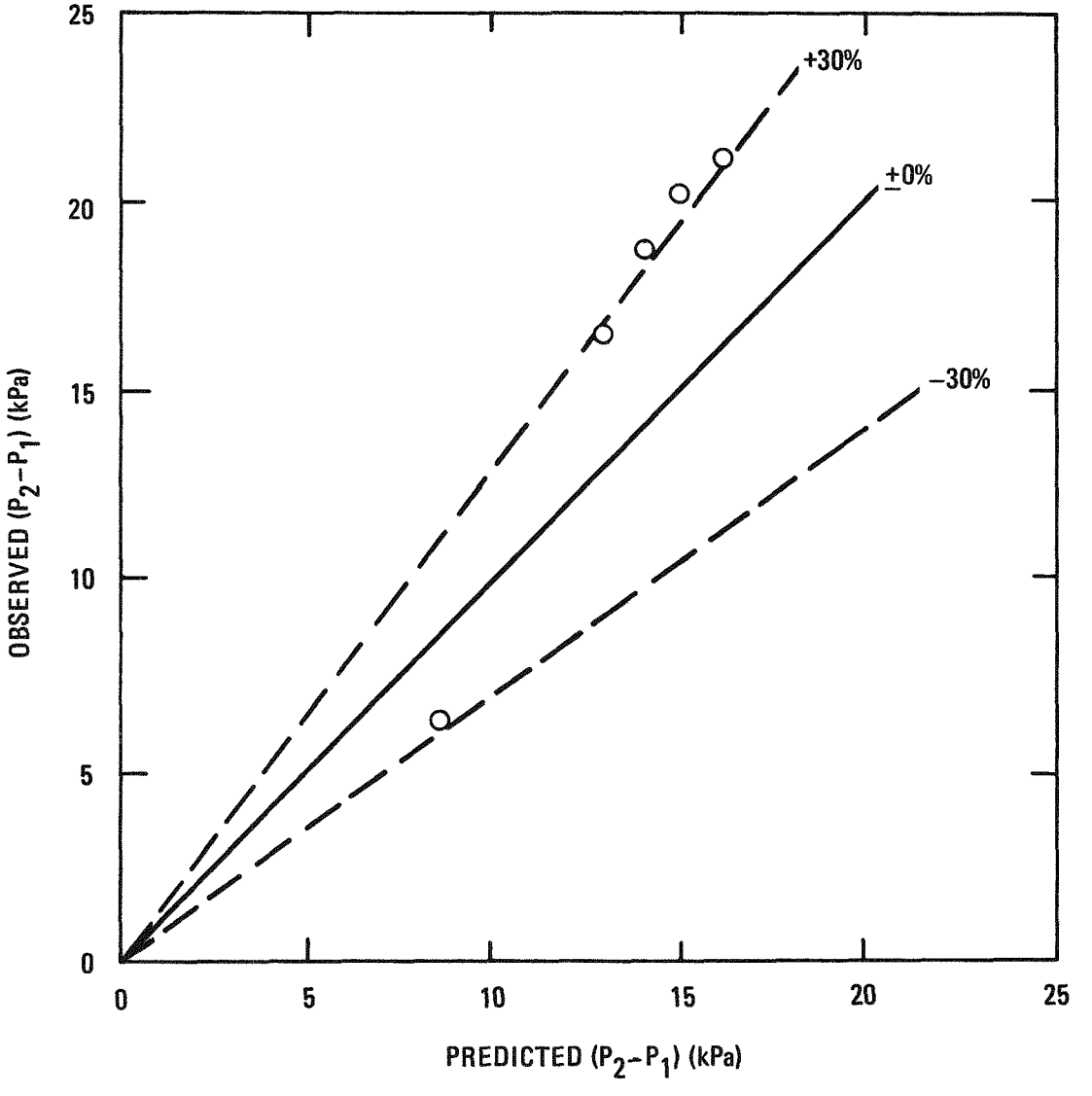

Fig. 7-15. Observed versus predicted pressure drop results for classifier recycle system using uncoated BISO fuel particles fed at 0.23 kg/s

product bunker (Fig. 7-16). Pressure drop data across the transport system were collected during the test and subsequently compared with predicted pressure drop results, as shown in Table 7-5 and Fig. 7-17.

REFERENCES

7-1. "Thorium Utilization Program Quarterly Progress Report for the Period Ending November 30, 1976," ERDA Report GA-A14214, General Atomic Company, December 30, 1976.

7-2. "Thorium Utilization Program Quarterly Progress Report for the Period Ending February 28, 1977," ERDA Report GA-A14304, General Atomic Company, March 1977.

7-3. Pneumatic Handling of Powdered Materials, Engineering Equipment Users Association (EEUA), Constable and Company, LTD., London, 1963.

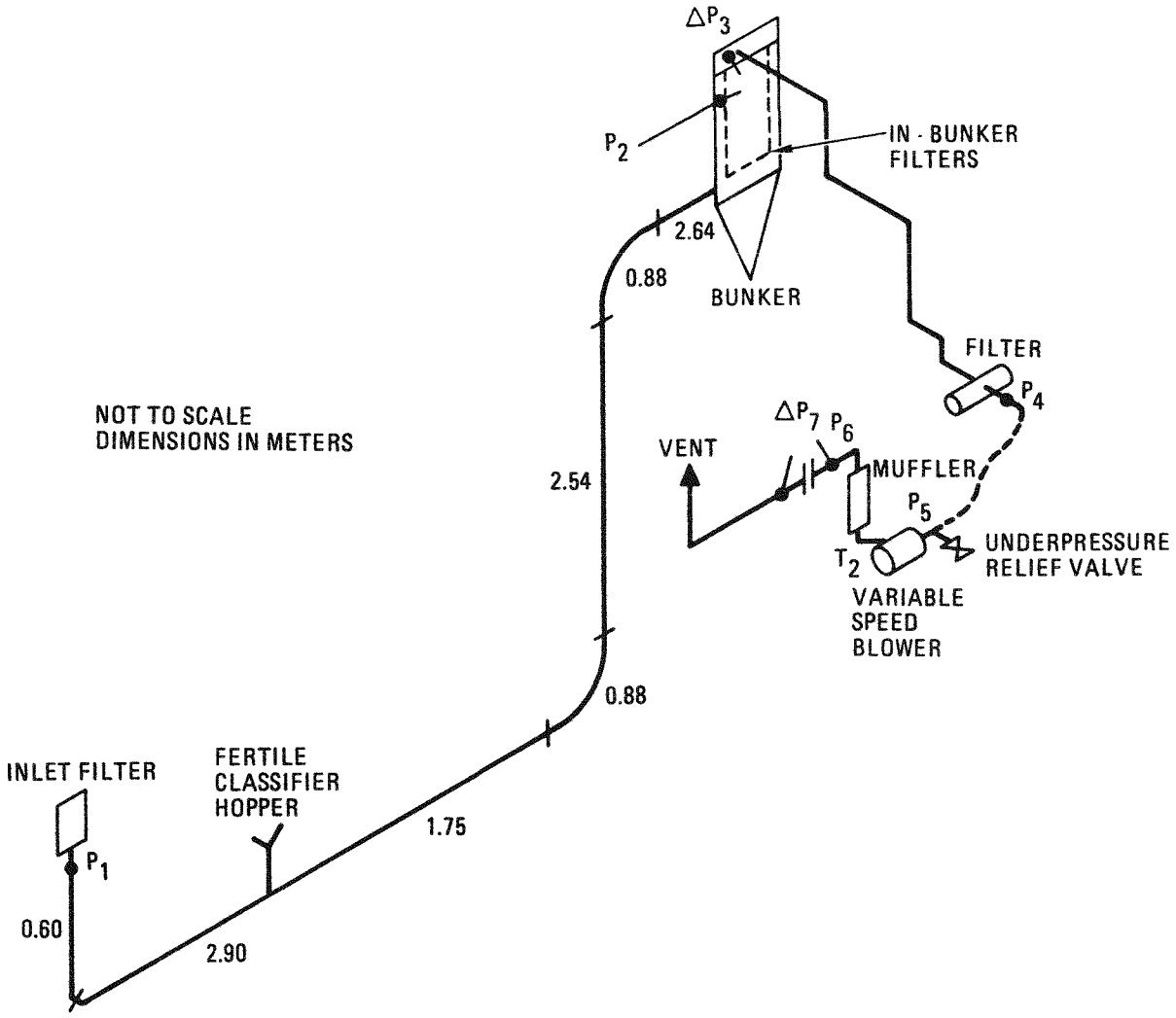

Fig. 7-16. BISO transport loop, secondary burner product removal system

TABLE 7-5
PRESSURE DROPS FOR CONVEYING UNCOATED BISO FUEL PARTICLES
IN THE BISO TRANSPORT LOOP OF THE SECONDARY
BURNER REMOVAL SYSTEM[a]

Mean Gas Velocity (m/s)	Calculated ΔP ($P_2 - P_1$) (kPa)	Observed ΔP ($P_2 - P_1$) (kPa)	Difference (Calc. - Obs.) (kPa)
27.5	14.86	15.93	-1.07
24.9	13.69	15.18	-1.49
22.5	12.91	13.44	-0.53
20.4	11.84	11.94	-0.10
18.1	11.00	10.70	+0.30

[a] Feed rate = 0.19 kg/s.

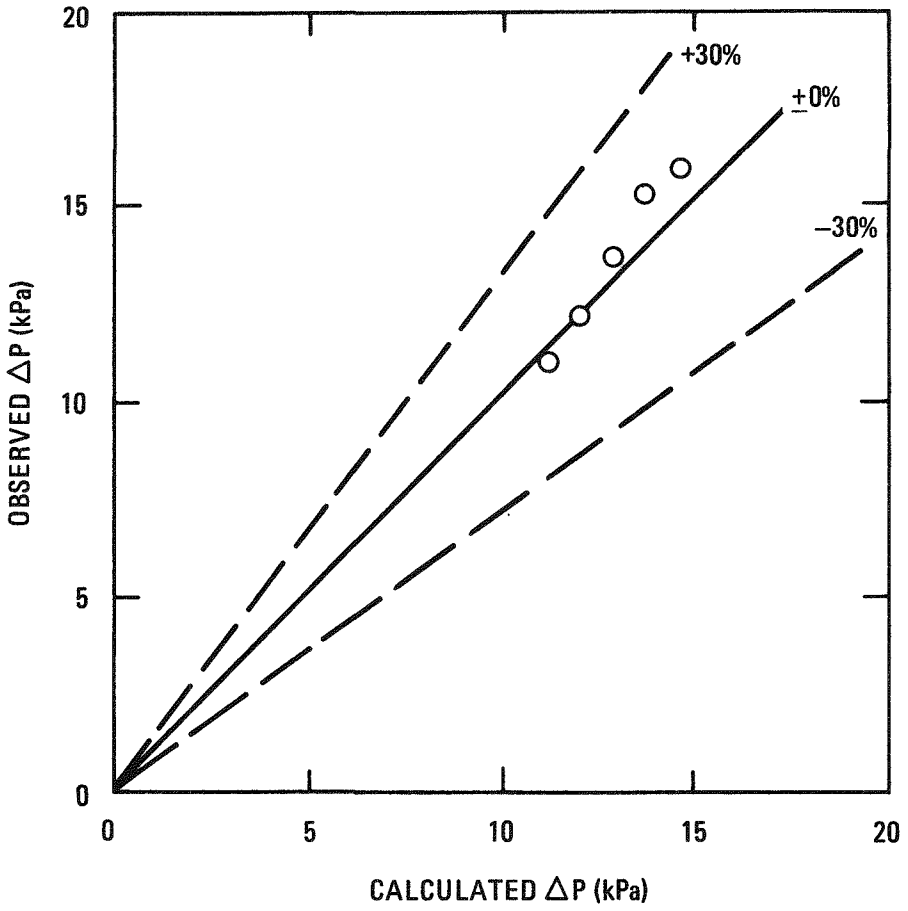

Fig. 7-17. Observed versus predicted pressure drop results for conveying uncoated BISO fuel particles in the BISO transport loop of the secondary burner removal system (feed rate = 0.19 kg/s)

8. GASEOUS EFFLUENT TREATMENT

8.1. SUMMARY

The conceptual design of an engineering-scale off-gas treatment system has begun. The system includes a CO/HT oxidizer, iodine adsorber, SO_2 adsorber, tritium/moisture removal unit, radon holdup bed, CO_2 adsorber, and NO_x converter, as well as their support and auxiliary systems such as heaters, coolers, condensers/demisters, and generators for iodine vapor and humidity. An engineering-scale semivolatile fission product removal unit and/or an electrostatic precipitator will be added to the system later after the completion of the developmental work on this unit at Idaho National Engineering Laboratory (INEL). The last step of the gaseous effluent treatment, i.e., the separation of krypton from CO_2 using the KALC process, is being developed at Oak Ridge National Laboratory (ORNL) on an engineering scale.

Due to the many similarities in the primary burner, secondary burner, and dissolver off-gas (BOG and DOG) treatment processes, most system component units will be shared, although each process will use a different process scheme. Process flow (PF) diagrams and preliminary control and instrumentation (C&I) diagrams on each (BOG and DOG) process have been completed, on which detailed piping and instrumentation (P&I) diagrams will be based.

The processes are to be monitored and controlled via various gas analyzers. Purchase orders for the gas analyzers and sampling system have been placed and the photoionization iodine detector and the gas chromatograph unit have already been received.

Molecular sieve adsorbents and catalysts have also been ordered after a preliminary sizing of the adsorption beds and catalytic reactors. A partial shipment of the molecular sieves has been received.

The conceptual design package including the design criteria (DC) and P&I diagrams will be completed next quarter, followed by initiation of a detailed design of an engineering-scale off-gas treatment system.

8.2. CONCEPTUAL DESIGN

The purpose of an engineering-scale off-gas treatment system is two-fold:

1. Establish the technical feasibility of the treatment process for desired decontamination factors on an engineering scale. The feasibility must be established on each component unit as well as on the integrated system.

2. Identify areas which need further development and obtain engineering data for scale-up, system improvement and process optimization, and demonstration of an integrated system operation.

The following design criteria have been established in order to achieve the goals stated above.

1. The overall treatment of the burner and the dissolver off-gas follows the process scheme discussed in an earlier quarterly report (Ref. 8-1).

2. The units are designed to operate on a cold engineering basis. Tracer level of radioactivity, however, can be employed in the test within the safety limits applicable to our pilot plant.

3. A test on an individual unit or on any combination of units is possible through the use of bypass lines. This will enable separate tests on burner off-gas (BOG) and dissolver off-gas (DOG) treatment processes in one off-gas treatment system.

4. The units are designed to give maximum flexibility in operating conditions (temperature, flow rate, concentrations, etc.).

5. Long-term tests on component units as well as on an integrated system with simulated BOG and DOG will precede the integration of the system with an existing engineering-scale burner or dissolver.

6. BOG treatment units are sized to handle the off-gas from one 0.20-m primary or secondary burner.

7. DOG treatment units are sized to handle the off-gas from the engineering-scale dissolver unit under design.

8. The process is monitored and controlled by in-line gas analyzers and temperature and flow sensors.

8.3. PROCESS FLOW DIAGRAMS

Three process flow diagrams (Figs. 8-1 through 8-3) have been developed for the burner and dissolver off-gas treatment processes. Figure 8-1 represents the treatment of primary burner off-gas. No separate process flow diagram has been developed for the secondary burner off-gas treatment since the process is essentially the same as that of the primary burner off-gas treatment except the iodine adsorber (and its auxiliaries) precede the CO/HT oxidizer unit. The establishment of the technical feasibility of PF565101 (Fig. 8-1) will automatically prove the alternate process for the secondary burner off-gas treatment, although the reverse is not true.

Two separate flow sheets (Figs. 8-2 and 8-3) have been developed for the dissolver off-gas treatment, in which the order of the iodine adsorber and the tritium/moisture removal unit is reversed. The feasibility of one process scheme does not automatically prove the other.

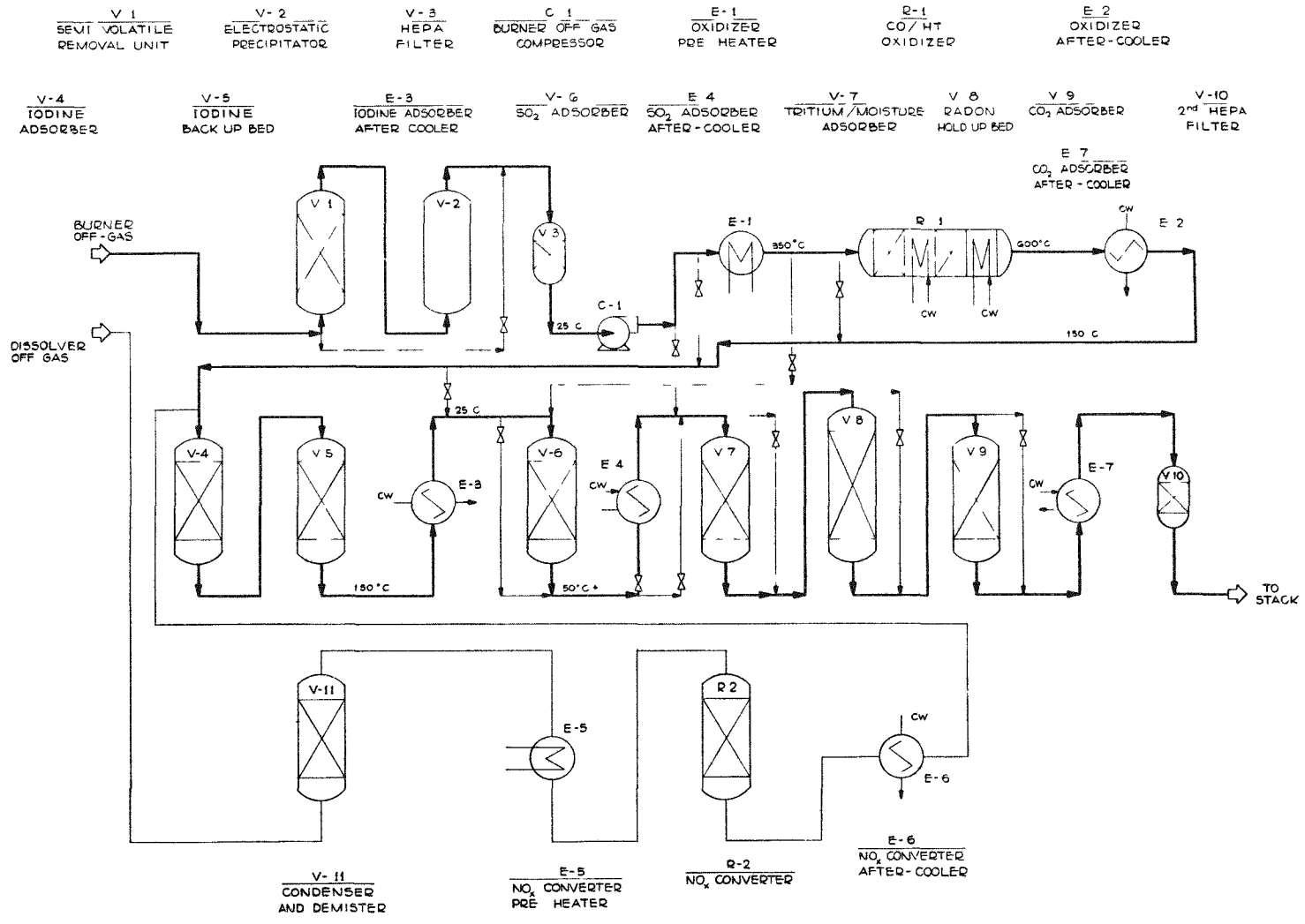

Fig. 8-1. Process flow diagram for burner off-gas

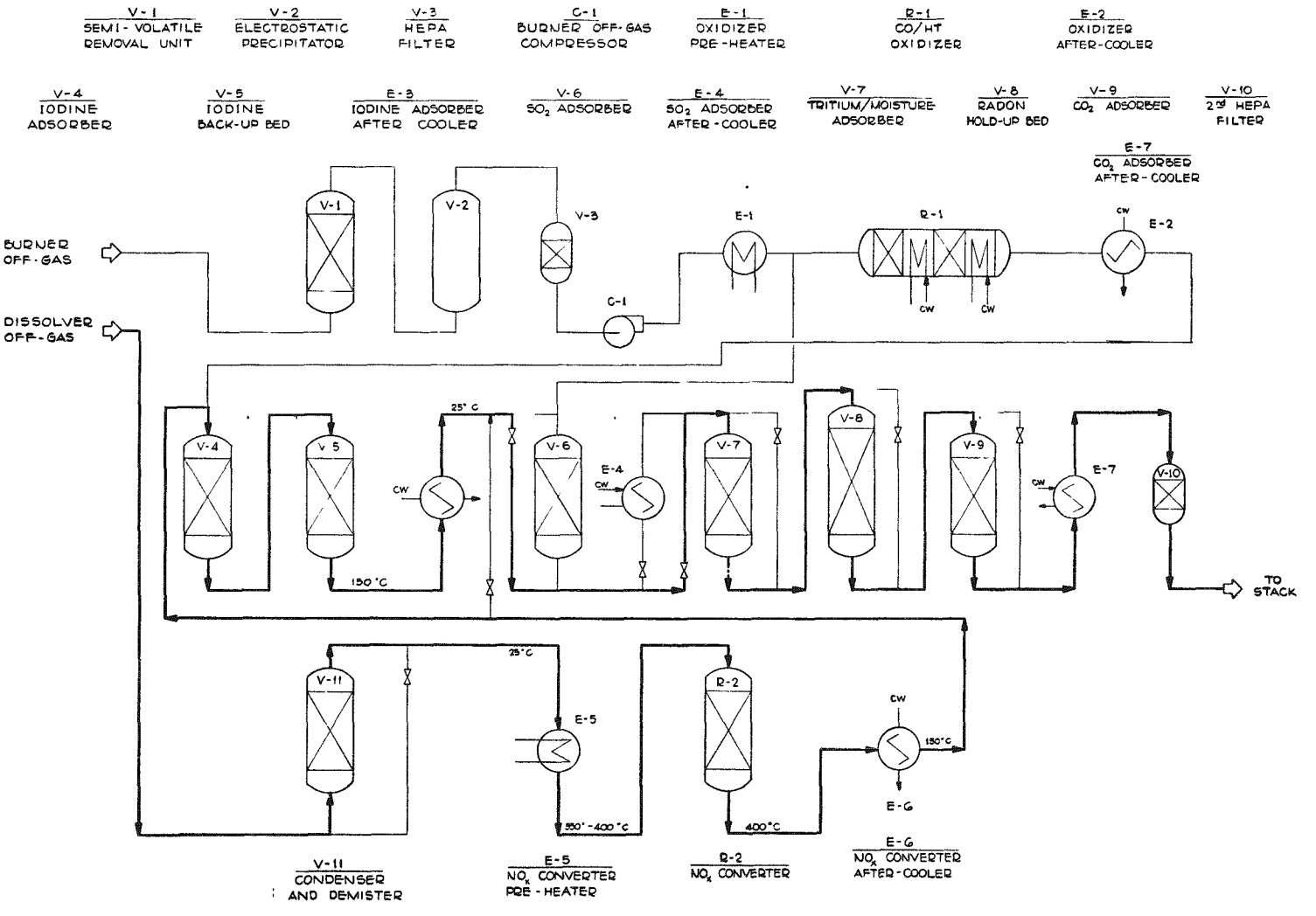

Fig. 8-2. Process flow diagram for dissolver off-gas

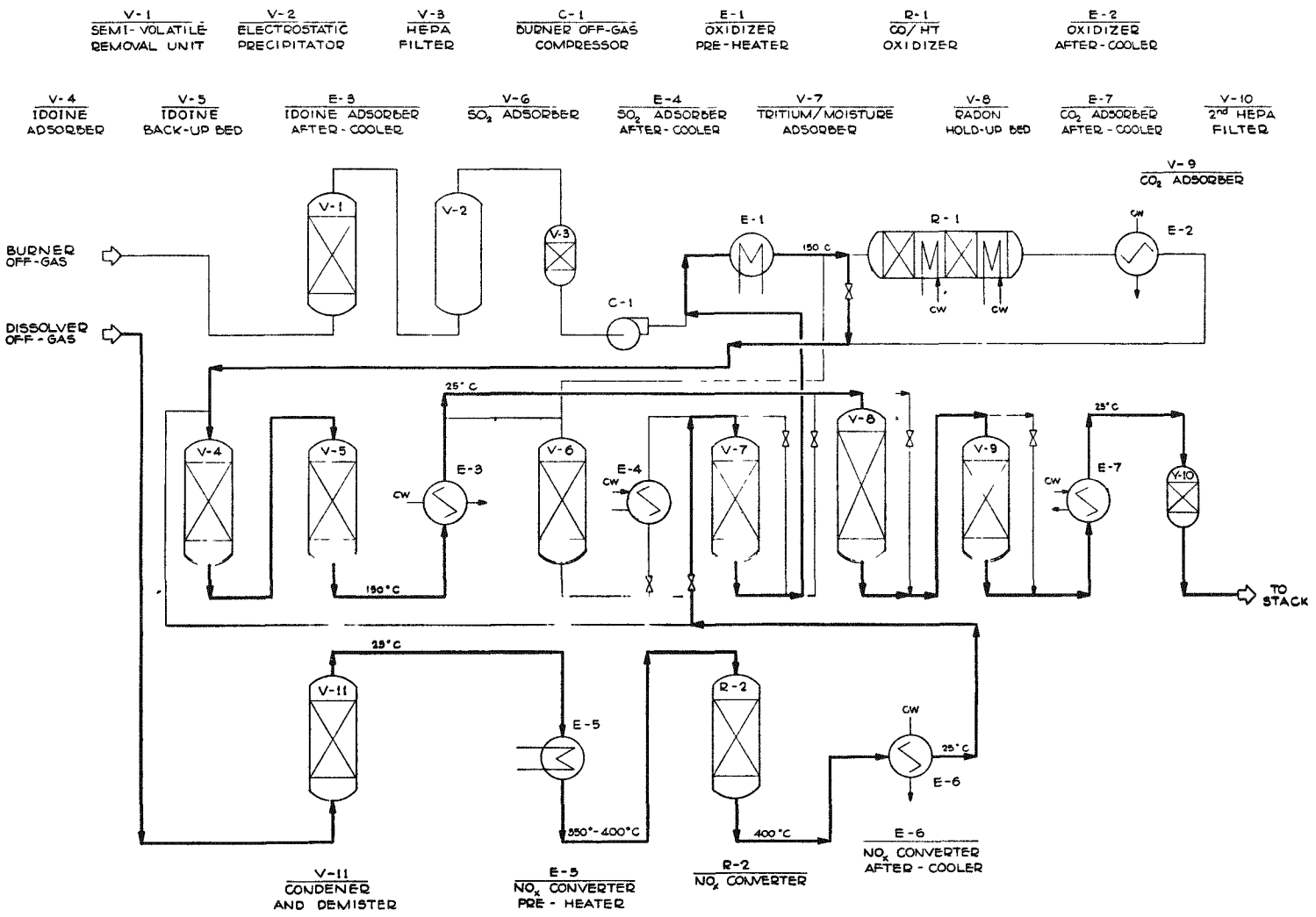

Fig. 8-3. Process flow diagram for dissolver off-gas (alternate)

The flow sheets show basically three trains. One train of equipment, consisting of iodine, SO_2, tritium, radon, and CO_2 adsorbers plus two heat exchangers, can be shared by both the BOG and DOG treatment processes.

A brief description of each flow diagram, using the main process lines to follow the flow of gas through the equipment, is presented below. A more detailed description of adsorbers and catalytic reactors has been presented previously (Ref. 8-2).

8.3.1. PF565101 - Burner Off-Gas

A flow of about 566 liters/min (20 SCFM) of burner off-gas will enter the system at 500°C. The process will take place in the following sequence:

V-1 Semivolatile Removal Unit

The semivolatile fission products such as ruthenium and cesium will plate out on a cold surface in this vessel. The exit temperature will be 100°C.

V-2 Electrostatic Precipitator

The negative electrode contained in this vessel will attract the positively charged ions so that the airborne nonvolatiles, as well as condensed semivolatiles, will be precipitated.

V-3 HEPA Filter No. 1

The high-efficiency particulate air filter will adsorb any particulates which escape from the preceding stages, in addition to removing from the stream other undesirable particles which might interfere with the CO oxidizer catalyst efficiency.

C-1 Burner Off-Gas Compressor

At this point the burner off-gas pressure will not be sufficiently high for the pressure drop encountered throughout the system. Therefore, C-1 will boost the pressure to a higher level. (This level is not yet known but will be available after a preliminary system design.)

E-1 Oxidizer Preheater

The gas stream will be heated by an electric coil to about 300°C.

R-1 CO/HT Oxidizer

The stream will then pass through this long horizontal complex of catalyst beds and interstage coolers, in which the carbon monoxide contents of the off-gas flow will react with added oxygen to produce carbon dioxide. The highly exothermic nature of the reaction might limit the percentage of CO reacted in each stage to 5%, requiring several stages with a final exit temperature of about 700°C.

E-2 Oxidizer After-Cooler

The gas will be cooled down to 150°C in this water cooler.

The following train, with the exception of the SO_2 adsorber and its after-cooler, will be common in all three schemes, sharing the burner off-gas as well as the dissolver off-gas treatment.

V-4 Iodine Adsorber

The gas will pass through a silver exchanged zeolite bed, leaving behind its iodine content. Due to its low concentration level,

the adsorption is essentially isothermal and will take place at 150°C.

V-5 Iodine Backup Bed

Any trace amount of iodine which might have survived the adsorption bed during breakthrough tests will be accumulated here so that the effluent stream is iodine free. This is also an isothermal process, maintained at 150°C.

E-3 Iodine Adsorber After-Cooler

The gas stream will be cooled down to 50°C by cooling water before entering the SO_2 removal step.

V-6 SO_2 Adsorber

The stream will carry up to 200 ppm SO_2, which will be adsorbed in this bed. The SO_2 adsorption is moderately exothermic; however, the low concentration level of SO_2 will not greatly raise the exit temperature.

E-4 SO_2 Adsorber After-Cooler

Exchanging its heat with cooling water, the gas stream will be cooled to 25°C (or lower if necessary) in E-4.

V-7 Tritium/Moisture Adsorber

Tritium, in the form of HTO, will be almost completely removed from the off-gas at this stage. This will be accomplished by diluting the HTO with 1000 times H_2O before adsorption. This is an isothermal process, which takes place on a molecular sieve adsorption bed.

V-8 Radon Holdup Bed

Radon removal will take place by adsorption on a mordenite molecular sieve bed that is long enough for the radon to decay to its nongaseous daughter products, which remain on the bed. The gas entering the bed should be free of moisture. The radon adsorption takes place at 250°.

V-9 CO_2 Adsorber

The removal of CO_2 will be carried out by a zeolite adsorption bed which can be regenerated. The purpose of this unit is to study CO_2 adsorption characteristics. CO_2 adsorption may be needed to concentrate the krypton stream after the KALC process or for the dissolver off-gas stream if CO_2 is used for sparging. This unit can be bypassed for normal test operation.

E-7 CO_2 Adsorber After-Cooler

The CO_2-free gas will be cooled to 25°C.

V-10 HEPA Filter No. 2

The final stage of the burner off-gas treatment will be in this filter. The last traces of the airborne contaminants will be removed from the stream before the KALC operation.

8.3.2. PF565201 - Dissolver Off-Gas

A gas stream of approximately 255 liters/min (9 SCFM), originated at the dissolvers, will enter the system by first passing through a condenser and demister at 25°C. The sequence of steps is as follows:

V-11 Condenser and Demister

Dissolver off-gas will enter the condenser in which the water vapor carried by the gas will be condensed and removed by a demister, or wire mesh, isothermally at 25°C.

E-5 NO_x Converter Preheater

An electric heater will heat the stream to about 350°C to prepare for NO_x conversion.

R-2 NO_x Converter

The NO_x content of the gas stream will react with the injected NH_3 to produce nitrogen and water. The catalyst will be zeolite. The conversion will be carried out at 350° to 400°C.

E-6 NO_x Converter After-Cooler

The conversion products will be cooled to 150°C using cooling water.

V-4 Iodine Adsorber

Same as PF565101.

V-5 Iodine Backup Bed

Same as PF565101.

E-3 Iodine Adsorber After-Cooler

Same as PF565101.

V-7 Tritium/Moisture Adsorber

Same as PF565101.

The tritium content of the dissolver off-gas is expected to be negligible. Because of the high moisture content of this stream, a commercial dryer can also be utilized.

V-8 Radon Holdup Bed

Same as PF565101.

V-9 CO_2 Adsorber

Same as PF565101.

E-7 CO_2 Adsorber After-Cooler

Same as PF565101.

V-10 HEPA Filter No. 2

Same as PF565101.

8.3.3. PF565202 - Dissolver Off-Gas (Alternate)

This is an alternate process for the treatment of the dissolver off-gas, with the same inlet conditions as PF565201. This method of treatment is the same as in PF565201 except for the NO_x converter effluent, which will be cooled to a lower temperature (25°C versus 150°C for PF565201), and demoisturization of the stream prior to iodine bed adsorption. This process will be selected only if the effectiveness of the catalyst bed in V-4

is noticeably diminished by the moisture content of the stream. The sequence for this process is as follows:

V-11 Condenser and Demister

Same as PF565201.

E-5 NO_x Converter Preheater

Same as PF565201.

R-2 NO_x Converter

Same as PF565201.

E-6 NO_x Converter After-Cooler

Same as PF565201 except for the outlet temperature of 25°C (versus 150°C in PF565201).

V-7 Tritium/Moixture Adsorber

Same as PF565201.

E-1 Oxidizer Preheater

This preheater will operate as an iodine adsorber preheater and will heat the demoisturized gas stream to 150°C before the gas reaches V-4, the iodine adsorber.

V-4 Iodine Adsorber

Same as PF565201.

V-5 Iodine Backup Bed

Same as PF565201.

E-3 Iodine Adsorber After-Cooler

Same as PF565201.

V-8 Radon Holdup Bed

Same as PF565201.

V-9 CO_2 Adsorber

Same as PF565201.

E-7 CO_2 Adsorber After-Cooler

Same as PF565201.

V-10 HEPA Filter No. 2

Same as PF565201.

REFERENCES

8-1. "Thorium Utilization Program Quarterly Progress Report for the Period Ending November 30, 1976," ERDA Report GA-A14214, General Atomic Company, December 1976.

8-2. "Thorium Utilization Program Quarterly Progress Report for the Period Ending August 31, 1976," ERDA Report GA-A14085, General Atomic Company, September 1976.

9. PLANT MANAGEMENT

9.1. SUMMARY

Availability requirements for major dry head-end systems were calculated as a function of reliability and maintenance downtime. Similar calculations were initiated for major wet head-end systems. The HET conceptual design work was completed, and the Conceptual Design Report sections assigned to GA were completed. HET technical review meetings were held during the quarter to discuss facility and equipment arrangement and design, Conceptual Design Report completion, cost estimating, and future program assignments.

9.2. MAINTAINABILITY AND RELIABILITY

9.2.1. Introduction

Work on Phase I of this study was initiated in January 1977. The objective of the Phase I study is to establish preliminary availability allocation requirements for the HRDF reprocessing facility and its major process systems, based on the HRDF recycle plant overall availability requirement. A specific near-term objective is to develop a methodology for establishing availability requirements of major systems.

During the preceding quarter, three assumed cases of HRDF dry head-end system capacities and an associated number of required parallel systems were defined, and the corresponding case functional diagrams and system operating profiles were prepared.

9.2.2. Activity

The availability requirements for major equipment systems in the dry head-end were calculated for an assumed level of 100% reliability and then were plotted as a function of probable upper and lower bounds of system reliability and maintenance downtime.

The methodology for establishing likely availability allocation requirement ranges was then extended to wet head-end systems. Functional diagrams and system operating profiles were prepared, and wet head-end system capacity data were generated. The system availability requirements were then calculated for an assumed level of 100% reliability.

Further effort on this study was deferred to provide personnel support to the commercialization study.

9.3. HOT ENGINEERING TEST REPROCESSING PRELIMINARY DESIGN

9.3.1. HET Project

All sections of Volume I, "Reprocessing Facility," of the Conceptual Design Report under GA responsibility have been completed. These sections include:

3.4. Anticipated Operating Plans.

4.0. Principal Safety, Fire, and Health Hazards.

12.3. Primary Burning System - System 1200.

12.4. Particle Classification and Material Handling System - System 1300.

12.5. Particle Crushing and Secondary Burning System - System 1400.

12.6. Dissolution and Feed Adjustment System - System 1500.

12.7. Solvent Extraction System - System 1800.

12.10. Intersystems Material Handling.

All of the above Conceptual Design Report sections were submitted for the 90% level document on schedule, all review comments have been acted upon, and the sections are in the process of publication.

During the present reporting period, the 60% and 90% level technical review meetings, on February 23-25 and April 12-13, 1977, respectively, were attended by project engineers. Mechanical equipment and arrangement drawings, facility design and mechanical specialties, Conceptual Design Report text, and the Conceptual Design Report cost estimate were reviewed. All action items arising from the technical review meetings were completed and have been incorporated into the appropriate Conceptual Design Report volumes for publication.

On April 15 and 18, 1977, GA project members met with the HETP Project Leader and Project Engineer to discuss GA tasks during the balance of FY-77 and participation in the HETF detail design effort scheduled to begin in FY-78. Tasks were tenatively agreed upon for FY-77. A GA proposal to participate as the principal contractor for HETF System 1200 - Primary Burning, System 1300 - Particle Classification and Material Handling, and System 1400 - Particle Crushing and Secondary Burning was presented and taken under consideration by the ORNL project members. A decision on the FY-78 proposal will be made after current ERDA programmatic reviews regarding the Thorium Utilization Program are resolved.

9.3.2. HETE - Reprocessing Systems

Mechanical equipment design and arrangement drawings and piping and instrumentation drawings were completed for all GA systems. A total of 53 mechanical drawings and 19 piping and instrumentation drawings were developed. The drawings were reviewed as part of the 60% and 90% technical review meetings, final action was completed on all comments, and the drawings have been transmitted for publication as part of the Reprocessing Facility Conceptual Design Report.

9.4. HRDF REMOTE MAINTENANCE

9.4.1. Introduction

During the quarter, study activities were continued toward establishing overall systems descriptions and design criteria for an integrated remote maintenance system for the HRDF-Reprocessing Head-End and Solvent Extraction Systems.

9.4.2. Activity

The preliminary draft of the head-end maintenance study report was reviewed internally. Efforts are now being directed toward final rewrite of the draft, with emphasis on developing detailed maintenance strategies. These are being formulated based on a compilation of the previous maintenance experiences which have proven successful. Specific criteria are also being established to provide guidance in determining plant layout, equipment arrangement, and configurations consistent with the maintenance strategy.

10. HET FUEL SHIPPING

10.1. SUMMARY

During the quarter, the HETP radioactive feed material shipping equipment Conceptual Design Report, which details the design effort, was published (Ref. 10-1). Related activities included development of detailed costs for use in conjunction with the HETP conceptual design cost estimate and identification of all system interfaces.

10.2. HETP SHIPPING EQUIPMENT CONCEPTUAL DESIGN EVALUATION

Initial activity involved selection of the basic shipping system based on its availability, suitability, licensability, and cost. After establishing the operational criteria, various candidate shipping casks were surveyed to determine their suitability. Because of the long-term nature of this program (availability not assured for long-term use) and considerations of cost associated with major facility modifications, it was decided to limit the final selection to three candidates. These were the FSV-1 cask, which was designed to transport the FSV fuel between the reactor and the Irradiated Fuel Storage Facility (IFSF), the PB-2 cask, which was designed to transport the Peach Bottom fuel between the Peach Bottom reactor and the IFSF, and a new cask specifically designed for HET.

Each of these systems was investigated in a systematic manner by identifying the important characteristics required, assigning weighted values to them based on their relative importance, assigning values to performance, and then evaluating the performance of the system against these characteristics. In this manner the cask system was "scored" based on its ability to perform within the given constraints. Table 10-1 is a

TABLE 10-1
WEIGHTED DESIRABILITY MATRIX

Candidate Shipping System	Availability	Suitability		Licensability	Cost					Σ
		Operation	Turnaround Time		Fuel Storage	Support Equip.	Operation	Lease	Buy	
FSV (Two Casks)	0.0	0.0	0.14	0.0	0.05	0.25	0.0	0.0		0.44
Peach Bottom	0.08	0.04	0.0	0.09	0.0	0.0	0.20	0.30		0.71
New Cask	0.0	0.4	0.14	0.0	0.0	0.0	0.0	0.30		0.48

summary of the calculations used to select the cask system. The results indicated that the PB-2 cask rated highest, and it was therefore chosen as the reference system for HET.

Once the basic system was chosen, the studies were directed toward definition of the system configuration. The approach chosen was to establish operational constraints and to evaluate the suitability of the various options by assigning weighted probabilities to each choice. In addition to the canister choice, selection of a single-element versus a multiple-element canister was made so that appropriate optimization of the system could be considered. A decision tree (Fig. 10-1) was prepared which shows that the cumulative probability (ranking preference) is highest for the single-element disposable canister with a welded closure. (This line has been darkened for clarity.) This configuration was then reviewed with the responsible interface organizations, both at the Idaho Chemical Processing Plant (ICPP) and ORNL, to determine if it is compatible with current overall system designs. Both organizations concurred with the proposed approach, and it was therefore adopted as the reference shipping system.

This system, which utilizes the PB-2 cask as the basic shipping vehicle, consists of four single-element carbon steel canisters (Fig. 10-2) approximately 0.46 m (18 in.) in diameter by 0.80 m (31.5 in.) long which are placed in the cavity. These canisters, which will be loaded in the IFSF, will utilize a welded closure and will form the primary containment for the shipping system. The cavity houses a tubular support assembly (Fig. 10-3) which provides support for the four loaded canisters when positioned within the cavity as shown in Fig. 10-4. Each end of the cask cavity is provided with an impact limiter assembly which protects the canisters during transport and in the event of exposure to the hypothetical accident conditions.

The original safety analysis report (SAR) for the PB-2 cask was reviewed to identify the original design basis used to license the cask. Once this was established, a detailed comparison was made between this

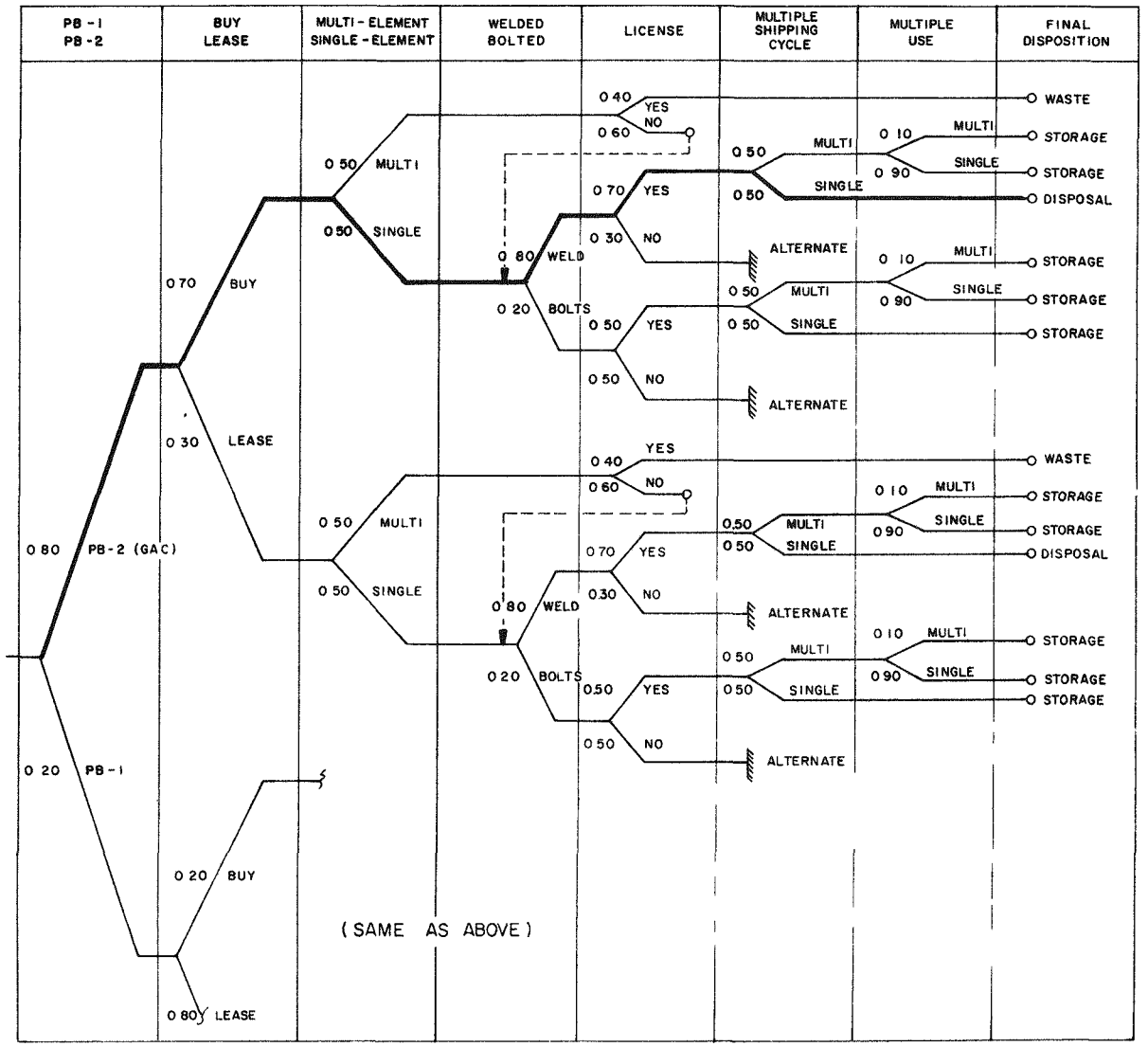

Fig. 10-1. Decision tree

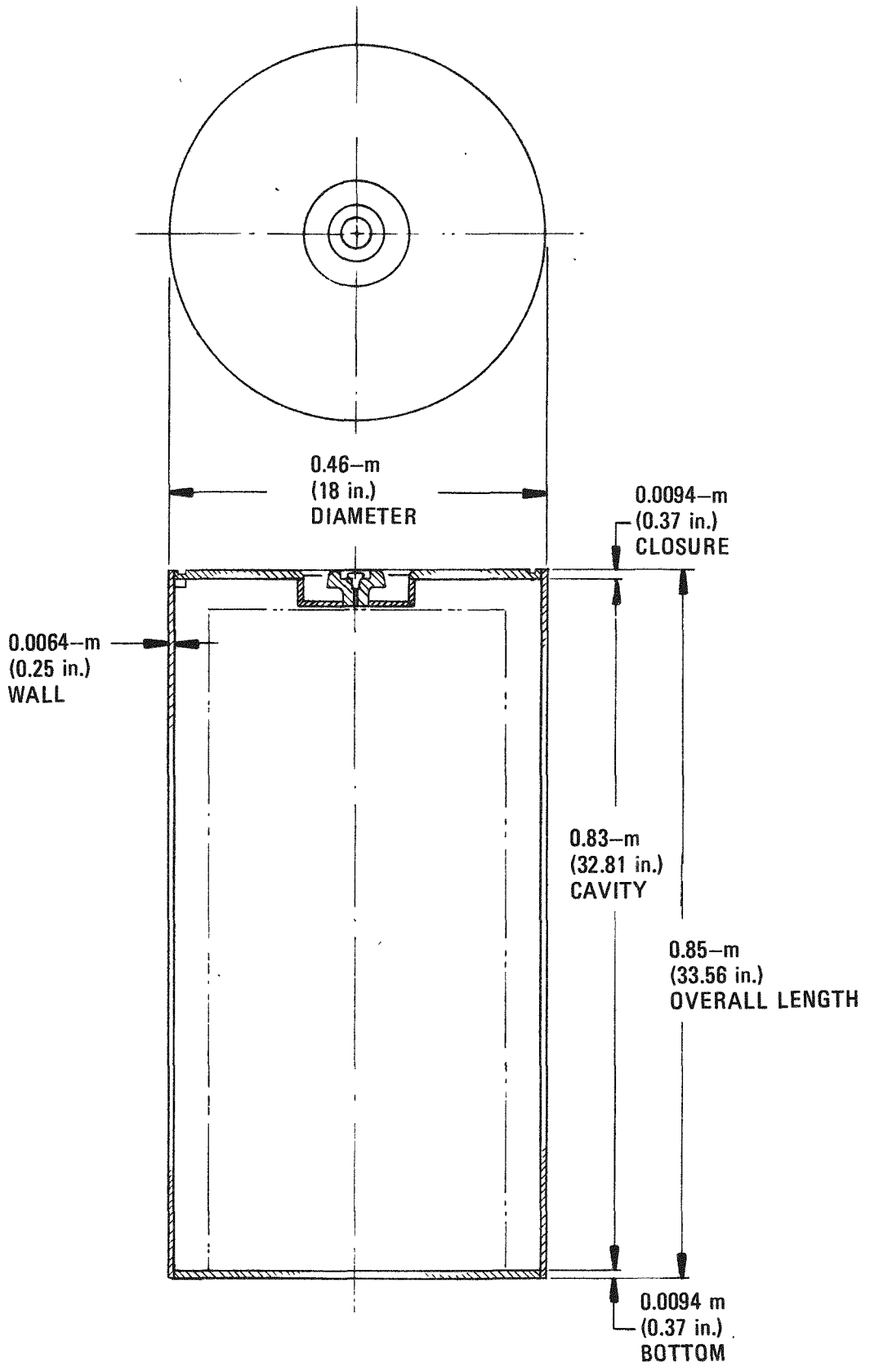

Fig. 10-2. Disposable fuel element shipping canister

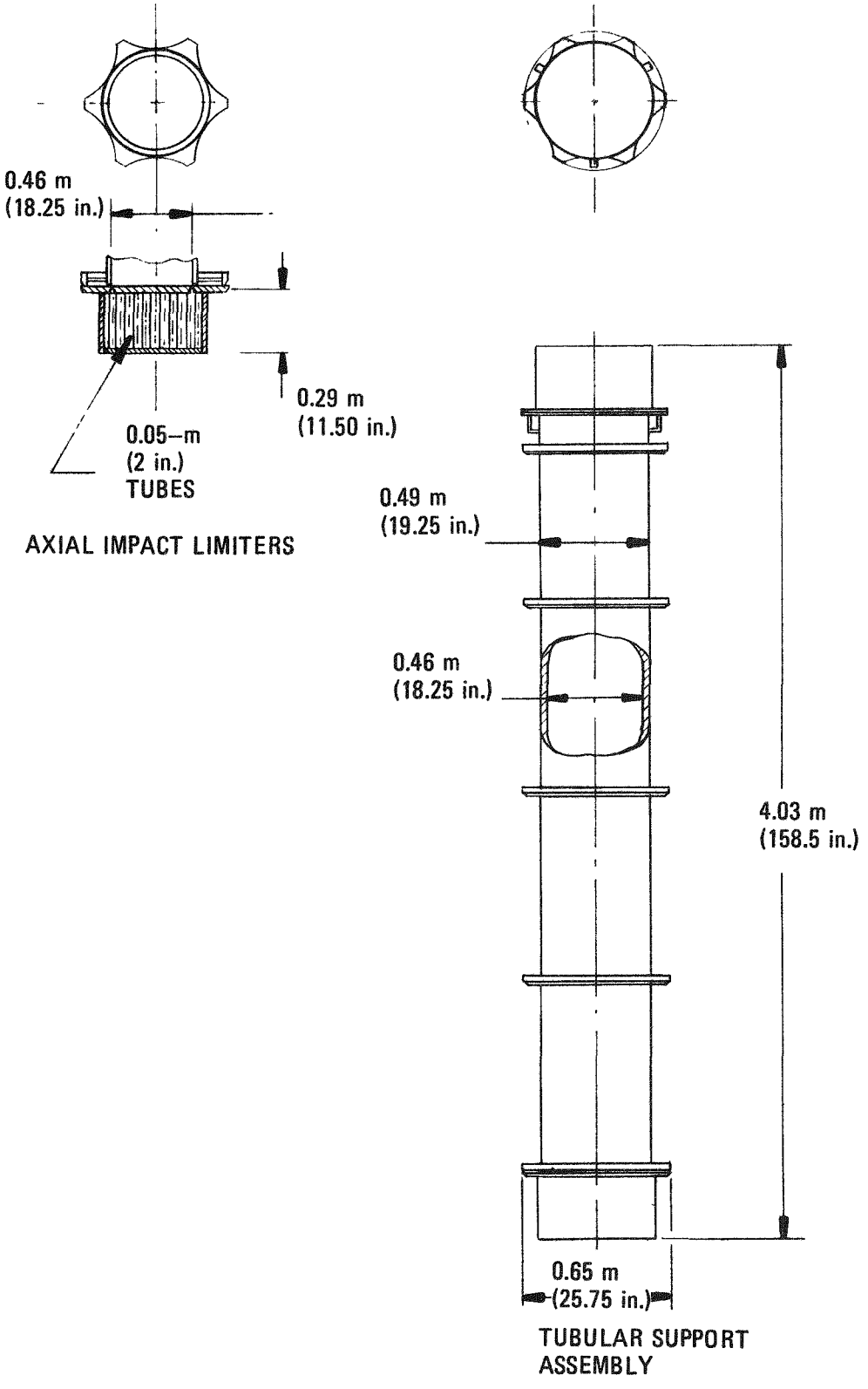

Fig. 10-3. Cask internal adapters

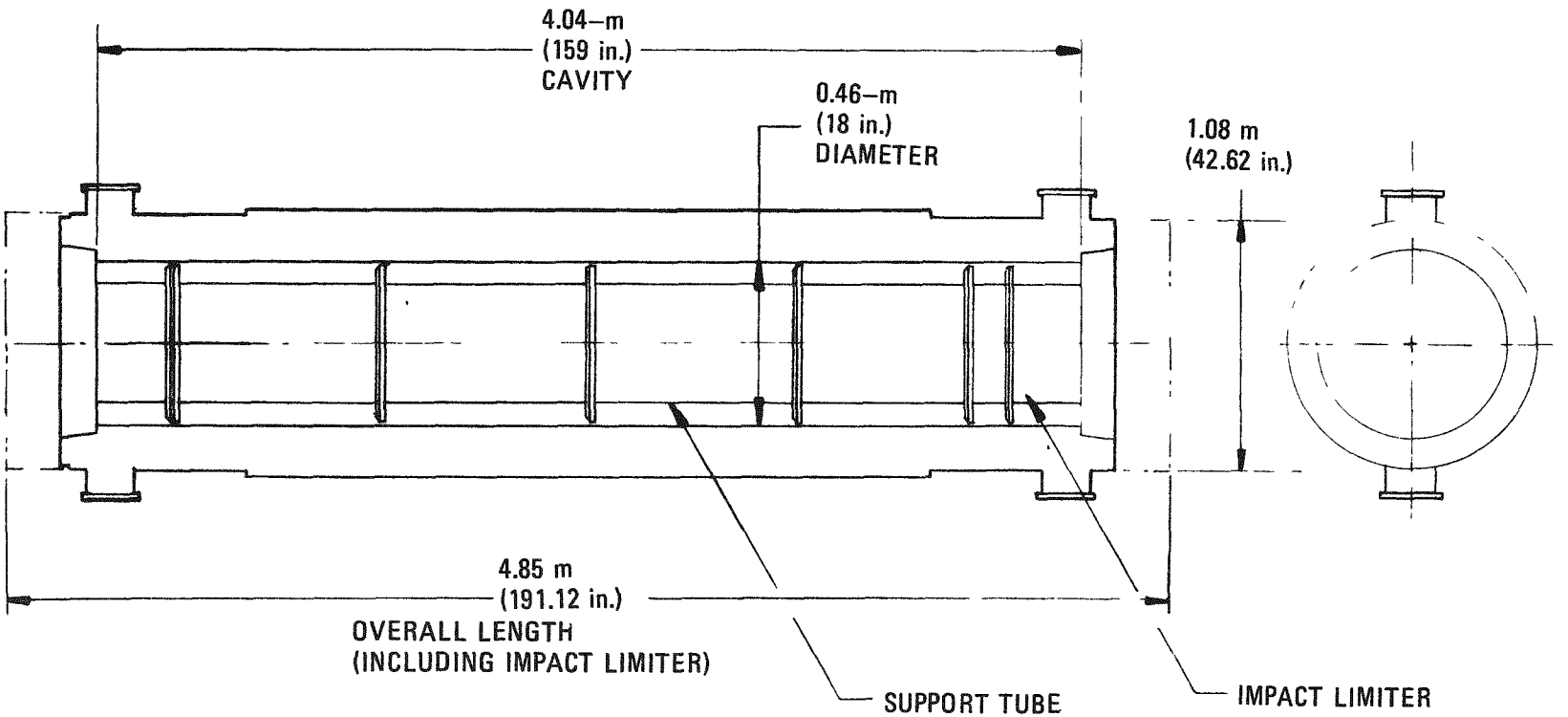

Fig. 10-4. PB-2 shipping cask, HETP fuel shipping configuration

design and the new configurations to determine the impact on licensibility of the reference shipping system. It was judged that the reference system would not present any significant relicensing problems.

In conjunction with the licensing assessment, the system operation was outlined in detail with specific attention to interface definition and identification of special support equipment. The operations at the ICPP are depicted in Figs. 10-5 and 10-6, and the canister unloading operations at ORNL (Building 3026D) are depicted in Fig. 10-7. Detailed lists of operations were provided along with lists of special tools or support equipment required at each site. Two specific areas of notable importance are the welding equipment required to close the canisters at the ICPP and the saw or cutting equipment required to open the canisters at ORNL. In both cases, outside equipment suppliers were contacted to determine the feasibility of these operations with regard to using equipment considered to be generally available in the commercial market. Equipment was found to be available in both cases. However, it will require some modification to adapt it to a remote cell environment.

Future design activities will be performed consistent with the requirements of the schedule shown in Fig. 10-8. This schedule is predicted upon having shipping equipment in place by the third quarter of 1982.

REFERENCE

10-1. Burgoyne, R. M., and E. J. Steeger, "Conceptual Design Report for HETP Radioactive Feed Material Shipping Equipment," ERDA Report GA-A14353, General Atomic Company, April 1977.

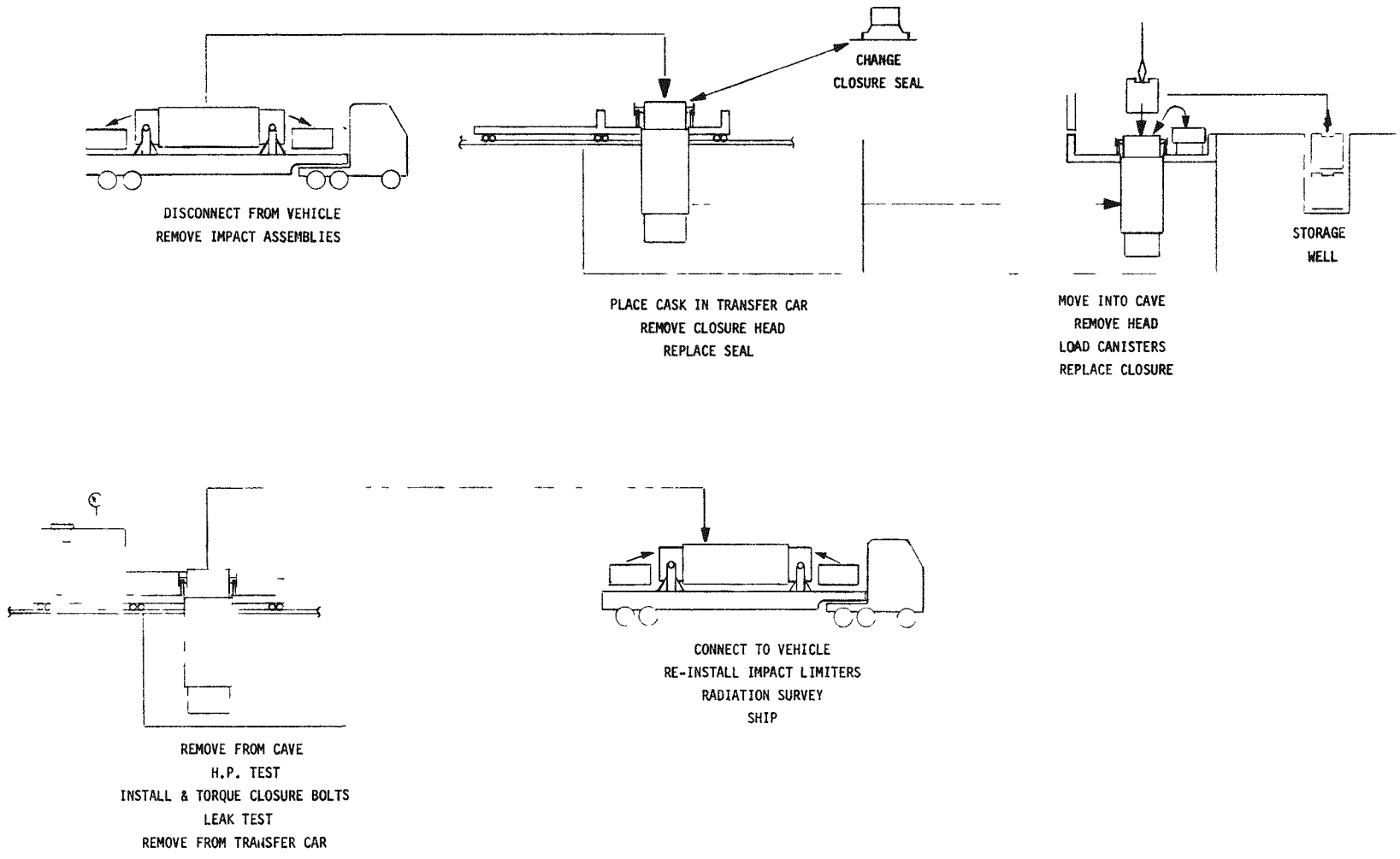

Fig. 10-5. Cask loading at ICPP

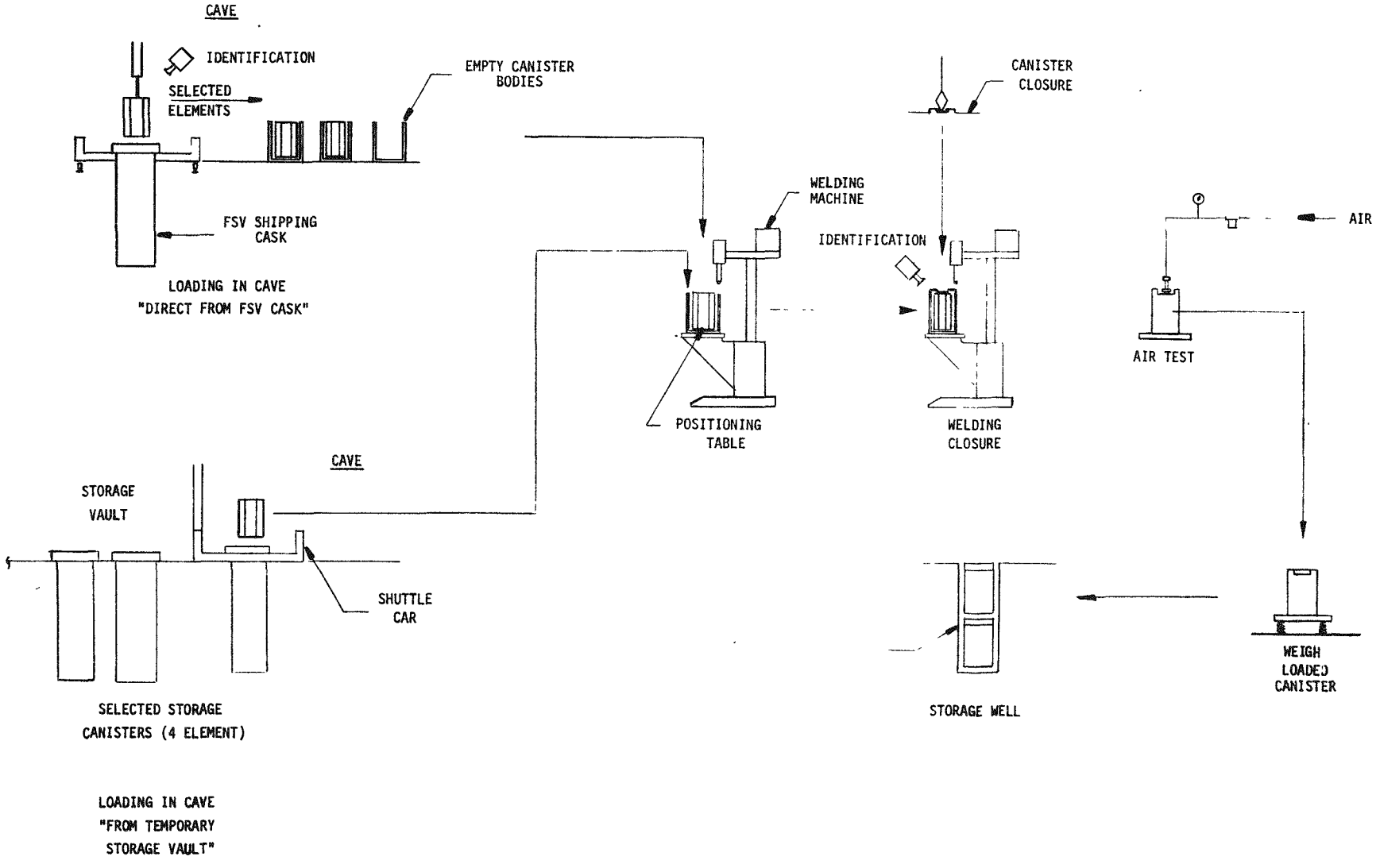

Fig. 10-6. Canister loading at ICPP

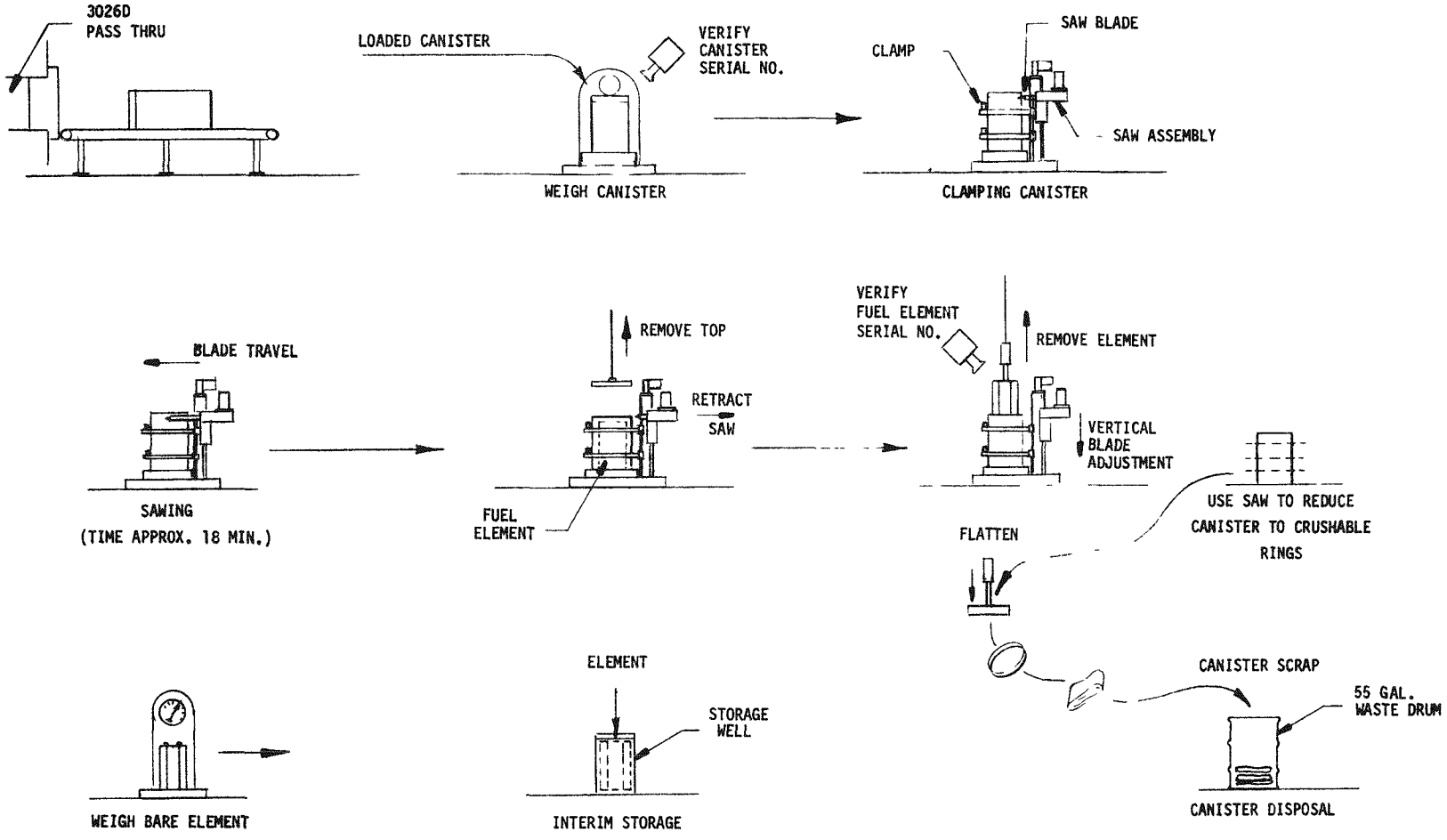

Fig. 10-7. Canister opening at ORNL Building 3026D

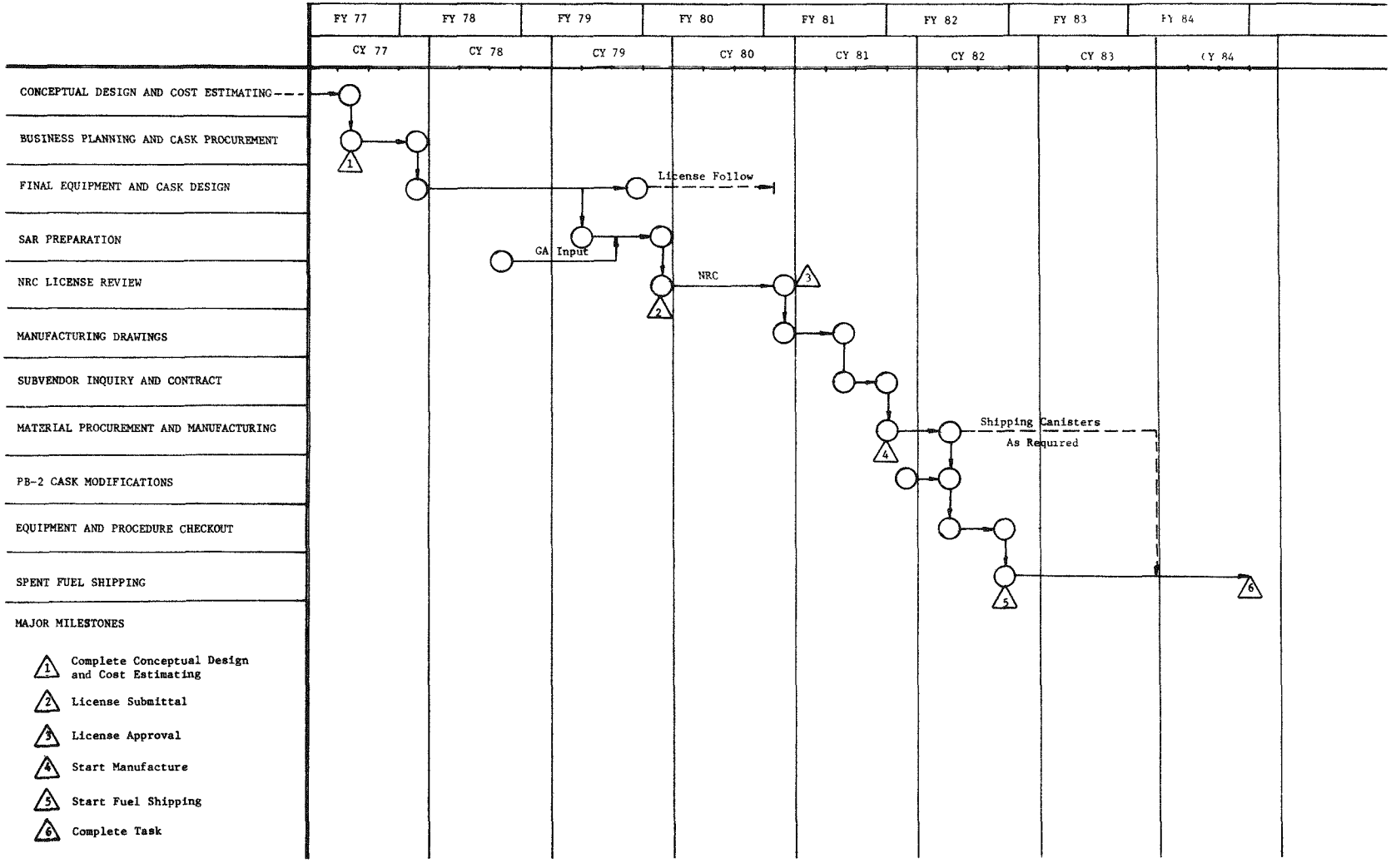

Fig. 10-8. HET shipping development schedule

11. HTGR RECYCLE DEMONSTRATION FACILITY

11.1. SUMMARY

Draft copies of the head-end process and off-gas treatment system sections of a topical report covering the Reprocessing Flowsheet Review and Material Balance Study were transmitted to ORNL for use in their commercialization study activity. HTGR spent fuel element impurities were compared with specifications for impurities in the feed to the resin-loading process in the Refabrication Plant of the HRDF, and required decontamination factors were estimated. A GASP IV simulation language package was purchased for comparison with the SIMSCRIPT language package as part of the reprocessing plant simulation study. Information was provided to ORNL, RAMCO, and cognizant GA personnel as part of HTGR commercialization studies.

11.2. REPROCESSING FLOWSHEET REVIEW AND MATERIAL BALANCE

11.2.1. Introduction

This study is part of the continuing technology assessment to ensure that (1) the proposed HRDF flowsheet incorporates recent technology development improvements and new design data, and (2) supporting technical programs are apprised of flowsheet design issues requiring resolution. The updated reprocessing flowsheet is intended to become an approved baseline document for HRDF design definition and to provide guidance for technical development activities.

During the preceeding quarter, topical report drafts covering the flowsheet review and material balances for the head-end process and off-gas treatment systems were completed and circulated for technical review.

11.2.2. Activity

During this reporting period, technical review comments were resolved and incorporated into the report drafts described above. Following management review and approval, draft copies of the head-end process and off-gas treatment system sections of the topical reports were transmitted to ORNL for use in their commercialization study.

11.3. REPROCESSING YIELDS AND MATERIAL THROUGHPUT

11.3.1. Introduction

This study defines the basis for material balances to accompany the HRDF reprocessing flowsheets being prepared as guidance to the development program. Head-end and off-gas treatment system material balances have been prepared as previously reported and are ready for publication. Solvent extraction balances will complete the activity.

11.3.2. Activity

Detailed material balances for Purex and Thorex solvent extraction are being prepared and will be included in the final report. A comparison of impurities present in HTGR spent fuel elements (Ref. 11-1) with specifications for uranyl nitrate feed solution to the resin-loading process for refabrication (Ref. 11-2) is shown in Table 11-1, along with the decontamination factors required to meet the specifications. Several of the specifications address metallic impurities that might be expected to enter the process stream through corrosion or erosion. Expected quantities of these contaminants have not been determined and are not included in the decontamination factor requirements.

11.3.3. Conclusions

As previously reported, definitive process yields cannot be predicted for the HRDF at present owing to insufficient experimental data and pending

TABLE 11-1
IMPURITY CONCENTRATIONS AND REQUIRED SOLVENT EXTRACTION DECONTAMINATION FACTORS
(EXCLUDING IMPURITIES ADDED IN PROCESSING)

Impurity	Specification, Max. Limit[a] (μg/g U)	Spent Fuel Element Concentration (μg/g U)[b]		DF Required	
		Fertile Stream	Fissile Stream	Thorex	Purex
Aluminum	75	--	--	--	--
Calcium plus magnesium	150	--	--	--	--
Chlorine plus fluorine	50	1224[c]	--	0[d]	0[d]
Chromium	150	--	--	--	--
Cobalt	75	2×10^{-3}	1×10^{-4}	0	0
Copper	200	--	--	--	--
Iron plus chromium	200	--	--	--	--
Lead	200	160	3×10^{-2}	0	0
Manganese	200	--	--	--	--
Molybdenum	200	117,118	277,525	600	1400
Nickel	150	7298	586	50	4
Phosphorous	200	5×10^{-3}	2×10^{-5}	0[d]	0[d]
Silicon	200	--	--[e]	--	0[e]
Sulfur	30	78,027[c]	31	0[d]	0[d]
Tantalum	200	--	--	--	--
Tin	200	341	473	2	3
Titanium	200	--	--	--	--
Tungsten	200	--	--	--	--
Vanadium	200	--	--	--	--
Zinc	200	--	--	--	--
Total of above elements	1200	204,168	278,615	200	250
Plutonium	30	91	47,050	3	1600
Thorium	600	3×10^{7}	2×10^{-1}	50[f]	
Total impurities,					
Burnable[g]	20 TEBC[h]	63,893[h,i]	56,131[h]	3200	2800
Nonburnable[j]	2 TEBC[h]	1,318[h]	3,745[h]	700[k]	1900[k]
Other[k]	None	1×10^{6}	2×10^{6}	0[k]	0[k]

[a] Ref. 11-2.

[b] Ref. 11-1 *Standard makeup fuel element (cooled 180 days).*

[c] Quantity includes contribution from graphite in fuel element.

[d] Element is assumed to volatilize during burning step.

[e] Silicon is expected to be disposed of as hulls, as a product of burning. Only a negligible residue should be in solution.

[f] Decontaminaton factor of 50 required after separation factor of 1000 for thorium from uranium is applied.

[g] Burnable elements include boron, cadmium, lithium, samarium, and gadolinium (Ref. 11-2).

[h] TEBC = total equivalent boron content.

[i] Includes boron from poison wafers.

[j] Nonburnable elements include aluminum, barium, calcium, chlorine, chromium, cobalt, copper, iron, indium, manganese, molybdenum, nickel, phosphorus, silicon, silver, tin, tungsten, vanadium, zinc, europium, and dysprosium.

[k] Other impurities present in fuel but with no specification limit in Ref. 11-2 include 37 fission and activation products. TEBC ≈1365 (fertile) and 3241 (fissile). The TEBC is principally attributable to neodynium and technicium. Assuming the maximum limit of 2 TEBC for nonburnable impurities applies would increase the required decontamination factor for Thorex from 700 to ∿1350 and for Purex from 1900 to ∿3500.

fuel design changes. However, deficiencies can be recognized and data needs identified as guidance to the experimental program so that appropriate information can be gathered for the HRDF conceptual design.

11.4. SIMULATION OF REPROCESSING PLANT OPERATING MODES

11.4.1. Introduction

The objective of this subtask is to develop a computerized simulation model of a typical HTGR fuel reprocessing plant. Specific problems to be studied and reported are:

1. The effects of system reliability on plant performance.

2. The dependence of system performance on the level of surge capacities available.

3. The effects of batch versus continuous operation on system performance.

11.4.2. Activity

A GASP IV simulation language package has been purchased. GASP IV capabilities will be compared with SIMSCRIPT capabilities for modeling reprocessing operations. The SIMSCRIPT language package is operative on the GA computer system, and several trial runs have been made to achieve familiarization with the language. Activity is at a low level owing to other priority assignments, pending recruiting of additional personnel.

11.5. HTGR COMMERCIALIZATION

11.5.1. Introduction

Contributions to commercialization studies during the quarter included:

1. Hanford Engineering Development Laboratory HTGR commercialization cost/benefit analysis and reactor strategy studies.

2. General Atomic Lead Plant Cost Estimate and Risk Analysis.

3. RAMCO Gas-Cooled Reactor Commercialization Study.

The General Atomic lead plant estimate is supportive to the RAMCO commercialization study.

11.5.2. Activity

Oak Ridge National Laboratory cost estimates for reprocessing and refabricating HTGR fuel were reviewed, and the revised input was submitted by ORNL to HEDL for the HTGR cost/benefit analysis.

The Ralph M. Parsons - GA 1975 Target Recycle Plant (TRP) cost estimate was updated to employ current year dollars and to reflect the lead plant fuel design. A 20,000 fuel element per year recycle plant representing the HRDF cost was factored from the TRP as input to the lead plant cost estimate. Financial risks that might be incurred in building and operating a recycle plant were identified as input to the lead plant risk analysis.

The following items were furnished to ORNL as input to the RAMCO commercialization study:

1. Spent fuel element and mass flow data for the HRDF.
2. HRDF reprocessing system capacities.
3. State-of-the-art summaries for HRDF shipping-receiving-storage and reprocessing functional areas.

The draft ORNL document "Fuel Cycle Technology Assessment Information Summary for RAMCO - Commercialization Study," was reviewed and comments were submitted to ORNL.

A letter report was furnished to RAMCO answering questions regarding the HTGR fuel cycle.

REFERENCES

11-1. Hamilton, C. J., et al., "HTGR Spent Fuel Composition and Fuel Element BLock Flow," ERDA Report GA-A13886, General Atomic Company, July 1, 1976.

11-2. Trauger, D. B., "Thorium Utilization Program: Interim II Specifications for Uranyl Nitrate Feed Solution to the Resin-Loading Process," Oak Ridge National Laboratory unpublished data, December 15, 1976.

12. NONPROLIFERATION ASSESSMENT FOR THORIUM FUEL CYCLES

12.1. SUMMARY

Alternate fuel cycles were defined for HTGRs, GCFRs, and heavy water reactors (HWRs) as part of the nonproliferation study. Specificaton trees and functional flow diagrams for fabricaton and reprocessing of alternate fuels were prepared. A brief assessment of the state of the art of various thorium fuel cycles was made to determine future development requirements.

12.2. ALTERNATE FUEL CYCLES/NONPROLIFERATION STUDY

12.2.1. Introduction

This study provides support to ORNL as lead contractor for an evaluation of the nonproliferation aspects of the thorium fuel cycle for various reactor designs. The objectives of the evaluation are to determine the potential for proliferation of nuclear weapons through diversion of fissile isotopes in thorium-based fuel cycles, to evaluate the economics of various thorium fuel cycles, and to determine the development required to attain commercial application of the thorium fuel cycles of interest.

General Atomic is providing support in assessment of the functional area of spent fuel reprocessing for HTGRs and other thermal reactors, as well as fast reactors, operating on thorium fuel cycles and/or low-enriched uranium (LEU) fuel cycles. The functional area of fresh fuel fabrication for HTGRs is also included in GA's scope of work. Work on this study was started in April 1977.

12.2.2. Activity

Alternate fuel cycle cases to be evaluated in this study are listed in a case matrix supplied by the lead contractor. The initial activity at GA

was to further define and describe candidate alternate fuel cycle cases for the HTGR, GCFR, and HWR. Specification trees and functional flow diagrams for the reprocessing of alternate fuels were prepared for these reactor types. Similarly, specification trees and functional flow diagrams were prepared for HTGR fresh fuel fabrication. Proliferation-critical functions were indicated in the specification trees and functional flow diagrams, and Level 0 design solutions were proposed. The relative proliferation attractiveness of process fuel materials in the assigned reactor fuel cycles was tentatively categorized as an aid to subsequent nonproliferation assessment of process functional systems. As a first step toward determining the development requirements necessary for attaining commercial application of thorium fuel cycles of interest, a brief assessment of the state of the art was included for functional systems appearing on the flow diagrams. Where feasible, candidate fuel cases were combined as single processing cases in order to reduce the ultimate nonproliferation assessment effort to as concise a matrix as possible.

APPENDIX A
TOPICAL REPORTS PUBLISHED DURING THE QUARTER

Ballard, A. S., "Interim Design Status and Operational Report for Semi-remote Handling Fixtures: Size Reduction System," ERDA Report GA-A14126, General Atomic Company, February 1977.

Sund, R. E., D. E. Strong, and B. A. Engholm, "HTGR Spent Fuel Element Decay Heat and Source Term Analyses," ERDA Report GA-A14140, General Atomic Company, February 1977.

Young, D. T., "Fluidized Combustion of Beds of Large, Dense Particles in Reprocessing HTGR Fuel," General Atomic Report GA-A14327, March 1977.

Burgoyne, R. M., and E. J. Steeger, "Conceptual Design Report for HETP Radioactive Feed Material Shipping Equipment," ERDA Report GA-A14353, General Atomic Company, April 1977.

APPENDIX B

DISTRIBUTION LIST

L. BROOKS	SV-101	J. F. WATSON	L-640
R. C. DAHLBERG	L-503	B. BAXTER	ORNL*
G. B. ENGLE	L-364	R. D. ZIMMERMAN	E-179
W. V. GOEDDEL	SV-101	M. H. MERRILL	L-510
A. J. GOODJOHN	E-217	H. C. CARNEY	E-086
T. D. GULDEN	L-444	A. H. SCHWARTZ	EA2-211
S. LANGER	TO-559	G. E. BENEDICT	E-249
G. B. MELESE d'HOSPITAL	TO-365	J. W. ALLEN	E-166
C. L. RICKARD	L-205	R. M. BURGOYNE	E-165
O. STANSFIELD	L-440	P. L. WARNER	E-167
H. B. STEWART	L-602	G. CHANDLER	E-161
J. J. SHEFCIK	E-244	N. W. JOHANSON	E-165
R. F. TURNER	L-507	J. S. RODE	E-174
R. C. NOREN	SVB-131	U-S PARK	E-243
B. YALOF	S-117		

LEGAL

WASHINGTON

15 DOCUMENT CENTER

177 TIC

---

*Room 215, Bldg. 4508
ORNL, P. O. Box X
Oak Ridge, Tenn. 37830

1 R. D. Thorne, Manager, SAN
U.S. ERDA
San Francisco Operations Office
1333 Broadway
Oakland, Ca. 94612

1 J. B. Radcliffe
PMRS-SD

1 Assistant Director, Commercial
Fuel Cycle Division of Nuclear
Fuel Cycle and Productions
U.S. ERDA
Washington, D. C. 20545

5 Chief, HTGR Fuel Recycle Branch
Division of Nuclear Fuel Cycle
and Productions
U.S. ERDA
Washington, D. C. 20545

2 Project Manager, HTGR Fuel
Reprocessing Development
Allied Chemical Corp.
P. O. Box 2204
Idaho Falls, Idaho 83401

1 Director, Reactor Division,
Attn: Fred E. Dearing
Oak Ridge Operations Office
U.S. ERDA
P. O. Box E
Oak Ridge, Tennessee 37830

1 Director, Advanced Gas-Cooled
Reactor Programs
Attn: P. R. Kasten
Oak Ridge National Laboratory
P. O. Box X
Oak Ridge, Tennessee 37830

1 C. E. Williams
Office of the Manager
Idaho Operations Office
U.S. ERDA
Idaho Falls, Idaho 83401

1 Barry Smith
Idaho Operations Office
U.S. ERDA
Idaho Falls, Idaho 83401

1 V.C.A. Vaughen
Chemical Technology Division
Union Carbide Co.
P. O. Box X
Oak Ridge, Tennessee 37830

1 W. D. Woods
1 E. E. Fisher
R. M. Parsons Co.
Pasadena, Ca 91124

1 Chong Lewe
Nuclear Utility Services
4 Research Place
Rockville, Maryland 20850

1 W. G. Price
Vice President - Generation
Delmarva Power and Light
800 King St.
Wilmington, Delaware 19899

1 J. D. Hornbuckle
So. Calif. Edison
P. O. Box 351
Los Angeles, Ca. 90053

1 G. F. Daebeler
Branch Head, Safety and
Licensing
1 R. F. Manty
Branch Head, Fuel Management
1 H. D. Honan
Philadelphia Electric
2301 Market St.
Philadelphia, Penn. 19101

1 P. U. Fischer
1 R. Finkbeiner
General Atomic Europe
Weinbergstrasse 109
8006 Zurich
Switzerland

1 Director, Office of Public Affairs,
U.S. ERDA
San Francisco Operations Office
1333 Broadway
Oakland, Ca. 94612

1 California Patent Group
U.S. ERDA
San Francisco Operations Office
1333 Broadway
Oakland, Ca. 94612

1 John Ganley
GAC Fuels Group
France
(via M. H. Merrill)

1 Mr. Claude Moreau
Commissariat a l'Energie Atomique
Centre d'Etudes Nucleaires de Saclay
BP No. 2
91190 Gif-sur-Yvette
France

1 J. L. McElroy
Battelle Northwest Laboratories
P.O. Box 999
Richland, Washington 99352

1 Dr. K. Hackstein
HOBEG
6450 Hanau/Main
Postfach 787
Germany

1 Dr. D. Stoelzl
Hochtemperatur Reaktorbau Gmbh
Gottlieb-Daimler-Strasse 8
D-68 Mannheim - 1
Postfach 5360
Germany

1 K. Notz
Oak Ridge National Laboratory
Oak Ridge, Tennessee 37830

1 A. L. Lotts, Program Manager
Thorium Utilization Program
Oak Ridge National Laboratory
P.O. Box X
Oak Ridge, Tennessee 37830